uOttawa

L'Université canadienne
Canada's university

FACULTÉ DES ÉTUDES SUPÉRIEURES ET POSTOCTORALES

uOttawa

L'Université canadienne
Canada's university

FACULTY OF GRADUATE AND POSDOCTORAL STUDIES

Peigang Cao

AUTEUR DE LA THÈSE / AUTHOR OF THESIS

Ph.D Chemical Engineering

GRADE / DEGREE

Department of Chemical and Biological Engineering

FACULTÉ, ÉCOLE, DÉPARTEMENT / FACULTY, SCHOOL, DEPARTMENT

A Membrane Reactor Process for the Production of Biodiesel

TITRE DE LA THÈSE / TITLE OF THESIS

Marc A. Dubé

DIRECTEUR (DIRECTRICE) DE LA THÈSE / THESIS SUPERVISOR

André Yves Tremblay

CO-DIRECTEUR (CO-DIRECTRICE) DE LA THÈSE / THESIS CO-SUPERVISOR

EXAMINATEURS (EXAMINATRICES) DE LA THÈSE / THESIS EXAMINERS

Ajay Dalai

Martin Ternan

Christopher Lan

Boguslaw Kruczek

Gary W. Slater

Le Doyen de la Faculté des études supérieures et postdoctorales / Dean of the Faculty of Graduate and Postdoctoral Studies

# A Membrane Reactor Process for the Production of Biodiesel

by

Peigang Cao

A thesis submitted to the Faculty of Graduate and Postdoctoral Studies
in partial fulfillment of the requirements for the degree of

**Doctor of Philosophy**

**in the Department of Chemical and Biological Engineering**
**University of Ottawa**

*Your file Votre référence*
*ISBN: 978-0-494-41628-0*
*Our file Notre référence*
*ISBN: 978-0-494-41628-0*

# Abstract

Biodiesel, a transesterified product of vegetable oil and animal fats, is considered as a promising diesel fuel substitute because it has properties similar to that of petroleum-based diesel fuel. The biodiesel market is among the fastest growing renewable energy markets and therefore, there is considerable interest in its production processes from industry and academia. However, the high cost of the feedstock and some technical challenges in biodiesel production such as the immiscibility of two of the reagents and the reversibility of the transesterification reaction call for innovative technologies to be developed. In addition, unreactable matter in the lipid feedstock may affect biodiesel purity. One promising solution to these issues is the use of a membrane reactor for biodiesel production.

The objectives of the proposed research project were to develop this new approach to produce biodiesel and to investigate different factors affecting the production process and the biodiesel purity. The eventual goal was the development and optimization of a continuous membrane reactor process.

Bench and pilot scale membrane reactors were designed and assembled to carry out the transesterification of different lipids with methanol. The membrane reactors integrate many procedures and reach several process integration objectives such as combining reaction and separation in a single unit, continuous mixing of raw materials, maintaining high mass transfer between the immiscible phases and maintaining two phases during the reaction. Several factors affecting the biodiesel production process and the biodiesel purity such as membrane pore size, volume ratio of feedstocks, recycling of the polar phase, catalyst (NaOH) concentration, and feedstock type and quality were investigated. Thus, a series of experiments using canola, palm, soybean and waste oils were performed at various alcohols to oil ratios, recycling proportions, catalyst (NaOH) concentrations, and residence times.

Carbon membranes of different pore sizes (namely, 0.05, 0.2, 0.5 and 1.4 micron) were shown to retain the unreacted lipid feedstock in the reactor, which indicated that the

oil droplets present in the reactor were larger than all the pore sizes; no triglycerides were found in the permeate. The effects of initial methanol/canola oil loading were also studied in semi-continuous mode. Permeate was observed at the 0.38, 0.47, and 0.64 initial methanol volume fractions ($\phi_1$) whereas it was not observed at $\phi_1 = 0.29$, which indicated that initial volume fractions of methanol up to 0.38 could be treated in the membrane reactor. A semi-empirical model was developed and validated as a predictive equation to determine phase inversion in the reactor. The membrane reactor produces a permeate stream which readily phase separates at room temperature into a FAME (fatty acid methyl ester)-rich non-polar phase and a methanol- and glycerol-rich polar phase. To decrease the overall methanol:oil molar ratio in the reaction system, the polar phase was recycled. Three recycle ratios were tested: 100, 75 and 50%, at the same residence time and operating conditions. The permeate consistently separated to yield a FAME-rich non-polar phase containing a minimum of 85 wt.% FAME (the remainder being methanol) as well as a methanol/glycerol polar phase. At the highest recycle ratio, the FAME concentration ranged from 85.7 to 92.4 wt.% in the FAME-rich non-polar phase. In addition, the overall molar ratio of methanol:oil in the reaction system was significantly decreased to 10:1 while maintaining a FAME production rate of 0.04 kg/min. The transesterifications were performed at 0.0, 0.01, 0.03, 0.05, 0.1, 0.5, and 1 wt% catalyst (NaOH) on an oil basis. It was found that a base catalyst concentration above 0.05 wt% for a one hour residence time (RT) and above 0.03 % for a two hour RT resulted in steady-state biodiesel production via the membrane reactor. Such catalyst amounts are 10 to 33 times lower than those employed in the industrial production of biodiesel, respectively (e.g., 0.5 to 1 wt% sodium hydroxide concentration). Meanwhile, it was demonstrated that the membrane reactor can be operated using a very broad range of feedstocks at highly similar operating conditions to produce biodiesel.

The total glycerine and free glycerine contents of the FAME produced were below the ASTM D6751 standard after only a single reaction step. Under essentially the same reaction conditions, a conventional batch reaction was not able to achieve the same degree of FAME purity. A kinetic study was conducted to seek the rate constants of transesterification in the membrane reactor at various catalyst (NaOH) concentrations and RTs. The proposed mathematical kinetic model fitted the experimental results well. It

was found that the catalyst (NaOH) concentration increased the reaction rates, and the RT had no significant influence on the reaction rates. The forward rate constants were over 450 % higher than previous work using a batch process. This was attributed to the excellent mixing in the membrane reactor loop, the higher methanol:oil molar ratio used in the study and the continuous removal of product from the reaction medium. The work shows the advantages of product removal in enhancing the reaction rate in transesterifying canola oil in a membrane reactor.

In conclusion, this work presents the first systematic study of biodiesel production using a membrane reactor. Among the most significant factors investigated were the completion of high purity biodiesel production process based on the permeate de-phasing discovery. Empirical models were selected for prediction of phase inversion in the reactor. Lower catalyst (NaOH) concentration than conventional process can be used in membrane reactor, and a very broad range of feedstocks can be used in the membrane reactor to produce biodiesel.

# Résumé

Le biodiésel, un produit transestérifié de graisses animales et d'huiles végétales, est considéré comme produit de remplacement pour le carburant diésel parce qu'il a des propriétés semblables. Le marché de biodiésel est parmi les marchés d'énergie renouvelables croissants les plus rapides et donc, il y a de l'intérêt considérable pour ses procédés de production. Cependant, le coût élevé de la matière de base et de quelques défis techniques dans la production du biodiésel tels que l'immiscibilité de deux des réactifs et de la réversibilité de la réaction de transestérification nécéssitent que les technologies innovatrices soient développées. En outre, la matière non-réactive dans la matière de base du lipide peut affecter la pureté du biodiésel. Une solution prometteuse est l'utilisation d'un réacteur de membrane pour la production du biodiésel.

Les objectifs de ce projet de recherche étaient de développer cette nouvelle approche pour produire le biodiésel et pour étudier différents facteurs affectant le procédé de production et la pureté du biodiésel. Le but ultime était le développement et l'optimisation d'un processus continu de réacteur de membrane.

Des réacteurs de membrane à l'échelle de banc et pilote ont été conçus et assemblés pour effectuer la transestérification de différents lipides avec du méthanol. Les réacteurs de membrane intègrent beaucoup de procédures et atteignent plusieurs des objectifs de processus d'intégration tels que combiner la réaction et la séparation dans une unité simple, le mélange continu des matières premières, maintenir le transfert de masse élevée entre les phases non-miscibles et maintenir deux phases pendant la réaction. Plusieurs facteurs affectant le procédé de production du biodiésel et de sa pureté telle que la taille de pore de membrane, le rapport de volume des matières de base, la réutilisation de la phase polaire, la concentration du catalyseur, et le type et la qualité de matière de base ont été étudiés. Ainsi, une série d'expériences en utilisant des huiles de canola, de paume, de soja et d'huiles de friture (yellow grease) a été exécutée à divers rapports d'alcool/lipide, taux de recyclage, concentrations de catalyseur, et temps de réaction.

Des membranes de carbone de différentes tailles de pore (notamment, 0.05, 0.2, 0.5 et 1.4 micron) ont maintenu les lipides dans le réacteur, qui a indiqué que les gouttelettes d'huile actuelles dans le réacteur étaient plus grandes que toutes les tailles de pore; aucun triglycéride n'a été décelé dans le perméat. Les effets du chargement initial d'huile de méthanol/canola ont été également étudiés en mode semi-continu. On a observé la production de perméat aux fractions initiales de volume de méthanol de 0.38, 0.47, et 0.64 tandis qu'on ne l'a pas observé à 0.29, qui ont indiquées que des fractions initiales de volume du méthanol jusqu'à 0.38 pourraient être traitées dans le réacteur de membrane. Un modèle a été développé et validé pour déterminer l'inversion de phase dans le réacteur. Le réacteur de membrane produit un perméat ou les phases se séparent aisément à la température ambiante dans une phase non-polaire riche en EMAG (ester méthylique d'acide gras) et une phase polaire riche en méthanol et glycérol. Pour diminuer le rapport molaire global de méthanol:huile dans le système de réaction, la phase polaire a été recyclée. Trois rapports de recyclage ont été examinés: 100, 75 et 50%, au mêmes temps de séjour et conditions de fonctionnement. Le perméat s'est uniformément séparé pour rapporter une phase non-polaire riche en EMAG contenant un minimum de 85% d'EMAG (le reste étant du méthanol) aussi bien qu'une phase polaire de méthanol/glycérol. Au plus haut rapport de recyclage, la concentration d'EMAG s'est étendue de 85.7 à 92.4% poids dans la phase non-polaire riche en EMAG. En outre, le rapport molaire global de méthanol:huile dans le système de réaction a été diminué à 10:1 tout en maintenant un taux de production d'EMAG de 0.04 kg/min. Les transestérifications ont été effectuées à des concentrations de catalyseur de 0.0, 0.01, 0.03, 0.05, 0.1, 0.5, et 1% en poids sur une base d'huile. On a constaté qu'une concentration basse en catalyseur au-dessus de 0.05% en poids pendant un temps de séjour d'une heure et au-dessus de 0.03% pendant un temps de séjour de deux heures a eu comme conséquence la production équilibrée de biodiesel par l'intermédiaire du réacteur de membrane. De tels montants de catalyseur sont de 10 à 33 fois inférieurs à ceux utilisés dans la production industrielle du biodiesel, respectivement (par exemple, 0.5 à 1 % en poids de concentration de hydroxyde de sodium). En même temps, on a démontré que le réacteur de membrane peut être opéré en utilisant une gamme très large des matières de base aux conditions de fonctionnement fortement semblables pour produire le biodiésel.

Les contenus de glycérine totale et de glycérine dans l'EMAG produite étaient au-dessous de la norme d'ASTM D6751 après seulement une étape simple de réaction. Dans essentiellement les mêmes conditions de réaction, une réaction en mode discontinu conventionnel ne pouvait pas réaliser le même degré de pureté d'EMAG. Une étude cinétique a été entreprise pour chercher les constantes des taux de réaction de la transestérification dans le réacteur de membrane chez de diverses concentrations de catalyseur et temps de séjour. Le modèle cinétique mathématique proposé a bien adapté les résultats expérimentaux. On a constaté que la concentration de catalyseur a augmenté les taux de réaction, et le temps de séjour n'a eu aucune influence significative sur les taux de réaction. Les constantes de taux de réaction étaient plus de 450% plus haut que le travail de Vicente. Ceci a été attribué à l'excellent mélange dans le réacteur de membrane et au déplacement continu du produit. Le travail montre les avantages du déplacement de produit en augmentant le taux de réaction en huile de canola de transestérification dans un réacteur de membrane.

En conclusion, ce travail présente la première étude systématique de la production du biodiésel à l'aide d'un réacteur de membrane. Parmi les facteurs les plus significatifs étudiés étaient l'accomplissement du procédé de production de biodiésel de grande pureté basé sur la découverte du déphasage du perméat. Des modèles empiriques ont été choisis pour la prévision de l'inversion de phase dans le réacteur. Des concentrations de catalyseur fortement inférieures à ceux du processus conventionnel peuvent être employées dans le réacteur de membrane, et une gamme très large des matières de base peut être employée dans le réacteur de membrane pour produire le biodiésel.

# Acknowledgements

This thesis would not have been possible if it were not for many people.

First and foremost, I would like to extend my deepest gratitude to my supervisors, Dr. Marc A. Dubé and Dr André Y. Tremblay; both of you gave me invaluable guidance, continued encouragement, and constructive advice throughout the course of this study, the perfect combination of your supervisions brought me out of the darkness of the unknown biodiesel world. I grew up and went through the challenges thanks to this unparalleled enlightenment.

I wish to express my sincere appreciation and gratitude to Professors Morris Kates (BCH), David McLean, and Marten Ternan for their helpful suggestions and instructive guidance. All the members in the Ottawa Biodiesel Research Group created a friendly, inspirational, supportive environment which helped me complete this research process. Thanks are due to Roza Tizvar, Fadi Ataya, Yongjun Zhang, Jehad Saleh, Katie Morse, and Julie Wijaya for their useful discussions and comments, our cooperation and friendship are precious to me.

I am grateful to the technicians in the Department of Chemical Engineering, University of Ottawa, Gérard Nina, Franco Ziroldo and Louis Tremblay for always being there when I needed help. Also, I would like to give my sincere thanks to all other people of the Department of Chemical Engineering, for their cooperation and generous help.

In these acknowledgements I must, of course, also mention my family, even though we were separated by the Pacific Ocean during most of the time of my study. To my wife Yuan Kang: without you and your prayers, I would have never dared to explore the world beyond my cocoon and have never grown into the person I am today. To my son Yucheng Cao: I was indebted to you everyday during our passed years, I did not commit to the responsibility as a father, which makes me feel guilty, but what you contribute to your father's PhD study is not measurable.

For the financial support during this project, I am grateful to the Ford Foundation with the mission to "**strengthen democratic values, reduce poverty and injustice,**

**promote international cooperation and advance human achievement**," which is and will be my credo forever; I am very proud of being a Fellow of the Ford Foundation.

I won't mention any other names in particular because I would be omitting the many mysterious backroom people in the team who were involved in making things a success!

# Table of Contents

# List of Figures

# List of Tables

# Nomenclature

This nomenclature lists some of the most frequently used abbreviations in this thesis. It is not meant to be exhaustive. Other symbols used in formulas, tables, and figures are explained in the text as they appear.

**List of abbreviation**

ASTM – American Society for Testing and Materials

CFPP – Cold flow plugging point

CGSB – Canadian General Standards Board

CN – cetane number, a dimensionless descriptor of the ignition quality of a diesel fuel, similar to the octane scale used for gasoline

DG – Diglyceride

FAAE – Fatty acid alkyl ester

FAEE – Fatty acid ethyl ester

FAME – Fatty acid methyl ester

FFA – Free fatty acid

FID – Flame ionization detector

GC – Gas chromatography

GHG – Greenhouse gas

GPC – Gel permeation chromatography

HP – Horsepower

HPLC – High performance liquid chromatography

ID – Inside diameter

MG – Monoglyceride

MR – Membrane reactor

MSTFA – N-methyl-N-(trimethylsilyl) trifluoracetamide

MWCO – Molecular weight cut-off

OD – Outside diameter

ppm – parts per million

psi – Pound per square inch

RT – Residence time

RRT – Relative retention time

TG – Triglyceride

THF – Tetrahydrofuran

TMP – Trans-membrane pressure

NREL – National Renewable Energy Laboratory in U.S.

NEB – Net energy balance

PUFA – Polyunsaturated fatty acid

**Symbols**

$k'$ – effective rate constants of reactions, L/(mole·min)

$k$ – rate constants of reactions, L/(mole·min)

[DG] – conc. of DG in the reactor base on the reactor volume, mol/L

$[DG]_{out}$ – conc. of DG in the permeate, mol/L

[FAME], –conc. of FAME in the reactor base on the reactor volume, mol/L

$[FAME]_{out}$ – conc. of FAME in the permeate, mol/L

[G] – conc. of glycerol in the reactor base on the reactor volume, mol/L

$[G]_{out}$ – conc. of glycerol in the permeate, mol/L

[Methanol] – conc. of the in membrane reactor base on the reactor volume, mol/L

$[Methanol]_{out}$ – conc. of methanol in the permeate, mol/L

[MG] – conc. of MG in the reactor base on the reactor volume, mol/L

$[MG]_{out}$ – conc. of MG in the permeate, mol/L

[TG] – conc. of TG in the reactor base on the reactor volume, mol/L

C – Constants

D or d – drop diameter, m or μm;

$D_{95}$ – diameter below which 95% of the volume is found, m or μm;

$F_{DG\text{-}in}$ – DG contained in feeding lipid, mol/min, be neglected for canola oil.

$F_{DG\text{-}out}$ – DG outflow rate, mol/min

$F_{FAME\text{-}out}$ – FAME outflow rate, mol/min

$F_{G\text{-}out}$ – glycerol outflow rate, mol/min

$F_{Methanol\text{-}in}$ – methanol feeding rate, mol/min

$F_{Methanol\text{-}out}$ – methanol outflow rate, mol/min

$F_{MG\text{-}out}$ – MG outflow rate, mol/min

$F_{TG\text{-}in}$ – TG feeding rate, mol/min

$J_p$ – membrane permeate flux, $m^3/(m^2\ s)$;

$K_{ow}$ – octanol-water partition coefficients;

$M_{Total\text{-}in}$ – mass flow rate of feeding feedstocks, g/min

$M_{Total\text{-}out}$, – mass flow rate of permeate, g/min

$MW$ – molecular weight, g/mol

$P$ – Pressure, Pa = kg/(m s);

$P_{crit}$ – critical pressure at which an oil droplet enters a pore, kPa

$r$ – Radius of the advancing portion of the oil droplet, m;

$R$ – Radius of the lagging portion of the oil droplet, m;

$R_{cp}$ – resistances associated with the concentration polarization, $m^{-1}$;

$R_g$ – resistances associated with the gel layer, $m^{-1}$;

$R_{in}$ – resistances associated with the internal pore fouling, $m^{-1}$;

$R_m$ – resistances associated with the membrane material, $m^{-1}$;

t – time, minute

U – Average velocity, m/s;

$V$ – Volume, $m^3$;

$V_0$ – volume of membrane reactor, L

$V_{out}$ – volume flow rate of permeate, L

$\theta$ – Contact angle, degree; oil-membrane surface

$\pi$ – osmotic pressure, Pa;

**Greek letters**

$\mu$ – viscosity, kg/m·s;

$\rho$ – density, $kg/m^3$;

$\rho_{out}$ – density of permeate from reactor, g/mL;

$\rho_{TG}$ – density of TG in the reactor, g/mL;

$\varepsilon$ – energy dissipation per unit mass per unit time, FL/MT;

$\sigma$ – interfacial tension, N/m; oil-alcohol;

$\dot{\gamma}$ – shear rate, $s^{-1}$

# Chapter 1 Introduction

# Chapter 1 - Introduction

Biodiesel is a cleaner burning diesel replacement fuel converted from biomass – mainly organic oils from seeds, corn, canola, animal fat, and even "used" oil - into liquid fuel. It is similar to and compatible with, conventional (fossil fuel) diesel energy, however it is more environmental friendly. Biodiesel, also known as fatty acid alkyl esters (FAAE), is defined as a fuel comprised of mono-alkyl esters of long chain fatty acids derived from vegetable oils or animal fats. A "mono-alkyl ester" is the product of the reaction of a straight chain alcohol, such as methanol or ethanol, with a fat or oil to form glycerol (also called glycerine) and the esters of long chain fatty acids through a transesterification process.

While, there are many technical and economic challenges hindering the widespread commercial use of biodiesel. The single most important factor in making biodiesel production economically viable is the use of low cost lipid feedstock (Zhang et al., 2003). The low cost feedstock gives rise to technological challenges which include water content, free fatty acid (FFA) content, and the effect of various components on biodiesel cold flow properties. With the use of low cost feedstock of dubious origin (e.g., waste oils, yellow grease), it is not surprising that product quality is an important issue. However, even in the case of high quality feedstock, product quality issues are important. For example, the ASTM D6751 standard for biodiesel allows 0.24% total glycerol in the final product. This implies that the reaction completion must be about 99.7% to meet the total glycerol standard for the fuel (Knothe et al., 2005). Although many downstream separation methods have been studied for purifying the biodiesel product, they are often energy intensive and require the addition of extracting solvents to the process. All these downstream processes involve the production of wastewaters and these often contain toxic elements (e.g., residual methanol and catalyst) which are evidently not in line with the environmentally driven ideals behind the use and production of biodiesel. Moreover, unsaponifiable material can be found in the lipid feedstock, even for virgin oil. Most of these unreactable materials will remain in the biodiesel product because of their solubility in the FAME. Distillation to separate these compounds from the FAME is not cost

effective for conventional biodiesel production. In addition to this, most commercially available biodiesel is produced in batch processes which have inherently large scale limitations.

A promising solution to the above issues is membrane reactor technology (Dubé et al., 2007). A membrane reactor is a reaction system where membranes and chemical reaction are integrated. It is a device for simultaneously carrying out a reaction and membrane-based separation in the same physical enclosure. Membrane reactor technology has been successfully applied to many chemical reaction processes (Hsieh, 1996). Transesterification is a classical reversible chemical reaction which could also be combined with membrane reactor technology. Previous research on biodiesel production in a membrane reactor by Liu (2004) was not a continuous process. That work was purely geared towards a proof of concept. The permeate contained only a very low concentration of FAME (~1 mol %), which was homogeneous at room temperature and required some downstream separation of the FAME and glycerol phases which were not straightforward. Furthermore, in that work, the actual molar ratio of methanol to oil was ~200:1, far higher than the commercial 6:1 ratio.

Thus, a number of important questions arise. How do the membrane properties such as pore size affect the biodiesel production process and what is the minimum methanol fraction at which the membrane reactor can operate? Can we recycle unused methanol to reduce the alcohol:oil ratio? Can we use lower amounts of catalyst? How does the reactor perform with different lipid feedstocks and can the use of a membrane reactor circumvent or facilitate overcoming technical issues such as high FFA contents? Can we use ethanol instead of methanol? The answers to these questions form the main objectives of this project.

## 1.1 Thesis Objectives

The overall objectives of this thesis were to develop a continuous membrane reactor process for the production of biodiesel, and to investigate several factors affecting the production process and the biodiesel purity. This was to be achieved through the construction and operation of a prototype continuous biodiesel membrane reactor. The permeate product from this novel reactor should be as high as possible in FAME

concentration with no (zero) traces of TG, and minimal amounts of DG or MG, and the overall molar ratio of methanol/oil should approach 6:1. The reactor should also provide the means to use low cost lipid feedstock.

Therefore, the specific objectives of the project were:

(i) To identify and quantify the effect of membrane pore size on the yield of biodiesel in a membrane reactor and to find out the feasible lowest alcohol fraction to maintain reactor operation.

(ii) To scale-up a prototype membrane reactor for continuous operation, and investigate the recycling of the polar phase (the methanol/glycerol-rich phase) of the permeate stream in order to decrease the overall molar ratio of methanol to lipid in the feed stream; to study any reaction inhibition due to the accumulation of glycerol in the reactor loop; and to identify the appropriate recycling conditions.

(iii) To explore the continuous production of biodiesel in the membrane reactor at different base catalyst concentrations and find the lowest feasible catalyst concentration.

(iv) To evaluate biodiesel product quality from different lipid feedstocks including low quality feedstocks (e.g., yellow grease) with high FFA contents using the membrane reactor and to identify the factors which influence the biodiesel quality from different lipid feedstocks.

(v) To study the kinetics of the transesterification in the continuous membrane reactor, calculate the rate constant in the kinetic model for the biodiesel production process, and compare the effects of residence time and catalyst concentration.

## 1.2 Outline of Approach

To achieve the above objectives, the following tasks were necessary: preliminary experiments using the original semi-continuous reactor, scale-up and construction of a prototype continuous membrane reactor and optimization of its design, layout, and operating parameters, experimental runs to fulfill objectives, sample analysis and characterization by GPC and GC, and data handling and interpretation.

To develop a continuous reaction process for the production of biodiesel and overcome the challenges due to the heterogeneity of the reaction system, incomplete conversion, use of high FFA feedstock and downstream purification, different factors

affecting the production process and the biodiesel purity were investigated. Figure 1.1 illustrates all the potential experimental variables for the membrane reactor study; the levels of the main experimental factors to be studied are shown in Table 1.1:

Table 1.1: Levels of main factors for the membrane reactor study

| Main factors | Range | Manipulated variable | Notes |
|---|---|---|---|
| Membrane pore size | 300 kD to 1.4 micron | Change membrane in reactor | Ceramic vs. carbon |
| Molar ratio of methanol:oil in reactor | 9.8:1 to 50:1 | Option 1: Change feed molar ratio<br>Option 2: Recycle the polar phase | |
| Temperature ($^{o}$C) | 45 to 65 | Adjust the heating bath temperature | |
| TMP (kPa) | 20 to 180 | Membrane fouling or adjust back pressure valve | |
| Catalyst (wt% based on total oil) | NaOH (0 to 1%) | Dissolve different amount of catalyst in the methanol. | |
| Residence time (h) | 15 min to 2 h | Adjust the feedstock feeding rate | |

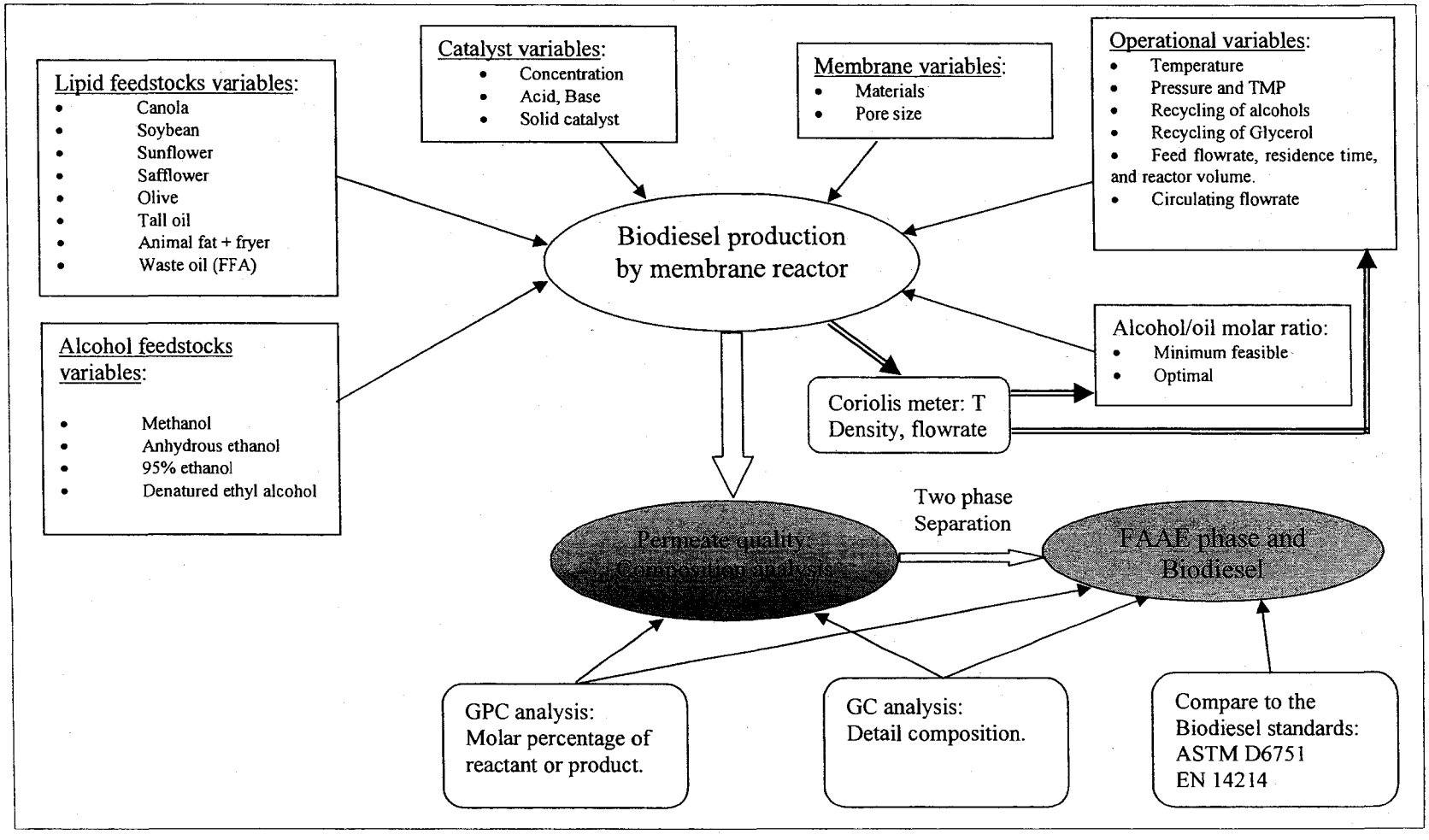


Figure 1.1: Experimental variables for the membrane reactor study

### 1.3 Organization of Thesis and Significance of the Contributions

This thesis consists of ten chapters. After Chapter 1 (Introduction), Chapter 2 (Theoretical Background) presents a literature review of biodiesel research and membrane reactors, a discussion on several factors affecting membrane reactor operation for biodiesel production, including the reactor's principle of operation, a brief overview of the nature of the feedstock, and the transesterification process. Chapters 3 to 7 each represent an independent publication submitted to a refereed scientific journal. Due to this structure, the repetition of some common ideas and elements (e.g., experimental procedures) was inevitable. Chapter 8 (General Discussion, Conclusions and Recommendations) relate to all chapters, and contains a general discussion, and conclusions and recommendations for future work. References and appendices (as appropriate) for each chapter are provided throughout the thesis. The general thesis appendix includes the membrane reactor operation guidelines, sample analysis methods and their related calibration curves, and all the experimental raw data.

**CHAPTER 3 - *Effect of Membrane Pore Size on the Performance of a Membrane Reactor for Biodiesel Production; published in Ind. Eng. Chem. Res., 2007, 46: 52-58.***

This chapter presents the effects of membrane pore size in the semi-continuous reactor and the initial methanol/canola oil loading. Four carbon membranes having different pore sizes of 0.05, 0.2, 0.5, and 1.4 micron were tested, with four different initial methanol volume fractions of 0.29, 0.38, 0.47, and 0.64. The initial oil loadings represent methanol/oil molar ratios of 11:1, 16:1, 23:1, and 46:1, and gel permeation chromatography (GPC) was used to analyze the composition of the permeate.

**CHAPTER 4 - *Methanol Recycling in the Production of Biodiesel in a Membrane Reactor; published in Fuel, 2008, 87:825-833.***

This study follows the de-phasing of the membrane reactor permeate stream upon cooling to room temperature. The two phases included a FAME (fatty acid methyl ester)-rich non-polar phase and a methanol- and glycerol-rich polar phase, respectively. To decrease the overall methanol:oil molar ratio in the reaction system, the polar phase was

recycled. Three recycle ratios were tested: 100, 75 and 50%, at the same residence time and operating conditions. This paper also illustrated the trans-membrane pressure (TMP), mass flowrate, and density of the membrane reactor retentate stream. The permeate stream composition and purity were reported.

**CHAPTER 5 - *Biodiesel production using ultra low catalyst concentrations; published in Energy & Fuels (in press)***

In this study, the lowest feasible catalyst concentrations using a membrane reactor were explored at varying catalyst concentrations and residence times (RT). Prior to all experiments, the free fatty acid in the canola oil was neutralized with sodium hydroxide. Experiments were performed at 0.0, 0.01, 0.03, 0.05, 0.1, 0.5, and 1 wt% catalyst on an oil basis. The RT effect on the permeate composition was also investigated.

**CHAPTER 6 - *High Purity Fatty Acid Methyl Ester Production from Canola, Soybean, Palm and Yellow Grease Lipids by mean of a Membrane Reactor; published in Biomass & Bioenergy (in press)***

Different lipid feedstocks including low quality feedstocks (e.g., yellow grease) with high FFA contents were transesterified in the continuous membrane reactor for biodiesel production under base-catalyzed conditions. The total glycerine and free glycerine content of the FAME produced were analyzed based on ASTM D6584 standard procedures. The effect of the fatty acid composition of the lipid feedstocks on the FAME purity was also investigated.

**CHAPTER 7 – *Kinetics of Canola Oil Transesterification in a Membrane Reactor; to be submitted to Ind. Eng. Chem. Res***

The transesterification of canola oil to biodiesel was conducted using a continuous membrane reactor in the presence of NaOH as a catalyst. Runs performed at 0.05, 0.1 and 0.5 wt% based on the oil content. Samples from the retentate and permeate streams were collected during the reaction and analyzed by GPC. The forward as well as the reverse reaction rate constants of all three steps involved in the transesterification were reported. A mathematical model was proposed.

## 1.4 References

Dubé M.A., Tremblay A.Y., Liu J., Biodiesel Production Using a Membrane Reactor. *Biores. Tech.,* 93:639, **2007.**

Hsieh H.P., Inorganic Membranes for Separation and Reaction, Membrane science and technology series 3, *New York NY 10160-0757: Elsevier Science.,* pp. 117-121, **1996.**

Knothe G., Krahl J., Van Gerpen J., *The Biodiesel Handbook*; AOCS Press: Champaign, Illinois, pp. 2-36, **2005**.

Liu J., Biodiesel production by membrane reactor from canola oil, M.A.Sc. thesis, University of Ottawa, **2004**.

Zhang Y., Dubé M.A., McLean D.D., Kates M., Biodiesel Production from Waste Cooking Oil: 1. Process Design and Technology Assessment. *Biores. Tech.,* 90:229, **2003**.

# Chapter 2 Theoretical Background

# Chapter 2 - Theoretical Background

## 2.1 Biodiesel Advantages and Challenges

Biodiesel is an alternative fuel for diesel engines that is gaining increased worldwide attention after reaching a considerable level of success in Europe and more recently in the U.S. The first industrial plant in the world with a biodiesel production capacity of 10,000 tons per year went into operation in Australia in 1991 (Agarwal and Das, 2001). Germany is currently the highest-producing nation in Europe, with an annual production of 650,000 tons in 2003, while France is second (Pahl, 2005). The biodiesel industry is currently enjoying exponential growth, and public policy will likely encourage further growth over time: for example, biodiesel sales in the U.S. have increased to 113 million L/yr in 2004, up from only 1.89 million L in 1999 (Williams, 2005). The federal government in Canada has also shown its commitment to biodiesel development in different ways, in its *Climate Change for Canada* document, it targeted 500 million L of production by 2010 (Torrie, 2002).

One of the main driving forces for biodiesel's widespread use is the limitation of greenhouse gas emissions ($CO_2$ being the major one) by the Kyoto Protocol. Along with ethanol and other biomass derived fuels, biodiesel is an important bioenergy. When plants photosynthesize, they use the sun's energy to pull $CO_2$ out of the atmosphere and incorporate it into biomass. Part of the solar energy is locked into the chemical structure within the biomass. There are a number of thermal, chemical or microbial processes that can be used to release this energy or convert it into a more convenient form for human use. As a form of bioenergy, biodiesel is nearly carbon-neutral, i.e., the $CO_2$ it produces on burning will be absorbed naturally from $CO_2$ in the air and recycled without an overall net increase in the atmospheric $CO_2$ inventory, thus making an almost zero contribution to global warming (Van Gerpen, 2005).

There are many distinct advantages of using biodiesel over conventional diesel fuel:

i) Considered to be environmental friendly, biodiesel is plant-, not petroleum-derived, one of the most renewable fuels currently available.

ii) It is biodegradable.

iii) It is derived from a renewable domestic resource, thus reducing dependence on and preserving petroleum. It can be domestically produced, offering the possibility of reducing petroleum imports.

iv) Reductions of most exhaust emissions relative to conventional diesel fuel, generating lower emissions of hydrocarbons, particulates and carbon monoxide;

v) Biodiesel has a relatively higher flash point, >150 $^{0}$C, indicating that it presents a very low fire hazard; leading to safer handing and storage.

vi) Biodiesel provides greater lubricity than petroleum diesel, thus reducing engine wear (Graboski and McCormick, 1998). In fact, biodiesel can be used as a lubricity enhancer for low-sulphur petroleum diesel formulations.

vii) Toxicity tests show that biodiesel is considerably less toxic than diesel fuel (Haws, 1997).

viii) Biodiesel can be used directly in most diesel engines without requiring extensive engine modifications.

However, there are some issues confronting biodiesel which prevents its widespread use. Biodiesel production costs are high due to the high cost of virgin vegetable oil, the main feedstock used in the process. The price of biodiesel is about 1.4-2.4 US$/US gal, compared with 1.0-1.5 US$/US gal for petroleum diesel (Coltrain, 2002). With the price of raw petroleum dramatically increasing these days, this gap is apparently becoming smaller, the Official Energy Statistics from the U.S. government reported in 2007 that the price of petroleum diesel is even higher than 2.4 US$/US gal (EIA, 2007). Recent work by Zhang et al. (2003) indicates that the use of waste frying oil can reduce the cost of biodiesel. Also, the cost of biodiesel could be reduced by the use of animal fats (Nye et al., 1983).

Generally speaking, biodiesel has a higher viscosity, and higher cloud and pour points than petroleum diesel, all of which are undesirable. The viscosity of biodiesel produced from low-priced recycled frying oil and animal fats is generally even higher than the ones produced from virgin oils. Cold flow properties such as cloud and pour points, which are especially important for the use of fuel in cold climates, are higher for

biodiesel (Chandra, 1998). Blending with diesel fuel is a solution to overcome the above concerns.

One debatable opinion is that biodiesel produces 5% more nitrous oxides ($NO_x$) than conventional diesel. Von Wedel (2004) corrected the misconception that biodiesel itself causes $NO_x$ emissions by explaining that $NO_x$ forms when nitrogen from the atmosphere combines with biodiesel oxygen atoms during combustion. Possible solutions include fuel additives and exhaust treatment devices.

Certainly the most famous argument against biodiesel was that of David Pimentel of Cornell University and Tad Patzek of the University of California-Berkeley in which they reported that the "net energy balance" of biodiesel is negative (Pimentel and Patzek, 2005). NREL (National Renewable Energy Laboratory in U.S.) responded to their study immediately, and Canadian industry and government officials also questioned many of their study's assumptions, and pointed to numerous studies that reached the opposite conclusion. Very few studies in the past few years have found that biodiesel has a negative energy balance (Van Gerpen and Shrestha, 2007). In 2005, Claude Robert, a senior analyst at Natural Resources Canada's Office of Energy Efficiency, who uses a modelling tool called GHGenius to estimate greenhouse-gas emissions and energy output, NRCan (Natural Resources Canada) has consistently found that biodiesel produces more energy than is used to produce it (Mayeda, 2005). Furthermore, Hill et al. (2006) concluded that biodiesel provides ~ 93% more energy than is required in its production.

## 2.2 Transesterification

Most commercial biodiesel is derived from vegetable oil. The direct use of vegetable oils in a vehicle engine could induce many problems such as injector fouling, ring sticking and varnish build-up on the cylinder walls (Ryan et al., 1984). Most of the problems associated with the use of vegetable oils (i.e., triglycerides (TG)) can be attributed to their high viscosity and to the reactivity of their polyunsaturated fatty acid components. Since the renewal of interest in vegetable oil-derived diesel during the late 1970s, four possible solutions to the problem of high viscosity were investigated: transesterification, pyrolysis, dilution, and micro emulsification (Schwab et al., 1987). It has been shown that the most practical way of overcoming the TG viscosity problem is

through the chemical reaction to form alcohol esters (biodiesel) via the transesterification (also called alcoholysis) process (Ma et al, 1999), which is a process that combines lipid feedstock (e.g., vegetable oils or animal fats) with alcohol (e.g., ethanol or methanol) in the presence of a catalyst (e.g., sodium or potassium hydroxide, sulphuric acid) to form fatty esters (e.g., ethyl or methyl ester).

Transesterification implies taking a TG molecule or a complex fatty acid, removing the glycerol and creating an alcohol ester. Figure 2.1 depicts the classical transesterification reaction scheme.

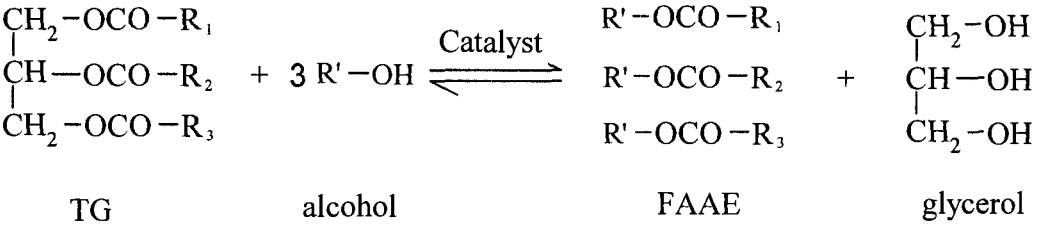


Figure 2.1: Stoichiometric reaction for conversion of TG to fatty acid alkyl esters

In Figure 2.1, $R_1$, $R_2$, and $R_3$ are long chain hydrocarbons (e.g., oleic acid - $(CH_2)_7CH{=}CH(CH_2)_7CH_3$), sometimes called fatty acid chains. The alcohol used for producing biodiesel is usually methanol (where the R' corresponds to $CH_3$).

Converting TG to methyl or ethyl esters through a transesterification process reduces the molecular weight to one-third that of the oil, reduces the viscosity by a factor of eight (Ma et al., 1999), and increases the volatility. There are many variables that influence the transesterification reaction rate, but the most important ones are temperature, catalyst type and concentration, alcohol to ester ratio, and mixing rate. The purity of the reactants, for example, the presence of water, FFAs, and other contaminants found in unrefined oils (or other feedstock) is also very important (Ma et al., 1998).

Transesterification consists of three reversible reaction steps. Figure 2.2 shows a detailed elementary reaction scheme of TG reacting with alcohol to produce diglyceride (DG), DG then reacting with another alcohol molecule to produce monoglyceride (MG), and the reaction of the MG with a third alcohol molecule to produce glycerol (Freedman et al., 1986).

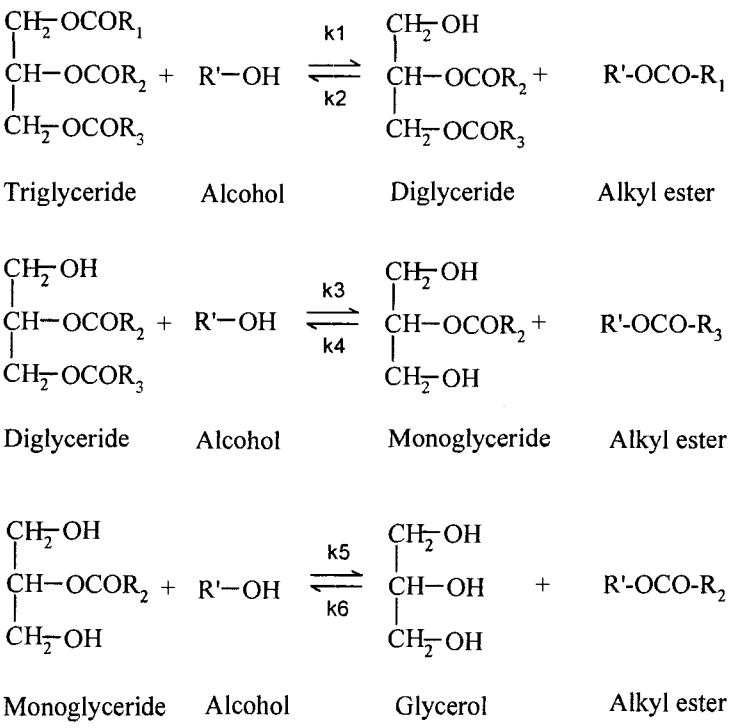


Figure 2.2: Elementary reaction scheme for transesterification of TG

Each of the reactions in Figure 2.2 is reversible with a different rate constant ($k_n$) denoting that the forward and reverse reactions take place at different rates. The reactions are all known to be second order or pseudo-second order (Freedman et al., 1986). The last step, the formation of glycerol from MG, is known to proceed more rapidly than the formation of MG from DG (Komers et al., 2001).

Despite the simple kinetic scheme shown in Figure 2.2, the reaction does not behave ideally. Due in part to the immiscibility of the oil and methanol phases, an initial lag time is usually attributed to limitations in the transfer of the methanol into the oil phase (Freedman et al., 1986; Noureddini and Zhu, 1997). One approach to overcoming this miscibility issue is to create a homogeneous reaction mixture using for example, THF as a co-solvent (Boocock et al., 1998). Another approach employs supercritical methanol (Saka and Kusdiana, 2001). While these approaches yield the desired results, they do involve additional costs for either downstream separation (e.g., removal of THF) or energy-related costs. Moreover, single-phase homogeneous solutions for biodiesel production will solubilize any unreactable or unsaponifiable matter in the feedstock into

the FAAE product. This will occur not only when converting low quality lipids, but even for virgin oil which can contain detectable amounts of unsaponifiable material (Van Gerpen et. al., 2004). The following question can be posed: "Can we take advantage of the heterogeneity of the system without adding solvent or trying to increase the interfacial area by intensifying the dispersion of oil into alcohol and to consequently enhance the interphase mass transfer and the chemical reaction?"

The transesterification process is reversible which implies that the reaction may not reach 100% completion under certain conditions. In fact, in most cases it will reach equilibrium and there will be some unreacted TG, DG and/or MG left in the reaction mixture. Recall that one standard for biodiesel quality concerns keeping the TG, DG, and MG to low levels. If one cannot prevent the attainment of equilibrium, is there a means of perhaps keeping the TG, DG and MG separate from the biodiesel product given the immiscibility of the methanol and oil?

As mentioned, the molar ratio of alcohol to oil plays a role in affecting the transesterification rate. This role would also extend to affecting the reaction equilibrium. In general, reactions can be encouraged to progress by adding an excess of one of the reactants or by removing one of the products. Current commercial practice is to add excess methanol to ensure that the reaction approaches completion. The most common commercial methanol/oil molar ratio is 6 to 1, rather than the stoichiometric molar ratio of 3 to 1. Increases in the molar ratio of methanol to oil could cause an increase in ester yield as well as a drop in the time required to achieve reaction equilibrium, which leads to a decrease in reactor residence time and an increase in reactor capacity (Michael and Gumpon, 2006). Of course, this comes at a significantly increased process operating cost.

The presence of FFA and water can cause serious difficulties for the transesterification. FFA in the lipid feedstock cannot be converted to biodiesel using an alkaline catalyst and will rather be converted to soap. High FFA contents also affect acid-catalyzed processes (see Figure 2.3). In this case, the reaction of FFA with methanol produces water which inhibits the esterification of the FFA and the transesterification of the glycerides (Romano, 1982; Freedman et al., 1984; Canakci and Van Gerpen, 1999).

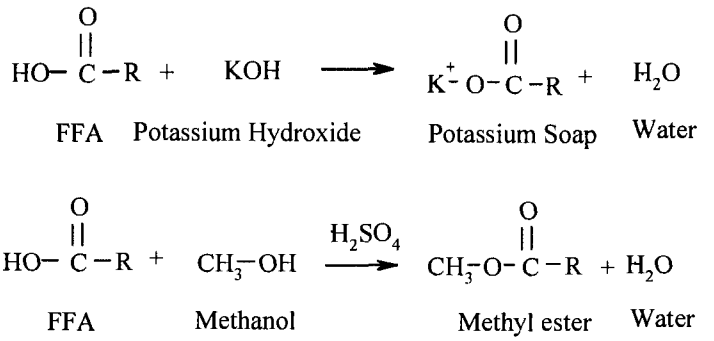


Figure 2.3: FFA effects in the transesterification

Because water catalyzes the hydrolysis of FA esters, all the substrates should be nearly anhydrous, the upper limit is about 0.1~0.3% water (Ma et al., 1999). For base–catalyzed process, water is the main cause for side reactions besides the alcoholysis – hydrolysis (saponification) of the transesterified oil and/or alkyl esters produced. The soap consumes the catalyst and reduces the catalytic efficiency, as well as causing an increase in viscosity. It is also responsible for the reduction in the concentration of the alcoholysis catalyst, and poses significant impediments to separating the FAME product from the polar methanol/glycerol phase (Fukuda et al., 2001). When water is present, particularly at high temperatures, it can hydrolyze the TG to DG and form FFA. Due to the unavoidable presence of FFA and water in low-grade lipid feedstock, the ideal reaction system should provide a way of either removing FFA or water (by separation or reaction) or to be capable of contending with the presence of a soap emulsion.

## 2.3 Properties of Feedstocks and By-product

### 2.3.1 Lipid reactants

Teall (2004) claimed that the biggest long-term production challenge facing biodiesel is finding viable feedstocks. Haas et al. (2004) reported that feedstock cost contributes more than 70% to the cost when it is produced from refined edible oils. Most commercial biodiesel is derived from vegetable oils. Vegetable oils are essentially mixtures of TG from various fatty acids; for example, canola oil contains 6 main major fatty acids (Gunstone et al., 1994), (see Table 2.1). The composition of vegetable oils varies with the plant source.

Table 2.1: Major fatty acids in canola oil.

| Fatty acid name | Structure | Composition (wt.%) |
|---|---|---|
| **Myristic:** 14 carbons, 0 double bonds (14:0) | R = - $(CH_2)_{12} - CH_3$ | <1 |
| **Palmitic:**16 carbons, 0 double bonds (16:0) | R = - $(CH_2)_{14} - CH_3$ | 1.5-6 |
| **Stearic:** 18 carbons, 0 double bonds (18:0) | R = - $(CH_2)_{16} - CH_3$ | 1-2.5 |
| **Oleic:** 18 carbons, 1 double bond (18:1) | R = - $(CH_2)_7$ CH=CH$(CH_2)_7CH_3$ | 52-66.9 |
| **Linoleic:** 18 carbons, 2 double bonds (18:2) | R = - $(CH_2)_7$ CH=CH-$CH_2$-CH=CH$(CH_2)_4CH_3$ | 16.1-31 |
| **Linolenic:** 18 carbons, 3 double bonds (18:3) | R = - $(CH_2)_7$ CH=CH-$CH_2$-CH=CH-$CH_2$-CH=CH-$CH_2$-$CH_3$ | 6.4-14.1 |

*Note: The oil from different manufacturers may contain small amounts of other fatty acids not listed here.*

The selection of the type of oil affects the production technology and product components (Kramer, 1995). Several kinds of vegetable oils have been used as feedstock for biodiesel production; it is well-known that the esterified oil has better fuel properties (Ma et al., 1999). The most commonly used oils for the production of biodiesel are soybean (Freedman et al., 1986; Noureddini and Zhu, 1997), sunflower (Antolín et al., 2002), palm (Darnoko and Cheryan, 2000a), rapeseed (Kusdiana and Saka, 2001), canola (Zhou et al., 2003), and cotton seed oils (Köse et al., 2002). Mustard oil is inedible but could be an attractive feedstock due to its cost effective production. In addition, biodiesel made from mustard oil has demonstrated good cold flow properties and high cetane ratings (Tyson et al., 2002). A broad variety of non-edible or industrial grade vegetable oils can also be used. Canola oil has the least amount of saturated fat of any vegetable oil, less than 7 percent; it is feedstock that results in a biodiesel that has excellent cold-flow properties (Coleman, 2006).

Benefits sought by the biodiesel industry are improved oxidative stability and improved cold flow properties. These can usually be achieved by modifying the composition of the vegetable oil. Polyunsaturated fatty acids (PUFA) improve cold flow properties but are most susceptible to oxidation. Biodiesel with low polyunsaturated fat levels, especially lower $C_{18:3}$ fatty acids, should also emit lower levels of nitrogen oxides (McCormick et al., 2001). Thus, one has to identify an optimal level of PUFA and target composition which is suitable for use as a feedstock to produce biodiesel with improved cold flow, improved ignition quality (CN), improved oxidative stability, and presumably reduced nitrogen oxide emissions.

The high cost of virgin oils, especially food-grade vegetable oils, limits their use in biodiesel production. Reducing the cost of the feedstock is necessary for biodiesel's long-term commercial viability. One way to reduce the cost of this fuel is to use less expensive feedstock like waste restaurant oils and rendered animal fats. FFA values increase as oil is used in a fryer. Used cooking oils typically contain 2-7% FFA, and animal fats contain from 5% to 30% FFA (Van Gerpen, 2005). As mentioned earlier, the FFA cannot be converted to biodiesel using an alkaline catalyst due to the formation of soap. Nonetheless, more robust chemical processes for producing biodiesel from high FFA feedstock do exist (Canakci and Van Gerpen, 2001). One approach is to utilize acid catalysts that do not form soaps (Aksoy et al., 1988; Liu, 1994). Although earlier work claimed that acid catalysts were too slow to be practical for converting TG to biodiesel (Canakci and Van Gerpen, 1999), Zhang et al. (2003) showed that an acid-catalyzed approach could indeed be economical.

A high FFA content is not the only drawback for using waste oils; waste oils are often hydrogenated and have a higher pour point, which may present some problems related to biodiesel flow at cold temperatures. Even though the waste oils are filtered using conventional means prior to use as a feedstock, there may remain some inert components which could have a deleterious effect on cold flow properties. A membrane reactor, which is in and of itself a filtration process, could potentially filter out these inert components.

### 2.3.2 Alcohol reactants

Commonly used short chain alcohols are methanol, ethanol, propanol and butanol. The transesterification yield is independent of the type of alcohol used. Therefore, the eventual selection of one of these alcohols will be based on cost and performance considerations. A key quality factor for the primary alcohol used for biodiesel production is the water content. It has been argued that water content is a more critical variable in the transesterification process than the presence of FFA (Ma et al., 1998, 1999). Unfortunately, all the lower alcohols are hygroscopic and are capable of absorbing water from the air.

The use of even longer-chain alcohols, either straight- or branched chains, in biodiesel production was described and it was determined that the FA esters of these alcohols offer the advantage of exhibiting lower freezing points than methyl ester biodiesel (Lee et al., 1995); this better cold flow characteristic is important for cold areas such as Canada. Viscosity increases with chain length (number of carbon atoms) and with increasing degree of saturation, so the viscosity of ethyl esters is slightly higher than that of methyl esters (Foglia et al., 1997). The higher prices of longer-chain alcohols currently prohibit their commercial application in biodiesel production. Table 2.2 lists the available prices of different alcohols based on a 210 L drum from Commercial Alcohols Inc. (Brampton, ON, Canada) in 2005. Thus, methanol and ethanol are preferred for biodiesel production.

Table 2.2: Price of alcohols

| **Alcohols** | **Price ($CAD/L)** |
|---|---|
| Methanol (anhydrous) | 0.95 |
| Denatured ethyl alcohol (anhydrous) | 1.54 |
| Ethanol (95%) | 1.76 |
| Ethanol (99.85%) | 1.86 |
| Isopropyl Alcohol (99%) | 2.30 |
| Isopropyl Alcohol (70%) | 2.00 |

Methanol is most often used commercially to produce biodiesel, since it is widely available, is inexpensive, and gives a reliable chemical reaction. Ethanol itself can be used today as an alternative fuel, a fuel extender, an oxygenate and an octane enhancer. Vegetable oil transesterification by ethanol has been reported in a number of studies (Clark et al., 1984; Peterson et al., 1991, 1995), though industrial-scale production of fatty acid ethyl ester (FAEE) has not been introduced so far. Ethanol is a promising option for alcohol used in biodiesel production.

Bio-ethanol (also called fermented ethanol, grain alcohol) is renewable and safer in terms of accidental or occupational exposure, but is more difficult and expensive to work with. Since fermentation uses water, bio-ethanol will require drying (Shuler and Kargi, 2002). Anhydrous ethanol is the best choice, but it may also be derived from fossil fuels and in that case, not pose such problems. Since chemical grade ethanol is typically denatured with poisonous material to prevent its abuse, ethanol that has been denatured with methanol is a good solution for the biodiesel production.

### 2.3.3 Catalysts

Most industrial processes for making biodiesel use a catalyst to initiate the transesterification reaction. The catalyst is required because the alcohol is sparingly soluble in the oil phase. The catalyst promotes an increase in solubility to allow the reaction to proceed at a reasonable rate.

Base catalysts are the most common, since the process is faster and the reaction conditions are moderated (Freedman et al., 1984). After the reaction, the base catalyst must be neutralized with a strong mineral acid. However, soap will form by two kinds of undesirable side-reactions: neutralising the FFA in the oil and TG saponification. Soap partially consumes the catalyst, decreases biodiesel yield and complicates the separation and purification steps.

With all of its drawbacks, sodium hydroxide (or rather, sodium methoxide) for ester conversion is by far the most commonly used base catalyst in industry today; the main reason is due to its effectiveness and cost. Efficient production of methyl ester usually requires 0.5 wt.% sodium hydroxide or more as the catalyst (Chandra, 1998). Potassium hydroxide can also be employed; the advantage of this catalyst is that the by-product

stream may have economic value as a soil fertilizer, due to its potassium content. However, its high cost is a disadvantage (Markolwitz, 2004). Potassium hydroxide is reportedly used more than sodium hydroxide in Europe, but not in North America.

When the base catalyst is mixed with alcohol, it forms an alkoxide group which is the true catalyst for the transesterification (Sridharan and Mathai, 1974; Ma et al, 1998). The mechanism of alkali-catalyst preparation is:

$$OH^- + R'OH \Leftrightarrow R'O^- + H_2O \qquad (2\text{-}1)$$

Here $R'$ is short alkali group and $R'O^-$ is the actual catalyst. Certainly, one can use catalysts in the methoxide (or ethoxide) form, which can be produced by the dissolution of metallic sodium in alcohol, directly for the transesterification. Vicente et al. (2005) concluded that near 100 wt.% biodiesel yields were only obtained with methoxide catalysts. These may be, however, prohibitively expensive and difficult to handle.

Acid-catalyzed systems are characterized by their slow reaction rates and high alcohol to oil ratio requirements (e.g., 20:1 and more). Often, acid-catalyzed reactions are used to convert FFAs to esters, or soaps to esters as a pre-treatment step for high FFA feedstocks. Residence times from 10 min to about 2 h are reported. The acid-catalyzed transesterification is much slower than the base-catalyzed reaction and also needs more extreme temperature and pressure conditions (Freedman et al., 1984; Schwab et al., 1987). For high FFA content oils such as waste frying oil, it is best to avoid soap formation. In addition, the acid catalyzes the FFA esterification to produce FAME, increasing the biodiesel yield. Among the many available acid catalysts, sulphuric acid has been shown to be the most effective in producing high yields of FAME (Dubé et al., 2004; Lotero et al., 2005). Although earlier work claimed that the acid–catalyzed process was too slow to be practical for converting TG to biodiesel (Canakci and Van Gerpen, 1999), Zhang et al. (2003) showed that an acid-catalyzed approach could indeed be economical. However, no large scale industrial synthesis had been report in commercial production (Knothe, 2005).

Other than the homogeneous catalysts listed above, recent research on the alcoholysis of oil has focused on the use of heterogeneous catalysts such as titanium-silicates, ion exchange resins, etc. This is because the advantage of homogeneous

catalysis at low temperatures is counteracted by the additional separation procedures the FAME products and by-products (i.e., glycerol) require. Residual catalyst must be removed and catalyst loss is inherent, raising the overall cost of production. In contrast, processes using heterogeneous catalysts usually require higher temperatures to be as effective. On the other hand, products do not necessitate complex separation procedures and, in most cases, catalysts can be recycled and reused for long periods of time. Lotero et al. (2006) grouped solid catalysts in three general categories: metal, base, and acid catalysts. Metal catalysts include metals, metal compounds and supported metal complexes. For example, zinc oxide supported on aluminium was employed as catalyst (Stern et al., 1999). Zeolites and metal catalysts have also been used for the transesterification of soybean oil (Suppes et al., 2004). Solid acid catalysts have the advantage of being easily removed by filtration and used for large scale production (Otera, 2003).

For the membrane reactor, an increase in acid catalyst concentration was found to increase the conversion of TG to FAME (Liu, 2004). $H_2SO_4$ concentrations between 0.5 and 2 wt.% increased conversion substantially but higher concentrations (e.g., 4 and 6 wt.%) did not have the same impact (<10% conversion increase). Thus, concentrations of acid beyond 2 wt.% are not necessary at 70°C. In addition, the reaction was more sensitive to temperature at high acid concentrations.

### 2.3.4 Glycerol

Glycerol (also called glycerine) is the major by-product of biodiesel production. It is chemically stable under normal storage and handling conditions. Glycerol is completely soluble in water and alcohol, slightly soluble in diethyl ester, ethyl acetate, and dioxane, and insoluble in hydrocarbons. It has no self-reactivity, nor spontaneous combustibility properties, its melting point is 18.17°C and its boiling point is 290°C at 101.3 KPa. Its specific gravity is 1.2620 which makes glycerol the only component in biodiesel production with a density higher than water. Its viscosity is 1499 mPa.s at 20°C.

Biodiesel containing excess free glycerol may result in the settling out of the glycerol during storage and create a very viscous mixture that can plug fuel filters and interfere with combustion. Glycerol is essentially insoluble in biodiesel so that almost all

glycerol is, theoretically, easily removed by settling or centrifugation. In practice, glycerol may remain in the biodiesel either as suspended droplets or in the very small amounts that do dissolve. The alcohol can act as a co-solvent to increase the solubility of glycerol in the biodiesel (Knothe, 2005).

The upward limit for free glycerol in biodiesel is 0.02 wt.% according to the ASTM standard, which means most glycerol should be removed from the biodiesel product during the purification process. Water-washing is the most popular and effective method to guarantee glycerol contents under the accepted levels, especially if hot water and multi-step washing are used. Another option for purification is distillation; the drawbacks are energy consumption and glycerol carry-over during distillation.

Of secondary importance in the biodiesel production process is the ability to sell the glycerol by-product for other applications. Unfortunately, in most conventional biodiesel production processes, the raw glycerol by-product is of relatively poor quality. The expected contaminants of the raw glycerol are the methanol and unused catalyst. Lower catalyst concentrations would yield a lower salt content in both the biodiesel and glycerol products.

## 2.4 Biodiesel

### 2.4.1 Standards for biodiesel usage

The primary criterion for biodiesel quality is adherence to appropriate standards. Only when the specifications are met, can the biodiesel be used in most diesel engines without modification while maintaining the engine's durability and reliability. To limit the amount of contaminants in biodiesel fuel, standards such as EN14214 (EN14213 when using biodiesel for heating oil purposes) in Europe and ASTM D6571 in the U.S. have become the prerequisite for market acceptance of biodiesel.

The Canadian General Standards Board (CGSB) requires that the pure biodiesel (B100) component in biodiesel blends must comply with ASTM D6571 or EN14214. The European specification EN14214 is very similar to the ASTM D6571, and is in fact slightly more stringent in a few areas. Therefore, ASTM D6571 is the minimum acceptable specification for B100 blend stock, which gives a stringent requirement about the properties of, for example, the fuel's flashpoint, ash level, and total and free glycerol.

Table 2.3 lists the details of the ASTM D6752 biodiesel standard which requires a free glycerine content of less than 0.020 wt.% and a total glycerine content of less than 0.240 wt.% based on ASTM method D6584.

Table 2.3: ASTM D 6751- Biodiesel component (B100) specifications

| **Property** | **ASTM Method** | **Limits** | **Units** |
|---|---|---|---|
| Flash Point | D93 | 130 min | °C |
| Water & Sediment | D2709 | 0.050 max | % vol |
| Kinematic Viscosity, 40°C | D445 | 1.0-6.0 | $mm^2/s$ |
| Sulfated Ash | D874 | 0.020 max | % mass |
| Sulfur | D5453 | 0.05 max | % mass |
| Copper Strip Corrosion | D130 | No. 3 max | |
| Cetane Index | D613 | 47 min | |
| Cloud Point | D2500 | Report | °C |
| Carbon Residue 100% sample | D4530* | 0.050 max | % mass |
| Acid number | D664 | 0.80 max | mg KOH/gm |
| Free Glycerine | D6584 | 0.020 max | % mass |
| Total Glycerine | D6584 | 0.240 max | % mass |
| Phosphorus Content | D4951 | 0.001 max | % mass |
| Distillation Temp. Atmospheric Equivalent Temp., 90% recovered | D1160 | 360 max | °C |

Because of the wide range of feedstock types and quality, achieving a consistently high purity biodiesel product is difficult. The production standards (ASTM D6751 and EN 14214) provide stringent requirements for:

- Free and total glycerine, thus limiting the presence of glycerine and acylglycerol (i.e., TG, diglyceride (DG), and monoglyceride (MG));
- Flash point, thus limiting the amount of residual alcohol;
- Acid value, thus limiting the presence of FFA; and
- Ash level, thus limiting the amount of residual catalyst.

Current commercial biodiesel production technologies face the challenge to achieve these standards while remaining profitable and environmentally friendly.

### 2.4.2 Biodiesel vs. petroleum diesel fuel

Petroleum diesel fuel is a "middle distillate" product of petroleum cracking. The conventional diesel fuel comprise of alkanes from n-C10 to n-C22 (Lane, 1980; Chandra, 1998). Similar to petroleum diesel fuel, biodiesel is also a mixture of organic compounds . Figure 2.4 shows the molecules of cetane and ethyl ester (biodiesel). Compared to cetane, alkyl esters are somewhat longer, and more importantly, contain two oxygen atoms. Since combustion is an oxidation reaction, the heating value of cetane, which contains no oxygen atoms, is higher than that of biodiesel. For this reason, biodiesel has slightly lower energy content than conventional diesel, e.g., soy biodiesel has a heating value of 37.2 MJ/Kg, while No.2 diesel fuel has about 42.6 MJ/kg (Freedman and Bagby, 1989; Knothe et al., 2005).

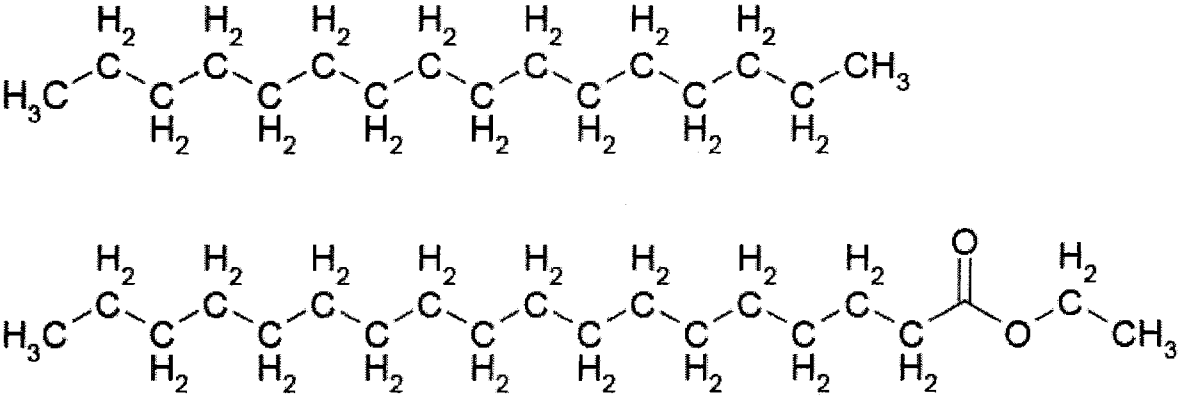

Figure 2.4: Molecules of cetane and ethyl ester

To conform to standard specifications (ASTM D6751 or EN-14214), there are standard GC methods in use today for analysis of the biodiesel products, one of which is EN-14103 used to determine the ester and linoleic acid methyl ester content. Other methods include EN-14105 / ASTM D 6584 (free and total glycerine and mono-, di- and triglyceride content) and EN-14110 (residual methanol). Figure 2.5 shows a gas chromatogram for biodiesel (B-100) conducted on the Varian CP-3800 GC in accordance

with EN-14103 (Duvekot, 2007). Compared to Figure 2.4 of petroleum diesel, biodiesel is chemically simpler since no more than ten fatty acid esters make up the biodiesel mixture which has similar properties to diesel.

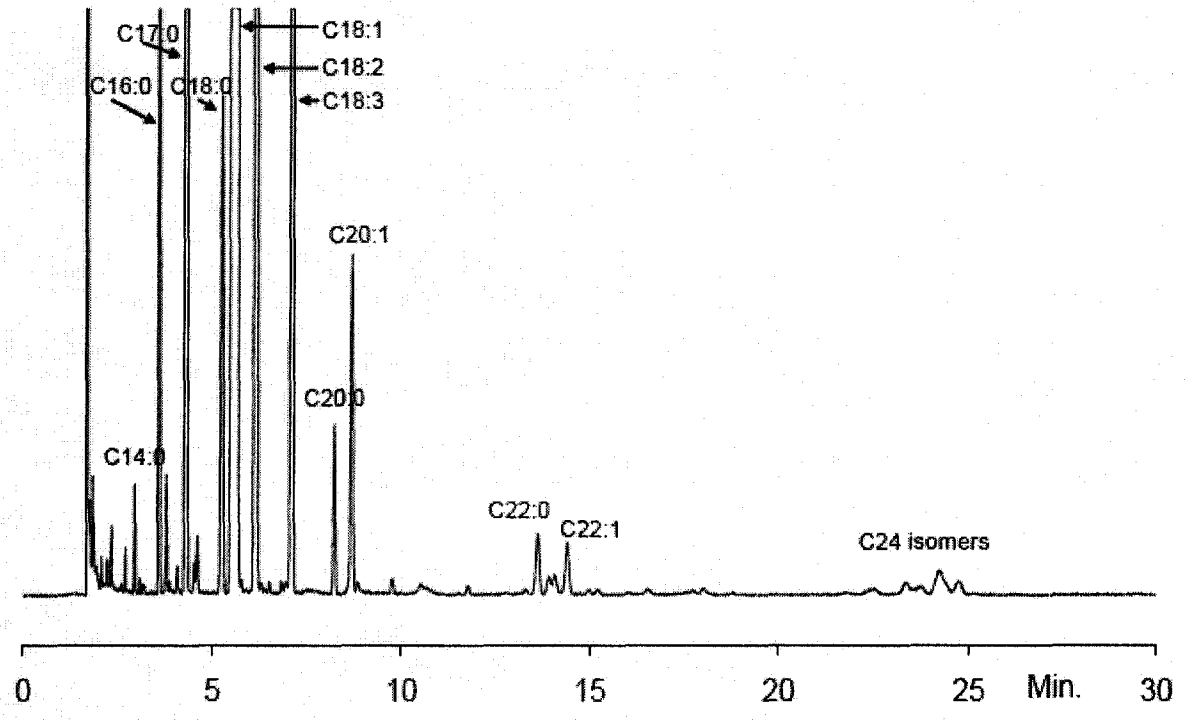


Figure 2.5: Biodiesel chromatogram (copy permission from Varian Inc.).

Unlike the fact that petroleum diesel is derived from limited fossil fuel resources, biodiesel is made from natural, renewable sources such as new and used vegetable oils and animal fats. Due to its biodegradable nature, biodiesel also dramatically reduces other emissions, and essentially no sulphur (a critical starting point for acid rain) and aromatic content, offers promise to reduce particulate and toxic emissions (Wang et al., 2000). In addition, biodiesel's biodegradability is about four times faster than conventional diesel (Peterson et al., 1996). Therefore, biodiesel can be an attractive fuel for use in environmentally sensitive aquatic areas, urban buses, underground mines, and national parks.

In the usage of biodiesel, just like conventional petroleum diesel, biodiesel operates in compression-ignition engines. Due to its miscibility with conventional diesel in all

ratios, biodiesel blends with diesel fuel show a near linear relationship for most of the fuel properties. Blends of up to 20% biodiesel (mixed with petroleum diesel fuels, called B20, 20% volume biodiesel: 80% volume diesel) can be used in nearly all diesel equipment and are compatible with most storage and distribution equipment. These low-level blends (20% and less) generally do not require any engine modifications. Table 2.4 lists the main properties of petroleum diesel and biodiesel.

Table 2.4: Comparison of typical properties of diesel, canola oil and biodiesel

| **Main items** | **Diesel** | **Canola** | **Biodiesel** |
|---|---|---|---|
| Density (kg/L) | 0.835 | 0.922 | 0.88 |
| Gross calorific value (MJ/L) | 38.3 | 36.9 | 33.3 |
| Viscosity ( $mm^2/s$ @ 37.8°C) | 3.86 | 37 | 4.7 |
| C:H ( ratio ) | 3.59 | 3.26 | 2.38 |
| Sulphur (%) | 0.15 | 0.0012 | <0.01 |

*Source: Adapted from Table 6.1 of BTCE (1994), www.afdc.doe.gov . The C:H ratio for biodiesel is taken from http://www.biodiesel.org/fleets/summary.shtml#attributes*

### 2.4.3 Issues confronting biodiesel

The earliest reported biodiesel product appeared in August 31, 1937 in a Belgian patent. The author, G. Chavanne (University of Brussels, Belgium) described the use of ethyl esters of palm oil as diesel fuel. After several decades of silence, the use of methyl esters of sunflower oil to reduce the viscosity of vegetable oil was reported at several technical conferences in 1980 and 1981 and this marked the beginning of the rediscovery and eventual commercialization of biodiesel (Schwab, 1987). From then on, the use of the word "biodiesel" in the literature expanded exponentially.

Biodiesel production costs are high due to the high cost of lipid feedstocks used in the process. Even when using the least expensive refined oil as feedstock, the lipids constitute between 70 to 85% of the overall production costs. Without government subsidies, biodiesel has a difficult time competing economically with petroleum diesel fuel. Production-oriented approaches to improving the economics of biodiesel have included the investigation of low cost lipids as feedstocks. The composition of these

alternate feedstocks, however, can require modification of existing technologies for their conversion into acceptable biodiesel fuels.

Other than the economic issue, conventional biodiesel production technology faces several challenges to achieve these standards while remaining profitable and environmentally friendly. Most commercial processes employ a base-catalyzed process which is unsatisfactory for the use of lower cost high FFA feedstock due to the formation of soaps. Although much is known about the biodiesel transesterification process, additional research is required to develop methods to overcome the reaction equilibrium limitations. The transesterification is reversible, which means 100% conversion of oil to biodiesel is impossible. In addition, the transesterification reaction system is essentially heterogeneous; oil conversion is often limited by the miscibility of the oil and alcohol phases.

In the biodiesel production process, downstream purification such as water washing to remove excess alcohol and catalyst may generate large amounts of toxic waste water, a desire to reduce the waste streams of spent catalyst and other by-products resulting from the traditional base-catalyzed transesterification reaction has stimulated research on alternative technological solutions.

## 2.5 Membrane Reactor

Membrane reactor technology had been successfully applied to many chemical reaction processes. The biodiesel production process employs transesterification which is a classical reversible chemical reaction and can be combined with membrane reactor technology. A membrane reactor is a device for simultaneously carrying out a reaction and membrane-based separation in the same physical enclosure. Membrane reactors are roughly categorized into two types: packed-bed membrane reactors and catalytic membrane reactors. Membrane reactors with packed-bed catalysts have separation zones separated from the reaction zone. On the other hand, in catalytic membrane reactors, reaction and separation occurs simultaneously (Hsieh, 1996).

In order to increase reaction rate, biodiesel production should be performed at higher pressures and temperatures. Compared to polymeric membranes, inorganic membranes have good high temperature and solvent stability. Membranes can play

different roles in a chemical reactor system: from selectively removing the main reaction product in order to increase the yield of equilibrium limited reactions, to enabling short contact times and hence increased selectivity in fast consecutive reactions. Separative membrane reactors can be used to selectively remove either products or by-products from the reaction zone. This can help overcome low conversions in equilibrium-limited reactions. Moreover, membrane-based separative reactors can also be used to selectively permeate reactant into the reaction zone in order to control excessive by-product formation. Beyond the separation functions, membranes can also be used to diffuse one reactant to another reactant (Lambrich and Schubert, 2005). All these characteristics of separative membrane reactors can be suitably applied to biodiesel production via transesterification of lipid feedstock.

### 2.5.1 Membrane materials & modules for biodiesel production

2.5.1.1 Membrane material

Inorganic membranes for membrane reactors can be inert or catalytically active; they can be either dense or porous, made from metals, carbon, glass or ceramics. They can be uniform in composition or composite, with a homogeneous or asymmetric porous structure. Membranes can be supported on porous glass, sintered metal, granular carbon or ceramics such as alumina. Different membrane shapes can be used: flat discs, tubes (dead-end or not), hollow fibers, or monolithic multi-channel elements for ceramic membranes (Hsieh, 1996), but also foils, spirals or helixes for metallic membranes (Sanchez and Tsotsis, 1996). The shape of the separative element induces a specific surface/volume ratio for the reactor, which often needs to be maximized for industrial applications.

The corrosive and thermal reaction conditions of transesterification make the use of inorganic membranes more suitable due to their mechanical and thermal stability. Most of the upper temperature limits for inorganic membranes can reach several hundreds of degrees Celsius, even the less stable carbon membranes can operate to as high as 165°C, which is more than enough for biodiesel production. In practice, the maximum operating temperature is dictated by the temperature limits for sealing the membrane, gaskets or other accessory materials that are required to provide leak-free

operation. Inorganic membranes are also much more resistant to chemical attack. In the highly basic (or acidic) conditions for typical biodiesel production, organic membranes would be quickly destroyed.

Selection of the inorganic membrane material of construction and pore size are key important to its operation for specific applications. The top micro-porous layer of the membrane must be defect-free (no cracks or pinholes) and have a preferably narrow pore size distribution to meet quality control needs. The selection of an optimal (or at least sub-optimal) membrane from the available commercial membrane manufacturers was one important aspect of this project. An ideal membrane should provide precise control of pore size with a high permeance and a low pressure drop. This is accomplished by carefully selecting the number of layers, the pore size of the layers, and the materials of construction to produce a product that will accomplish the desired separation. Porous inorganic membranes are currently made from glass, alumina, zirconia, titania, silver and stainless steel, etc. A variety of membrane materials have been investigated and an overview of commercially available systems has been given by Hsieh (1991). Alumina, zirconia and, more recently, titania membranes are used in many large scale applications. Carbosep membranes (Novasep Co., France) are made of a zirconia layer attached to a porous carbon supporting tube assembled into modules. Kerasep membranes produced by the same company attach the alumina or titania to a monolithic alumia-titania support. In general, many commercial products provide a separation layer of thickness in the 10-20 μm range, with a bulk support and intermediate layer thickness ranging from 1 to 2 mm.

Carbon is a material that is well known for its corrosion resistance. Carbon membranes are typically a composite structure of a very thin layer of porous carbon (10 μm thick) applied to the internal surface of a narrow diameter carbon and carbon-fibre support tube. Carbon membranes are made by mixing graphite with an organic binder and sintering the mixture at high temperature (i.e., several hundred degrees Celsius). At these temperatures, the organic binder is partially carbonized and holds the resulting graphite structure together.

Ceramic membranes are more popular in practical industrial applications. Siskens (1996) described many advantages of ceramic membranes: chemical and thermal stability, narrow pore size distribution, high porosity, high flux, mechanical strength, long lifetime,

etc. Aside from withstanding the reaction conditions, chemical and thermal stability also permits the ceramic membrane to be cleaned more efficiently when dirty feedstock such as waste oil is used. With ongoing membrane material research and development, the disadvantages of higher price and brittleness are being overcome.

2.5.1.2 Membrane element and module

The membrane element is the basic unit for the application. The element shape may be a sheet, single tube, hollow fiber, or multi-channel monolith. Details of these configurations are available in many references (Zeman and Zydney, 1996; Cheryan, 1986). Obviously a monolithic multi-channel shape provides more filtration area per unit volume than a sheet and single tube. For laboratory applications, a single tube is the best option due to its convenience for modeling. The carbon membrane element mentioned above is in the tube style. The relatively large tube diameters permit large cross flow velocities, which generally result in turbulent flow, and thus give reasonable permeate and retentate fluxes.

A membrane module is made up of membrane elements put into a housing or casing. A membrane module is actually a manifold assembly containing a membrane or membranes to separate the streams of feed, permeate, and retentate. In a lab setup, a membrane module may be a stand-alone loop, which may be operated in batch or continuous mode. Often a few membrane modules are combined in parallel or in series, to become a continuous loop or stage for industrial applications.

Resembling shell and tube heat exchangers, the basic concept of the tubular membrane module for biodiesel production is a straight membrane element tube put into a tubular housing which is made of stainless steel to withstand the chemically aggressive transesterification conditions. This tubular design for biodiesel production facilitates the aggressive operating conditions of the transesterification process as well as potential antifouling cleaning. As mentioned before, the gasket for the seal is crucial for the membrane module's successful operation. In the meantime, membranes can be bundled to increase the surface area for larger scale applications.

The main characteristics of the membrane used in our lab scale membrane reactor are shown in Table 2.5. It was shown that this carbon membrane was able to resist the

high acid and base environments for biodiesel production (Dubé et al., 2007). Another type of ceramic membrane used for this study had a different configuration, which was a multi-lumen membrane with a complex support structure.

Table 2.5: Characteristics of carbon membrane

| Configuration | Single channel tubular |
|---|---|
| inside diameter (mm) | 6 |
| outside diameter (mm) | 8 |
| length (mm) | 1200 |
| membrane area ($m^2$) | 0.022 |
| maximum operating temperature | 165 |
| pore size (μm) | 0.05, 0.2, 0.5, and 1.4 |

A monolithic multi-channel honeycomb shape provides more filtration area per unit volume than a sheet and single tube. The microporous ceramic membranes used in this study were produced by TAMI, Nyons, France. One membrane among those listed was coated (by the manufacturer) with a thin layer of inorganic oxides ($TiO_2$ or $\gamma$-$Al_2O_3$) on the surface channels. The support structure was shaped into a multi-channel tubular style which provided a larger membrane surface. Scanning electron micrographs suggest that the membrane consists of a percolation system with a spongy structure (Mullet et al., 1999). Physical details of one kind of membrane used in the prototype membrane reactor circulating loop are shown in Table 2.6.

### 2.5.2 Reactor system

Liu (2004) found that a micro-porous inorganic membrane reactor can selectively permeate FAME, methanol and glycerol during the transesterification from the reaction zone. Due to its immiscibility in methanol, the vegetable oil molecules are trapped in oil droplets forming an emulsion. At proper temperature and pressure conditions, the droplets cannot pass through the pores of the membrane. GPC analysis revealed that vegetable (canola) oil did not appear in the permeate side. The experiment was carried out in a semi-continuous membrane reactor. A certain amount of virgin canola oil

(normally less than one third of the reactor volume) was charged into the reactor initially, and then methanol with catalyst was fed continuously into the reactor. The permeate was a homogeneous mixture of FAME, methanol, glycerol and catalyst without oil, which permeated through the membrane via a backpressure valve and was collected in a tank.

Table 2.6: Characteristics of a ceramic membrane

| | |
|---|---|
| Commercial name | Daisy, TAMI |
| Configuration | 8 channels tubular |
| inside diameter (mm) | 6 |
| outside diameter (mm) | 25 |
| length (mm) | 1178 |
| membrane area ($m^2$) | 0.2 |
| Ceramic support material: | titanium oxide |
| Active layer material: | titanium oxide |
| Max. operating temperature ($^0C$) | up to 150 |
| Operating pH range | 0 to 14 |
| Bursting pressure (bars) | > 90 |
| MWCO (kDaltons) | 300 kD |

The operation of the membrane reactor is based on the immiscibility of the lipid feedstock in alcohol and the miscibility of the FAAE in alcohol. Transesterification is believed to occur at the surface of the oil droplets suspended in alcohol (Ataya et al., 2006). The products of transesterification, namely FAAE (or biodiesel) and glycerol, as well as the catalyst (either base or acid) are soluble in the alcohol. The FAAE forms a layer around the lipid oil droplet surface. As the FAAE layer grows, the FAAE diffuses

into the alcohol phase and passes through the membrane along with the glycerol and catalyst due to its solubility in the alcohol. The oil and alcohol are immiscible at the reaction temperature (e.g., 65°C). The droplets of oil cannot pass through the pores of the membrane due to their large size of several hundred microns (Collins and Knudsen, 1970), whereas the membrane pore size is below 1.4 micron (the biggest membrane pore size used in our laboratories).

As mentioned, the transesterification requires the reaction of the oil and alcohol, which creates a heterogeneous emulsion. As the liquid emulsion flows along the surface of the membrane, the components with a droplet size smaller than the membrane pore size pass through the membrane leaving behind larger components. The pressure driven membrane process for the flux of liquids through the membrane is governed by a size exclusion mechanism (Hsieh, 1991). So, one can say that the separation efficiency of inorganic membranes depends on, to a large extent, the microstructural features of the membrane/support composites such as pore size and its distribution, pore shape, porosity and tortuosity.

One could describe the membrane reactor for biodiesel production as an emulsion reactor. The membrane reactor used in this study combines two distinctly different functions, i.e., reaction and separation into a single operation. The combination of these two functions in the same unit creates a synergy: the retention of unreacted oil in the reactor results in a product of high purity such as cannot be achieved without extensive and costly downstream separations by other technologies and the removal of the products enhances the yield of the reaction by shifting the conversion to the right of the equilibrium.

## 2.6 Summary

From our search of the literature, we have found no reports on the production of biodiesel using a membrane reactor other than the work performed in our laboratories. The emulsion membrane reactor is a new concept in the biodiesel field.

Transesterification is a three-step reversible chemical reaction, which is also a heterogeneous reaction system due to the immiscibility of the oil and the alcohol phases. A membrane reactor can take advantage of this, and by allowing the biodiesel product to

selectively pass through the membrane, the reaction equilibrium can be shifted to the right giving higher yields and most importantly, providing a biodiesel product of unusually high quality.

As the feedstock for biodiesel production, the lipid and alcohol qualities and composition are important factors in the transesterification process. In particular, the presence of FFA in low cost feedstock needs to be studied in the membrane reactor.

Carbon and ceramic membranes appear to be suitable inorganic membranes for transesterification at higher temperatures and pressures. The size exclusion effect is the known mechanism of membrane operation for biodiesel production. Membrane pore size effects, alcohol fraction limit, low catalyst concentration, and different feedstocks should be fully explored through experimentation.

## 2.7 References

Agarwal A.K.; Das L.M., Biodiesel Development and Characterization for Use as a Fuel in Compression Ignition Engines, *J. Eng. Gas Turb. & Power*, 123: 440-447, **2001**.

Aksoy H. A.; Kahraman I.; Karaosmanoglu F.; Civelekoglu H., Evaluation of Turkish Sulphur Olive Oil as an Alternative Diesel Fuel, *J. Am. Oil Chem. Soc.*, **1988**.

Antolín G.F.; Tinaut V.; Briceño Y.; Castaño V.; Pérez C.; Ramírez A. I., Optimization of Biodiesel Production by Sunflower Oil Transesterification, *Biores. Tech.*, **2002**.

Ataya F.; Dubé M.A.; Ternan M., Single-Phase and Two-Phase Base-Catalyzed Transesterification of Canola Oil to Fatty Acid Methyl Esters at Ambient Conditions, *Ind. Eng. Chem. Res.*, 45:5411, **2006**.

Boocock D.G.B.; Konar S.K.; Mao V.; Lee C.; Buligan S., Fast Formation of High-purity Methyl Esters from Vegetable Oils, *J. Am. Oil Chem. Soc.*, 75:1167-1172, **1998**.

Canakci M.; Van Gerpen J., A Pilot Plant to Produce Biodiesel from High Free Fatty Acid Feedstocks, *ASAE Annual International Meeting,* **2001**.

Canakci M.; Van Gerpen J., Biodiesel Production via Acid Catalysis, *Trans. ASAE,* **1999**.

Chandra B.P., A Critical Review of Biodiesel as a Transesterification Fuel in Canada, *Report of Transportation Systems Branch Air Pollution Prevention Directorate, Environment Canada,* **1998**.

Cheryan M., Ultrafiltration Handbook, *Technomic Publishing Company, Lancaster, Pennsylvania, U.S.A.,* 250-256, **1986.**

Clark S. J.; Wagner L.; Schrock M.D.; Piennaar P. G., Methyl and Ethyl Soybean Esters as Renewable Fuels for Diesel Engines, *J. Am. Oil Chem. Soc.,* 61: 1632–1638, **1984**.

Coleman B., Canola: An Excellent Feedstock for Biodiesel, *Biodiesel Magazine*, 1:50, **2006**.

Coltrain D., Biodiesel: Is It Worth Considering?, *Presentation at Risk and Profit Conference, Kansas State University, Manhattan, Kansas,* **2002**.

Darnoko D.; Cheryan M., Continuous Production of Palm Methyl Esters, *J. Am. Oil Chem. Soc.*, **2000a.**

Dubé M.A.; Tremblay A.Y.; Liu J., Biodiesel Production Using a Membrane Reactor, *Biores. Tech., 93*, 639, **2007.**

Dubé M.A.; Zheng S.; McLean, D.D.; Kates, M., A Comparison of Attenuated Total Reflectance-FTIR Spectroscopy and GPC for Monitoring Biodiesel Production, *J. Am. Oil Chem. Soc., 81:* 599, **2004**.

Duvekot C., Determination of Total FAME and Linolenic Acid Methyl Esters in Biodiesel According to EN -14103, *Application Specialist Marketing GC Solutions, Varian, Inc.,* **2007.**

Energy Information Administration (EIA), This Week in Petroleum Reports, http://tonto.eia.doe.gov/oog/info/twip/twip.asp, the statistical agency of the U.S. Department of Energy, accessed on November 11, **2007**.

Foglia T.A.; Nelson L.L.; Dunn R. O.; Marmer W. N., Low-temperature Properties of Alkyl Esters of Tallow and Grease, *J. Am. Oil Chem. Soc.,* 74: 951-955, **1997**.

Freedman B.; Pryde E.H.; Mounts T.L., Variables Affecting the Yields of Fatty Esters from Transesterified Vegetable Oils, *J. Am. Oil Chem. Soc., 61*, 1638, **1984**.

Freedman B.; Butterfield R.O.; Pryde, E. H., Transesterification Kinetics of Soybean Oil, *J. Am. Oil Chem. Soc., 63*, 1375, **1986**.

Freedman B.; Bagby M.O., Heats of Combustion of Fatty Esters and Triglycerides, *J. Am. Oil Chem. Soc.,* 66:1601-1605, **1989.**

Fukuda H.; Kondo A.; Noda H., Biodiesel Fuel Production by Transesterification of Oils, *J. Biosci. Bioeng.*, **2001**.

Graboski M. S.; McCormick R.L., Combustion of Fat and Vegetable Oil Derived Fuels in Diesel Engines, *Prog. Energy Comb. Sci.*, **1998**.

Gunstone F.D.; Harwood J.L.; Padley F.B., The Lipid Handbook, 2nd edn., Chapman & Hall, London, **1994.**

Haas M. J.; Scott K. M.; Marmer W. N.; Foglia T.A., In situ Alkaline Transesterification: an Effective Method for the Production of Fatty Acid Esters from Vegetable Oils, *J. Am. Oil Chem. Soc,* **2004**.

Haws, R., Chemical Oxygen Demand, Biochemical Oxygen Demand and Toxicity of Biodiesel, *Proceedings of the conference on commercialization of biodiesel: Environmental and health benefits*, **1997**.

Hill J.; Nelson E.; Tilman D.; Polasky S.; Tiffany D., Environmental, Economic, and Energetic Costs and Benefits of Biodiesel and Ethanol Biofuels, *PANS*, 103:30, July **2006**.

Hsieh H.P., General Characteristics of Inorganic Membranes, *Inorganic membrane characterization and application,* Elsevier, Amsterdam, **1991**.

Hsieh H.P., Inorganic Membranes for Separation and Reaction, *Membrane science and technology series 3*, Elsevier, Amsterdam, **1996.**

Knothe G.; Krahl J.; Van Gerpen J., The Biodiesel Handbook; *AOCS Press*: Champaign, Illinois, pp. 44-46, **2005**.

Komers K.; R. Stloukal; Machek J.; Skopal F., Biodiesel from Rapeseed Oil, Methanol and KOH 3. Analysis of composition of actual reaction mixture, *Eur. J. Lipid Sci. Tech.*, **2001**.

Köse M. T.; Aksoy H.A., Immobilized Candida Antarctica Lipase-catalyzed Alcoholysis of Cotton Seed Oil in a Solvent-free Medium, *Biores. Tech.*, **2002**.

Kramer W., The Potential of Biodiesel Production, *Oil and Fats Int.*, **1995**.

Lambrich U.; Schubert H., Emulsification Using Microporous Systems, *J. Membrane Sci.*, **2005.**

Lane J.C., Gasoline and Other Motor Fuels, *Encyclopedia of Chemical Technology*, 3rd edn., New York, 11:682-689, **1980**.

Lee I.; Johnson L.A., Use of Branched-chain Esters to Reduce the Crystallization Temperature of Biodiesel, *J. Am. Oil Chem. Soc.,* 72: 1155-1160, **1995.**

Liu J., Biodiesel Production by Membrane Reactor from Canola Oil, M.A.Sc. thesis, University of Ottawa, **2004.**

Liu K., Preparation of Fatty Acid Methyl Esters for Gas-chromatographic Analysis of Lipids in Biological Materials, *J. Am. Oil Chem. Soc.*, **1994.**

Lotero E.; Goodwin J. G.; Bruce D. A.; Suwannakarn K.; Liu Y.; Lopez D. E, The Catalysis of Biodiesel Synthesis, Clemson SC 29634-0909, USA, *Catalysis,* The Royal Society of Chemistry, 19: 20-25, **2006.**

Lotero E.; Liu Y.; Lopez D. E.; Suwannakarn K.; Bruce D. A.; Goodwin J. G., Synthesis of Biodiesel via Acid Catalysis, *Ind. Eng. Chem. Res.*, 44 : 5353 -5363, **2005.**

Ma F.; Clements L.D.; Hanna M. A., The Effects of Catalyst Free Fatty Acids and Water on Transesterification of Beef Tallow, *Trans. ASAE,* **1998.**

Ma F.; Clements L. D.; Hanna M. A., Biodiesel Production: A Review, *Biores. Tech.,* 70:1, **1999.**

Markolwitz M., Consider Europe's Most Popular Catalyst, *Biodiesel Magazine,* 1: 20-22, **2004.**

Mayeda A., Study Lights Fire under Biodiesel Producers, *Source: CanWest News Service, http://www.iogen.ca/news_events/iogen_news/2005_07_20.html*, accessed on Jul. 20, **2005.**

McCormick R.L.; Graboski M.S.; Alleman T.L.; Herring A.M., Impact of Biodiesel Source Material and Chemical Structure on Emissions of Criteria Pollutants from a Heavy Duty Engine, *Env. Sci. Tech.,* 35: 1742-1747, **2001.**

Michael A.; Gumpon P., The Modeling of the Biodiesel Reaction, Prince of Songkla University, Thailand, http://journeytoforever.org/biofuel_library/macromodx.html, accessed on Nov. 20, **2006.**

Mullet M.; Fievet P.; Reggiani J.C.; Pagetti J., Wicking Technique Combined with Electrical Resistance Measurements for Determination of Pore Size in Ceramic Membranes, *J. Mater. Sci.*, 34:1905, **1999.**

Noureddini H.; Zhu D., Kinetics of Transesterification of Soybean Oil, *J. Am. Oil Chem. Soc.,* **1997.**

Nye M.J.; Williamson T.W.; Deshpande S.; Schrader J.H.; Snively W.H.; Yurkewich T.P.; French C.L., Conversion of Used Frying Oil to Diesel Fuel by Transesterification: Preliminary Tests, *J. Am. Oil Chem. Soc.*, **1983**.

Otera J., Esterification-methods, Reactions and Applications, *Wiley-VCH-GmbH and Co,* **2003.**

Pahl G., Biodiesel: Growing a New Energy Economy, *Chelsea Green Publishing Company,* pp 5-45, **2005**.

Peterson C.; Möller G.; Haws R.; Zhang X.; Thompson J.; Reece D., Ethyl Ester Process Scale-up and Biodegradability of Biodiesel, *For the United States Department of Agriculture Final Report, No. 303*, November **1996**.

Peterson C.L.; Feldman M.; Korus R.; Auld D.L., Batch Type Transesterification of Ethyl and Methyl Esters of Winter Rape Oil, *ASAE Paper No. 89-6569,* **1991.**

Peterson C.L.; Reece D.L.; Hammond B.J.; Thompson J.C.; Beck S., Commercialization of Idaho Biodiesel (HYSEE) from Ethanol and Waste Vegetable Oil, *ASAE Paper No. 956738,* **1995.**

Pimentel D.; Patzek T.W., "Ethanol Production Using Corn, Switchgrass, and Wood; Biodiesel Production Using Soybean and Sunflower," *Natural Resources Research*, 14(1): 65-75, **2005.**

Romano S., Vegetable Oils – A New Alternative, P*roceedings of the Int. Conf. on Plant and Vegetable Oils as Fuels, ASAE*, **1982**.

Ryan T. W.; Dodge L. G.; Callahan T. J., The Effect of Vegetable Oil Properties on Injection and Combustion in Two Different Diesel Engines, *J. Am. Oil Chem. Soc.*, **1984**.

Saka S.; Kusdiana D., Biodiesel Fuel from Rapeseed Oil as Prepared in Supercritical Methanol, *Fuel, 80,* **2001**.

Sanchez J.; Tsotsis T.T., Current Developments and Future Research in Catalytic Membrane Reactors, *Membrane Science and Technology Series,* Elsevier, Amsterdam, **1996**.

Schwab A.W.; Bagby M.O.; Freedman B., Preparation and Properties of Diesel Fuels from Vegetable Oils, *Fuel,* 66: 1372-1378, **1987.**

Shuler M.L.; Kargi F., Bioprocess Engineering: Basic Concepts textbook, *Prentice Hall,* **2002.**

Siskens C. A. M., Application of Ceramic Membrane in Liquid Filtration, *Membrane science and technology series 4,* Elsevier, Amsterdam, **1996..**

Sridharan R.; Mathai I.M., Transesterification Reactions, *J. Sci. Ind. Res.,* 33: 178–187, **1974.**

Stern R.; Hillion G.; Rouxel J. J.; Leporq S., Process for the Production of Esters from Vegetable Oils or Animal Oils Alcohols, *U.S. Patent 5,908,846*, **1999**.

Suppes G.J.; Dasari M.A.; Doskocil E.J.; Mankidy P.K.; Goff M.J., Transesterification of Soybean Oil with Zeolite and Metal Catalyst, *Appl. Catal. A: General,* 257: 213–223, **2004.**

Teall R., Biofuels Workshop & Trade Show Sees Success, *The First-ever Biofuels workshop & Trade Show-Western & Pacific Region, Biodiesel Magazine,* **2004**.

Torrie R., Commentary on the Government of Canada's "Climate Change Plan for Canada", s*ee www.torriesmith.com,* **2002**.

Tyson K. S.; Brown J.; Moora M., Industrial Mustard Crops for Biodiesel and Biopesticides, *National Renewable Energy Laboratory,* **2002**.

Van Gerpen J., Biodiesel Processing and Production, *Fuel Processing Technology*, 86: 1097-1107, **2005**.

Van Gerpen J.; Shrestha D., Biodiesel Energy Balance, Department of Biological and Agricultural Engineering, University of Idaho, see *www.uidaho.edu/bioenergy/NewsReleases/Biodiesel%20Energy%20Balance_v2a.pdf*, accessed on April 15, **2007**.

Van Gerpen J; Shanks B; Pruszko R; Clements D; Knothe G., Biodiesel Production Technology, National Renewable Energy Laboratory, NREL/SR-510-36244; **2004**.

Vicente G.; Mercedes M.; José A., Integrated Biodiesel Production: a Comparison of Different Homogeneous Catalysts Systems, *Biores. Tech.,* 96:1425-1429, **2005.**

Von Wedel R., First-ever Biofuels Workshop & Trade Show-Western & Pacific Region, *Cytoculture International Inc.,* **2004**.

Wang W.G.; Lyons D.W.; Clark N.N.; Gautam M., Emissions from Nine Heavy Trucks Fueled by Diesel and Biodiesel Blend without Engine Modification, *Env. Sci. Tech.,* 34: 933–939, **2000.**

Williams J., Presidential presence, *Biodiesel Magazine,* July, 7: 22-23, **2005**.

Zeman L.J.; Zydney A.L., Microfiltation and Ultrafiltration Principles and Applications, *Marcel Dekker, Inc.,* 331-341, 380-381, 575-576, **1996.**

Zhang Y.; Dubé M.A.; Mclean D.D.; Kates M., Biodiesel production from waste cooking oil: 2. Economic assessment and sensitivity analysis; *Biores. Tech.,* 90:239, **2003**.

Zhang Y.; Dubé, M. A.; Mclean D. D.; Kates M., Biodiesel Production from Waste Cooking Oil: 1. Process Design and Technology Assessment. *Biores. Tech.,* 90: 229, **2003**.

Zhou W.; Boocock D. G. B., Phase Distributions of Alcohol, Glycerol, and Catalyst in the Transesterification of Soybean Oil , *J. Am. Oil Chem. Soc.,* 83:1047-1052, **2006.**

Zhou W.; Konar S. K; Boocock D. G. B., Ethyl Esters from the Single-phase Base-catalyzed Ethanolysis of Vegetable Oils, *J. Am. Oil Chem. Soc.,* **2003**.

## Chapter 3

# Effect of Membrane Pore Size on the Performance of a Membrane Reactor for Biodiesel Production

*Ind. Eng. Chem. Res.*, **2007**, 46, 52-58.

similar properties to petroleum-based diesel, but it is biodegradable and non-toxic. [1] One of the main driving forces for biodiesel's widespread use is the net reduction of greenhouse gas emissions to the atmosphere on a lifecycle basis. Along with ethanol and other biomass-derived fuels, biodiesel is an important source of renewable energy.

The main components of biodiesel, fatty acid alkyl esters (FAAEs), are comprised of mono-alkyl esters of long chain fatty acids, the product of the reaction of a straight chain alcohol with lipid (triglycerides or TG). Transesterification of TG consists of three reactions steps. Figure 3.1 shows a detailed elementary reaction scheme of the reaction of TG with alcohol to produce a diglyceride (DG), the reaction of the DG with alcohol to produce a monoglyceride (MG), and finally the reaction of the MG with alcohol to produce glycerol; each step yields FAAEs. [2]

In Figure 3.1, $R_1$, $R_2$, and $R_3$ are long chain hydrocarbons (e.g., palmitic acid - $(CH_2)_{14}$-$CH_3$), sometimes called fatty acid chains. The alcohol used for producing biodiesel is usually methanol (where the $R'$ corresponds to $CH_3$). The use of methanol in the reaction produces fatty acid methyl esters (FAMEs). Each of the reactions is reversible with a different rate constant ($k_n$). The forward and reverse reactions take place at different rates. The reactions are all known to be second-order or pseudo-second order. [3] The third step, formation of glycerol from MG, proceeds more rapidly than the second step, formation of a MG from a DG. [4]

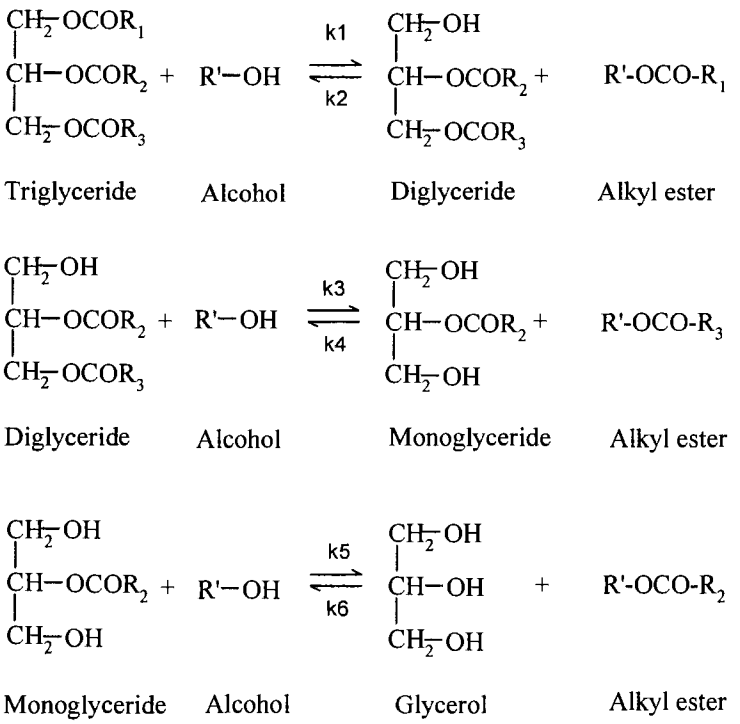


Figure 3.1: Elementary reaction scheme for transesterification of TG

The production of biodiesel presents several technical challenges. First, below a FAME concentration of 70 wt. %, the transesterification is essentially a heterogeneous, mass transfer limited reaction. Above this FAME concentration, the reaction mixture forms a single phase [5, 6]. One approach to overcoming this immiscibility issue is to create a homogeneous reaction mixture using for example, THF as a co-solvent; [7] another approach employs supercritical methanol. [8] Although these approaches yield the desired results, they do involve additional costs for either downstream separation (e.g., removal of THF) or energy-related costs. In addition, the unreactable materials that are present might also be solubilized and be retained in the biodiesel product. The reversible nature of the transesterification means that the reaction can never reach 100% completion. Subsequently, there will always be unreacted glycerides, leaving unconverted or partially converted material in the biodiesel. This issue is of particular importance due to the strict guidelines regarding the purity of commercial biodiesel. For example, the ASTM D6751 standard for biodiesel allows 0.24% total glycerol in the final product; which implies that the reaction completion must be about 99.7% to meet the total glycerol standard for the fuel [1]. The high cost of virgin oils favors the use of lower cost feedstocks, which are high

in water and/or free fatty acid (FFA). In this case, a higher concentration of catalyst is required for the reaction: either a strong acid or a strong base. The base catalyzed reaction can result in a saponification side reaction that hinders the production of biodiesel and reduces catalytic efficiency, as well as causing an increase in viscosity and even the potential difficulty in achieving separation of glycerol and the water wash stream [9]. Subsequently, a 2-step acid/base or 1-step acid reaction is used even though its reaction time is longer than the base-catalyzed reaction [10]. In addition, downstream purification processes such as water washing to remove unreacted alcohol and catalyst may generate large amounts of wastewaters that are energy intensive to treat. Downstream processes involving the production of wastewaters are evidently not in line with the environmentally driven ideals behind the use and production of biodiesel. These problems can potentially be overcome through the use of a membrane reactor in the production of biodiesel. [11]

In this paper, the development of a novel semi-continuous membrane reactor to produce high quality biodiesel is described. We hope to further modify this reactor so that it can be used on a continuous basis. The goals of this project were to determine the limit of the initial methanol to oil ratio on the operation of the reactor and the effect of membrane pore size on the retention of oil in the reactor. This information forms the basis to establish the versatility of the reactor technology and for the future design of such reactors.

### 3.3 Theoretical Basis of the Membrane Reactor

A membrane reactor is a reaction system where membranes and chemical reactions are combined. It is a device for carrying out a reaction and membrane-based separation simultaneously in the same physical enclosure or in close proximity. Membrane reactor technology had been successfully applied to many chemical reaction processes. [12] The transesterification of lipids is a classical reversible chemical reaction which could also be combined with membrane reactor technology.

In the case of membrane reactors involving gases, progress towards commercialization has been rather slow mainly due to problems of membrane stability

and the need to obtain high permeation rates and high permselectivity. [13] Much of the work on membrane reactors has concentrated on reactions involving gases. The greatest hurdle is in maintaining membrane performance with respect to gas permeation and permselectivity. In the case of an emulsion membrane reactor, there is an additional barrier helping the separation which is phase transfer. Ultrafiltration and microfiltration membranes can be made of corrosion resistant materials and offer greater stability and availability than gas separation membranes. The implementation of such membrane reactors is not expected to encounter the same difficulties as those found in gaseous systems.

Recently, Dubé et al. [11] applied membrane reactor technology to the production of biodiesel. They found that a micro-porous inorganic membrane reactor could selectively permeate FAME, methanol and glycerol during the transesterification process. The membrane module is the key component of the reactor system (see Figure 3.2). It consists of a porous membrane tube placed in a shell-and-tube configuration. The immiscibility of the lipid feedstock in methanol and the miscibility of the FAME in methanol permit an easy separation of the products from the reactants. As shown in Figure 3.2, transesterification is believed to occur at the surface of the oil droplets suspended in methanol [11]. Both the products of transesterification, namely FAME or biodiesel and glycerol, as well as the catalyst (either base or acid) are soluble in the methanol. As the FAME forms, it diffuses into the methanol phase. Because of the positive pressure difference across the membrane, the FAME/alcohol/glycerol/catalyst phase passes though the membrane into the permeate stream. The oil and alcohol are immiscible at the reaction temperature (e.g., 65 °C) and the oil molecules aggregate to form droplets dispersed in the alcohol as an emulsion. The oil droplets cannot pass through the membrane pores due to their large size relative to the membrane pore size.

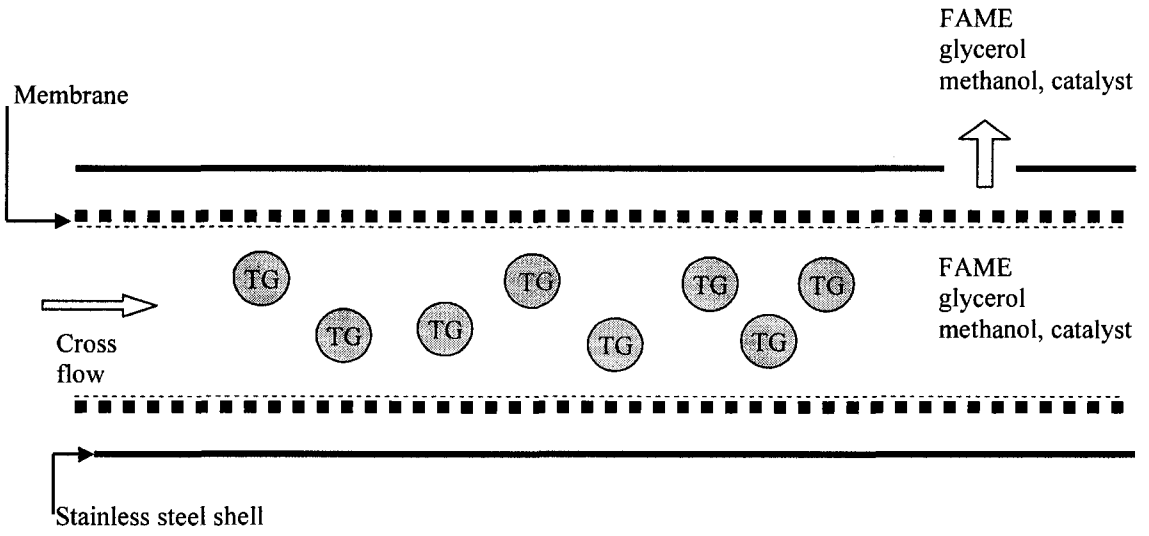


Figure 3.2: Schematic diagram of membrane module for biodiesel production.

The membrane offers a barrier to the passage of oleophilic substances present in lipid feedstocks. This introduces inherent reliability in the production of biodiesel that parallels the use of distillation in petroleum processes. The vapor-liquid interface ensures product quality in distillation, as the oleophilic-hydrophilic phase boundary does in the membrane reactor. The membrane serves to retain the smallest oleophilic droplets within the reactor. Thus, the membrane reactor offers inherent process reliability compared to batch processes.

Figure 3.3 depicts this semi-continuous membrane reactor. Briefly, a circulation pump, membrane module and heat exchange system make up a circulating loop within which the transesterification reaction occurs at a controlled temperature and pressure. A feed pump and a backpressure valve interface between this pressurized loop and atmospheric conditions.

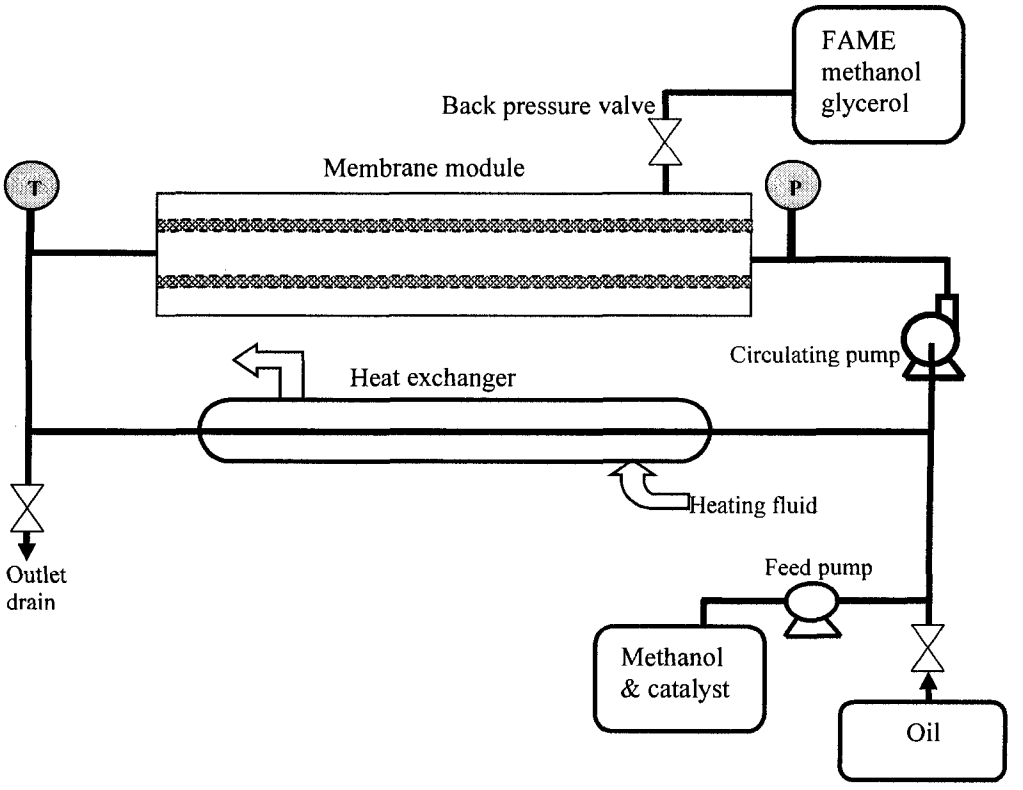


Figure 3.3: Flow diagram for semi-continuous membrane reactor.

For the purpose of membrane selection, it is important to estimate the size of the dispersed oil droplets in the continuous alcohol phase. The minimum particle size in the oil-methanol emulsion can be estimated from the work of DeRoussel et al. [14]. Based on a continuous methanol phase and an internal tube diameter of 6 mm; at 65°C and a cross-flow velocity of 3 m/s, the ratio, $\mu_c\dot{\gamma}/\sigma$, equals 102 $m^{-1}$, ($\mu_c$ = viscosity of the continuous phase, $\dot{\gamma}$ = shear rate in the tubular membrane reactor and $\sigma$ = interfacial tension)[14]. According to DeRoussel et al. [14], the average drop size for this emulsion is 44 microns with a lower and upper size limit of 12 and 400 microns, respectively. The largest membrane pore size selected in this work, 1.4 microns, was nearly one order of magnitude smaller than the lower oil drop size limit of 12 microns.

Maintaining a heterogeneous state within the reactor is important for its operation. The miscibility of the reactants and the partitioning of products obtained from the membrane reactor can be estimated using the octanol-water partition coefficients ($K_{ow}$) shown in Figure 3.4. Values of $K_{ow}$ were obtained from group contributions as described

in ref. 15. Representative lipid species were taken as follows: MG, 1-monoolein, FFA, oleic acid, FAME, methyl oleate, FAEE, ethyl oleate, DG, 1,3-diolein, and TG, triolein.

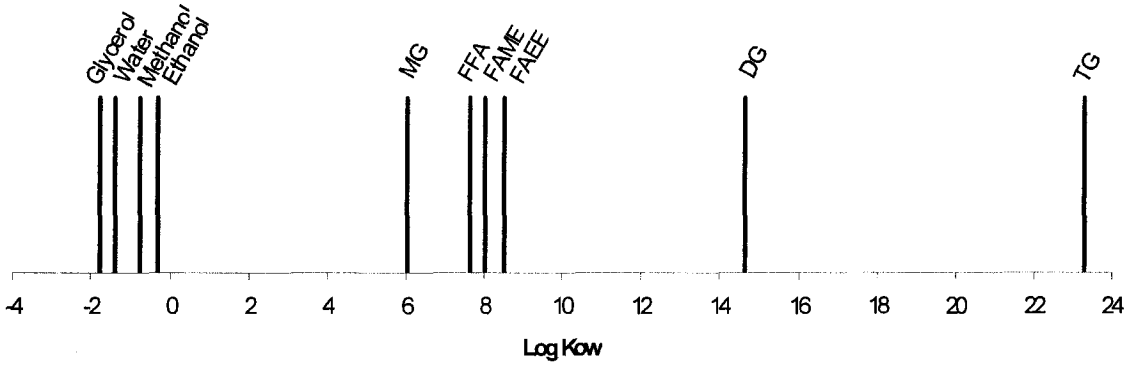


Figure 3.4: $K_{ow}$ Values of reaction mixture components in biodiesel production

The octanol-water coefficient $K_{ow}$ is the ratio of the equilibrium concentration of a species in octanol to that in water at a specified temperature. $K_{ow}$ represents the tendency of a chemical species to partition itself between an organic and an aqueous phase. This implies that species having similar values of $K_{ow}$ will be miscible. DG and TG have $\log(K_{ow})$ values of 14.64 and 23.29, respectively and are not miscible in methanol ($\log(K_{ow}$ ) value of -0.77). While MG and FAME have $\log(K_{ow})$ values of 6.04 and 8.02, respectively, and are miscible in methanol. Thus, it is reasonable to expect that DG and TG would be retained in the membrane reactor while MG and glycerol may be present in the mobile methanol phase and actually permeate through the membrane. However, it is also known that MG is so unstable that it will transesterify to FAME rapidly. [4] This would allow us to speculate that, under appropriate conditions, MG may permeate through the membrane but will likely react readily and, thus, no traces of MG would be found in the permeate product stream.

One concern is that the pores of the membrane will most likely plug in the event of phase inversion if the oil were to become the continuous phase. Qualitatively, the phase with the larger volume fraction tends to be continuous for two immiscible liquids. However, phase continuity is affected by viscosity. The phase having the lower viscosity

will have a tendency to flow around the higher viscosity phase. Jordhamo et al. [16] proposed a model expressing the point of phase inversion in a two phase system. The model assumes equal importance for the viscosity and the volume fraction of the components,

$$\frac{\phi_1}{\phi_2} = \frac{\mu_1}{\mu_2} \tag{1}$$

Where $\mu_1$ and $\mu_2$ represent the viscosity of the pure constituents and $\phi_1$ and $\phi_2$ are the volume fractions of the constituents at phase inversion.

When the viscosities of the two components differ widely, significant deviations between the predicted and experimental results are observed. A semi-empirical version of eq. 1 was proposed by Ho et al. [17] as:

$$\frac{\phi_1}{\phi_2} = 1.22 \times \left( \frac{\mu_1}{\mu_2} \right)^{0.29} \tag{2}$$

Substituting values for the viscosity of oil and methanol at 65°C into eq. 2 gives a value of $\phi_1/\phi_2 = 0.44$. Solving for $\phi_1$ we obtain $\phi_1 = 0.31$. This indicates that, at 65°C, the lowest initial volume fraction of methanol, where methanol is maintained as a continuous phase in the emulsion, is 0.31.

### 3.4 Experimental Section

#### 3.4.1 Materials

Canola oil (No Name®, Toronto, ON, Canada) was purchased at a local food store. Tetrahydrofuran (THF, 99.98% purity, EMD Chemicals Inc., Gibbstown, NJ, USA), hydrochloric acid (HCl, 36.5-38%, reagent grade, Fisher Scientific Co., Nepean, ON, Canada), methanol (99.85% purity, Commercial Alcohols Inc., Brampton, ON, Canada), and sodium hydroxide (NaOH, reagent grade, ACP Chemicals Inc., Montreal, QC, Canada) were all used as received. Solvents and analytical reagents were of high performance liquid chromatography (HPLC) grade.

### 3.4.2 Membranes and reactor equipment

Carbon is a material that is well known for its corrosion resistance. Carbon membranes are typically produced as a composite structure. A thin layer of porous carbon (10 micron thick) is applied to the internal surface of a narrow diameter carbon and carbon-fibre support tube. Carbo-cor membranes (Koch Membrane Systems, Inc., Wilmington, DE, USA) were used in the reactor. The single channel tubular membranes had an inside diameter of 6 mm, an outside diameter of 8 mm and a length of 1200 mm resulting in a membrane area of 0.022 $m^2$. The maximum operating temperature is 165 °C. Four different membrane pore sizes were employed: 0.05, 0.2, 0.5 and 1.4 microns.

A schematic diagram of the membrane reactor system was shown earlier in Figure 3.3. For the experimental reactor, a diaphragm pump (Milton Roy Company, Ivyland, PA) was used to feed the methanol to the system, while a seal-less centrifugal canned motor pump (Labcor Inc. Concord, ON, Canada) was used to circulate the mixture in the loop. A temperature-controlled bath (Neslab Instruments, Inc., Portsmouth, NH) was used to control the reaction temperature. Temperature was monitored using a temperature probe placed in the reactor loop. The total volume of the reactor was 320 mL.

### 3.4.3 Experimental Procedure

A given amount of vegetable oil was charged into the reactor, and then a solution of catalyst in methanol was continuously fed into the pressurized loop shown in Figure 3.3 and circulated with the circulating pump. Detailed procedures are as follows: A methanol/NaOH solution (0.5 wt.% NaOH by weight of oil) was fed into the reactor using the feed pump until the system was full (and all air had been displaced out of the reactor). Canola oil was then injected into the system upstream of the feed pump at the injection valve (see Figure 3.3). The drain valve was simultaneously opened to allow the excess methanol/NaOH solution to leave. Any remaining air was purged from the system. The back pressure valve was activated and the heat exchanger and circulating pump were turned on. When the temperature reached 55°C (after ~25 min), the feed pump was activated. The pressure in the reactor gradually increased to reach a maximum ranging from 400 to 550 kPa until permeation occurred. After permeation, the pressure decreased from this maximum and could be controlled at 207 kPa for the remainder of the run.

Maintaining pressure in the reactor was necessary to prevent cavitation in the circulating pump and boiling at the surface of the heat exchanger in the reactor loop (shell side temperature = 80 °C). The feed pump was set to a flow rate of 3.3 mL/min required to permeate 500 mL of methanol/catalyst solution in 2.5 hours. Once the permeate began to flow, samples were taken every ten minutes up to one hour and then for every fifteen minutes until 500 mL of methanol/catalyst solution was fed to the system. The transesterification reaction was immediately quenched in each sample vial by the addition of 12N hydrochloric acid in methanol down to a pH of 7.0. When 500 mL of methanol/catalyst solution had permeated through the system, the pumps and heat exchanger were stopped and the system completely drained. The volume of oil remaining in the final retentate was measured. Following each run, the system was flushed for 30 min with pure methanol and then drained. Samples were analyzed using gel permeation chromatography (GPC). The initial oil injection masses were selected as 100, 150, 175 and 200 g corresponding to initial methanol volume fractions of 0.64, 0.47, 0.38 and 0.29, respectively. The experimental conditions are found in Table 3.1.

Table 3.1: Experimental conditions.

| **Run** | **Membrane pore size (μm)** | **Initial injection mass of oil (g)** | **Initial molar ratio of methanol to injection oil** | **Initial volume fraction of methanol at 65 °C** |
|---|---|---|---|---|
| 1 | 0.05 | 100 | 46.0 | 0.64 |
| 2 | 0.05 | 150 | 22.7 | 0.47 |
| 3 | 0.05 | 175 | 16.0 | 0.38 |
| 4* | 0.05 | 200 | 11.0 | 0.29 |
| 5 | 0.2 | 100 | 46.0 | 0.64 |
| 6 | 0.2 | 150 | 22.7 | 0.47 |
| 7 | 0.2 | 175 | 16.0 | 0.38 |

| | | | | |
|---|---|---|---|---|
| 8 | 0.5 | 100 | 46.0 | 0.64 |
| 9 | 0.5 | 150 | 22.7 | 0.47 |
| 10 | 0.5 | 175 | 16.0 | 0.38 |
| 11 | 1.4 | 100 | 46.0 | 0.64 |
| 12 | 1.4 | 150 | 22.7 | 0.47 |
| 13 | 1.4 | 175 | 16.0 | 0.38 |
| 14* | 1.4 | 200 | 11.0 | 0.29 |

* No permeate was observed at the 200g loadings

### 3.4.4 Characterization

GPC meets our objective to quickly analyze diverse and numerous samples accurately for the purposes of assessing reactor operation. [18] For GPC analysis, each 20 mL sample of neutralized permeate (or retentate) was filtered through a 0.2 μm polytetrafluoroethylene (PTFE) syringe filter into a clean vial. Approximately 0.04 g of sample was combined with 2 g of THF in a vial for analysis. A Waters Corp. GPC system consisting of a pump, flow controller, differential refractometer and auto-sampler were used for the analysis. Waters Millennium 32$^{TM}$ software was utilized for analysis. The columns used were two 300 x 7.5 mm Phenogel columns of 3 μm and 100 Å pore size (Phenomenex, Torrance, CA) connected in series. The mobile phase was HPLC grade THF at a flow rate of 0.5 mL/min at 25°C. The sample injection loop was 20 μL with a running time of 60 minutes.

## 3.5 Results and Discussion

### 3.5.1 Effect of oil injection mass

Permeate was readily obtained from the membrane reactor at oil injection masses of 100, 150 and 175 g. This was not the case at the 200 g loading where both membranes tested at this level (0.05 and 1.4 micron) did not produce permeate at the operating

pressure of 207 kPa. This indicates that methanol was no longer the continuous phase in the emulsion. As seen in Table 3.1, the volume fraction of methanol at the 200 g oil loading was 0.29, whereas at the 175 g oil injection mass, $\phi_1$ was 0.38.

The semi-empirical model proposed by Ho et al. [17] was found to give a reasonable prediction of phase inversion. The model predicts phase inversion at $\phi_1 = 0.31$ which is between the values of $\phi_1$ for the 200 and 175 g loadings. The results validate the use of the model proposed by Ho et al. [17] in estimating the maximum oil loading in a membrane reactor operated in semi-continuous mode. The simpler model proposed by Jordhamo et al. [16] (eq. 1) was found to be unsuitable for the prediction of phase inversion yielding a minimum value of $\phi_1 = 0.023$, which is well below our experimental observation of phase inversion.

Figure 3.5 shows an increase in FAME production as the oil loading in the reactor increases (the rest of figures were put in the appendix). This is consistent with expectations as the more oil put into the system, the more FAME can be produced.

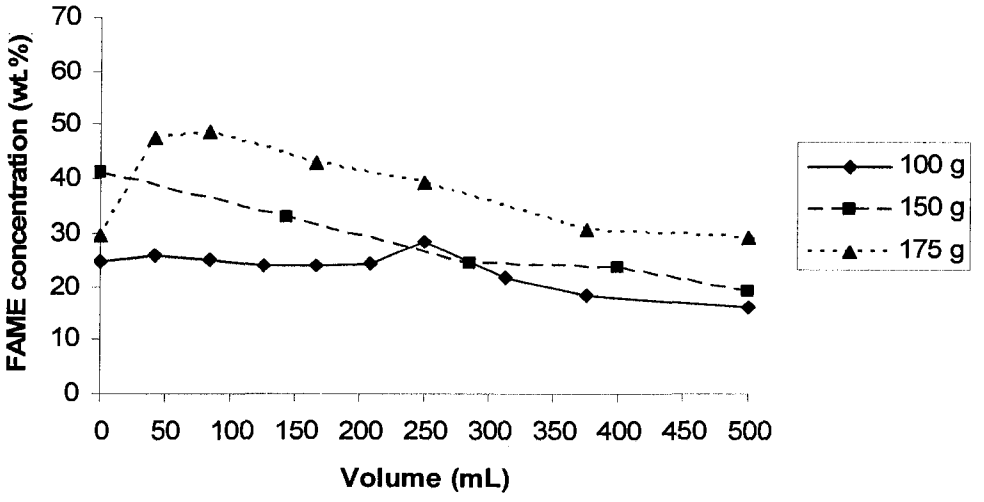


Figure 3.5 : Concentration of FAME in the permeate stream vs. the volume of methanol/NaOH injected for various initial oil loadings and membrane with 0.5 micron pore sizes.

### 3.5.2 Effect of membrane pore size

For all runs, no oil (TG) was found in the permeate stream as confirmed by GPC analysis. All permeate samples obtained from the membrane reactor were clear, amber in color and formed a single phase at 65°C. These observations indicate that the smallest oil droplet sizes in the reactor were greater than 1.4 microns. This is in agreement with the calculation of the lower drop size limit of 12 microns according to DeRoussel et al. [14].

### 3.5.3 Conversion and purity of the permeate

As oil (TG) was never found in the permeate, the unreacted oil was estimated from the weight of the oil phase remaining in the reactor at the end of each run. Table 3.2 reports the conversion for each run, where: conversion was determined as follows:

$$Conversion = \frac{\text{(initial weight of TG - weight of TG remaining in the reactor)}}{\text{initial weight of TG}} \times 100\%$$

A complete conversion beyond 99% is not expected for this reaction mixture, as some components of vegetable oils cannot be saponified. [19] The unsaponifiable materials are typically trace compounds having very low volatility and are stable towards bases. These can include sterols, alcohols and high molecular weight hydrocarbons. This is an inherent advantage of the reactor as several of these unreactable substances are oleophilic and are retained in the TG phase within the reactor.

The area under each curve in Figure 3.5 corresponds to the amount of FAME produced in a run. Figure 3.6 shows the amount of FAME produced considering both the integrated value of each FAME curve from Figure 3.5 and the FAME left in the reactor. It was assumed that the concentration of FAME left in the reactor equaled the concentration of FAME in the last permeate sample. It is seen from Figure 3.6 that the same amount of injected oil produces almost the same amount of FAME. In other words, the membrane pore size range studied did not affect the final conversion.

Table 3.2: Conversion for each run.

| **Run** | **Membrane pore size (μm)** | **Initial injection mass of oil (g)** | **Conversion of oil (wt.%)** |
|---|---|---|---|
| 1 | 0.05 | 100 | 90.8 |
| 2 | 0.05 | 150 | 94.8 |
| 3 | 0.05 | 175 | 93.5 |
| 4 | 0.05 | 200 | --- |
| 5 | 0.2 | 100 | 93.6 |
| 6 | 0.2 | 150 | 88.9 |
| 7 | 0.2 | 175 | 98.7 |
| 8 | 0.5 | 100 | 92.0 |
| 9 | 0.5 | 150 | 97.9 |
| 10 | 0.5 | 175 | 95.5 |
| 11 | 1.4 | 100 | 91.9 |
| 12 | 1.4 | 150 | 96.9 |
| 13 | 1.4 | 175 | 96.1 |
| 14 | 1.4 | 200 | --- |

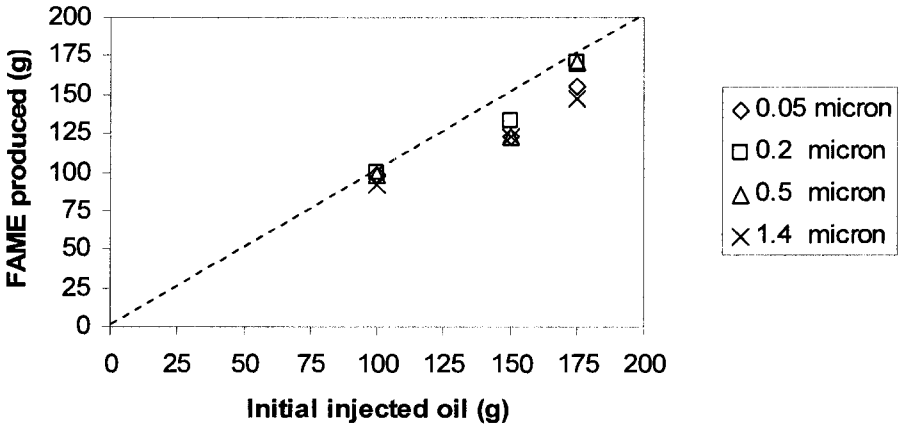


Figure 3.6: Comparison of the amount of FAME produced by transesterification vs. the initial amount of oil in the reactor.

The total reaction time had the most significant effect on conversion (see Figure 3.7). The flow of methanol needed to reach a targeted reaction time of 2.5 hours for a fixed volume of methanol/catalyst solution (500 mL), while maintaining a pressure of 207 kPa in the reactor, was difficult to set and control using the diaphragm pump. This resulted in variable reaction times and final conversions. As seen in Figure 3.7, longer total reaction times led to higher conversions. Most conversions were above 90% providing a good evaluation of reactor performance. It should be noted that the principal reason for reaching full conversion in a batch reactor is to reduce the amount of TG left in the FAME product. As the membrane reactor retains TG, achieving full conversion prior to removing product from the reactor is unnecessary.

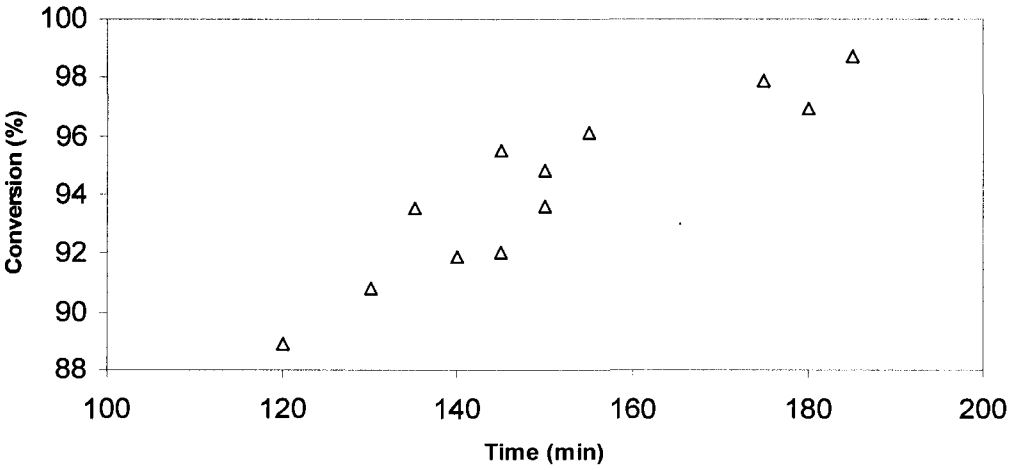


Figure 3.7: Conversion vs. total reaction time of each run.

For all runs, the GPC analyses showed that neither TGs nor MGs were present in the permeate stream. Although traces of DG were detected in several runs, there was no trend associating changes in pore size with DG concentration. Higher initial oil loadings resulted in increasingly higher DG contents in the permeate stream which paralleled the trend for FAME concentration (see Figure 3.8). From Figure 3.8, for all runs irrespective of initial oil loading or pore size, there was no DG observed in the permeate when the FAME concentration was lower than 25 to 35 wt.%. Above this range, the DG concentration increased with the FAME concentration in the permeate. DGs are an intermediate product of the transesterification process. They can either reside within the hydrophobic oil droplet, form a micelle, or be solubilized in a continuous FAME-rich methanol phase. As mentioned earlier, the solubility of DGs in pure methanol are very low because of to the difference in their respective $K_{ow}$ values. However, values of $K_{ow}$ for FAME and DG are fairly close and FAME can compatibilize the continuous methanol phase to solubilize more DG, and allow it to permeate through the membrane. Therefore, keeping FAME concentrations under 25% eliminates DG from the permeate to produce a higher quality biodiesel.

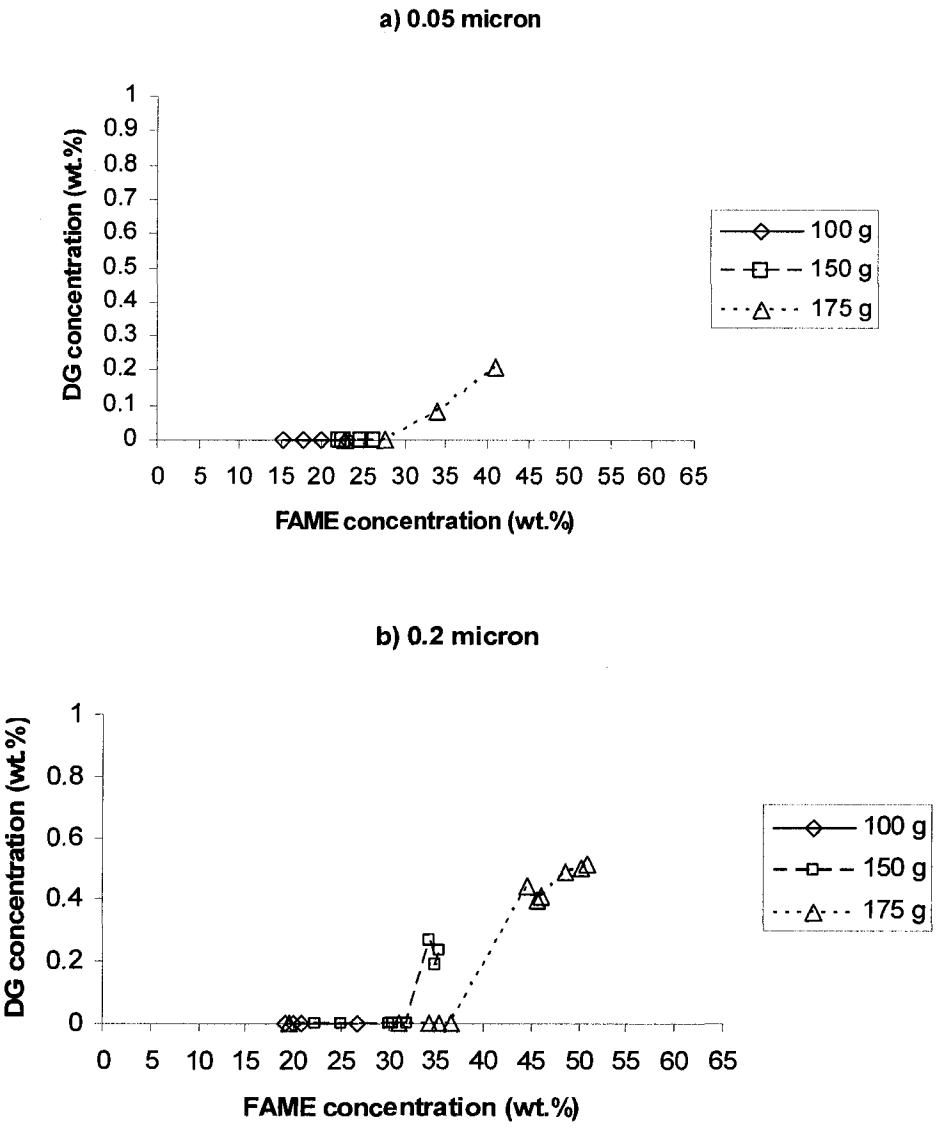


Figure 3.8: Concentration of DG in the permeate stream vs. concentration of FAME for various membrane pore sizes and initial oil loadings.

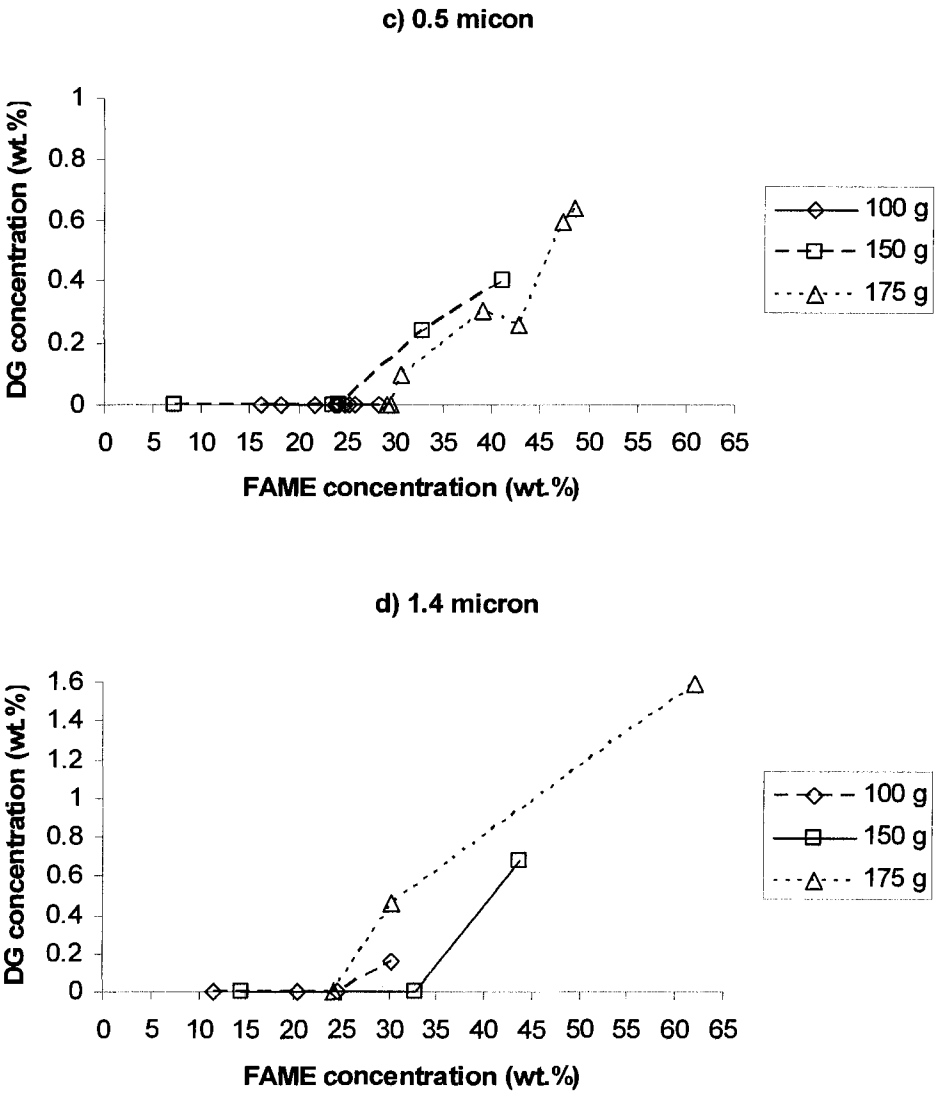


Figure 3.8: Concentration of DG in the permeate stream vs. concentration of FAME for various membrane pore sizes and initial oil loadings. (continued)

### 3.5.4 De-phasing of the permeate stream

When the experiments were carried out, the permeate from the membrane reactor eluted as a clear, amber, homogeneous solution. Within approximately 10 minutes, once room temperature was reached, the permeate samples separated into two phases with a clear boundary. The absence of particles in the permeate enhanced the de-phasing process. In addition, as the experiment progressed, the extent of de-phasing diminished, until

homogeneous samples were collected. GPC analysis revealed that the homogeneous samples were those with the lowest percentage of FAME.

Table 3.3: Composition of the upper and lower phase for permeate samples taken at 20 and 70 min from the start of permeation [a]

| **Phase** | **FAME (wt.%)** | **Glycerol (wt.%)** | **Methanol (wt.%)** | **Calculated Density (g/mL)** |
|---|---|---|---|---|
| Lower (20 min ) | 82.2 | 0 | 17.8 | 0.863 |
| Upper (20 min) | 21.4 | 6.2 | 72.4 | 0.828 |
| Lower (70 min) | 79.7 | 0 | 20.3 | 0.861 |
| Upper (70 min) | 20.6 | 5.7 | 73.7 | 0.825 |

[a] membrane pore size 0.2 micron and 150 g initial oil injection.

Table 3.3 shows the composition of the different phases. The lower phase in both of these samples was the FAME-rich phase, with an average mass composition of 82.2% after 20 min and 79.7% after 70 min from the start of permeation (run with membrane pore size 0.2 micron and 150 g initial oil injection). All samples of the FAME-rich phase taken throughout the run had non-detectable levels of glycerol using GPC. For most batch operations using a 6:1 methanol to oil ratio, the upper phase is the FAME-rich phase. In our results we found the upper phase to be the methanol-rich phase containing glycerol. This indicates that the amount of FAME in the FAME-rich phase was such that its density was greater than the density of the methanol-rich phase. One important finding was that the location (top or bottom) of the FAME-rich phase and methanol-rich phase changed from the normal location due to the glycerol content. At 1.25 g/mL, the density of glycerol at is much higher than those of both FAME (0.879 g/mL) and methanol (0.792 g/mL) (all densities @ 20°C). Consequently, particular mixtures can lead to different densities for the methanol-rich and FAME-rich phase. If recycling of the

methanol-rich phase is of interest, attention must be given to the composition of the phases.

The above observations indicate that the methanol-rich phase of the de-phased permeate can be recycled to the reactor in order to decrease the overall methanol:oil molar ratio and recycle the FAME in this phase. To reach a commercial methanol to oil molar ratio of 6:1, it is entirely practical to cool the permeate to allow for phase separation and recycle the methanol-rich phase to the reactor. The initial oil loadings represent methanol:oil mole ratios of 11:1, 16:1, 23:1, and 46:1. This opens the possibility of reaching methanol:oil mole ratios of 6:1 with a single recycling step.

### 3.6 Conclusions

Canola oil was successfully transesterified using methanol and NaOH in a membrane reactor. All tested carbon membranes of different pore sizes (namely, 0.05, 0.2, 0.5 and 1.4 micron) could retain the canola oil in the reactor, which indicated that the oil droplets present in the reactor were larger than all the pore sizes. In addition, the same amount of oil loading produced almost the same amount of FAME while the membrane pore size did not affect the final conversion. Initial volume fractions of methanol up to 0.38 could be treated in the membrane reactor. While no permeate flow was obtained at the lowest initial methanol volume fraction of 0.29. The semi-empirical model of Ho et al. [17] was validated as a predictive equation to determine phase inversion in the reactor.

Neither TG nor MG were present in the permeate stream by GPC analysis, and keeping FAME concentrations under 25% could eliminate DGs from the permeate to produce a higher quality biodiesel. Permeate de-phasing can occur at room temperature: the FAME-rich phase contained undetectable levels of glycerol by GPC, which is beneficial in more economic downstream processes for biodiesel purification; and the polar, methanol-rich phase can be recycled to the reactor and permit the continuous production of biodiesel.

In this work, the initial oil loadings represent methanol:oil mole ratios of 11:1, 16:1, 23:1, and 46:1. To decrease the overall methanol:oil molar ratio in the biodiesel production process via a membrane reactor, further work related to recycling conditions and methods will be explored.

### 3.7 Acknowledges

The authors would like to thank the financial support from Natural Sciences and Engineering Research Council of Canada (NSERC) and the Ford Foundation.

### 3.8 References

(1) Knothe, G.; Krahl J.; Van Gerpen, J. *The Biodiesel Handbook*; AOCS Press: Champaign, Illinois, **2005**, pp. 2-36.

(2) Freedman, B.; Pryde, E. H.; Mounts, T. L. Variables Affecting the Yields of Fatty Esters from Transesterified Vegetable Oils. *J. Am. Oil Chem. Soc.*, **1984**, *61*, 1638.

(3) Freedman, B.; Butterfield, R. O.; Pryde, E. H. Transesterification Kinetics of Soybean Oil. *J. Am. Oil Chem. Soc.*, **1986**, *63*, 1375.

(4) Komers, K.; Stloukal, R.; Machek, J.; Skopal F. Biodiesel from Rapeseed Oil, Methanol and KOH 3: Analysis of Composition of Actual Reaction Mixture. *Eur. J. Lipid Sci. Tech.*, **2001**, *103*, 359.

(5) Zhou, H., Lu, H., Liang, B., Solubility of Multicomponent Systems in the Biodiesel Production by Transesterification of Jatropha curcas L. Oil with Methanol, *J. Chem. Eng.*, **2006**, *51*, 1130.

(6) Noureddini, H.; Zhu, D. Kinetics of Transesterification of Soybean Oil. *J. Am. Oil Chem. Soc.*, **1997**, *74*, 1457.

(7) Boocock, D. G. B.; Konar, S. K.; Mao, V.; Sidi, H. Fast One-Phase Oil-Rich Processes for the Preparation of Vegetable Oil Methyl Esters. *Biomass and Bioenergy*, **1996**, *11*, 43.

(8) Saka, S.; Kusdiana, D. Biodiesel Fuel from Rapeseed Oil as Prepared in Supercritical Methanol. *Fuel.*, **2001**, *80*, 225.

(9) Ma, F.; Clements, L. D.; Hanna, M. A. Biodiesel Production: A Review. *Biores. Tech.*, **1999**, *70*, 1.

(10) Zhang, Y.; Dubé, M. A.; Mclean D. D.; Kates M. Biodiesel Production from Waste Cooking Oil: 1. Process Design and Technology Assessment. *Biores. Tech.*, **2003**, *90*, 229.

(11) Dubé, M.A.; Tremblay, A.Y.; Liu, J. Biodiesel Production Using a Membrane Reactor. *Biores. Tech.*, **2007**, *93*, 639.

(12) Hsieh, H. P., Inorganic Membranes for Separation and Reaction, Membrane science and technology series 3, *New York NY 10160-0757: Elsevier Science.*, **1996**, pp. 117-121.

(13) Dixon, A. G. Recent Research in Catalytic Inorganic Membrane Reactors. *Int. J. Chem. React. Eng.* **2003**, *1*, R6.

(14) DeRoussel, P.; Khakhar, D.V.; Ottino, J.M., Mixing of viscous immiscible liquids. Part 2: Overemulsification—interpretation and use, *Chem. Eng. Sci.*, **2001**, *56*, 5531.

(15) Allen, D.; Shonnard, D., Green Engineering: Environmentally Conscious Design of Chemical Processes, *EPA's Green Engineering Textbook,* ISBN# 0-13-061908-6, **2001**.

(16) Jordhamo, G. M.; Manson, J. A.; Sperling, L. H. Phase Continuity and Inversion in Polymer Blends and Simultaneous Interpenetrating Networks. *Polym. Eng. Sci.*, **1986**, *26*, 517.

(17) Ho, R. M.; Wu C. H.; Su A.C. Morphology of Plastic/Rubber Blends. *Polym. Eng. Sci.*, **1990**, *30*, 511.

(18) Dubé, M. A.; Zheng, S.; McLean, D. D.; Kates, M. A Comparison of Attenuated Total Reflectance-FTIR Spectroscopy and GPC for Monitoring Biodiesel Production. *J. Am. Oil Chem. Soc.*, **2004**, *81*, 599.

(19) Van Gerpen J. Cetane Number Testing of Biodiesel, National Biodiesel Board, Report gen-187; National Biodiesel Board: Jefferson City, MO, Sept **1996.**

## 3.9 Appendix

Figures 3.9 show the increase in conversion with the increased injection mass of oil for FAME concentration at 0.05, 0.2 and 1.4 micron membrane pore sizes, which is the supplement of Figure 3.5 shown in paper. It can be seen that as the mass of oil injected increases, so does the peak height. This is consistent with expectations as the more oil put into the system, the more FAME can be produced.

**a) 0.05 micron**

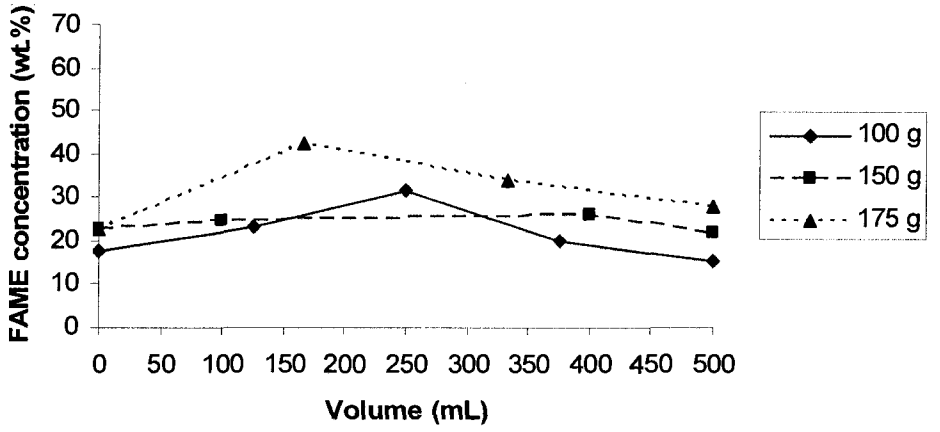


**b) 0.2 micron**

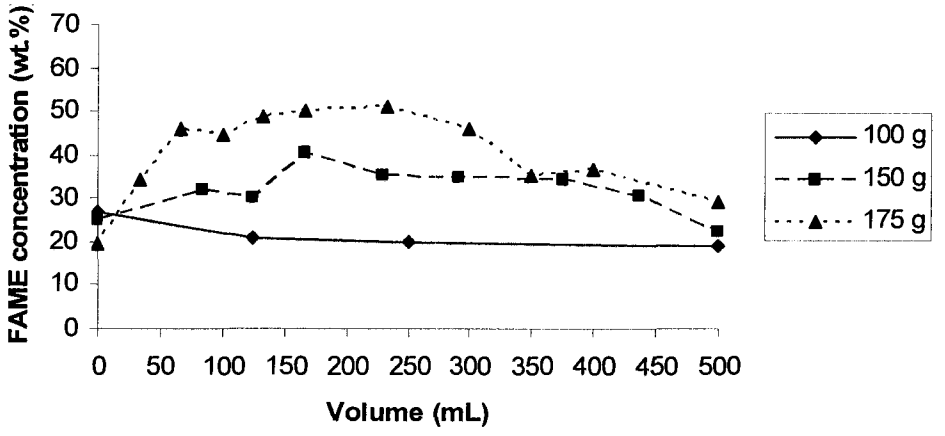

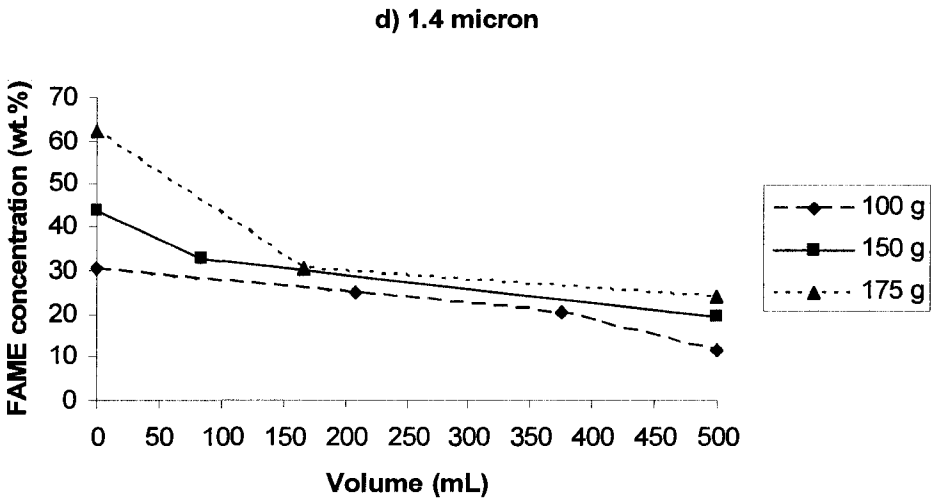


Figure 3.9: Concentration of FAME in the permeate stream vs. the volume of methanol/NaOH injected for various initial oil loadings at 0.05, 0.2 and 1.4 micron membrane pore sizes.

# Chapter 4

# Methanol Recycling in the Production of Biodiesel in a Membrane Reactor

*Fuel,* **2008**, 87: 825-833.

## 4.2. Introduction

Biodiesel is a cleaner burning diesel alternative fuel converted from biomass into liquid fuel. It is similar to and compatible with petroleum diesel such that it can be used as blends without engine modification [1]. As a form of bioenergy, biodiesel is nearly carbon-neutral having no overall net increase in the atmospheric $CO_2$ inventory, making an almost zero contribution to global warming [2]. Thus, it is more environmentally friendly than petrodiesel.

Biodiesel or fatty acid methyl ester (FAME) is defined as a fuel comprised of mono-methyl esters of long chain fatty acids derived from vegetable oils or animal fats. A mono-methyl ester is the product of the reaction of methanol with a fat or oil (i.e., triglyceride or TG) to form glycerol (also called glycerin) and the esters of long chain fatty acids. Figure 4.1 shows a detailed elementary reaction scheme for the reaction of TG with methanol to produce a diglyceride (DG); the reaction of DG with methanol to produce a monoglyceride (MG); and finally the reaction of MG with methanol to produce glycerol; each step yields a FAME molecule [3, 4].

In Figure 4.1, $R_1$, $R_2$, and $R_3$ are long chain hydrocarbons (e.g., palmitic acid - $(CH_2)_{14}$-$CH_3$)), sometimes called fatty acid chains. Each of the reactions is reversible with a different rate constant ($k_n$) denoting that the forward and reverse reactions take place at different rates. The reactions are all known to be second order or pseudo-second order [4]; the last step, formation of glycerol from MG, proceeds more rapidly than the formation of MG from DG [5].

There are two key roadblocks to the development of a continuous biodiesel production process. These are the reversibility of the transesterification reaction when full conversion is desired, and the immiscibility of the lipid and alcohol feedstocks. The reaction system is essentially heterogeneous as the non-polar (mostly TG) and polar (mostly methanol) phases are immiscible. The formation of a saponified reaction product with a basic catalyst promotes emulsification, allowing the reaction to proceed rapidly [6]. The reversible nature means that the reaction can never reach 100% completion (typically, 98% or lower [1]). Subsequently, for batch biodiesel production, there will tend to be unconverted or partially converted material contaminating the biodiesel. This is of particular importance due to the strict guidelines regarding commercial biodiesel purity

for use in diesel engines. Both these problems can potentially be overcome through the use of a membrane reactor [7].

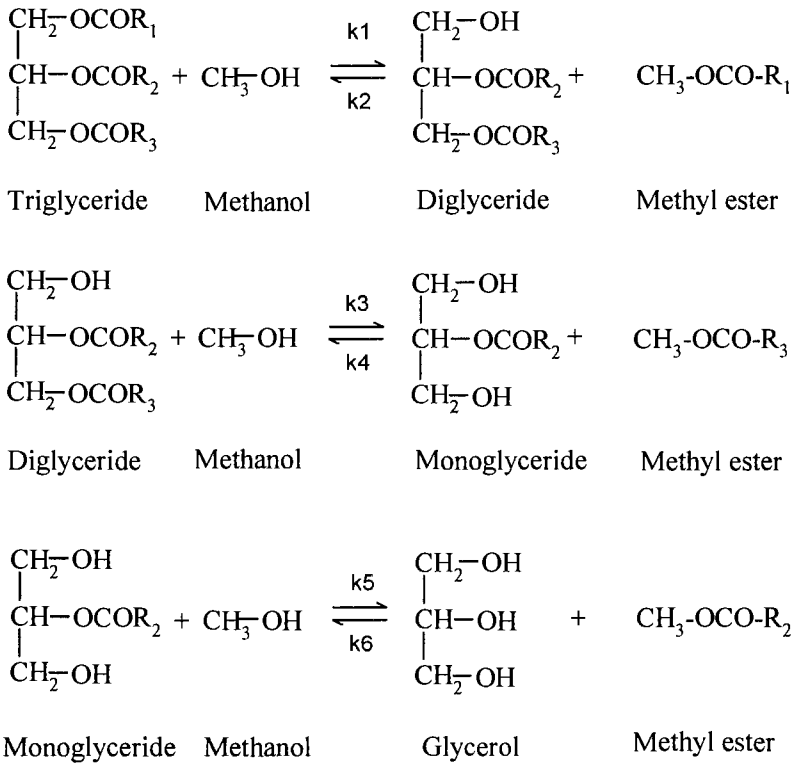


Figure 4.1. Elementary reaction scheme for transesterification of TG.

Membrane reactors can be used to carry out a reaction and a membrane-based separation simultaneously in the same physical enclosure [8]. Ideally, the membrane reactor system will separate any unreacted material from the product, so that the reactants are retained inside the reactor for a longer residence time and the products are removed from the reactor in the permeate. Recently, Dubé et al. [7] applied membrane reactor technology to a biodiesel production process. They found that a micro-porous inorganic membrane reactor could selectively remove fatty acid methyl ester (FAME), methanol and glycerol during the transesterification from the TG. The biodiesel membrane reactor is based on the general principle that oil particles form droplets in hydrophilic environments. When the reactants are mixed, oil droplets with diameters larger than the membrane pore size are formed [9]. A continuous phase comprising FAME, methanol and glycerol, readily permeates through the membrane while the oleophilic phase

containing TG is retained. This permits removal of a very pure product irrespective of reaction completion.

Most commercial transesterification processes for biodiesel production are conducted as batch reactions using methanol:oil feed ratios ranging from 10:1 to 12:1 (i.e., methanol volume fractions of 0.29 and 0.33, respectively). The advantages of continuous reaction systems over batch systems are well-known. A novel semi-continuous membrane reactor has been developed to produce biodiesel on a large-scale and is currently being extended to continuous operation [10]. The membrane reactor was shown to operate effectively in semi-continuous mode at volume fractions of methanol greater than 0.38 [9]. The permeate from the membrane module readily separated into two phases with a clear boundary at room temperature. The lower phase was a methanol/glycerol-rich polar phase and the upper one was a FAME (or biodiesel)-rich non-polar phase. The polar phase contained mostly methanol (>70 wt.%) in addition to glycerol and some FAME. To decrease the overall methanol:oil molar ratio of the process, recycling of the polar phase would be necessary. Because the methanol and catalyst are distributed predominantly in the polar phase [11], recycling would make full use of the methanol and save catalyst while maintaining the molar ratio in the reaction mixture high enough to overcome the reversibility of the reaction. On the other hand, an upper limit to the recycle ratio may exist beyond which the reaction rate may be compromised. The recycling ratios were selected to achieve an overall alcohol use similar to that found in commercial applications and up to a 0.5 volume fraction of methanol in the reactor (i.e., no recycling).

In this paper, we report on recycling of the polar phase of the permeate stream of the membrane reactor used for biodiesel production. The goals of this study are: to decrease the overall molar ratio of methanol to lipid in the biodiesel production process; to monitor membrane performance indicators such as trans-membrane pressure (TMP) in face of the accumulation of glycerol in the reactor loop; and to seek feasible recycling conditions.

## 4.3 Experimental

### 4.3.1 Material

Canola oil (No-Name®, Toronto, ON, Canada) was purchased at a local food store. Tetrahydrofuran (THF, 99.98% purity, EMD Chemicals Inc., Gibbstown, NJ, US), hydrochloric acid (HCl, 36.5-38%, reagent grade, Fisher Scientific Co., Nepean, ON, Canada), methanol (99.85% purity, Commercial Alcohols Inc.; Brampton, ON, Canada) and sodium hydroxide (NaOH, reagent grade, ACP Chemicals Inc.; Montreal, QC, Canada) were all used as packaged. Other chemicals (e.g., standards) were obtained from commercial sources. Solvents and analytical reagents were of high performance liquid chromatography (HPLC) grade.

### 4.3.2 Equipment and membrane

A schematic of the membrane reactor is shown in Figure 4.2. The figure shows the main sub-systems which include: reagent feed system; backpressure valve and cooling system for permeate; circulation pump; membrane module; Coriolis meter; heat exchange system, and safety and relief valve system.

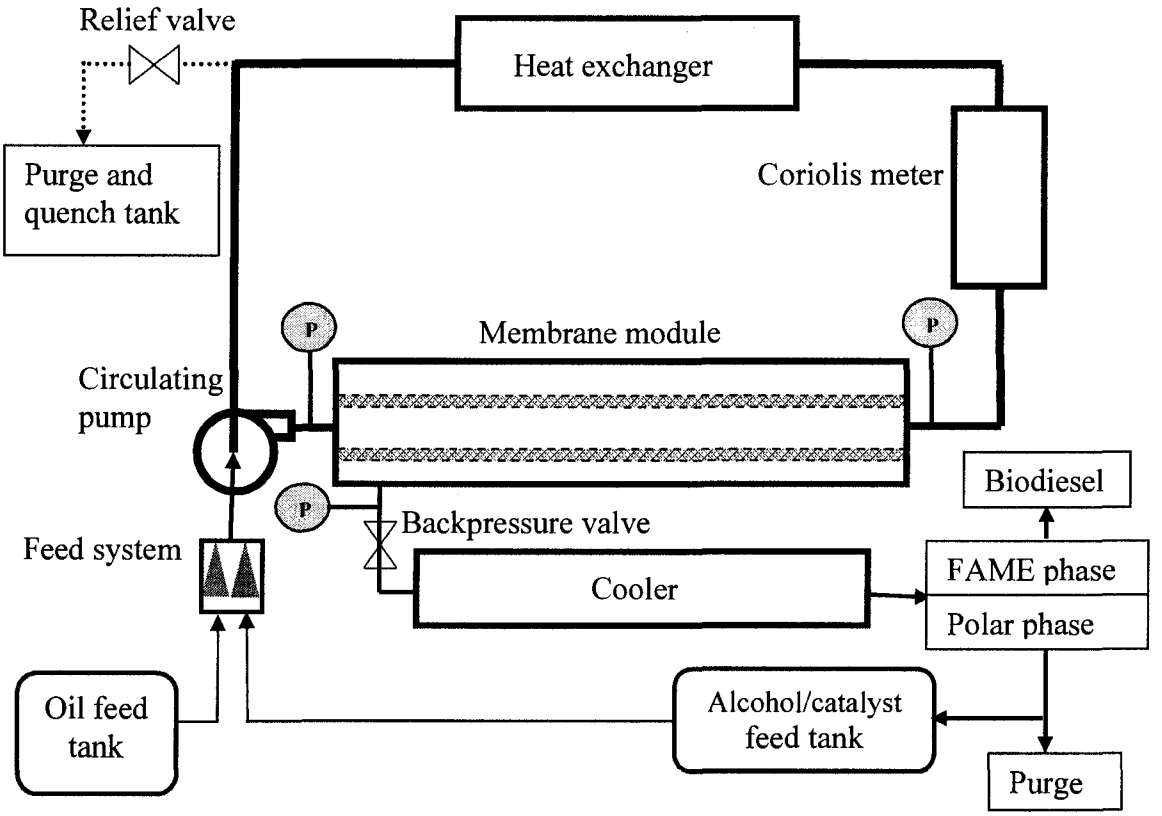


Figure 4.2: Schematic diagram of the membrane reactor

The circulating pump, membrane module, Coriolis meter and heat exchanger make up a circulating loop within which the transesterification reaction occurs at a controlled temperature and pressure. A feed system and a backpressure valve interface between this pressurized loop and atmospheric conditions. The feedstock oil and methanol/catalyst are pumped proportionately into this pressurized loop and circulated with the circulating pump. The multi-component mixture flows in the retentate side of the membrane as a suspended mixture of lipids dispersed in a methanol-rich phase. The FAME/methanol/glycerol phase permeates through the membrane and is collected for purification and/or recycling. The permeate stream is brought to atmospheric conditions by the backpressure valve and cooler. The permeate cooler reduces the temperature, thus preventing the volatilization of methanol on release to atmospheric conditions. The retentate stream passes through the Coriolis meter, is then heated by a heat exchanger, and the fluid is then looped back to the feed side of the circulation pump. The Coriolis

meter in our system is the Proline Promass 83 (Endress and Hauser, Greenwood, IN, US) which can provide mass flowrate data corrected for any temperature variations and density. The heat exchanger (Neslab Instruments, Inc., Portsmouth, NH, U.S.A.) is used to control the temperature within the reactor. The overall internal volume of the membrane reactor is 6.0 L.

Effective biodiesel reactions require temperatures on the order of 65°C and a strong base or acid catalyst. An inorganic carbon membrane was used due to its thermal stability and its resistance to chemical attack [7]. Ceramic membranes are popular in commercial applications. Siskens [12] described many advantages of ceramic membranes: chemical and thermal stability, narrow pore size distribution, high porosity, high flux, mechanical strength, long lifetime, etc. Aside from withstanding the reaction conditions, chemical and thermal stability also permits the ceramic membrane to be cleaned more efficiently when dirty feedstock such as waste oil is used. In this study, a filtanium™ ceramic membrane (TAMI, Nyons, France) constructed of a titanium oxide support and active layer was employed. The molecular weight cut off (MWCO) of the membrane was 300 kD and its configuration was multi-channel tubular. No TG was found in the permeate stream, as confirmed by gel permeation chromatography (GPC) analysis. The smallest calculated oil droplet size in the membrane reactor from Cao et al. [9] was 12 microns. This greatly exceeds the membrane pore size of the 300 kD membrane, which is expected to be approximately 0.02 microns as calculated by the size of a 300 kD dextran molecule [13]. This value is also in good agreement with dynamic light scattering measurements performed on 246 kD dextran, which yielded a range of particle sizes from 0.01 to 0.04 microns with an average of 0.025 microns [14].

### 4.3.3 Procedures

Three runs were carried out to compare different recycling ratios: 100%, 75% and 50% by volume, e.g., 75% recycling implies that every 0.75 L of polar phase was mixed with 0.25 L methanol with 1 wt.% (by weight of oil) NaOH catalyst and pumped into the reactor circulating loop at a feed rate of 3 L/h, while the feed rate of canola oil was also kept at 3 L/h.

Initially, 3 L of methanol/NaOH solution (1 wt.% NaOH by weight of oil) was charged into the reactor through the feed system. Three litres of canola oil were then injected into the reactor. The back pressure valve was shut initially and the heat exchanger and circulating pump were turned on. When the temperature of the reaction mixture reached 65°C (after ~60 min), the feed system was activated and both the methanol/catalyst and oil feed rates were each set to 3 L/h (i.e., the reactor residence time was 1 h). The canola oil and methanol/catalyst/recycled polar phase streams were fed continuously into the pressurized loop. The back pressure valve regulated the membrane reactor pressure to ~275.8 kPag (40 psig). Almost immediately after the feed streams were fed to the reactor, permeate began to flow.

Reactor pressure, temperature, trans-membrane pressure (TMP), mass flowrate, and density were recorded continuously. Permeate samples were taken every 20 min up to 8 h or when the TMP approached 173.4 kPa. The reaction was immediately halted in each sample vial by the addition of 12N hydrochloric acid in methanol to a pH of 7.0. Meanwhile, the permeate was collected into a 4 litre Erlenmeyer flask, cooled to room temperature, and allowed to separate for a 0.5 to 1 h period into non-polar and polar phases. The polar phase was transferred to a feed tank and recycled as described above. Over the course of a typical reaction for a 1 h residence time, the polar phase was transferred to the feed tank about 4 times. After each run, the pumps and heat exchanger were stopped and the system completely drained. Following each run, the membrane was backwashed and the system was flushed for 30 min with pure methanol and drained.

After over one year of operation, no decreases in permeate flux were observed. The membrane was operated in a cross-flow mode and the concentration of base used in catalyzing the reaction was typical of that used in aqueous cleaning solutions for membranes.

### 4.3.4 Characterization

GPC was used to quickly analyze the permeate samples. Each 20 mL sample of neutralized permeate (or retentate) solution was filtered through a 0.2 μm polytetrafluoroethylene (PTFE) syringe filter into a clean vial. To about 0.04 g of sample was added ~2 g of THF in a 4 mL vial. A Waters Corp. GPC system consisting of a pump,

flow controller, differential refractometer and auto-sampler was used. Waters Millennium 32$^{TM}$ software was utilized for analysis. The columns were two 300 x 7.5 mm Phenogel columns of 3 μm and 100 Å pore size (Phenomenex, Torrance, CA) connected in series. The GPC analysis was conducted according to the method shown by Dubé et al. [15] and Darnoko et al. [16]. The mobile phase was HPLC grade THF at a flowrate of 0.5 mL/min at 25°C. The sample injection loop was 20 μL with a running time of 60 minutes. A calibration curve was generated from six standards: triolein (TG), diolein (DG), monoolein (MG), methyl oleate (FAME), glycerol and methanol. The injection masses were plotted against the peak area. The calibration curves of the standard solutions showed good linearity. The retention times of the standards are shown in Table 4.1. The canola oil feedstock contained roughly 67.9% oleic acid (18:1), 18.8% linoleic acid (18:2), 6.6% linolenic acid (18:3), 4.4% palmitic acid (16:0) and 2.3% stearic acid (18:0) [17]. Given that the majority of the methyl ester was derived from oleic acid (i.e., 67.9%) and that 95.6% of all FAME produced contained 18 carbons in its alkanoate chain, methyl oleate was used as the sole standard for FAME in the GPC calibration curve.

Table 4.1: The retention times of standards for GPC

| Standard | Retention time (min) |
|---|---|
| Triolein (TG) | 24.57 |
| Diolein (DG) | 25.45 |
| Monoolein (MG) | 27.12 |
| Methyl oleate (FAME) | 28.68 |
| Glycerol | 30.95 |
| Methanol | 35.2 |

## 4.4 Results and Discussion

### 4.4.1 Methanol: oil molar ratio

The most important purpose of recycling the polar phase is to decrease the overall methanol:oil molar ratio while maintaining two phases in the reactor and a 50% volume

fraction of oil in the reactor [9] All three runs were started at a methanol:oil molar ratio of 23.93 (volume ratio methanol:oil = 1:1). As shown in Figure 4.3, three different polar phase recycle ratios were employed. For the 50% polar phase recycle case, the polar phase from the membrane reactor permeate was blended in a 50:50 polar phase: fresh methanol (fresh methanol includes 1 wt.% NaOH catalyst) volume ratio. The 75 and 100% recycle cases employed 75:25 and 100:0 polar phase: fresh methanol volume ratios, respectively. As seen in Figure 4.3, eventually these schemes resulted in overall methanol: oil ratios in the reactor of 15:1, 12:1 and 10:1 for the 50, 75 and 100% recycle cases, respectively.

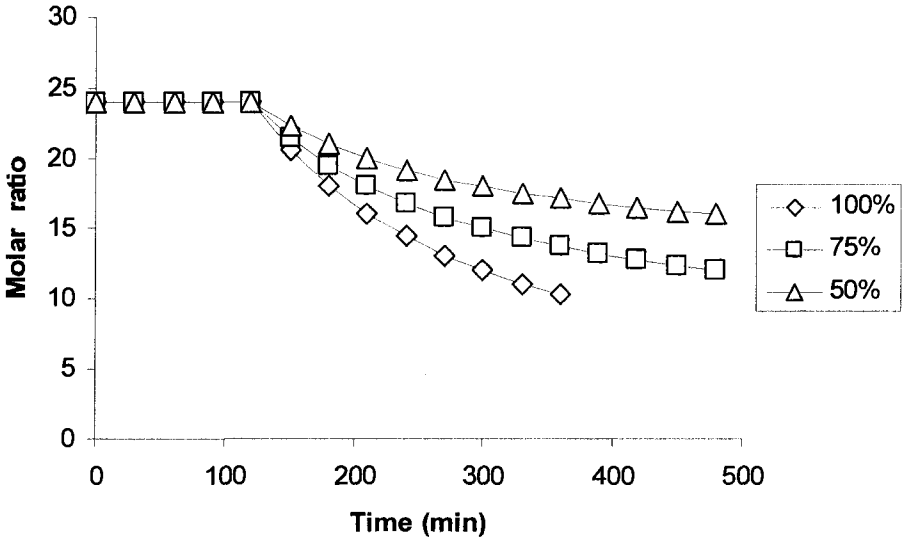


Figure 4.3: Cumulative overall methanol: oil molar ratio trends at 50, 75 and 100% recycle ratios.

### 4.4.2 Permeate de-phasing and recycling

At each recycle ratio, upon cooling to 15°C, the permeate separated instantaneously into two distinct phases. A clear demarcation was observed at the FAME-rich and methanol-rich phase interface. In the FAME-rich phase, the composition was >85 wt.% FAME with the remainder consisting mostly of methanol and trace amounts of DG and catalyst. The methanol and catalyst could be easily removed with a single water

wash step. Figure 4.4 shows a typical GPC chromatogram of the non-polar (FAME-rich) permeate phase prior to water washing. No TG or glycerol was detected and other than the occasional trace amounts of DG, these samples contained only FAME and methanol (compare to Table 5.1). Evidently, this indicates a high purity FAME product.

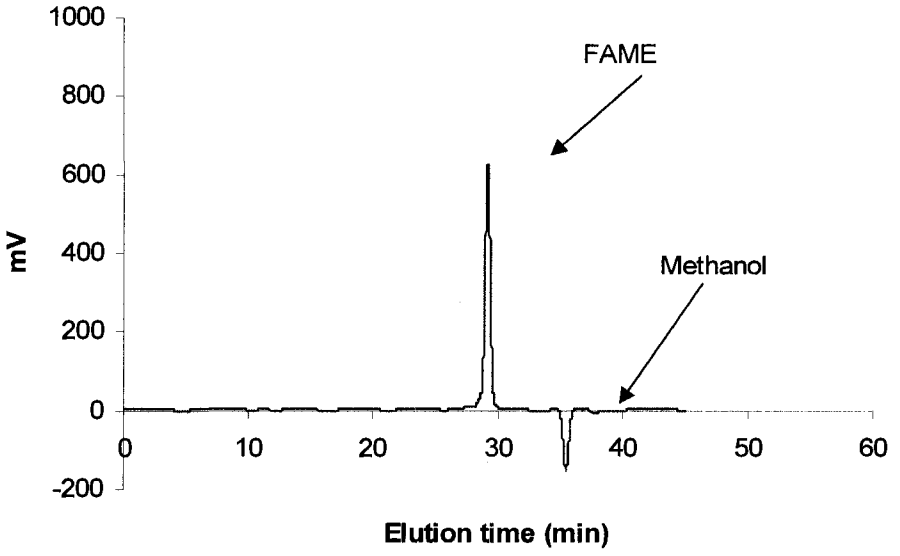


Figure 4.4: Typical GPC chromatogram of FAME-rich phase from permeate.

At the completion of the runs, the membrane reactor retentate was observed to contain a stable interfacial emulsion similar to that obtained in a batch reactor run under identical process conditions. A conventional batch reaction could require several hours to achieve complete separation of the FAME-rich and methanol/glycerin-rich phases. This is because emulsions from the oil or soaps produced during the reaction process may act as emulsifiers or dispersants to prevent phase separation. The situation in a batch reactor would even be worse when using high free fatty acid feedstock. In that case, significant reduction in biodiesel yield would result. The membrane is thus performing an additional purification function by retaining emulsions within the reactor (retentate). This was tested by employing the membrane reactor as a batch reactor, i.e., without permitting the outflow of permeate. The entire content of the reactor was emptied and greater than 3 h was required to achieve an effective separation of the reactor contents. A separate and stable emulsion layer was visible between the two phases.

### 4.4.3 Effect of glycerol on TMP and flowrate

In the circulating loop, the density and mass flowrate of the reaction mixture was monitored using a Coriolis meter. During the first 120 min of the reaction (i.e., prior to commencing recycling), all three recycle ratio runs gave similar results in terms of density (see Figure 4.5). It was observed during that period, that the density of the reaction mixture slightly increased, due largely to the production of glycerol, and then stabilized to a steady-state value. Once recycling was initiated (at 120 min), an increase in density was observed for all runs as seen in Figure 4.5. Glycerol has a significantly higher density (1.26 g/mL at 25°C) than the other reactants (all <0.95 g/mL at 25°C). Not surprisingly, the density increase of the reaction mixture for the 100% recycling ratio was the most rapid. The 75 and 50% recycling ratios exhibited lower density increases.

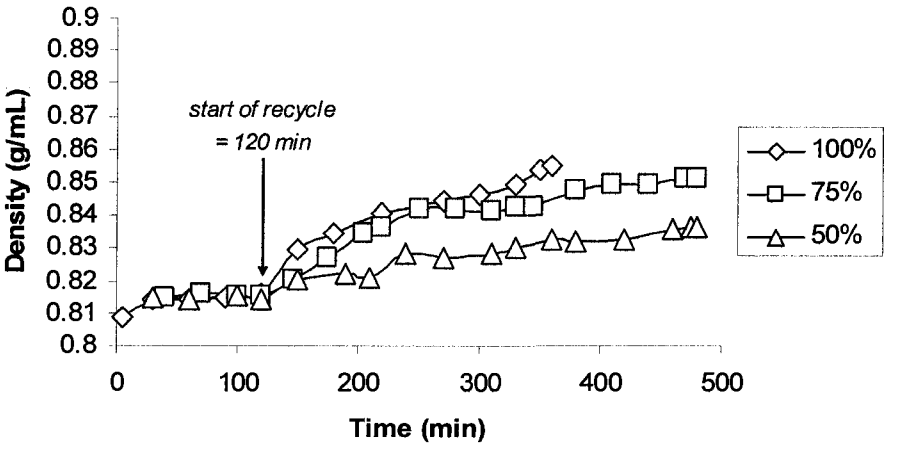


Figure 4.5: Density profiles of reaction mixture at different recycling ratios.

The mass flowrate in all cases decreased slightly over time. The pressure drop across the membrane module multiplied by the volume flowrate at a certain period of time (or PV work) was calculated. Even though the density was changing, the PV work transferred to the fluid by the circulating pump remained constant. For all recycle ratio

runs, similar results for the PV work at 1 h were achieved: 20000, 19900, and 20200 Nm, respectively, for the 100, 75 and 50% recycle ratios.

Figure 4.6 shows the TMP trends for each recycle case. As mentioned earlier, all reactants were fed at a constant rate, which implies that the data presented here are at constant permeate flux. The TMP profiles are correlated with the increasing viscosity of the reaction mixture. In other words, the higher the glycerol content in the reactor (or higher recycle ratio), the higher the TMP. The results indicate that in order to operate at a 100% recycle ratio, higher temperatures would be needed to reduce the viscosity of the permeate. Otherwise, as one can see in Figure 4.6, the TMP for 100% recycle will increase sharply after 137.9 kPa (20 psi). This is well below the recommended maximum membrane operating pressure of 1000 kPa (145 psi).

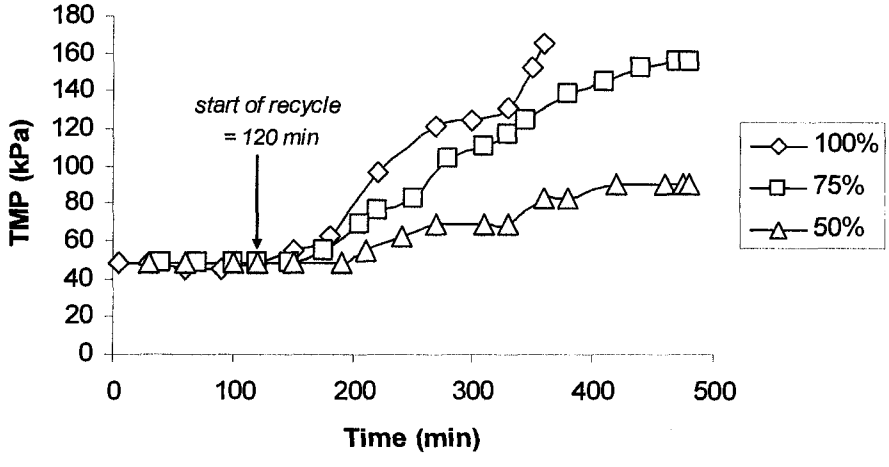


Figure 4.6: TMP profiles at different recycle ratios

Figure 4.7 depicts the TMP trends with glycerol concentration in the permeate stream. Under the reaction conditions studied, it is clear that the glycerol content played an important role in the TMP increase. When the glycerol content was lower than 6 wt.%, the TMP was in the 50-60 kPa range. However, increases in the average glycerol content resulted in increases in TMP. As can be seen in the figure, beyond glycerol concentrations of 6 wt.%, the TMP increased linearly and the slope for each recycle case

was essentially the same. The membrane reactor can function properly even at glycerol contents as high as 17.6 wt.%. Actually, even for a conventional 6:1 methanol to oil molar ratio batch reaction (assuming an oil conversion of 100%), the glycerol content in the final FAME/glycerol/methanol mixture would be ~8.5 wt.%. The corresponding TMP would be only 90 kPa. The membrane reactor can operate at TMPs far beyond that point.

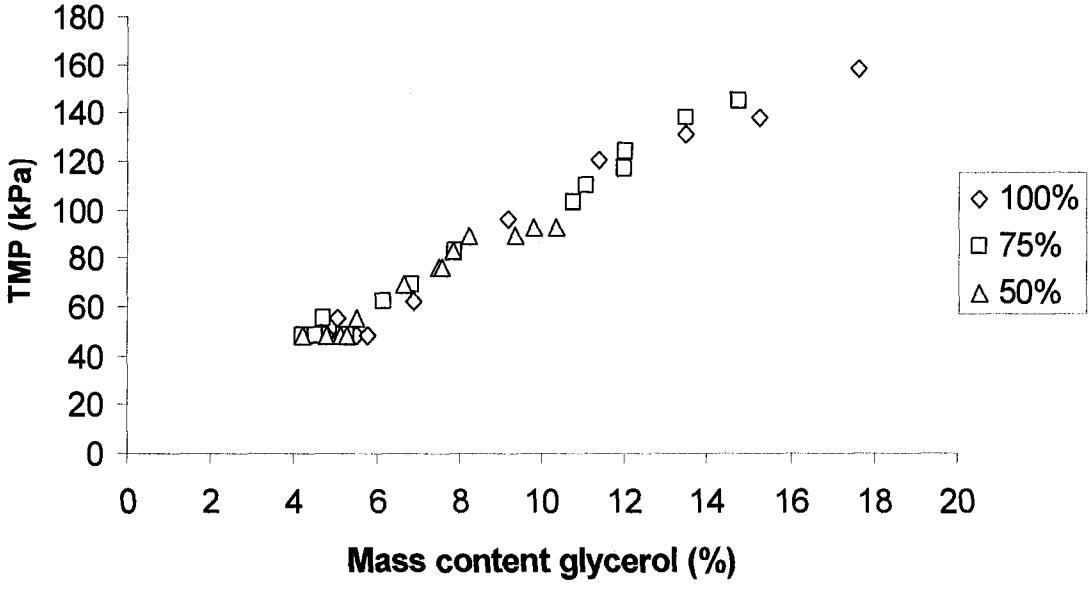


Figure 4.7: TMP vs. glycerol content in permeate stream at 50, 75 and 100% recycle ratios.

### 4.4.4 Permeate composition

Figures 4.8 through 4.10 show the composition of the polar phase and non-polar FAME-rich phase from the de-phased permeate stream at different recycle ratios. For the 100% recycle ratio (see Figure 4.8), no fresh methanol was added to the system during recycle, and thus the methanol concentration in the polar phase showed a distinct decrease. The FAME concentration in the polar phase decreased from 11.01 to 2.98 wt.%, which means that more FAME was distributed into the non-polar phase with recycling. At the same time, the glycerol concentration exhibited a dramatic increase: after 2 h of recycling, its concentration in the polar phase reached 40.4 wt.%. The colour of the polar phase also changed from amber to dark brown. The FAME concentration in the FAME-

rich non-polar phase increased from 85.7 to 92.4 wt.%. The remaining part of that phase, i.e., methanol was therefore reduced. No glycerol was detected in the FAME-rich non-polar phase. This implies that recycling also facilitates the production of a higher purity FAME and reduces the amount of water-washing necessary to achieve the desired fuel specification.

Glycerol is highly soluble in methanol and is found mainly in both the reactor and permeate methanol phases. Over time, glycerol accumulated in both these phases. Thus, it would be important to purge the accumulated glycerol when running continuously by removing part of the methanol-rich phase from the permeate stream prior to it being reused in the reactor. The 75 and 50% recycle ratio cases exhibited the same trends of compositions as the 100% recycle case although to a lesser extent (see Figures 4.9 and 4.10, respectively).

Figure 4.11 shows the overall methanol, glycerol and FAME concentrations in the permeate stream based on the data from Figures 4.8 through 4.10. This reflects the composition of the permeate as it exits the reactor loop prior to phase separation. For all three runs, the methanol concentration decreased. The FAME concentration increased and remained in the range 55 to 60 wt.% after 40 min. It appears that FAME concentration was independent of the recycle ratio. The overall glycerol concentration increased with time for all cases with the 100% recycle ratio case showing the most dramatic increase. As mentioned earlier, the glycerol content reached as high as 17.6 wt.%, which is much higher than the level for biodiesel batch production at the most ambitious commercial conditions, i.e., 8.54 wt.% for a methanol:oil molar feed ratio of 6:1. Thus, a glycerol purge stream, either from the permeate or retentate side, would be necessary to remove the accumulated glycerol and to keep the TMP to a reasonable level.

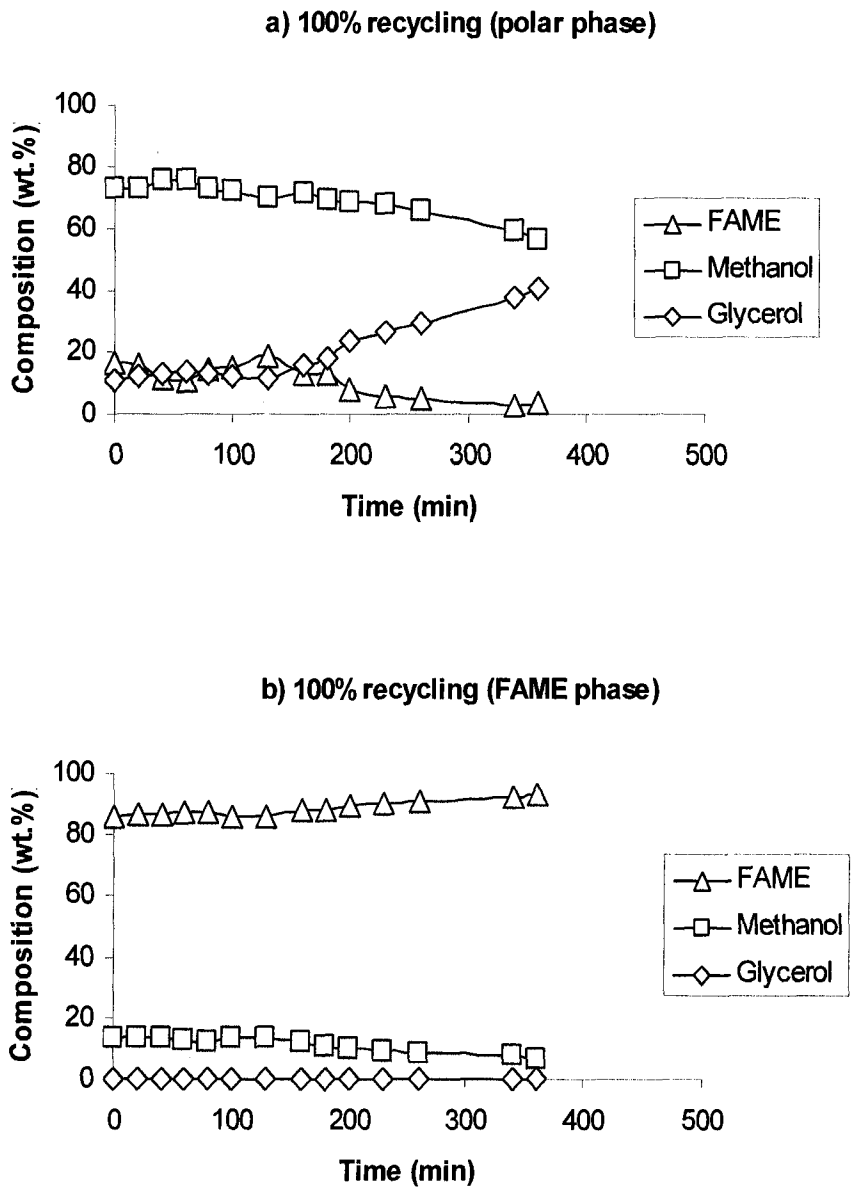


Figure 4.8: Mass composition of polar and non-polar permeate phases at 100% recycle ratio.

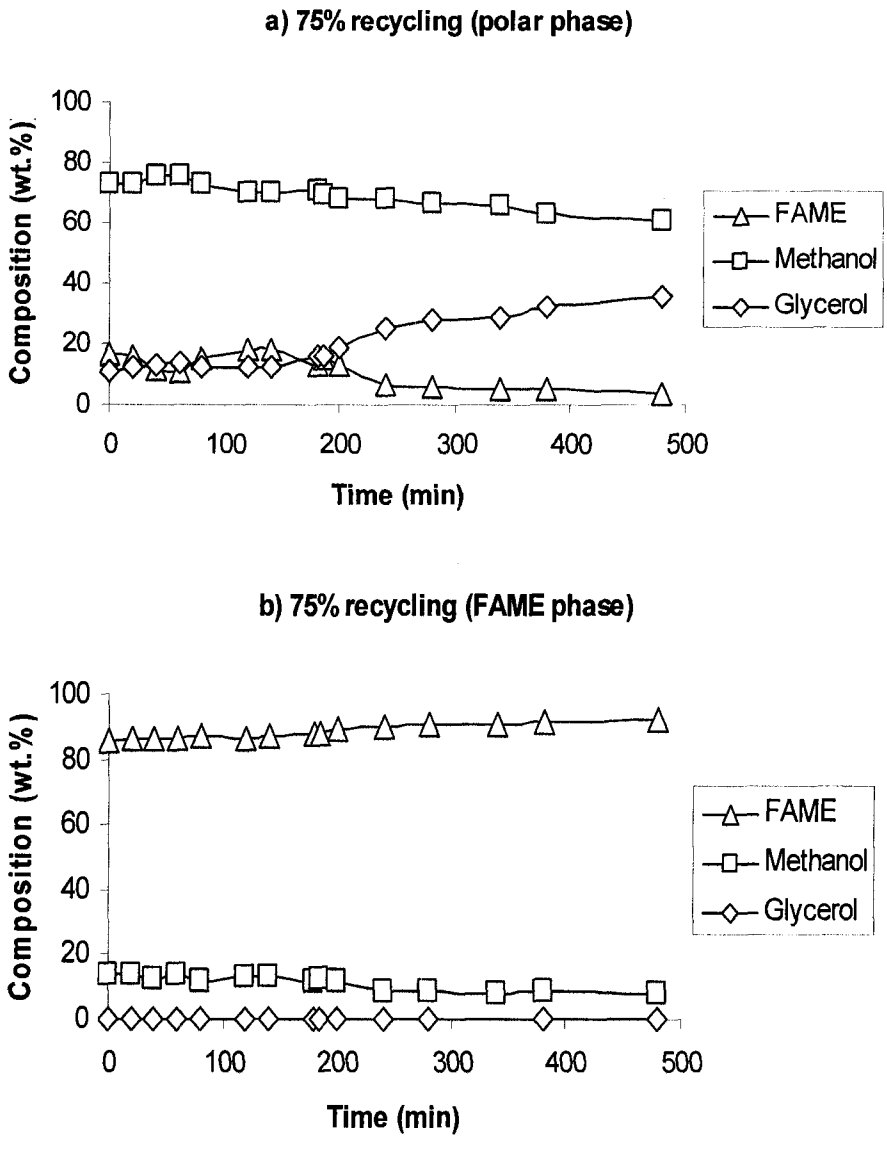


Figure 4.9: Mass composition of polar and non-polar permeate phases at 75% recycle ratio.

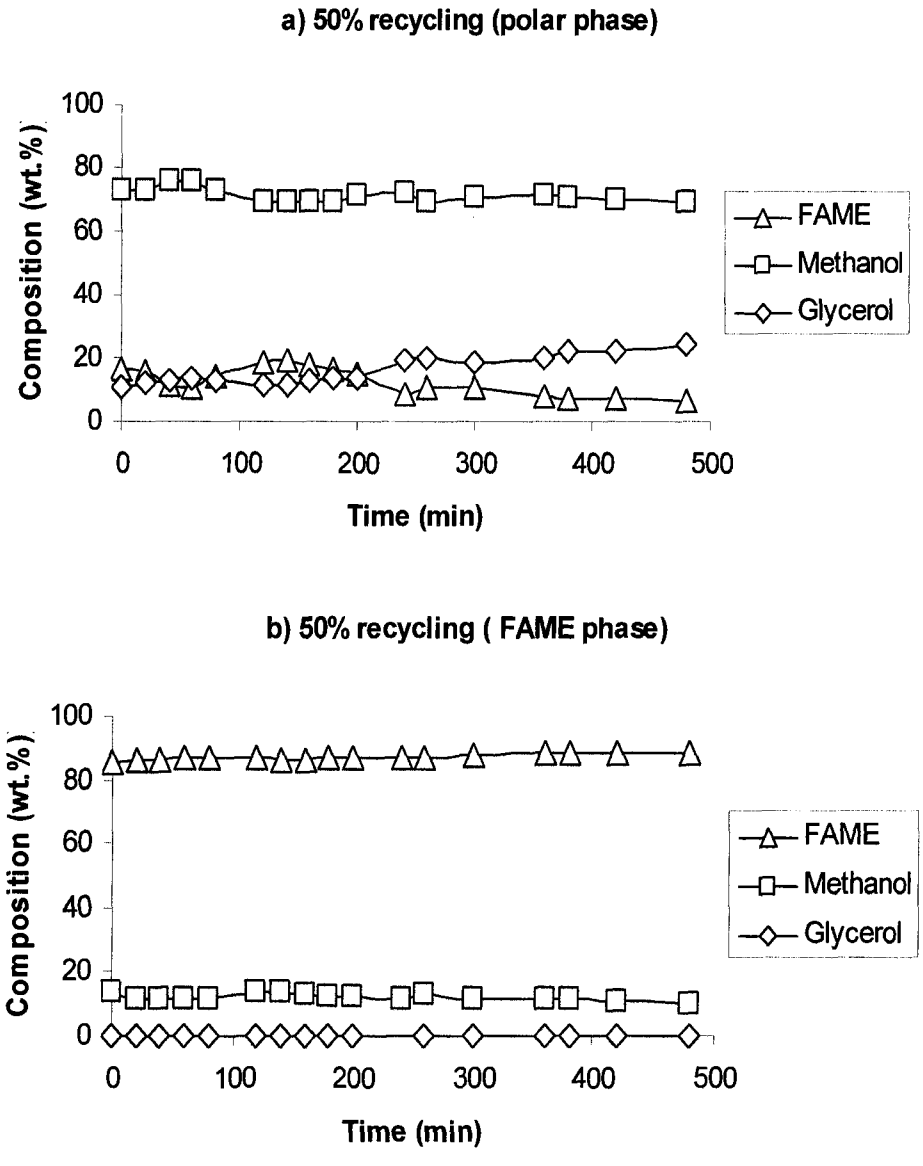


Figure 4.10: Mass composition of polar and non-polar permeate phases at 50% recycle ratio.

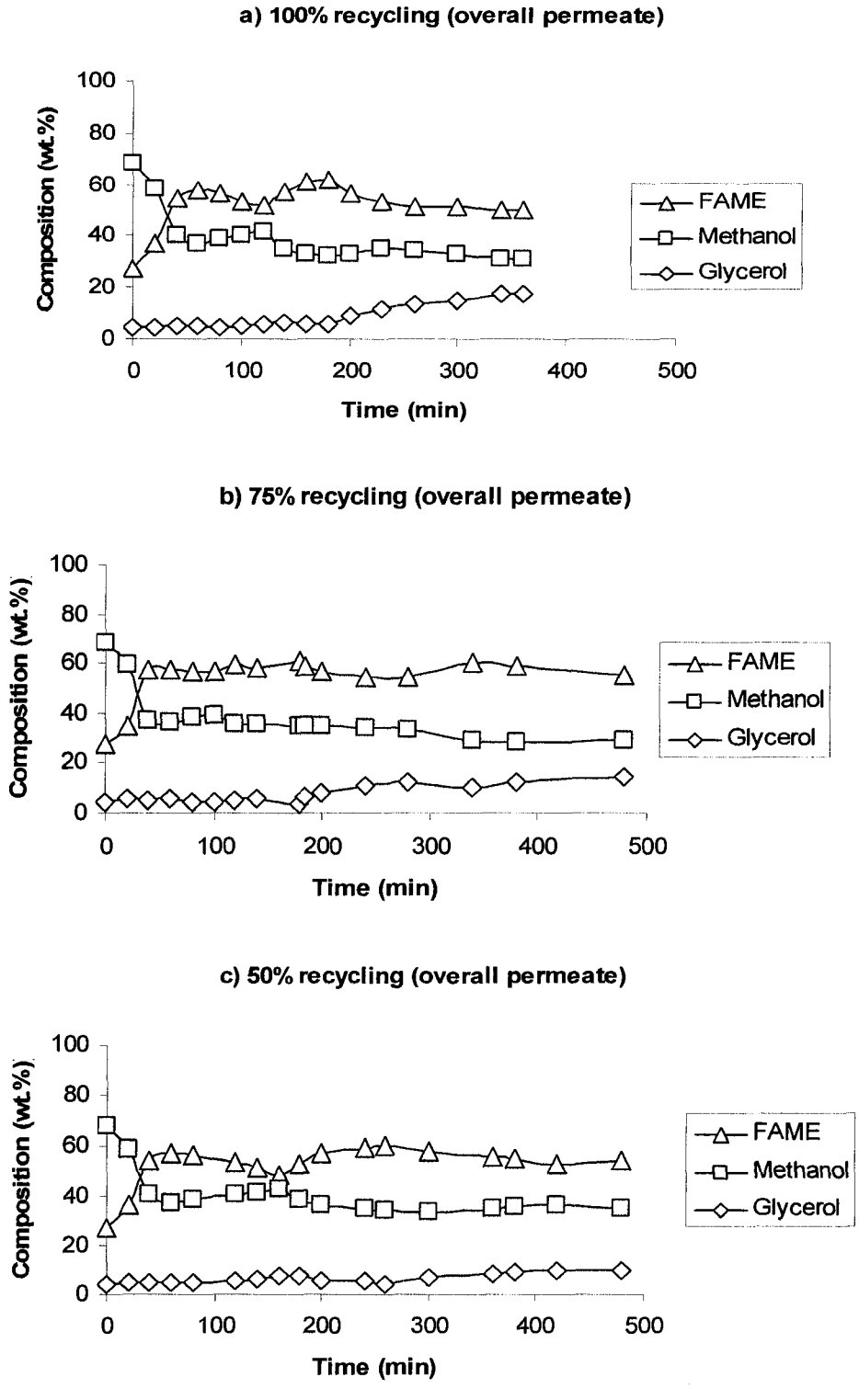


Figure 4.11: Concentrations in the permeate stream.

### 4.4.5 FAME Production

As can be seen in Figures 4.8b, 4.9b and 4.10b, the FAME concentration in the FAME-rich non-polar permeate phase was in the range 85 to 93 wt.% and showed a slow increase with time. For each run, every two hours, the FAME phase density was measured as reported in Table 4.2. Only slight increases in density were measured due to the absence of glycerol in the FAME-rich non-polar permeate phase. Based on these densities, the FAME production in the membrane reactor can be calculated. Figure 4.12 shows the cumulative FAME production with time. The data from the three runs overlap, which implies that recycling has no effect on the transesterification reaction rate. In other words, there was no significant glycerol inhibition in the membrane reactor when glycerol concentrations were 17.6 wt.% or lower in the permeate stream.

Table 4.2: Density of FAME phases for each case

| Time period of each run | Density for 100% recycle (g/mL) | Density for 75% recycle (g/mL) | Density for 50% recycle (g/mL) |
|---|---|---|---|
| 0~120 min (before recycle) | 0.853 | 0.853 | 0.852 |
| 121~240 min (recycle) | 0.860 | 0.856 | 0.857 |
| 241~360 min (recycle) | 0.872 | 0.867 | 0.861 |
| 361~480 min (recycle) | -- | 0.869 | 0.865 |

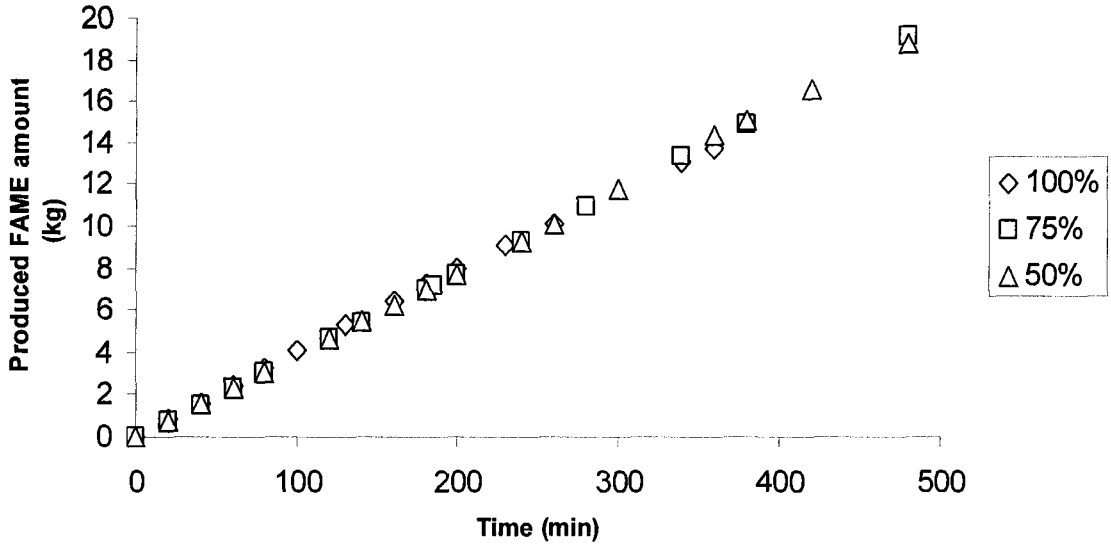


Figure 4.12: Cumulative production of FAME with time at 50, 75 and 100% recycle ratios.

Figure 4.13 shows the FAME production rate from the membrane reactor vs. glycerol concentration. Even over a broad glycerol concentration range (3.6 to 17.6 wt.%), the FAME production rate remains within a narrow range (0.0355 to 0.0425 kg/min) which implies that the reaction rate of TG is always within the range 0.0354 to 0.0423 kg/min. During the experimental period, the TG feed rate was exactly within this range, implying that the membrane reactor can be operated at residence times less than one hour and that productivity can be improved.

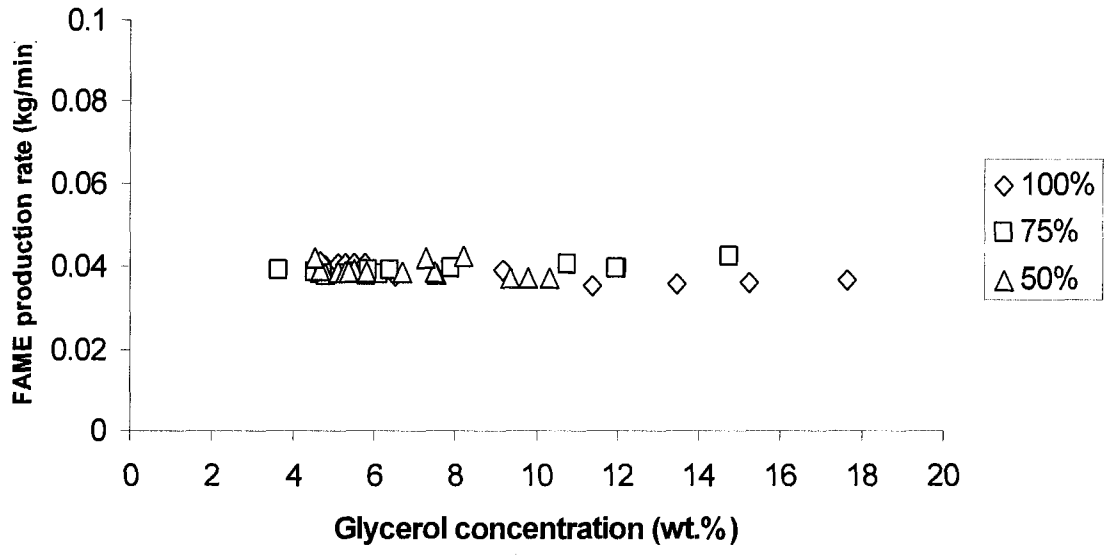


Figure 4.13: FAME production rate vs. glycerol concentration in permeate stream at 50, 75 and 100% recycle ratios.

### 4.4.6 Purity of the permeate stream

Permeate leaving the reactor was immediately cooled, as shown in Figure 4.2, to 15°C. This caused slight amounts of non-reacted DG to remain in the FAME product. In an industrial application, the homogeneous permeate would be kept at reaction temperature until all the DG would be transformed to FAME. Trace amounts of DG were detected in the FAME-rich non-polar permeate phase. No DG was found in the polar phase for all samples in all runs. This undoubtedly had to do with the fact that DG is more hydrophobic and prefers to reside in a non-polar environment. We have previously observed that when the FAME concentration is higher than 35 wt.% in the permeate stream, the DG will solubilize into the permeate stream [9]. After recycling, the average DG concentrations in the FAME-rich non-polar permeate phase were 0.34, 0.34, and 0.32 wt.% for the 100, 75 and 50% recycle ratio cases, respectively. From Figure 4.11, we observe that the FAME concentrations reached 55 wt.% or higher, which explains the presence of DG in the permeate.

If residence time or catalyst concentration is increased, conversion will increase, which increases the concentration of FAME in the reactor. Elevated concentrations of FAME can lead to the dissolution of TG, DG and MG into a single phase in batch

reactors [1]. As the concentration of FAME increases in the methanol phase, so does the solubility of DG in this phase. This is why DG is transported through the membrane pores above 35 wt.% FAME concentrations in methanol [9]. Thus, reducing the residence time and/or lowering the catalyst concentration to decrease the FAME concentration in the retentate side should prevent the occurrence of DG in the permeate.

### 4.5 Conclusions

Continuous biodiesel production was successfully conducted using canola oil, methanol, and NaOH in a membrane reactor. The permeate stream phase separated readily at room temperature allowing for separate polar (methanol- and glycerol-rich) and non-polar (FAME-rich) phases. This enabled the polar phase to be recycled to the feed side of the membrane reactor at various volume ratios. Recycling of the polar phase resulted in a reduction of the overall methanol:oil ratios in the reaction system to 15:1, 12:1 and 10:1 for the 50, 75 and 100% recycle cases, respectively. All of the catalyst and glycerol was also recycled as they were found exclusively in the polar phase.

In the non-polar (FAME-rich) part of the phase separated permeate stream, no TG, MG or glycerol were detected. It should be noted that the samples were not water washed prior to analysis. Therefore, a high purity FAME product, free of non-saponifiable materials was produced.

The recycled glycerol was shown to exert significant influence on the fluid density in the reaction loop and to increase the trans-membrane pressure (TMP). It was shown that the reactor could operate at TMPs well beyond that equivalent to a 6:1 methanol:oil molar ratio in a batch reaction. One could, however, operate at recycle and operating conditions equivalent to a 6:1 overall methanol:oil ratio but glycerol must be purged to prevent glycerol accumulation within the membrane reactor. In addition, no significant glycerol inhibition of the production of FAME was detected in the membrane reactor. FAME concentrations in the permeate were found to be independent of the recycling ratios, and were maintained between 55 and 60 wt.% after 40 min of reaction time for all recycle ratios tested. The FAME production rate ranged from 2.13 to 2.55 kg/h. This production rate could be improved by operating the membrane reactor at lower residence times.

## 4.6 Acknowledgements

The authors would like to thank the Natural Sciences and Engineering Research Council of Canada (NSERC) and the Ford Foundation for financial support.

## 4.7 References

[1] Knothe G., Krahl J., and Van Gerpen J., The Biodiesel Handbook, AOCS Press: Champaign, Illinois 61826-3489, 2005; 1:2-36.

[2] Van Gerpen J., Biodiesel Processing and Production, Fuel Processing Technology, 2005; 86:1097-107.

[3] Freedman, B., Pryde E. H., and Mounts, T. L., Variables Affecting the Yields of Fatty Esters from Transesterified Vegetable Oils. J. Am. Oil Chem. Soc., 1984; 61:1638-43.

[4] Freedman, B., Butterfield, R. O., and Pryde, E. H., Transesterification Kinetics of Soybean Oil, J. Am. Oil Chem. Soc., 1986; 63:1375-80.

[5] Komers K., Stloukal R., Machek J. and Skopal F., Biodiesel from Rapeseed Oil, Methanol and KOH 3: Analysis of Composition of Actual Reaction Mixture, Eur. J. Lipid Sci. Tech., 2001; 103:363-71.

[6] Van Gerpen J., Shanks B., Pruszko R., Clements D., and Knothe G., Biodiesel Production Technology, National Renewable Energy Laboratory, NREL/SR-510-36244, 2004; (p. 30).

[7] Dubé, M.A., Tremblay, A.Y., and Liu, J., Biodiesel Production Using a Membrane Reactor. Biores. Tech., 2007; 93:639-47.

[8] Koros W.J., Ma Y.H., and Shimidzu T., Terminology for Membranes and Membrane Processes, IUPAC, J. Membrane Sci., 1996; 120:149-159.

[9] Cao P., Tremblay A.Y., Dubé M.A., and Morse K., Effect of Membrane Pore Size on the Performance of a Membrane Reactor for Biodiesel Production, Ind. Eng. Chem. Res., 2007; 46:52-58.

[10] Tremblay, A.Y., and Dubé, M.A., Biodiesel Production using Membrane Reactors, PCT Patent filed February 27, 2006.

[11] Chiu C, Goff M. J., and Suppes G. J., Distribution of Methanol and Catalysts between Biodiesel and Glycerin Phases. Bioenergy, Food, and Natural Products, 2005; 51:1274-8.

[12] Siskens, C. A. M., Application of Ceramic Membrane in Liquid Filtration, Membrane Science and Technology Series 4: Fundamentals of Inorganic Membrane Science and Technology, Elsevier Science, 1996; 13:238-42.

[13] Granath, K., and Kwist, B., Molecular Weight Distribution Analysis by Gel Chromatography on Sephadex, J. Chromatography, 1967; 28:69-81.

[14] Porsch, B., and Sundelof, L. O., Size-Exclusion Chromatography and Dynamic Light-Scattering of Dextrans in Water - Explanation of Ion-Exclusion Behavior. J. Chromatography A, 1994; 669:21-30.

[15] Dubé, M. A., Zheng, S., McLean, D. D., and Kates, M., A Comparison of Attenuated Total Reflectance-FTIR Spectroscopy and GPC for Monitoring Biodiesel Production. J. Am. Oil Chem. Soc., 2004; 81:599-603.

[16] Darnoko, D., Cheryan, M., and Perkins, E.G., Analysis of Vegetable Oil Transesterification Products by Gel Permeation Chromatography. J. Liq. Chrom. Rel. Technol., 2000; 23:2327-35.

[17] Lang, X., Dalai, A. K., Reaney, M. J., and Hertz, P.B., Preparation and Evaluation of Vegetable Oil Derived Biodiesel Esters as Lubricity Additives. Tribotest, 2006; 8:131-150.

# Chapter 5

# Biodiesel production using ultra low catalyst concentrations

*Energy & Fuels,* accepted on March 26, 2008

wt% for a one hour residence time (RT) and above 0.03 % for a two hour RT resulted in the steady-state biodiesel production via the membrane reactor. Such catalyst amounts are 10 to 33 times lower than those employed in the industrial production of biodiesel (e.g., 0.5 to 1 wt% sodium hydroxide concentration). Mono and triglycerides were not detected in any of the biodiesel produced in this single reaction step process. The RT in the reactor caused no obvious effect on permeate composition.

The results demonstrated that maintaining the phase separation between the oil and methanol at all times during the reaction and the ability of the membrane to separate these phases were key in obtaining high quality product. Unreacted triglycerides and unsaponifiable, oleophilic impurities in the lipid feedstock were not integrated into the final biodiesel as in conventional processes due to the presence of two phases in the reactor. The results illustrate the advantages in using a membrane reactor to produce biodiesel, where products are continuously removed from the reactor in a different phase than the lipid reactant.

**Keywords:** Biodiesel production, low catalyst use, improved glycerol quality, membrane reactor.

## 5.2 Introduction

Biodiesel is a clean-burning, renewable, liquid fuel that can be used instead of petroleum diesel in compression-ignition engines. Biodiesel is sometimes used in its pure form, B100, but most often as a 5 vol.% (B5) or 20 vol.% (B20) blend with petrodiesel. Minor engine modifications may be required in older diesel engines to avoid the dissolution of various seals when B100 biodiesel is utilized; however, B5 or B20 blends can be used in unmodified diesel engines.

Transesterification, also referred to as alcoholysis, is a process that combines triglycerides (TG) with alcohol (e.g., methanol) in the presence of a catalyst (e.g., sodium hydroxide or NaOH) in order to yield fatty acid methyl esters (FAME or biodiesel) and glycerol. Figure 5.1 depicts the classical transesterification reaction.

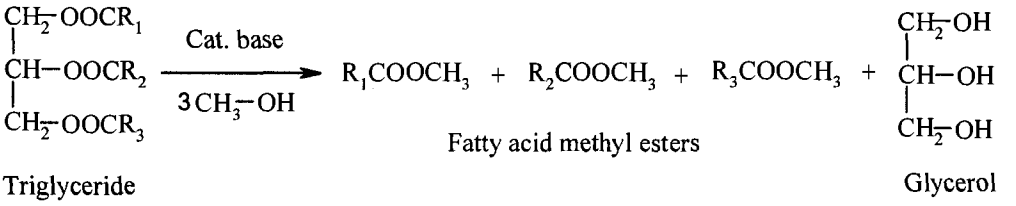


Figure 5.1: The overall reaction for the conversion of TG to FAME.

Here, $R_1$, $R_2$, and $R_3$ represent hydrocarbon chains. The conversion of triglyceride oils to methyl esters through a transesterification process reduces the viscosity of the oil by a factor of eight and increases its volatility. There are many variables that influence the reaction time of the transesterification as well as the conversion efficiency, but the most important ones include the temperature, the catalyst type and its concentration, the alcohol to ester ratio, and the mixing rate.[1] The purity of the reactants, e.g., the absence of water, free fatty acid (FFA), or other contaminants found in unrefined oils (or other feedstocks), is also very important.[2]

Although it is possible to conduct transesterification without the addition of catalyst, this approach requires high pressures (20 MPa) and temperatures (350°C).[3] Kusdiana and Saka have developed a catalyst-free method for biodiesel fuel production by employing supercritical methanol.[4] The optimum condition for the transesterification of rapeseed oil to biodiesel fuel was found to be 350°C, at a pressure of 43 MPa, with a molar ratio of 42:1 of methanol to oil. The great advantage of this method was that FFAs present in the oil could be simultaneously esterified with supercritical methanol.[5]

Both homogeneous and heterogeneous catalysts have been used for transesterification reactions. Homogeneous catalysts can be either bases or acids.[6] The most common catalysts are strong mineral bases such as sodium hydroxide (NaOH), sodium methoxide and potassium hydroxide (KOH). After the reaction, the basic catalyst requires neutralization with a strong mineral acid. The reason that basic catalysts are the most frequently used, is that the process is faster and the reaction conditions are moderate.[7] In fact, when a base, such as NaOH, KOH or potassium carbonate ($K_2CO_3$) is used as a catalyst, it reacts with an alcohol to form an alkoxide group which is the genuine catalyst for the transesterification.[2] This reaction is shown below where, $R'$ is a short alkali group, and $R'O^-$ is the actual catalyst:

$$OH^- + R'OH \Leftrightarrow R'O^- + H_2O \qquad (1)$$

Nonetheless, when employing base catalysts, soap can form by two kinds of undesirable side-reactions; either by neutralization of the FFA in the oil or by TG saponification. The formation of soap partially consumes the catalyst, complicates the separation and purification steps and decreases biodiesel yield.

Using KOH as a catalyst for producing biodiesel has the advantage that the production waste stream may have an economic value as a soil fertilizer, due to its potassium content. Moreover, KOH dissolves in methanol much more easily than NaOH.[8] However, high cost and lower purity are big disadvantages for the use of KOH.[9] Thus, a means of obtaining a direct transesterification with base catalysts would be to use methoxide, potassium ethoxide and sodium ethoxide, which can be produced by the dissolution of metallic sodium in alcohol. Vicente et al. concluded that near 100 wt% biodiesel yields could only be obtained with the direct use of methoxide catalysts,[6] but these are expensive and require special care in handling.

More recently, research on alcoholysis of oil has focused on the use of heterogeneous catalysts. These heterogeneous catalysts include enzymes, titanium-silicates, anion exchange resins and other solid catalysts. Solid acid catalysts have the advantage of being easily removed by filtration and can be used for large-scale production. For instance, zinc oxide supported on aluminum has been successfully employed as a catalyst.[10] Zeolites and metal catalysts have also been used for the transesterification of soybean oil.[11] Other than with chemical catalysts, biodiesel can also be synthesized from oils and fats through the use of biocatalysts.[12]

In conventional biodiesel production, an important issue is the final conversion of TG as the equilibrium reaction must be pushed to completion in two to three reaction steps. A membrane reactor technology can be introduced for biodiesel production to overcome this issue.[13] The membrane reactor technology takes advantage of the heterogeneous alcohol/lipid system leaving unreacted TG within the membrane reactor. Pushing the reaction to completion prior to product removal is not necessary with the use of a membrane reactor as high purity product is continually being removed from the reactor.

Generally, a higher concentration of catalyst drives the reaction equilibrium to the product side. It also increases the rate of reaction, thus resulting in higher productivity.[14] In the previous study, the acid catalyst concentration has been found to affect the reaction rate and conversion of canola oil to FAME in a membrane reactor under semi-continuous operation. An acid concentration of between 0.5 and 2 wt% (based on TG) substantially increased the conversion. Acid concentrations higher than 2 wt% were deemed unnecessary.[13]

Excess alkali catalyst causes the formation of soaps. As suggested by Freedman et al.,[7] the concentration of base catalyst used in industry should not exceed 1 wt% of the oil. The higher catalyst concentration required for complete conversion has another drawback, which is the higher salt content in the final biodiesel product, resulting in more extensive downstream water washing.

For biodiesel production from a membrane reactor, one important question that can arise is what would happen if the base catalyst concentration changed? Would a very low concentration of catalyst affect the final biodiesel purity in the membrane reactor? In the present paper, concentrations of base catalyst (NaOH) in the range 0 to 1 wt% were investigated in a membrane reactor at two different residence times (RT). The objective was to determine the minimum concentration of base catalyst that would lead to a feasible production of FAME.

## 5.3 Experimental Section

### 5.3.1 Materials.

Sodium hydroxide (ACS Reagent grade (NaOH, EMD Chemicals Inc.; NJ, USA) with a minimum purity of 97 wt% was used in this study. The lipid feedstock consisting of canola oil was a "no-name" brand marketed by Loeb grocery stores, and was purchased at a local food store. Methanol (99.85% purity, Commercial Alcohols Inc.; Brampton, ON, Canada), tetrahydrofuran used in the GPC analysis (THF, 99.98% purity, EMD Chemicals Inc., Gibbstown, NJ, USA), and hydrochloric acid (HCl, 36.5-38%, reagent grade, Fisher Scientific Co., Nepean, ON, Canada) were all used as received. Solvents and analytical reagents were of high performance liquid chromatography (HPLC) grade.

### 5.3.2 Equipment.

Figure 5.2 shows a schematic representation of the membrane reactor used in the present study. The seven main sub-systems of this membrane reactor system included: a feeding pump system; a permeate system including a backpressure valve and cooler; a circulation pump; a membrane module; a Coriolis meter; a heat exchange system; a safety and relief valve system.

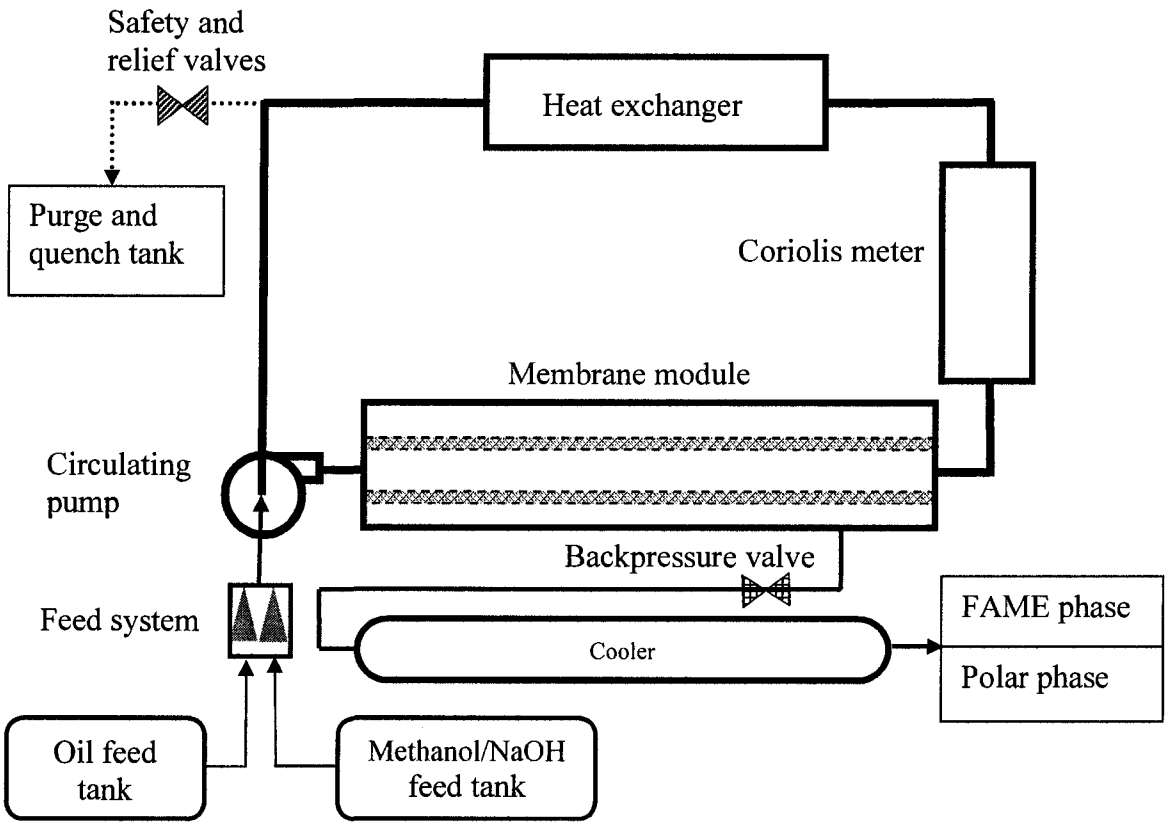


Figure 5.2: A schematic representation of the membrane reactor.

The circulating pump, membrane module, Coriolis meter and heat exchanger made up a circulating loop within which the transesterification reaction occurred at a controlled temperature and pressure. A feed system fed both the oil and methanol/catalyst solution to the reactor during the entire run. For safety considerations, backpressure valves were installed on all entry points to the loop. The Coriolis meter in the system was

a Proline Promass 83 model (Endress and Hauser, Greenwood, IN, US) that provided mass flowrate data corrected for temperature variations and density. A heat exchanger was used to control the temperature in the reactor. A Neslab Instruments, Inc., (Portsmouth, NH, U.S.A.) heating bath was used to control the temperature within the reactor. In the present study, a filtanium™ ceramic membrane (TAMI, Nyons, France) consisting of a titanium oxide support and an active layer was employed. The molecular weight cut off (MWCO) of the membrane was 300 kD and it had a multi-channel tubular configuration. The overall internal volume of the membrane reactor was 6.0 L.

### 5.3.3 Procedures.

The feedstock oil and methanol/catalyst solution were pumped in a 1:1 volume ratio into the pressurized loop and circulated with the circulating pump. For the 1 hour RT, the oil and methanol feed rates were 45 and 39.5 g/min, respectively. This gave an overall flow rate of 3 L/h of oil and 3 L/h of methanol to the reactor. Since oil is fully retained by the reactor,[15,16] the residence time for oil in the 6 L reactor was 1 h. For the 2 h RT, the oil and methanol feed rates were 22.4 and 19.8 g/min, respectively. This gave an overall flow rate of 1.5 L/h of oil and 1.5 L/h of methanol to the reactor. The residence time for oil in the 6 L reactor was 2 h. The one hour RT was selected for comparison with industrial practice where a residence time of one hour is typical in continuously stirred reactors (CSTR) used in the transesterification of soy oil.[17]

The multi-component mixture flowed on the retentate side of the membrane forming an emulsion of lipids dispersed in a methanol-rich phase. The FAME/methanol/glycerol phase permeated through the membrane and was collected. The permeate stream was brought to atmospheric conditions by the backpressure valve and cooler. The role of the permeate cooler was to reduce the temperature, thus preventing the volatilization of methanol on the release to atmospheric conditions. The retentate, passed through the Coriolis meter was heated by the heat exchanger, and finally looped back to the feed side of the circulation pump.

All the runs were performed at a temperature of 65°C and an initial pressure of 173 kPa (25 psi). The experimental conditions are listed in Table 5.1. This pressure in the reactor was selected to prevent cavitation in the circulation pump as the operating

temperature in the reactor was at the normal boiling point of methanol. The design of the membrane reactor shown in Figure 5.2 permits the decoupling of the reactor pressure and the trans-membrane pressure (TMP) (pressure across the membrane). This is achieved by locating the backpressure valve on the permeate line after the membrane. The permeate composition profile was measured and the operating parameters of the membrane reactor were monitored over a time period of 1-3 h.

Table 5.1: Experimental conditions used in this work.

| NaOH concentration* (% by weight of oil ) | Residence time (RT) (h) | |
|---|---|---|
| 1 | 1 | |
| 0.5 | 1 | |
| 0.1 | 1 | |
| 0.05 | 1 | 2 |
| 0.03 | 1** | 2 |
| 0.01 | 2** | |
| 0 | 2** | |

*The oil feedstock was neutralized with NaOH prior to the run. The numbers represent the catalyst added above that required for neutralization. All feedstock was titrated using phenolphthalein as the acid-base indicator.

** The trans-membrane pressure (TMP) increased, indicating oil accumulation in the reactor at these operating conditions.

The amount of base required to neutralize the FFA in the oil was 0.02 wt% NaOH (on an oil basis). This was determined by titration with phenolphthalein. This amount of base, required for neutralization, was not included in the catalyst concentration reported in this work. The methanol/NaOH solution was prepared by totally dissolving the calculated amount of NaOH into pure methanol. For each experiment, 3 L of a methanol/NaOH solution at a concentration according to Table 5.1 was initially charged into the reactor through the oil feed pump. Three liters of canola oil were then injected

into the reactor. The backpressure valve was shut and the heat exchanger and circulating pump were turned on. When the temperature of the reaction mixture reached 65°C (after ~60 min), the feed system was activated and both the methanol/catalyst and oil feed rates were set to 3 L/h or 1.5 L/h (i.e., the reactor RT was 1 h and 2 h, respectively). The canola oil and methanol/catalyst solutions were fed continuously into the pressurized loop.

Almost immediately after the feed streams were fed to the reactor, the permeate began to flow. The reactor pressure, temperature, and TMP were recorded continuously. Permeate samples were taken every 15 min during the first hour and then every 30 min up to 2.5 h or until the TMP reached 173.4 kPa. After each run, the pumps and heat exchanger were stopped and the system completely drained. Following each run, the membrane was backwashed with pure methanol and the system was flushed for 30 min with pure methanol and then drained.

### 5.3.4 Characterization.

The analysis of the permeate samples included several steps. Immediately after taking a sample it was neutralized to pH = 7 by the addition of 12N hydrochloric acid in methanol. The sample was then passed through a 0.2 μm polytetrafluoroethylene (PTFE) syringe filter and analyzed by gel-permeation chromatography (GPC) to evaluate the influence of a number of variables affecting the transesterification according to the methods reported by Dubé et al.[18] Smaller portions of the samples (0.04 g) were weighed into gas permeation chromatography (GPC) vials and diluted with THF to obtain 20 mg/mL sample solutions for GPC analysis. The GPC system (Waters Corp.) consisted of a pump, a flow and temperature controller, a differential refractive index detector, and two 300 × 7.5 mm Phenogel columns of 3 μm and 100 Å pore size (Phenomenex) connected in series. The system was operated by Waters Millennium 32 software. HPLC-grade THF was used as the mobile phase at a flow rate of 0.05 mL/min at 25°C. The sample injection loop was 200 μL and the injected sample volume was 20 μL. The running time required for product characterization was approximately 60 min. Calibration curves were generated for the following standards (Sigma-Aldrich): triolein (TG), diolein (DG), monoolein (MG), methyl oleate (FAME), and glycerol. The areas under the peaks

in the chromatograms for the product samples were used, together with the calibration curves, to determine the mass of the constituents (TG, DG, MG, FAME and glycerol) present in the permeate samples.

### 5.4 Results and Discussion

As previously mentioned, canola oil and the methanol/catalyst solution were continuously fed to the membrane reactor in a 1:1 volumetric ratio to have at least a 50 volume % of methanol in the reactor. This feed ratio was selected in order to maintain a continuous methanol-rich phase within the reactor. The presence of this continuous methanol-rich phase permits the removal of products (e.g., FAME and glycerol) from the reactor through the pores of the membrane. Should the reaction not occur, oil will be retained in the reactor as it is not soluble in methanol. Eventually oil will form the continuous phase within the reactor and the TMP will increase. A run was performed without catalyst to establish the basis for a non-reacting case. The TMP for this run, performed at 0 wt% catalyst (wt catalyst/wt oil), is shown in Figure 5.3 a). It can be seen that the pressure drop across the membrane is relatively constant until 45 min, at which point it increases sharply. Based on the amount of oil fed to the reactor in the 45 min, the volume fraction of methanol in this membrane reactor was calculated to be 0.331. Cao et al.[15], using a smaller reactor having a 300 mL volume, have shown that oil is the continuous phase in a membrane reactor at methanol volume fractions lower than 0.31. The sharp increase in the TMP in Figure 5.3 a) is in excellent agreement with Cao et al.[15]. The methanol volume fraction decreased steadily until the 60 min mark at which point it had reached the value of 0.275 and the TMP was 140 kPa. The run was stopped at this point. A sharp increase in the TMP was taken as an indication that oil had become the continuous phase within the membrane reactor. This observation was used to establish if, at a given catalyst concentration and RT, a sufficient amount of oil had been transformed into FAME to allow for the continuous operation of the membrane reactor.

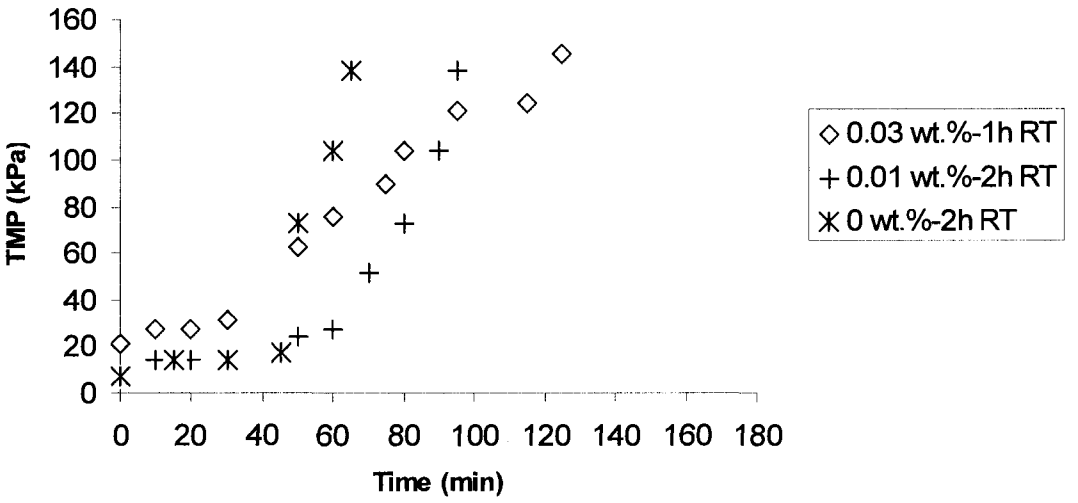


a)

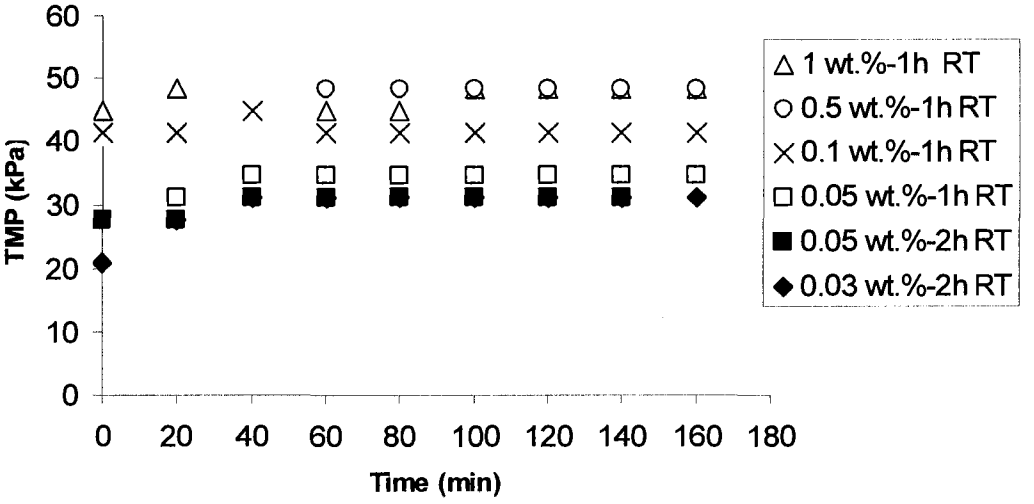


b)

Figure 5.3: TMP trends as a function of time. a) for the reaction conditions that did not permit the continuous operation of the reactor and b) for those that did. Catalyst (NaOH) concentrations and residence times are indicated in the legend.

For all runs, TG was not detected in the permeate stream, indicating that the membrane was highly efficient at retaining oil droplets within the membrane reactor. The GPC analyses revealed that transesterification occurred in the reactor. The GPC results

also indicated that any dissolved oil present in the methanol phase within the membrane reactor had reacted at the catalyst concentrations used in this work.

The TMP across the membrane was monitored for all runs. These results are shown in Figure 5.3 a), for the reaction conditions that did not permit the continuous operation of the reactor and in Figure 5.3 b) for those that did. It can easily be seen in Figure 5.3 a) that at catalyst concentrations of 0.03 wt% at a RT of one hour and 0.01 wt% at a RT of two hours, an insufficient amount of oil is reacted at 65°C to permit the continuous operation of the reactor. This sets a lower bound with respect to the catalyst concentration, under these experimental conditions, for the continuous operation of the membrane reactor. Other runs performed above 0.05 wt% at a RT of one hour and 0.03 wt% at a RT of two hours were easily performed continuously within the membrane reactor as evidenced by the very stable TMP for all operating times shown in Figure 5.3 b). The amount of oil remaining in the reactor after each run was determined and tabulated in Table 5.2. It can be seen that the conditions above 0.05 wt% at a RT of one hour and 0.03 wt% at a RT of two hours (Figure 5.3 b)) allow for the continuous reaction of the oil fed to the reactor and the continuous removal of FAME product via the permeate stream. At these successful conditions, all of the oil fed to the reactor was converted into FAME. At the higher catalyst concentrations, almost all of the oil initially in the reactor had been transformed into FAME. The results indicate that the RT in the reactor could be reduced for all successful steady state runs as no oil accumulated in the reactor under these conditions.

The results found in Table 5.3 indicate that the amount of methanol in the reactor was approximately 50% for all runs. When FAME is produced in the membrane reactor, it enters the continuous methanol-rich phase circulating in the reactor. Under the reaction conditions, FAME, methanol and glycerol are mutually soluble in this phase. As previously mentioned, the membrane retains the oil droplets (non-continuous phase) in the reactor and allows for the permeation of the methanol-rich continuous phase. As both oil and methanol are continuously fed to the reactor loop, the continuous phase is forced to leave the reactor as permeate via the membrane pores. The concentration of FAME in the permeate stream plotted versus time is shown in Figure 5.4 for all runs performed in this work. Figure 5.4 a) illustrates the FAME concentration for the runs performed at a

one hour RT and Figure 5.4 b) those performed at a two hour RT. It can be seen in Figure 5.4 a) that all runs performed at a one hour RT steadily produced above 50 wt% FAME in the permeate except for the catalyst concentration of 0.03 wt % which did not provide sufficient reactivity for the continuous operation of the membrane reactor as discussed above. In Figure 5.4 b) it can also be seen that the 0.01 wt% (two hour RT) run also produced low concentrations of FAME in the permeate due to insufficient reaction as discussed in the TMP considerations above.

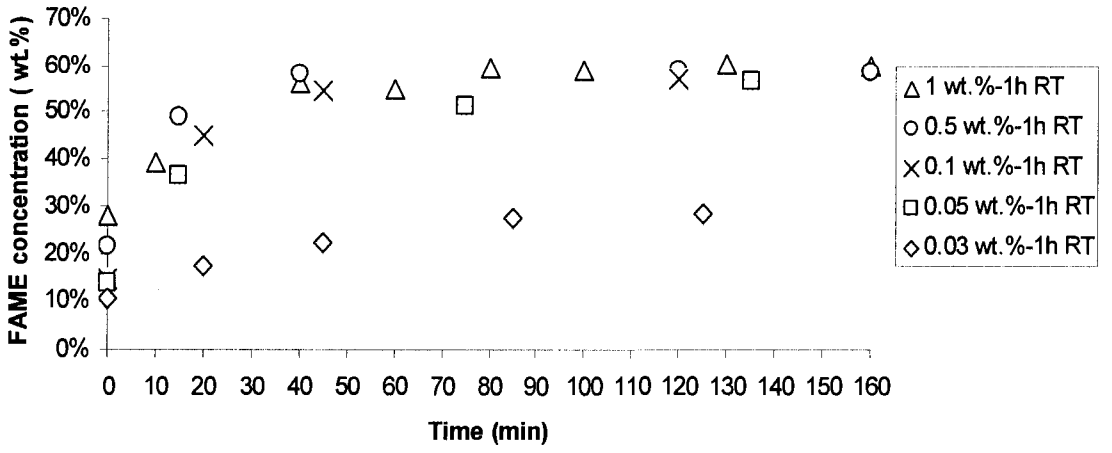


a)

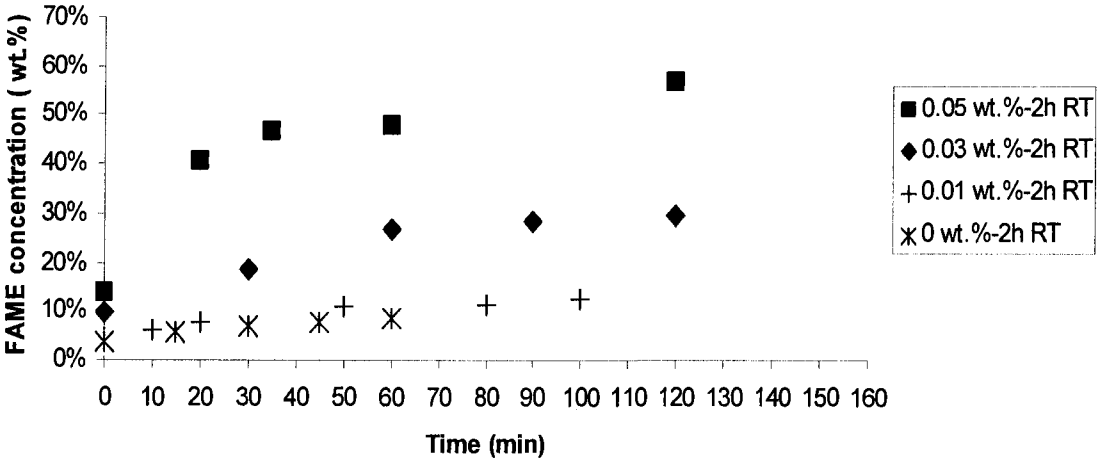


b)

Figure 5.4: The FAME concentration in the permeate as a function of time. Catalyst(NaOH) concentrations and residence times are indicated in the legend.

The concentration of catalyst used industrially in a two to three stage reaction process is approximately 0.5 wt% sodium hydroxide. The lower concentration of 0.05 wt% at a RT of one hour is one order of magnitude lower than this value. If a 2 hour RT is used, then the concentration of 0.03 wt% can be used. This is 10 to 33 times lower than the lower concentrations used in industry which ranges from 0.5 to 1 wt%.[6,7,19-22] At these low catalyst concentrations, the color and quality of the glycerol is substantially improved. In addition to this, depending on the feedstock, the color of the biodiesel will improve at the lower catalyst concentrations. Figure 5.5 shows the absorbance of methanol-rich phase and FAME-rich phase of the permeate from different catalyst concentrations using a spectrometer at 600 nm wavelength. It can be seen that the absorbance of glycerol phase decreases almost linearly with catalyst concentration, and the color of FAME-rich phase is improved below 0.1 wt% catalyst concentration.

All permeate samples with a FAME concentration higher than 20 wt% phase separated on cooling at room temperature. Figure 5.6 illustrates the concentration of the FAME-rich phase of the room temperature separated permeate for the successful steady state runs. The concentration of FAME in this phase is independent of the catalyst concentration used. This indicates that the remaining methanol and glycerol in the FAME-rich phase will contain on average 10 to 33 times less catalyst than found in the present industrial use. This implies less washing to meet ASTM standards, less sorbents required if magnesol or amberlite resins, for example, are used to purify the FAME. The color of the methanol-rich phase was much lighter when a catalyst concentration of 0.05 wt % was used vs. that produced using a 0.5 wt% catalyst concentration. This follows the absorbance results shown in Figure 5.5 and suggests that fewer degradation products are formed at the lower catalyst concentrations. The polar methanol-rich phase will be recycled and form what is known as a glycerol co-product. This suggests that a more valuable co-product glycerol containing less salts and degradation products is obtained at lower catalyst concentrations.

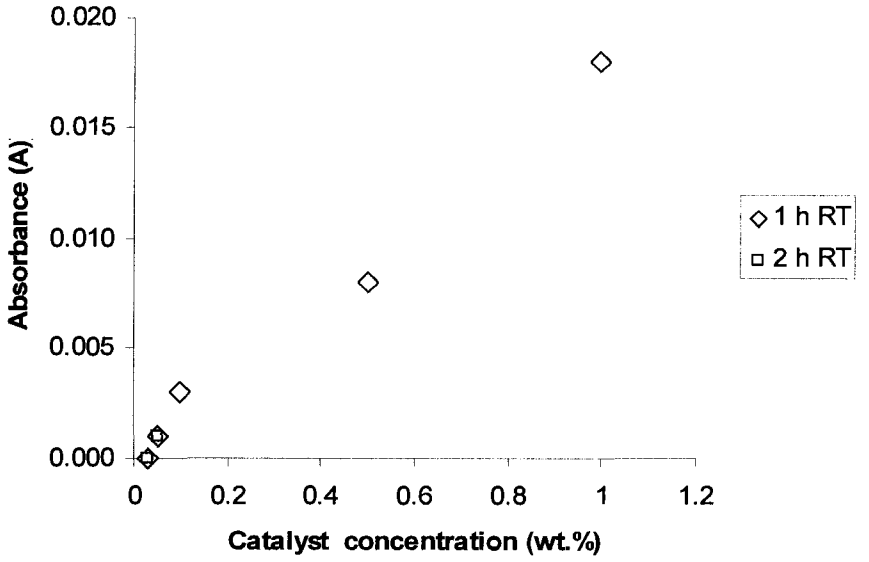


a)

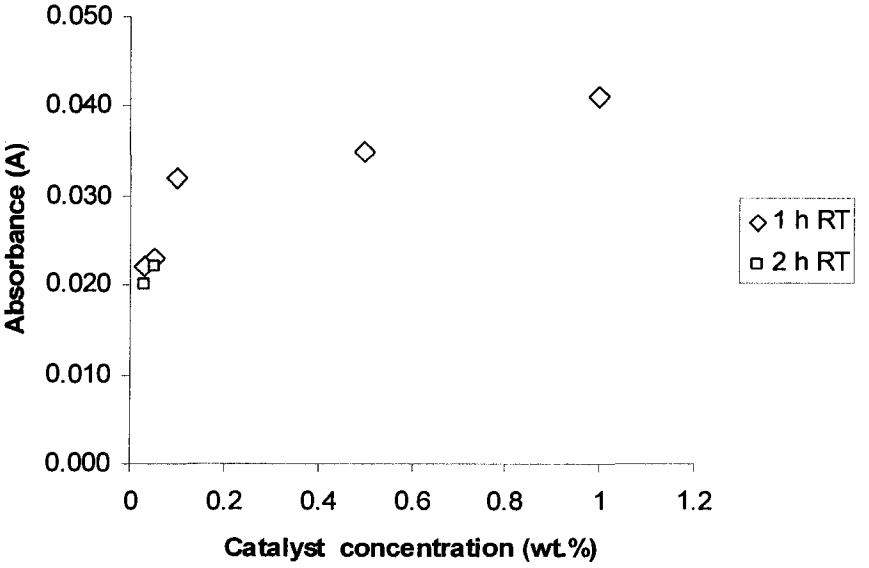


b)

Figure 5.5: Absorbance of a) methanol rich phase and b) FAME rich phase of the phase separated permeate at different catalyst concentrations.

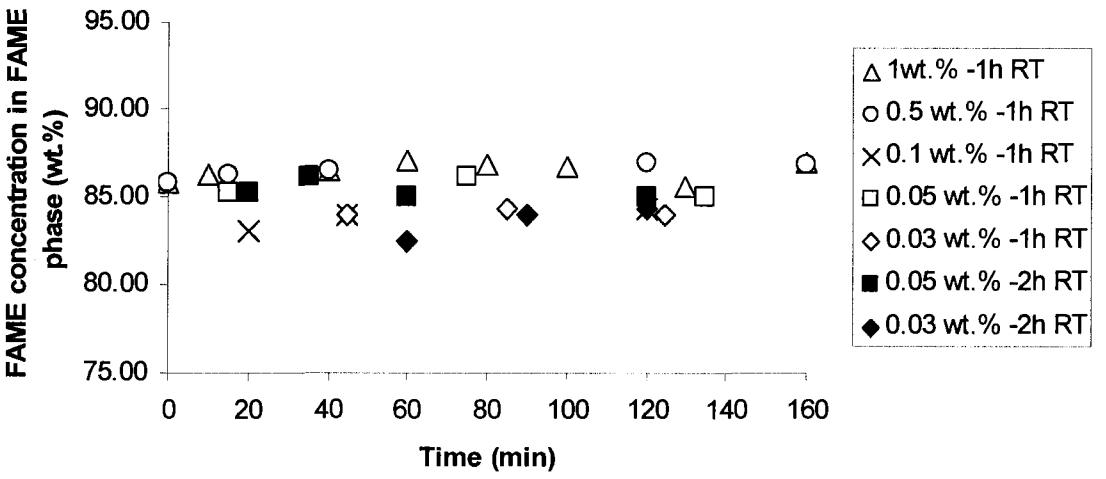


Figure 5.6: FAME concentration in the FAME-rich phase of the permeate as a function of time. Catalyst (NaOH) concentrations and residence times are indicated in the legend.

The composition of the permeate at steady state (the last sample taken in the run) is listed in Table 5.4. The change in catalyst concentration did not have a significant impact on the composition of FAME in the permeate at steady state. This ranged from 56.6 to 59.8 wt% FAME for all runs except the 0.03 wt% two hour RT run. The concentration of FAME in the permeate form this run was almost the same as that of the successful steady state 0.03 wt% two hour RT run (see Table 5.4).

Table 5.5 lists the concentrations of the two phases formed when the permeate was allowed to cool to room temperature. The last sample taken in each run is reported in Table 5.4. It can be seen that a high quality FAME phase is obtained by phase separation. No TG or MG were found in this phase, which implies that the FAME obtained from this process will be free of TG and MG and contain very low levels of DG.

The concentration of DG in the permeate leaving the reactor (non-phase-separated permeate stream) was plotted vs. the FAME concentration in this stream in Figures 5.7 and 5.8 for the one hour and two hour RTs, respectively. It can be seen that a relation exists between the concentration of FAME and DG in the overall, non phase separated permeate stream. At concentrations below 35 wt% FAME there is no DG in the permeate whereas at concentrations above 35 wt%, trace amounts of DG appear. At the higher FAME concentration, the trace DG can easily be removed from the FAME by further

reacting the FAME phase of the permeate with fresh methanol and catalyst in a batch reactor to produce higher quality biodiesel. Alternatively the reactor can be operated at low FAME concentrations in the permeate to produce high quality FAME which does not need further reaction.

Table 5.6 lists the time of appearance of the first signs of phase separation for all studied samples. From the table it can be concluded that higher catalyst concentrations increased the speed of the transesterification reaction, as also seen in the conversions found in Table 5.2, leading to greater production of FAME and glycerol and the possibility of operating at shorter residence times.

For the present study, the methanol to oil feed molar ratio was always kept at 24:1. Recycling of the polar methanol-rich phase can be used to decrease the overall methanol to oil molar ratio in the biodiesel production process via a membrane reactor. Mole ratios of 10:1, methanol:oil were obtained in previous work.[16]

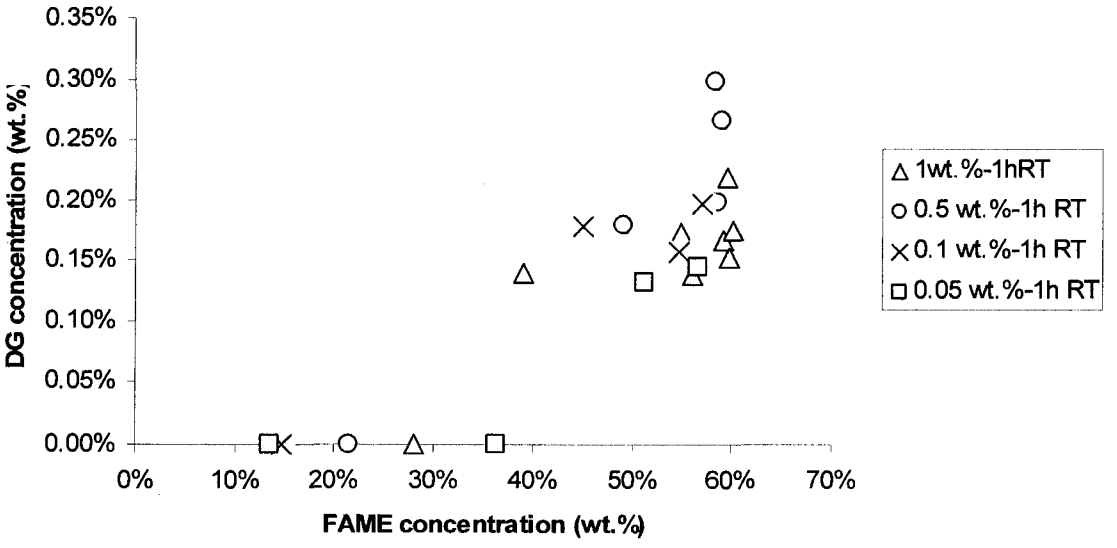


Figure 5.7: Concentration of DG vs. that of FAME in the non phase separated permeate stream for different catalyst concentrations at a 1 h residence time. Catalyst (NaOH) concentrations are indicated in the legend.

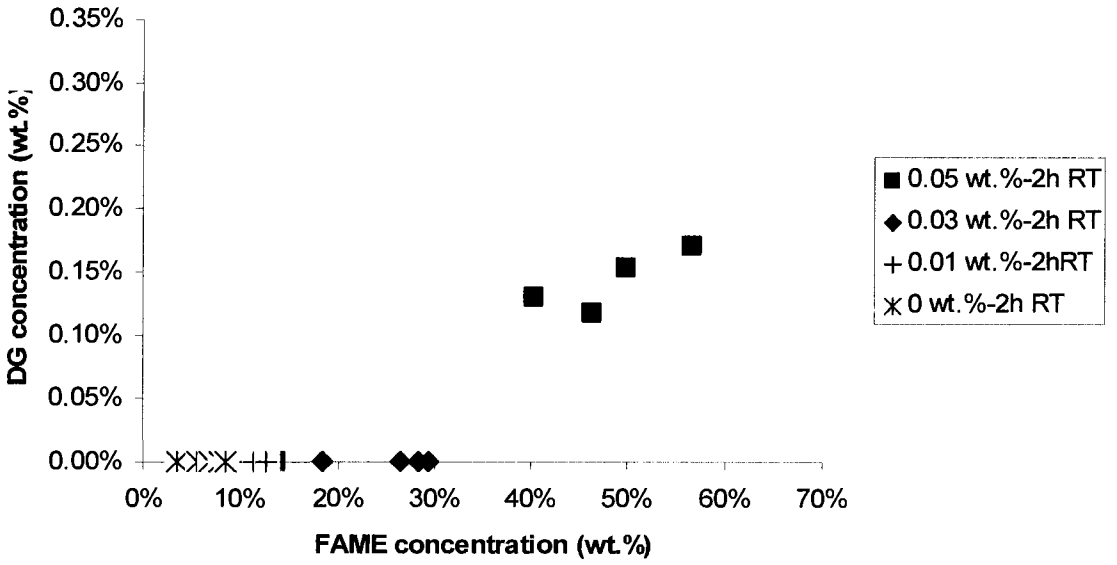


Figure 5.8: Concentration of DG vs. that of FAME in the non phase separated permeate stream for different catalyst concentrations at a 2 h residence time. Catalyst (NaOH) concentrations are indicated in the legend.

Table 5.2: Effect of catalyst concentration on the conversion of oil fed to the reactor and the conversion of oil initially in the reactor.

| Residence time (RT) (h) | Catalyst concentration (wt% on oil basis) | Total run time (min) | Steady state TMP (kPa) | Oil remaining in reactor at the end of the run (g) | Volume fraction of oil in the reactor at the end of the run | Conversion of oil fed to the reactor (wt.%) | Conversion of oil initially in the reactor (wt.%) |
|---|---|---|---|---|---|---|---|
| 1 | 0.03 | 120 | - | 3191.2 | 0.58 | 90.0 | 0.0 |
| 1 | 0.05 | 180 | 32.3 | 1870.7 | 0.34 | 100.0 | 37.6 |
| 1 | 0.1 | 180 | 41.8 | 605.2 | 0.11 | 100.0 | 79.8 |
| 1 | 0.5 | 180 | 46.3 | 110.0 | 0.02 | 100.0 | 96.3 |
| 1 | 1 | 180 | 46.2 | 55.0 | 0.01 | 100.0 | 98.2 |
| | | | | | | | |
| 2 | 0 | 60 | - | 3961.4 | 0.72 | 3.1 | 0.0 |
| 2 | 0.01 | 90 | - | 3521.3 | 0.64 | 56.5 | 0.0 |
| 2 | 0.03 | 180 | 30.2 | 2090.8 | 0.38 | 100.0 | 30.3 |
| 2 | 0.05 | 180 | 29.5 | 1595.6 | 0.29 | 100.0 | 46.8 |

Table 5.3: Methanol and oil fed to the reactor and overall volume fraction of methanol in the reactor during a run for all residence times and catalyst concentrations.

| Residence time (RT) (h) | Catalyst concentration (wt% on oil basis) | Total run time (min) | Initial methanol in reactor (g) | Total methanol fed to the reactor during the run (g) | Initial oil in reactor (g) | Total oil fed to the reactor during the run (g) | Mass Methanol total (in reactor at start + fed during run) (g) | Mass Oil Total (in reactor at start + fed during run) (g) | Volume of Methanol total (in reactor at start + fed during run) (mL) | Volume of Oil Total (in reactor at start + fed during run) (mL) | Volume fraction of methanol fed to the reactor during the run |
|---|---|---|---|---|---|---|---|---|---|---|---|
| 1 | 0.03 | 120 | 2373 | 4740.5 | 2739 | 4394.2 | 7113.5 | 7133.2 | 9004.4 | 7838.7 | 0.535 |
| 1 | 0.05 | 180 | 2373 | 6228.3 | 2739 | 7145.5 | 8601.3 | 9884.5 | 10887.7 | 10862.1 | 0.501 |
| 1 | 0.1 | 180 | 2373 | 6696.4 | 2739 | 7929.4 | 9069.4 | 10668.4 | 11480.2 | 11723.5 | 0.495 |
| 1 | 0.5 | 180 | 2373 | 6768.8 | 2739 | 8097.5 | 9141.8 | 10836.5 | 11571.9 | 11908.2 | 0.493 |
| 1 | 1 | 180 | 2373 | 6570.1 | 2739 | 8154.2 | 8943.1 | 10893.2 | 11320.4 | 11970.6 | 0.486 |
| | | | | | | | | | | | |
| 2 | 0 | 60 | 2373 | 1164.3 | 2739 | 1249 | 3537.3 | 3988 | 4477.6 | 4382.4 | 0.505 |
| 2 | 0.01 | 90 | 2373 | 1701.2 | 2739 | 1770.5 | 4074.2 | 4509.5 | 5157.2 | 4955.5 | 0.510 |
| 2 | 0.03 | 180 | 2373 | 3716.3 | 2739 | 3283.8 | 6089.3 | 6022.8 | 7708.0 | 6618.5 | 0.538 |
| 2 | 0.05 | 180 | 2373 | 3492.6 | 2739 | 4146.6 | 5865.6 | 6885.6 | 7424.8 | 7566.6 | 0.495 |

Table 5.4: Steady state compositions for the overall permeate for the successful runs.

| Residence time (h) | NaOH concentration (wt.%) | Steady state values of the permeate (wt.%) | | | | | |
|---|---|---|---|---|---|---|---|
| | | TG | DG | MG | FAME | Glycerol | Methanol |
| 1 | 1 | 0 | 0.14 | 0 | 59.8 | 4.2 | 35.9 |
| | 0.5 | 0 | 0.19 | 0 | 58.7 | 4.6 | 36.6 |
| | 0.1 | 0 | 0.13 | 0 | 57.0 | 4.8 | 38.0 |
| | 0.05 | 0 | 0.07 | 0 | 56.6 | 5.3 | 38.0 |
| | 0.03 | 0 | 0.0 | 0 | 28.4 | 6.2 | 65.4 |
| 2 | 0.05 | 0 | 0.11 | 0 | 56.7 | 5.4 | 37.8 |
| | 0.03 | 0 | 0 | 0 | 29.5 | 3.4 | 67.1 |
| | 0.01 | 0 | 0 | 0 | 12.6 | 3.0 | 84.4 |
| | 0.0 | 0 | 0 | 0 | 8.4 | 2.9 | 88.6 |

Table 5.5: Steady state compositions for the phase separated permeate, FAME rich phase and methanol rich phase for the successful runs.

| RT (h) | NaOH concentration (wt.%) | Steady state compositions for the FAME rich phase (wt. %) | | | | | | Steady state compositions for the methanol rich phase (wt. %) | | | | | |
|---|---|---|---|---|---|---|---|---|---|---|---|---|---|
| | | TG (wt.%) | DG (wt.%) | MG (wt.%) | FAME (wt.%) | Glycerol (wt.%) | Methanol (wt.%) | TG (wt.%) | DG (wt.%) | MG (wt.%) | FAME (wt.%) | Glycerol (wt.%) | Methanol (wt.%) |
| 1 | 1 | 0.0 | 0.24 | 0.0 | 86.9 | 0.0 | 12.8 | 0.0 | 0.0 | 0.0 | 11.9 | 11.4 | 76.6 |
| | 0.5 | 0.0 | 0.32 | 0.0 | 86.8 | 0.0 | 12.9 | 0.0 | 0.0 | 0.0 | 11.8 | 12.1 | 76.1 |
| | 0.1 | 0.0 | 0.31 | 0.0 | 84.3 | 0.0 | 15.4 | 0.0 | 0.0 | 0.0 | 10.2 | 13.1 | 76.7 |
| | 0.05 | 0.0 | 0.24 | 0.0 | 85.0 | 0.0 | 14.8 | 0.0 | 0.0 | 0.0 | 13.8 | 13.2 | 73.0 |
| | 0.03 | 0.0 | 0.00 | 0.0 | 84.0 | 0.0 | 16.0 | 0.0 | 0.0 | 0.0 | 9.6 | 8.4 | 82.0 |
| 2 | 0.05 | 0.0 | 0.28 | 0.0 | 85.0 | 0.0 | 14.7 | 0.0 | 0.0 | 0.0 | 14.0 | 13.6 | 72.4 |
| | 0.03 | 0.0 | 0.00 | 0.0 | 84.3 | 0.0 | 15.7 | 0.0 | 0.0 | 0.0 | 12.0 | 6.9 | 81.0 |

Table 5.6: Time of appearance of the first signs of phase separation of the permeate on cooling to room temperature for all samples.

| RT (h) | NaOH concentration *(wt.% by weight of oil ) | Time of appearance of phase separation (min) |
|---|---|---|
| 1 | 1 | 0 |
| 1 | 0.5 | 0 |
| 1 | 0.1 | 8 |
| 1 | 0.05 | 15 |
| 2 | 0.05 | 18 |
| 1 | 0.03 | 25 |
| 2 | 0.03 | 30 |

## 5.5 Conclusions

Biodiesel is becoming a key component in the motor diesel pool because of its attractive features. Increasing biodiesel consumption requires optimized production processes that are compatible with high production capacities and that feature simplified operations, high yields, as well as the absence of chemical requirements of the catalyst and the minimization of waste streams.

It has been demonstrated that a membrane reactor can drive the reversible transesterification towards the product FAME, even at very low catalyst concentrations. All NaOH concentrations above 0.05 wt% produced permeate streams with very similar FAME concentrations. No TG or MG was detected in the permeate stream. The results indicate that, even at these low catalyst concentrations, unreacted TG was unable to pass through the membrane and enter the permeate stream to contaminate the biodiesel product. The unique advantage of the membrane reactor of not having to push the reaction to completion before obtaining product, has been fully demonstrated in this work. Furthermore, the concentrations of catalyst used in the reaction have been reduced 10 to 33 fold compared to those used industrially. From the perspective of a steady state biodiesel production, the lowest catalyst concentration under the operating conditions

used in this work was 0.05 wt% at an RT of one hour and 0.03 wt% at an RT of two hours.

Biodiesel production at lower catalyst concentrations will decrease the economic cost of production due to the lower consumption of catalyst, reduce the downstream processing needed to obtain ASTM biodiesel and greatly improve the quality of the biodiesel by eliminating unreacted oils and non saponifiable, oleophilic, substances from entering the biodiesel as is currently occurring in batch processing. Because less water wash steps will be needed to remove residual catalyst in the FAME phase, a higher quality glycerol by-product is obtained, which renders the biodiesel process more in line with the environmentally driven ideals behind the use and production of biodiesel. In addition to this, the visual quality of the co-product glycerol and the biodiesel are improved. The RT in the membrane reactor was found not to have significant effects on the permeate stream profile, and the FAME-rich phase had a very similar composition for catalyst concentrations above 0.03 wt%. This resulted in phase separation of the permeate stream, and thus a consistent purification process at varying catalyst concentrations and the continuous production of TG free high purity biodiesel.

## 5.6 Acknowledgements

The authors would like to thank the Natural Sciences and Engineering Research Council of Canada (NSERC) and the Ford Foundation for financial support.

## 5.7 References

(1) Ma, F.; Clements, L. D.; Hanna, M. A. Biodiesel production: A review. *Biores. Tech.* **1999**, *70*, 1-15.

(2) Ma, F.; Clements, L. D.; Hanna, M. A. The effects of catalyst free fatty acids and water on transesterification of beef tallow. *Trans. ASAE.* **1998,** *41*, 1261-1264.

(3) Dasari, M. A.; Goff, M. J.; Suppes, G. J. Noncatalytic alcoholysis of soybean oil. *J. Am. Oil Chem. Soc.* **2003**, *80*, 189-192.

(4) Kusdiana, D.; Saka, S. Kinetics of transesterification in rapeseed oil to biodiesel fuel as treated in supercritical methanol. *Fuel.* **2001**, *80*, 693–698.

(5) Kusdiana, D.; Saka, S. Methyl esterification of free fatty acids of rapeseed oil as treated in supercritical methanol. *J. Chem. Eng. Jpn.* **2001**, *34,* 383–387.

(6) Vicente, G.; Martínez, M.; Aracil, J. Integrated biodiesel production: a comparison of different homogeneous catalysts systems. *Biores. Tech.* **2004**, *92*, 297-305.

(7) Freedman, B.; Pryde, E. H.; Mounts, T. L. Variable affecting the yield of fatty ester from transesterified vegetable oils. *J. Am. Oil Chem. Soc.* **1984**, *61,* 1638-1643.

(8) Peterson, C.; Möller, G.; Haws, R.; Zhang, X.; Thompson J.; Reece, D. Ethyl ester process scale-up and biodegradability of biodiesel, University of Idaho - College of Agriculture. Final Report No. *303*, November, **1996.**

(9) Markolwitz, M. Consider Europe's most popular catalyst. *Biodiesel Mag.* **2004**, *1,* 20-22.

(10) Stern, R.; Hillion, G. Process for the production of esters from vegetable oils or animal oils alcohols. U.S. Patent *5,908,846*, **1999**.

(11) Suppes, G. J.; Dasari, M. A.; Doskocil, E. J.; Mankidy, P. K.; Goff, M. J. Transesterification of soybean oil with zeolite and metal catalyst. *Appl. Catal. A: General.* **2004,** *257*, 213–223.

(12) Shimada, Y.; Watanabe, Y.; Sugihara, A.; Tominaga, Y. Enzymatic alcoholysis for biodiesel fuel production and application of the reaction to oil processing. *J. Mol. Catal B: Enzymati.* **2002**, *17,* 133–142.

(13) Dubé, M. A.; Tremblay, A. Y.; Liu, J. Biodiesel production using a membrane reactor. *Biores. Tech.* **2007**, *93*, 639-647.

(14) Antolin, G.; Tinaut, F. V.; Briceno, Y.; Castano, V.; Perez, C.; Ramirez, A. I. Optimization of biodiesel production by sunflower oil transesterification. *Biores. Tech.* **2002**, *83*, 111-114.

(15) Cao, P.; Tremblay, A. Y.; Dubé, M. A.; Morse, K. Effect of membrane pore size on the performance of a membrane reactor for biodiesel production. *Ind. Eng. Chem. Res.* **2007,** *46*, 52-58.

(16) Cao, P.; Dubé, M. A.; Tremblay, A. Y. Methanol recycling in the production of biodiesel in a membrane reactor. *Fuel.* **2008,** *87*, 825-33.

(17) Hass, M. J.; McAloon, A. J.; Yee, W. C.; Foglia, T. A. A process model to estimate biodiesel production costs. *Biores. Tech.* **2006,** *97,* 671-78.

(18) Dubé, M. A.; Zheng, S.; McLean, D. D.; Kates, M. A comparison of attenuated total reflectance-FTIR spectroscopy and GPC for monitoring biodiesel production. *J. Am. Oil Chem. Soc.* **2004**, *81*, 599-603.

(19) Lotero, E.; Goodwin, J. G.; Bruce, D. A.; Suwannakarn, K.; Liu, Y.; Lopez, D. E. The catalysis of biodiesel synthesis. *Catalysis.* **2006,** *19,* 41–83.

(20) Zhang, D. Crystallization characteristics and fuel properties of tallow methyl esters. Master thesis, Food Science and Technology, University of Nebraska–Lincoln, **1994.**

(21) Zhang, Y.; Dubé, M. A.; McLean, D. D.; Kates, M. Biodiesel production from waste cooking oil. 1. Process design and technological assessment. *Biores. Tech.* **2003,** *89,* 1–16.

(22) Barnwal, B. K.; Sharma, M. P. Prospects of biodiesel production from vegetable oils in India. *Renew. Sust. Energy Rev.* **2005**, *9,* 363–78.

Chapter 6

# High Purity Fatty Acid Methyl Ester Production from Canola, Soybean, Palm and Yellow Grease Lipids by mean of a Membrane Reactor

*Biomass & Bioenergy,* accepted on January 22, 2008

## 6.2 Introduction

Biodiesel is a renewable, biodegradable alternative to petroleum diesel, produced from vegetable oils or animal fats. Most commercial biodiesel comes from vegetable oil. Although the use of vegetable oil as a fuel has a long history, its use was abandoned when comparatively inexpensive petroleum-based fuels became available. The direct use of vegetable oils in a vehicle engine could bring many problems such as injector fouling, ring sticking and varnish build-up on the cylinder walls [1]. Most of the problems associated with the use of vegetable oil can be attributed to its high viscosity and to the reactivity of its polyunsaturated fatty acid components, i.e., of the triglycerides (TG). It has been shown that the most practical way of overcoming the TG viscosity problem is through chemical reaction to form alcohol esters (a.k.a. biodiesel) via the transesterification process [2].

Different lipids have different fatty acid chain compositions. There are six major types of fatty acid chains that are common in lipids, with other components present in relatively smaller amounts. Table 6.1 shows the fatty acid composition of various lipid feedstocks [3-6]. The biodiesel produced from these different lipids are mixtures of the corresponding fatty acid methyl ester (FAME).

The most commonly used lipids for the production of biodiesel are vegetable oils, such as soybean, canola, and palm oils [7 - 9] as listed in Table 6.1. Sunflower, rapeseed, and cotton seed oils have also been used for biodiesel production [10 -12]. The type of oil used is largely a factor of where the biodiesel is being produced and what type of oil is abundant there. Thus, rapeseed and sunflower oils are used in Europe, palm oil predominates in biodiesel production in tropical countries, and soybean oil is the major feedstock in the United States. Canada is a large producer of canola oil (1.6 Mt annually reported by the Canola Oil Council of Canada [13]), which has the least amount of saturated fat of any vegetable oil, less than 7 percent; biodiesel from canola oil has excellent cold-flow properties [14].

Table 6.1: Major fatty acids in some oils and waste lipids

| Lipids | **Fatty acid composition (wt.%)** | | | | | |
|---|---|---|---|---|---|---|
| | Myristic (14:0) | Palmitic (16:0) | Stearic (18:0) | Oleic (18:1) | Linoleic (18:2) | Linolenic (18:3) |
| Soybean [3] | -- | 7.8 | 4.2 | 24.25 | 53.05 | 6.25 |
| Canola [3] | -- | 3.75 | 1.75 | 59.45 | 23.55 | 10.25 |
| HPO: RBDPO (25:75) [4] | 1.4 | 43.9 | 17.0 | 30.1 | -- | -- |
| Yellow grease [5] | 0.84 | 15.88 | 8.43 | 48.43 | 20.11 | 1.89 |
| Brown grease [6] | 1 | 23 | 10 | 50 | 15 | -- |

There are several issues confronting commercial biodiesel production. The first challenge is that the transesterification reaction is mass transfer limited. The lipids and methanol are immiscible under normal reaction conditions, which limits the transfer of the methanol into the oil phase [15]. Improved mixing using ultrasonic static mixers [16], or larger pumps could be a solution, but these may significantly increase energy costs. One approach to overcoming this miscibility issue is to create a homogeneous reaction mixture using for example, THF as a cosolvent [17]. Another approach employs supercritical methanol [11]. While these approaches yield the desired results, they do involve additional costs for either downstream separation (e.g., removal of THF) or energy-related costs.

Reaching complete conversion of the TG is a challenge in light of the chemical equilibrium of the reaction. Typical single-step batch processes yield biodiesel with high levels of TG, diglyceride (DG) and monoglyceride (MG) which implies a loss of reactants as well as a failure to meet the bound glycerol levels required by the ASTM standard. In addition, the residual TG, DG and MG may result in the production of glycerine over time which would further violate the ASTM D6571 standard.

One way to achieve higher conversions includes adding excess amounts of methanol to drive the reaction to the product side, which results in additional costs for the removal of the excess methanol. Other approaches include operating at higher temperatures and pressures or higher catalyst concentrations, however, this can lead to higher energy costs, and the higher catalyst concentrations can result in a poor quality glycerine by-product. Yet another approach involves a multi-step water wash of the FAME product but this incurs costs and, of course, may result in the generation of a large waste-water stream. Finally, one needs to also consider unreactable matter that can be found in the lipid feedstock. Table 6.2 shows that one can encounter 0.3% unsaponifiable matter in refined oils and 1.6% unsaponifiable matter in crude oils. Most of this unreactable matter will remain in the FAME product because distillation is not cost effective for conventional biodiesel production and purification.

Table 6.2: Average composition for crude and refined soybean oil [18]

| **Items** | **Crude Oil** | **Refined Oil** |
|---|---|---|
| Triglycerides, wt.% | 95 – 97 | >99 |
| Phosphatides, wt.% | 1.5 – 2.5 | 0.003 – 0.045 |
| Unsaponifiable Matter, wt.% | 1.6 | 0.3 |
| Plant sterols, wt.% | 0.33 | 0.13 |
| Tocopherols, wt.% | 0.15 – 0.21 | 0.11 – 0.18 |
| Hydrocarbons, wt.% f | 0.014 | 0.01 |
| Free fatty acids, wt.% | 0.3 – 0.7 | < 0.05 |
| Trace Metals | | |
| Iron, ppm | 1 – 3 | 0.1 – 0.3 |
| Copper, ppm | 0.03 – 0.05 | 0.02 – 0.06 |

The high cost of virgin vegetable oil is the most important issue in the economic evaluation of the biodiesel process [19]. Reducing the cost of the feedstock is necessary for biodiesel's long-term commercial viability. One way to achieve this cost reduction is to use less expensive feedstocks such as waste frying oils and rendered animal fats. Free fatty acid (FFA) values increase as oil is used in a fryer. Used cooking oils typically

contain 2-7% FFA, and animal fats contain from 5 to 30% FFA [20]. Lower cost feedstocks such as low-grade or waste oils, animal fats, yellow grease, and brown grease are high in FFA (and often water) which leads to the production of soaps in the FAME product when a base catalyst is used. This makes the separation of the biodiesel from unreacted methanol and lipids exceedingly difficult [2]. Eventually, the various compounds found in such low grade feedstocks can lead to the formation of substances (e.g., stearates) which result in poor flow properties at low temperatures [21]. One approach is to utilize acid catalysts to avoid soap formation by esterification of the FFA to FAME [22]. In these cases, capital costs are incurred due to the need for more reaction vessels, and the reaction kinetics is far slower than in the base-catalyzed process. Although earlier work claimed that the acid–catalyzed process was too slow to be practical for converting TG to biodiesel [23], Zhang et al. showed that an acid-catalyzed approach could indeed be economical [24].

Traditional downstream purification methods such as water washing to remove excess methanol and catalyst may generate large amounts of waste water and incur high energy costs. Most commercially available biodiesel is produced in batch processes which have inherent large scale limitations. Continuous production brings the benefits of less downtime and a more stable operation [25]. One example is the continuous biodiesel production through an oscillating flow reactor [26].

Recently, Dubé et al. [27] applied membrane reactor technology for the semi-continuous production of FAME. The ultimate goal was to develop a continuous reaction process for the production of biodiesel and overcome the challenges due to mass transfer limitations, incomplete conversion, use of high FFA feedstocks and downstream purification, and to combine reaction and separation into a single processing unit to reduce the size of current batch operations, and maintain high mass transfer between the immiscible phases.

This paper describes a prototype continuous membrane reactor, which evolved from a lab-scale semi-continuous system for biodiesel production. Herein, we report results from the use of different lipid feedstocks in the biodiesel membrane reactor and quantify the effect of each of these on FAME purity.

## 6.3 Continuous Membrane Reactor and Experimental Methods

### 6.3.1 Principle of Operation

Due to the immiscibility of the lipid feedstock and methanol, under a broad range of conditions, the reaction mixture will exist as an emulsion of lipid droplets suspended in a continuous methanol-rich phase. These lipid droplets are of a size large enough to be excluded from passing through the membrane pores.

Figure 6.1 illustrates the membrane reactor principle using a schematic diagram. Operation of the membrane reactor consists of continuously feeding the lipid feedstock and an methanol/catalyst mixture via separate streams into the membrane reactor system. The reaction mixture is circulated in a loop through the tubular membrane. The membrane reactor is operated in a cross-flow mode as opposed to a dead-end filtration device.

Transesterification occurs at the lipid droplet-methanol interface [28]. The products of transesterification, namely FAME and glycerine, as well as the catalyst (either base or acid) are soluble in the methanol. Thus the retentate side of the membrane consists of a suspended mixture of lipids dispersed in a FAME/methanol/glycerine/catalyst solution. When a positive pressure difference across the membrane, referred to as the trans-membrane pressure (TMP), is built up, the FAME/methanol/glycerine/catalyst phase selectively passes though the micro-porous membrane into the permeate stream while the emulsified lipid droplets are retained because their size exceeds that of the membrane pores [29].

A key to insuring high quality biodiesel production is to maintain a separate lipid phase within the membrane reactor system. FAME has good solvent properties, which will not only result in an increase in solubility of DG in the permeate stream, but also could lower the interfacial surface tension between the methanol and the lipid, especially at higher temperatures. This would result in the lipid/FAME/methanol mixture to become a single phase [30] and permit unreacted TG to pass though the membrane pores into the permeate stream. This would result in poor quality biodiesel product with bound glycerine content exceeding ASTM standards.

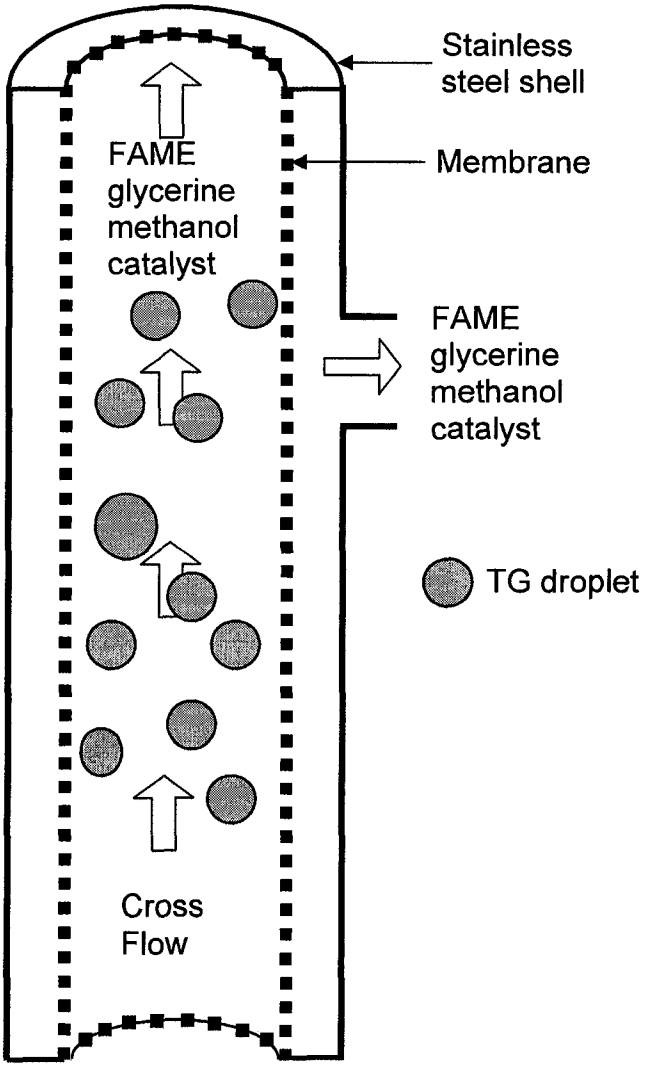


Figure 6.1: Membrane module schematic for biodiesel production
(Drawing is not to scale).

### 6.3.2 Prototype reactor and biodiesel production process

To investigate the use of different lipid feedstocks in the membrane reactor and realize a continuous biodiesel production process, a prototype membrane reactor was constructed. This prototype evolved from a previously constructed semi-continuous membrane reactor system [27]. A schematic of the prototype biodiesel membrane reactor system is shown in Figure 6.2. The reactor system consists of a circulation pump, a membrane module, a Coriolis meter, a heat exchange system, and safety and relief valves.

These make up a circulating loop within which the transesterification reaction occurs at a controlled temperature and pressure. The overall internal volume of the membrane reactor is 6.0 L.

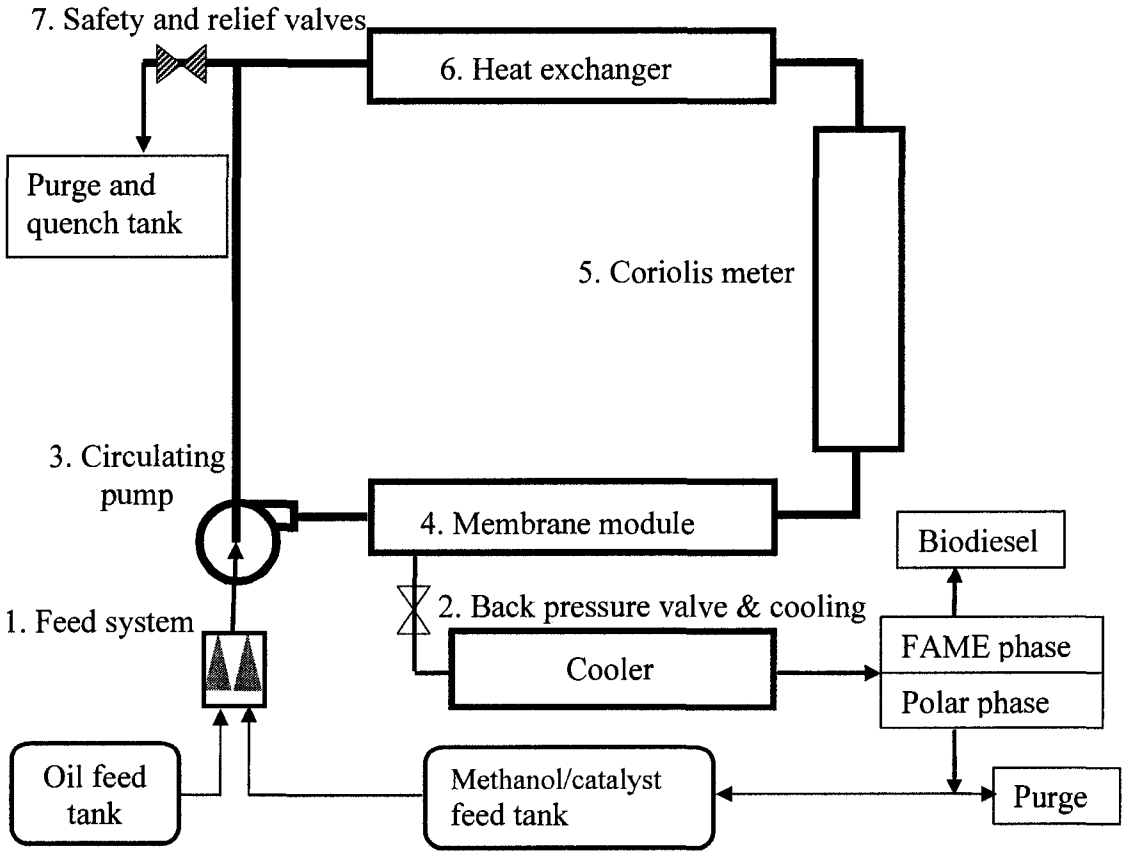


Figure 6.2: Schematic of the reactor.

In this study, a filtanium™ ceramic membrane (TAMI, Nyons, France) constructed of a titanium oxide support and active layer was employed. The molecular weight cut off (MWCO) of the membrane was 300 kD and its configuration was multi-channel tubular [31]. In addition, the system uses a reagent feed system and a backpressure valve interface between this pressurized reaction loop and atmospheric conditions. The feedstock lipid and methanol/catalyst can be pumped into this pressurized loop and circulated with the circulating pump. Thus, as mentioned above, the membrane is operated as a cross-flow filtration device. The permeate which passes through the

membrane is brought to atmospheric conditions by a backpressure valve and a permeate cooler. Cooling the permeate to ambient conditions prevents the volatilization of methanol on release to atmospheric conditions and accelerates phase separation. The permeate stream is a single phase at the reaction temperature but easily separates into a FAME-rich phase and a methanol/glycerine-rich phase upon cooling to ambient conditions.

Recycling the methanol/glycerine-rich phase allows one to achieve methanol:lipid ratios comparable to commercial batch biodiesel production [31]. Nevertheless, a relatively high methanol:lipid molar ratio (e.g., 23.9:1) is maintained in the circulating loop whereas the overall process methanol:lipid molar ratio is kept reasonably low (e.g., 10:1). The high molar ratio of methanol to lipid helps drive the reaction towards completion, due to the reversible nature of the reaction, and also reduces the concentration of intermediate products such as DG and MG.

The Coriolis mass flow meter provides interesting and useful on-line information such as mass flow rate, density, and temperature, and the mass flow rate data is internally corrected for any temperature variations. The retentate stream passes through the Coriolis mass flow meter, is then heated by a heat exchanger, and the fluid is then looped back to the feed side of the circulation pump. The temperature, pressure, TMP, density and mass flowrate are graphically displayed on the PC screen and recorded. LABVIEW$^{TM}$ software was used to control the system and acquire the data.

The procedure for producing biodiesel using this continuous membrane reactor is straightforward. Initially, a measured amount of methanol/catalyst solution is charged into the reactor through the feed system. The remaining reactor volume is filled with the lipid feedstock, which can be pre-heated if necessary. The back pressure valve is closed initially to prevent permeate flow through the membrane. The heat exchanger and circulating pump are then started. When the temperature reaches the intended reaction temperature (e.g., 65$^{o}$C), the feed system is activated. Continuous feeding of methanol/catalyst and/or lipid feedstock at a controlled molar ratio ensures a trans-membrane pressure causing the permeation of FAME/methanol/glycerine/catalyst while retaining the lipid feedstock inside the membrane reactor loop. During that time, the residence time can be adjusted by tuning the feeding rates and the back pressure valve

can be set to regulate the membrane reactor pressure. When the reactor is operated under certain conditions [31], the permeate stream undergoes a straightforward phase separation after cooling to ambient conditions. The FAME-rich phase may then undergo further purification, if necessary, to produce ASTM quality biodiesel, while the methanol/glycerine-rich phase is recycled to the membrane reactor.

### 6.3.3 Experimental materials and conditions

Different lipids such as virgin canola oil, soybean oil, a hydrogenated palm oil/refined, bleached and deodorized palm oil (HPO/RBDPO) blend, and yellow grease and brown grease, were tested in the membrane reactor system. The canola oil was the "no-name" brand marketed by Loeb grocery stores, which was purchased at a local food store. Soybean oil (Goudas brand) was supplied from Goudas Food Products Co. Ltd. (Concord, ON, Canada). The HBO/RBDPO 25:75 wt.% blend was supplied from Golden Jomalina Food Industries (Malaysia). Two kinds of low-grade lipids were tested, one was a yellow grease containing greater than 10 wt.% FFA, and another was a brown grease containing greater than 17 wt.% FFA content.

Sodium hydroxide (97% purity, NaOH, EMD Chemicals Inc.; NJ, USA), methanol (99.85% purity, Commercial Alcohols Inc.; Brampton, ON, Canada), tetrahydrofuran (THF, 99.98% purity, EMD Chemicals Inc., Gibbstown, NJ, USA), and hydrochloric acid (HCl, 36.5-38%, reagent grade, Fisher Scientific Co., Nepean, ON, Canada) were all used as received. All other solvents and analytical reagents were of high performance liquid chromatography (HPLC) grade.

All runs employed methanol and were conducted at a reaction temperature of 65oC. The residence time (RT) of the membrane reactor was set to 1 h and molar ratios of methanol:lipid for both initial loading and continuous feeding were kept at 23.9 (volume ratio methanol:lipid = 1:1). NaOH catalyst at a concentration of 0.5 wt% based on lipid mass was used in all runs. The FFA contained in the low-grade lipids was neutralized using NaOH.

### 6.3.4 Characterizations

Gel permeation chromatography (GPC) was used to analyze both phases from the permeate stream. Each 20 mL sample of permeate solution was filtered through a 0.2 μm polytetrafluoroethylene (PTFE) syringe filter into a clean vial. To about 0.04 g of sample was added ~2 g of THF in a 4 mL vial. A Waters Corp. GPC system consisting of a pump, flow controller, differential refractometer and auto-sampler was used. Waters Millennium 32$^{TM}$ software was utilized for analysis. The columns were two 300 x 7.5 mm Phenogel columns of 3 μm and 100 Å pore size (Phenomenex, Torrance, CA) connected in series. The GPC analysis was conducted according to the method shown by Dubé et al [32]. The mobile phase was HPLC grade THF at a flow rate of 0.5 mL/min at 25°C. The sample injection loop was 20 μL with a running time of 60 min. A calibration curve was generated from six standards: triolein (TG), diolein (DG), monoolein (MG), methyl oleate (FAME), glycerine and methanol. The injection masses were plotted against the peak area. The calibration curves of the standard solutions showed good linearity.

GC analysis was used to determine the free and total glycerine using ASTM method D6584, which is included in the ASTM D6751 biodiesel standard. After silylating with N-methyl-N-(trimethylsilyl) trifluoracetamide (MSTFA), the FAME sample was injected onto a capillary column for separation and a flame ionization detector (FID) was used for detection. MG, DG, and TG were determined by comparison to monoolein, diolein, and triolein standards, respectively. The GC for our project analysis was a Varian, Inc. model CP-3800 gas chromatograph, equipped with a 1079 injector, 8410 Auto-sampler and FID detection, using He as the carrier gas. A high temperature WCOT Fused Silica column was used and the stationary phase was VF-5HT. The column length was 15 m and the inside and outside diameters were 0.32 and 0.45 mm, respectively. After setting the instrument operating variables, ~100 mg of sample was weighed into a 10 mL septa vial. Exactly 100 μL of each internal standard and MSTFA silylating agent were added to the vial. The vial was shaken and allowed to sit for a minimum of 15 min at room temperature. Then, ~8 mL of n-heptane was added to the vial, which was then briefly shaken. One μL of the reactant mixture was then injected into the GC. A calibration curve was generated from four standards (i.e., triolein (TG), diolein (DG), monoolein (MG), and glycerine) and two internal standards (i.e., 1,2,4 -

butanetriol for glycerine and 1,2,3 –tricaproylglycerol (tricaprin) for glycerides). Each standard was injected two times at five different concentrations. The calibration curves of the standard solutions showed good linearity. (Note: the standard solutions were a Biodiesel package from the Sigma-Aldrich Company, sample concentrations were 50 μg $cm^{-3}$ TG, 50 μg $cm^{-3}$ DG, 100 μg $cm^{-3}$ MG, and 5 μg $cm^{-3}$ glycerine (injection volume was 10 μl); internal standards butanetriol and tricaprin solutions had concentrations of 1000 μg $cm^{-3}$ pyridine and 8000 μg $cm^{-3}$ pyridine, respectively (injection volume was 1 μL).

## 6.4 Results and Discussion

### 6.4.1 Operational parameters

For all runs, the lipid feedstock and methanol/NaOH feed rates were 45 and 39.5 g/min respectively. The reaction temperature was controlled at 65°C. During the reaction, the densities of the reaction mixtures slightly increased, due largely to the production of glycerine, and then stabilized to a steady-state value (see Table 6.3). In addition, both the mass flowrates of the reaction mixture and the TMP were kept at constant levels during the reaction (see Table 6.3). Interestingly, the operational parameters for the different lipid feedstocks were very similar and, in other words, the membrane reactor was fully capable of handling the different lipid feedstocks from an operational point of view.

Table 6.3: Steady state values of operational parameters

| Lipids | TMP (kPa) | Density of reaction mixture (g $cm^{-3}$) | Mass flowrate of reaction mixture (g/min) |
|---|---|---|---|
| Soybean | 37.9 | 0.812 | 19200 |
| Canola | 41.4 | 0.813 | 19200 |
| Palm | 40.0 | 0.813 | 19200 |
| Yellow grease | 40.2 | 0.814 | 19100 |
| Brown grease | 43.1 | 0.814 | 19200 |

### 6.4.2 Purification function of membrane and permeate de-phasing effect

In batch processes and in the presence of a base catalyst, impurities such as FFA and unsaponifiable matter will result in the formation of an emulsion which makes the separation of the FAME product from the glycerine difficult [19]. The membrane used in the reactor system had a 300 kD molecular weight cut-off (MWCO). This provided an excellent means to retain emulsions. The permeate streams from all lipid feedstocks tested were clear, without any visible emulsions, even for the high FFA low-grade lipids, yellow grease and brown grease. A post-reaction comparison of the FAME-rich portion of the permeate stream and the retentate stream during the yellow grease run showed an obvious difference. The retentate stream became cloudy with a thick soap layer in the middle after water washing, e.g., when 2 L of retentate was washed with 2 L water, the soap layer was about 350 mL. Even after a subsequent two hours settling time, it was difficult to identify and separate the upper and lower phases. On the other hand, the permeate stream easily separated into a FAME-rich phase and a methanol/glycerol-rich phase. Immediately after water washing the FAME-rich phase, a clear boundary existed between the FAME-rich phase and the water wash phase. The FAME product was of exceptional purity without any evidence of particulate matter.

For all lipid feedstocks tested, i.e., soybean oil, canola oil, palm lipid, yellow grease and brown grease, immediate phase separation of the permeate stream occurred after cooling to room temperature. For all cases, the upper phase in the permeate stream was the methanol/glycerine-rich phase and the lower phase was the FAME-rich phase when the methanol to lipid volume ratio was kept at 1:1 (molar ratio is 23.9).

Results of GPC analyses of the permeate streams are reported in Table 4, wherein the upper and lower phase compositions are shown for the permeate stream from each lipid feedstock. It is important to note that no water washing was performed on these samples prior to GPC analysis. In the lower FAME-rich phase, the FAME concentration varied from 79.07 to 86.36 wt.%, and no glycerine was detected. All the glycerine was distributed in the methanol/glycerine-rich phase because methanol and glycerine have similar polarities. Meanwhile, DG was detected in the FAME-rich phase because of DG's hydrophobicity. It has been previously shown that when the FAME concentration is lower than 35 wt.%, DG could be retained in the membrane reactor [29]. For this study,

FAME concentrations in the permeate streams were far above 35 wt.%, thus allowing the FAME to dissolve more DG, thereby allowing DG to permeate through the membrane. Only the DG residing within the hydrophobic oil droplet, or forming its own micelle larger than membrane pore size would be retained in the reactor.

Comparing the two phases for each feedstock in Table 6.4, the compositions are quite similar. This implies that the membrane reactor can be operated using a very broad range of feedstocks at fairly constant operating conditions.

Table 6.4: Composition of the FAME-rich phase and methanol/glycerine-rich phase of permeate samples from different lipid feedstocks

| Lipid feedstock | Composition of the FAME-rich phase (wt.%) | | | | Composition of the methanol/glycerine-rich phase (wt.%) | | | |
|---|---|---|---|---|---|---|---|---|
| | FAME | Glycerine | DG | Methanol | FAME | Glycerine | Methanol | DG |
| Soybean | 86.36 | N.D. | 0.13 | 13.51 | 11.32 | 12.97 | 75.72 | N.D. |
| Canola | 84.21 | N.D. | 0.20 | 15.59 | 14.53 | 11.96 | 73.51 | N.D. |
| Palm | 82.47 | N.D. | 0.50 | 17.03 | 18.39 | 9.28 | 72.33 | N.D. |
| Yellow grease | 79.07 | N.D. | 0.38 | 20.55 | 19.06 | 7.73 | 73.21 | N.D. |
| Brown grease | 83.42 | N.D. | 0.41 | 16.17 | 15.41 | 11.38 | 73.21 | N.D. |

*N.D. = not detectable

### 6.4.3 Biodiesel analysis results

The GPC analytical results in Table 6.4 show that no TG or MG were detected in the permeate stream for any lipid feedstock. The low glycerine content in the FAME-rich phase of the permeate stream has important implications in terms of water washing for biodiesel purification. The final biodiesel product must meet the ASTM D6751 standard, which requires that the free glycerine content is less than 0.020 wt.% and the total glycerine content is less than 0.240 wt.%. Table 6.5 lists the free glycerine and total glycerine contents of the FAME from each lipid feedstock based on the ASTM D6584 standard procedures. All FAME samples were prepared by using the FAME-rich phase

from the permeate stream and subjected each of these to 6 water washes using water at one third the volume of the FAME-rich phase for each wash. An additional FAME sample produced from canola oil after recycling the methanol/glycerine-rich phase was also analyzed for reaction conditions [31]. As shown in Table 6.5, FAME produced using the membrane reactor easily meets the free glycerine and total glycerine ASTM standards even for the low-grade lipid feedstock cases. The FAME produced using methanol/glycerine recycling contained slightly higher glycerine content than that without recycling. This implies that recycling had no apparently negative impact on FAME purity in terms of its free and total glycerine contents.

Table 6.5: GC results according to ASTM D6584

| **Lipid Feedstock** | Biodiesel from membrane reactor (wt.%) | | Biodiesel from batch reaction (wt.%) | |
|---|---|---|---|---|
| | Total glycerine | Free glycerine | Total glycerine | Free glycerine |
| Soybean | 0.0685 | 0.00763 | -- | -- |
| Canola | 0.0712 | 0.00654 | 0.131 | 0.0124 |
| Palm | 0.124 | 0.0117 | -- | -- |
| Yellow grease | 0.0989 | 0.00735 | 0.685* | 0.0234* |
| Brown grease | 0.104 | 0.0138 | 0.797* | 0.0171 |
| Canola oil with methanol recycle | 0.0929 | 0.00749 | -- | -- |

* does not meet the ASTM standard

Transesterifications of canola oil, yellow grease, and brown grease were carried out in conventional batch reactions at methanol:lipid molar ratios of 23.9:1 at the same reaction conditions as in the membrane reactor. The free glycerine and total glycerine contents of the FAMEs are also listed in Table 6.5. Comparing the FAME produced in the membrane reactor to that from a batch reaction, it was found that the FAME produced from canola oil met ASTM standards in both cases. However, for the batch reaction case, the total glycerine and free glycerine were almost twice that for the membrane reactor run. For the yellow grease and brown grease feedstocks, the FAME produced in the batch

reaction did not meet the ASTM standard whereas the membrane reactor easily accomplished the task.

### 6.4.4 Effect of fatty acids composition of lipids on biodiesel quality

In the FAME-rich permeate phase, TG, MG, and free glycerine were not detectable via GPC. In this case, total glycerine appears to be due solely to the presence of DG. The variation in DG content in the FAME-rich phase of the permeate stream for the different lipid feedstocks can be explained by the different FAME compositions obtained from each of these feedstocks. From Table 6.1, it can be expected that the different fatty acid composition of the lipid feedstocks resulted in correspondingly different FAME compositions. FAMEs of different molecular weights and structure have different affinities to DG. The value of the octanol-water partition coefficient, $K_{ow}$, can be used to illustrate this affinity difference. $K_{ow}$ is the ratio of the equilibrium concentration of a species in octanol to that in water at a specified temperature. $K_{ow}$ represents the tendency of a chemical species to partition itself between an organic and an aqueous phase. This implies that species having closer values of $K_{ow}$ will have a stronger affinity towards each other, and thus be more miscible. Methyl esters of myristic, palmitic, stearic, oleic, linoleic, and linolenic acid have $\log(K_{ow})$ values of 6.27, 7.25, 8.23, 7.73, 7.51, and 7.3, respectively, as calculated using a group contribution method described in ref. [33]. The following equation was used to estimated the average $K_{ow}$ values of FAME mixtures from different lipids. $K_{ow\text{-}i}$ refers to the $K_{ow}$ value of the methyl ester of myristic, palmitic, stearic, oleic, linoleic, or linolenic acid. $W_i$ refers to the fatty acid weight percentage in the lipid feedstock (see Table 6.1):

$$Average K_{ow} = \frac{\sum K_{ow-i} W_i}{\sum W_i}$$

DG has a $\log(K_{ow})$ value of 14.64 if di-olein is used as a model compound. Thus, the methyl ester of stearic acid has the strongest affinity towards DG, and higher stearic acid contents in a lipid feedstock should produce FAME with a stronger affinity towards DG. For example, the HPO/RBDPO blend (palm lipid) contained 17.0 wt.% stearic acid,

which is higher than any other lipid studied here (see Table 6.1). The average $K_{ow}$ value of the corresponding FAME mixture should be higher.

Figure 6.3 illustrate the relationship between the total glycerine content in the FAME-rich permeate phase and the average log($K_{ow}$) value for FAME mixtures from different lipid feedstocks. The soybean FAME mixture has the smallest $K_{ow}$ value, which implies that DG would have the least affinity to its corresponding FAME mixture. As shown in Tables 6.4 and 6.5, the lowest DG and total glycerine contents were exhibited by the soybean biodiesel.

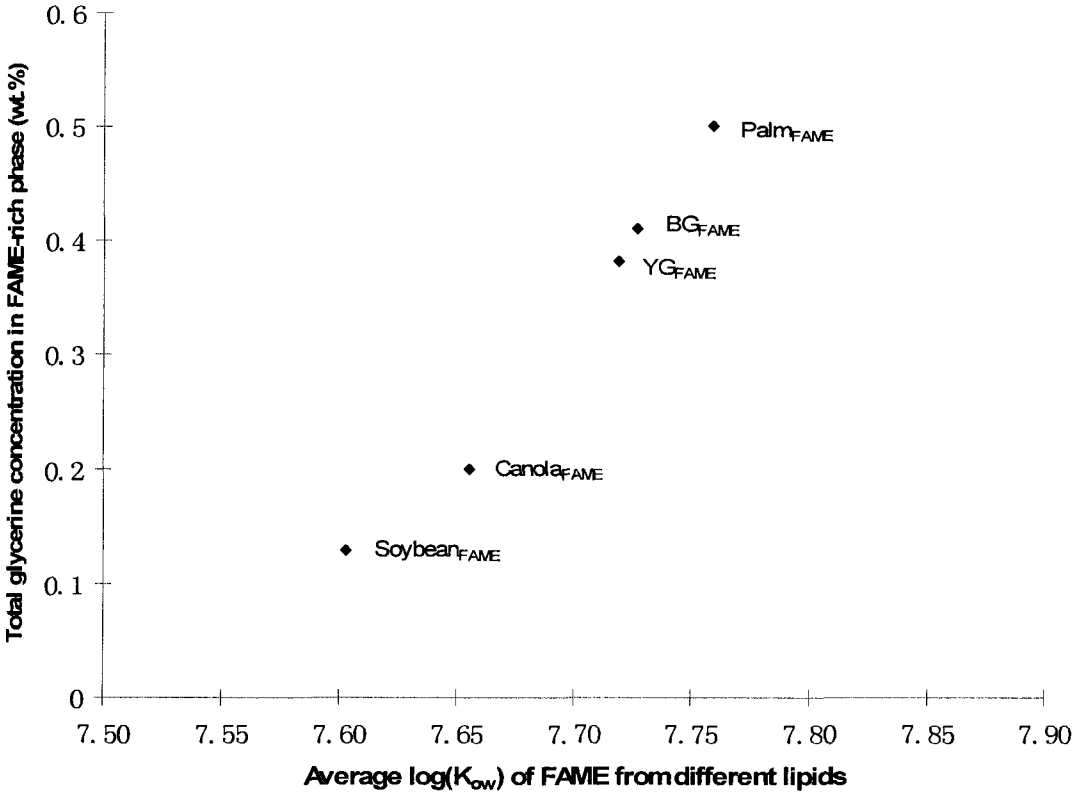


Figure 6.3: Total glycerine concentration in FAME-rich phase vs. average log($K_{ow}$) of FAME from different lipids

For soybean biodiesel and canola biodiesel, the total glycerine content in the FAME-rich phase were far lower than the 0.24 wt.% ASTM standard. This implies that a high quality biodiesel can be easily achieved by using the membrane reactor even without a final water wash step.

## 6.5 Conclusions

Different lipid feedstocks including low quality feedstocks (e.g., yellow grease) with high FFA contents were successfully transesterified in a continuous membrane reactor for biodiesel production under base-catalyzed conditions. Despite the fairly broad range of feedstocks, the membrane reactor delivered a fairly consistent performance at one set of operating conditions and enabled the production of high quality FAME.

GC analysis based on the ASTM D6584 standard confirmed the production of high purity FAME from different lipid feedstocks using a continuous membrane reactor. The FAME from each feedstock, including that from low-grade lipids, completely met and exceeded the ASTM D6751 standard. The glycerine content of FAME produced using a membrane reactor is significantly lower than that produced via a conventional batch reaction.

The FAME quality was significantly affected by the fatty acid composition of the lipid feedstocks. The percentage of FAME with less affinity to DG was directly related to the fatty acid composition of the original feedstock. This permitted the production of FAME with a total glycerine content lower than the 0.24 wt.% ASTM standard without a post-reaction water wash for soybean and canola oil-based FAME.

## 6.6 Acknowledgements

The authors would like to thank the financial support from Natural Sciences and Engineering Research Council of Canada (NSERC) and the Ford Foundation.

## 6.7 References

[1] Ryan TW, Dodge LG, Callahan TJ. The effect of vegetable oil properties on injection and combustion in two different diesel engines. Journal of American Oil Chemists' Society 1984; 61:1610-9.

[2] Ma F, Clements LD, Hanna MA. Biodiesel production: A review, Bioresource Technology 1999; 70:1-15.

[3] Knothe G, Krahl J, Van Gerpen J. The biodiesel handbook, AOCS Press: Champaign, Illinois, USA; 2005.

[4] Omar Z, Let CC, Seng CC, Rashid NA. Crystallisation and rheological properties of hydrogenated palm oil and palm oil blends in relation to crystal networking. European Journal of Lipid Science and Technology 2005; 107:634-40.

[5] Plascencia A, Estrada M, Zinn RA. Influence of free fatty acid content on the feeding value of yellow grease in finishing diets for feedlot cattle. Journal of Animal Science 1999; 77:2603-9.

[6] Tyson SK. Brown grease feedstocks for biodiesel, National Renewable Energy Laboratory, USA 2002; http://www.nrbp.org/pdfs/pub32.pdf. accessed on January 3, 2008.

[7] Freedman B, Butterfield RO, Pryde EH. Transesterification kinetics of soybean oil. Journal of American Oil Chemists' Society 1986; 63:1375-80.

[8] Zhou W, Konar SK, Boocock DGB. Ethyl esters from the single-phase base-catalyzed ethanolysis of vegetable oils. Journal of American Oil Chemists' Society 2003; 80:367-71.

[9] Darnoko D, Cheryan M. Continuous production of palm methyl esters, Journal of American Oil Chemists' Society 2000; 77:1269-72.

[10] Antolín GF, Tinaut V, Briceño Y, Castaño V, Pérez C, Ramírez A I. Optimization of biodiesel production by sunflower oil transesterification. Bioresource Technology 2002; 83:111-4.

[11] Kusdiana D, Saka S. Kinetics of transesterification in rapeseed oil to biodiesel fuel as treated in supercritical methanol. Fuel 2001; 80:693-8.

[12] Köse Ö, Tüter M, Aksoy HA. Immobilized Candida antarctica lipase-catalyzed alcoholysis of cotton seed oil in a solvent-free medium. Bioresource Technology 2002; 83:125-9.

[13] Canola Council of Canada report. Overview of Canada's canola industry, 2005; www.canola-council.org/ind_overview.html, accessed on January 3, 2008.

[14] Coleman B. Canola: An excellent feedstock for biodiesel. Biodiesel Magazine 2006; 1:25-6.

[15] Noureddini H, Zhu D. Kinetics of transesterification of soybean oil. Journal of American Oil Chemists' Society 1997; 74:1457-63.

[16] Stavarache C, Vinatoru M, Nishimura R, Maeda Y. Transesterification of vegetable oil in the presence of low ultrasonic irradiation. Ultrasonics Sonochemistry 2004; 12:367-72.

[17] Boocock DGB, Konar SK, Mao V, Lee C, Buligan S. Fast formation of high purity methyl esters from vegetable oils. Journal of American Oil Chemists' Society 1998; 75:1167-72.

[18] Van Gerpen J, Shanks B, Pruszko R, Clements D, Knothe G. Biodiesel production technology. National Renewable Energy Laboratory, NREL/SR-510-36244; 2004.

[19] Zhang Y, Dubé MA, Mclean DD, Kates M. Biodiesel production from waste cooking oil: 2. Economic assessment and sensitivity analysis. Bioresource Technology 2003; 90:229-40.

[20] Van Gerpen J. Biodiesel processing and production. Fuel Processing Technology 2005; 86:1097-107.

[21] Prakash CB. A critical review of biodiesel as a transportation fuel in Canada. Report of Transportation Systems Branch Air Pollution Prevention Directorate, Environment Canada; 1998.

[22] Aksoy HA, Kahraman I, Karaosmanoglu F, Civelekoglu H. Evaluation of Turkish sulphur olive oil as an alternative diesel fuel. Journal of American Oil Chemists' Society 1988; 65:936-8.

[23] Canakci M, Van Gerpen J. Biodiesel production via acid catalysis, Transactions of the American Society of Agricultural Engineers 1999; 42:1203-12.

[24] Zhang Y, Dubé MA, Mclean DD, Kates M. Biodiesel production from waste cooking oil: 1. Process design and technology assessment. Bioresource Technology 2003; 89:1-16.

[25] Forssell P, Parovuori P, Lonko P, Poutanen K. Enzymatic transesterification of rapeseed oil and Lauric acid in a continuous reactor. Journal of American Oil Chemists' Society 1993; 70:1105-8.

[26] Harvey AP, Mackley MR, Seliger T. Process intensification of biodiesel production using a continuous oscillatory flow reactor. Journal of Chemical Technology and Biotechnology 2003; 78:338-41.

[27] Dubé MA, Tremblay AY, Liu J. Biodiesel production using a membrane reactor. Bioresource Technology 2007; 98:639-47.

[28] Ataya F, Dubé MA, Ternan M. Single-phase and two-phase base-catalyzed transesterification of canola oil to fatty acid methyl esters at ambient conditions. Industrial & Engineering Chemistry Research 2006; 45:5411-7.

[29] Cao P, Tremblay AY, Dubé MA, Morse K. Effect of membrane pore size on the performance of a membrane reactor for biodiesel production. Industrial & Engineering Chemistry Research 2007; 46:52-8.

[30] Zhou H, Lu H, Liang B. Solubility of multicomponent systems in the biodiesel production by transesterification of Jatropha curcas L. oil with methanol. Journal of Chemical & Engineering Data 2006; 51:1130-5.

[31] Cao P, Dubé MA, Tremblay AY. Methanol recycling in the production of biodiesel in a membrane reactor. Fuel 2008; 87:825-833.

[32] Dubé MA, Zheng S, McLean DD, Kates M. A comparison of attenuated total reflectance-FTIR spectroscopy and GPC for monitoring biodiesel production. Journal of American Oil Chemists' Society 2004; 81:599-603.

[33] Allen D, Shonnard D. Green engineering: Environmentally conscious design of chemical processes, Prentice Hall PTR: Upper Saddle River, NJ, USA; 2001.

# Chapter 7

# Kinetics of Canola Oil Transesterification in a Membrane Reactor

To be submitted to ***Industrial & Engineering Chemistry Research***

## 7.2 Introduction

The necessity for alternative energy sources across the globe is increasing as non-renewable resources are being depleted. It is for this reason that biodiesel has been the focus of many studies as an environmentally friendly and renewable replacement for petroleum diesel. Biodiesel is obtained by transesterifying lipids of vegetable or animal origin with alcohols. Triglycerides (TG) react with alcohols in a reaction which is catalyzed by acid or base. This produces fatty acid alkyl esters (FAAE) and glycerine as a co-product. The characteristics and composition of the final biodiesel product will vary with the type of lipid reacting with the alcohol.[1]

The transesterification reaction has a low rate of reaction due to the immiscibility of the two reactants as oil and alcohol require vigorous stirring to promote good inter-phase contact.[2] Boocock et al. proposed the use of tetrahydrofuran (THF) to overcome this difficulty,[3] which reduced the reaction time to less than 15 min depending on the catalyst concentration. However, single-phase homogeneous solutions for biodiesel production will solubilize hydrophobic unreactable or unsaponifiable matter in the feedstock and retain it in the FAAE product. This will occur not only when converting low quality lipids, but even when converting virgin oil which can contain detectable amounts of unsaponifiable material.[4] Other efforts such as using microwave or ultrasonic irradiation have also been made to accelerate the transesterification.[5,6] The reversibility of transesterification also interferes with the completion of this process, which implies the existence of glyceride in the final biodiesel product.

A membrane reactor technology has been proposed to produce high quality biodiesel.[7,8,9] The membrane reactor integrates reaction and separation in a single unit, provides continuous mixing of raw materials and maintains high mass transfer between the immiscible phases. It was found that this novel reactor enabled the continuous separation of reaction products (FAAE/glycerol in alcohol) from the original lipid feed, which shifts the reversible transesterification to the product side. Meanwhile, the straightforward separation of the FAAE phase in the permeate stream also enabled the recycling of the polar phase to the membrane reactor, thus lowering the overall alcohol to lipid molar ratio to 10:1.[10]

Some researchers have reported reaction kinetics for both acid and base- catalyzed transesterification processes. At 32°C, transesterification was 99% completed in 4 h when using base catalyst (NaOH) while at 60°C, the reaction was completed in 1 h.[11] The transesterification of soybean oil with methanol was reported to proceed with pseudo-first-order or second-order kinetics, whereas the reverse reaction was second–order.[12] The methanolysis of sunflower oil at a molar ratio of methanol:oil of 3:1 was reported to begin with second-order kinetics but the rate decreased due to the formation of glycerol.[13] Noureddini and Zhu studied the kinetics of transesterification of soybean oil.[14] They used the same reaction model proposed by Freedman et al.[12] and performed experiments at various mixing intensities, as measured by the Reynolds number. The reaction rates for the reverse reaction of the first two reactions were found to be larger than the rate constants for the forward reactions. In addition, second-order kinetics of palm oil transesterification were studied in batch mode,[15] Vicente et al. conducted a comprehensive study on the kinetics of sunflower oil transesterification with a 6:1 molar ratio of methanol:oil.[16] The kinetic parameters of a homogeneous base-catalyzed methanolysis of soybean oil have been determined by Doell et al.,[17] the rate constants were reported much larger than those reported by Karmee et al. for a methanolysis of Pongamia oil;[18] but in Doell's work, THF was added to the reaction mixture with a methanol:oil molar ratio of 27:1 to achieve and maintain a monophasic system throughout the reactions.

We investigated the transesterification of canola oil with methanol using a membrane reactor. Methanol was the alcohol used in the reaction because of its low cost and high reactivity compared to longer chain alcohols[19] and the FAAE produced was fatty acid methyl ester (FAME). The membrane reactor runs employed a continuous feed of oil and methanol and the product was continuously removed from the reaction zone simultaneously. The present study was focused on the effect of residence time and catalyst concentration on the reaction rates. A similar modeling approach to the works of Freedman and Vicente was used with the modification that an identical volume of permeate phase left the membrane reactor to the combined oil and methanol fed to the reactor. The six reaction rate constants in the model were estimated from measurements performed on the contents of the reactor (retentate) and the product stream (permeate).

## 7.3 Experimental

### 7.3.1 Material

Food grade canola oil (No-Name®, Toronto, ON, Canada) was purchased at a local food store. Methanol (99.85% purity) was purchased from Commercial Alcohols Inc. Brampton, ON, Canada. Tetrahydrofuran (THF, 99.98% purity, EMD Chemicals Inc., Gibbstown, NJ, US) used for HPLC analysis, and both hydrochloric acid (HCl, 36.5-38%, reagent grade, Fisher Scientific Co., Nepean, ON, Canada) and sodium hydroxide (NaOH, reagent grade, ACP Chemicals Inc.; Montreal, QC, Canada) were used as packaged.

### 7.3.2 Continuous membrane reactor

A schematic drawing of the membrane reactor is shown in Figure 7.1. The figure shows the feed system, backpressure valve and cooling system for permeate, circulation pump, membrane module, heat exchange system, and safety and relief valve system.

The circulating pump, membrane module and heat exchanger make up a circulating loop within which the transesterification reaction occurs at a controlled temperature and pressure. A feed system and a backpressure valve regulate the pressure in the loop. The feedstock oil and methanol/catalyst are pumped proportionately into this pressurized loop and circulated using the circulating pump. The multi-component mixture flows on the retentate side of the membrane as a suspended mixture of lipids dispersed in a methanol-rich phase. The FAME/methanol/glycerol phase permeates through the membrane and is collected for purification and/or recycling. The permeate stream is brought to atmospheric conditions by the backpressure valve and cooler. The cooler reduces the temperature of the permeate, thus preventing the volatilization of methanol on release to atmospheric conditions. The retentate stream is heated by a heat exchanger, and the fluid looped back to the feed side of the circulation pump. A thermal fluid is used in the heat exchanger. The fluid is heated and circulated by a thermal bath (Neslab Instruments, Inc., Portsmouth, NH, U.S.A.). In this study, a filtanium™ ceramic membrane (TAMI, Nyons, France) constructed of a titanium oxide support and active layer was employed. The overall internal volume of the membrane reactor is 6.0 L.

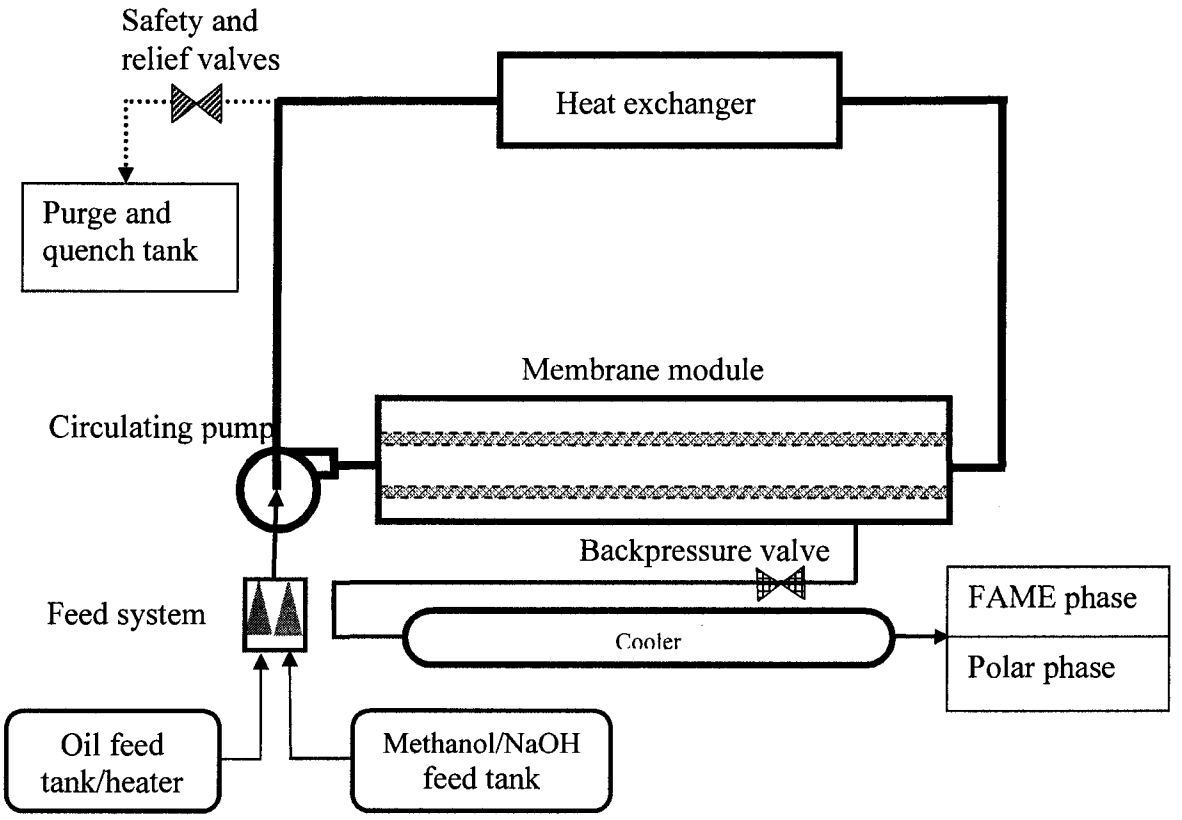


Figure 7.1: A schematic of the membrane reactor.

### 7.3.3 Experimental procedures

For all runs, the methanol:oil volume ratio fed to the reactor was 1:1. Four runs were carried out to compare different residence times; 15, 30, 45 and 60 min. The catalyst concentration for these four runs was held constant at 0.5 wt.% NaOH by weight of oil. Another two runs were carried out to compare the lower catalyst concentrations of 0.1 wt. % and 0.05 wt.% at a 60 min residence time.

Initially, for all runs, 6 L of methanol and catalyst were charged to the reactor through the feed system, and heated to 65°C. At the same time, canola oil was preheated to 65°C in the oil feed tank. With the circulation pump off, three litres of canola oil were then quickly pumped into the reactor displacing 3 litres of methanol. The permeate back pressure valve was shut initially and the heat exchanger and circulating pump were turned on. The circulation pump was then switched on and the feed system activated.

Both the methanol/catalyst and oil feed rates were each set according to the residence time. The canola oil and methanol/catalyst solution were fed continuously to the pressurized loop. Almost immediately after the feed streams were fed to the reactor, permeate began to flow. Reactor pressure, temperature and trans-membrane pressure (TMP) were recorded continuously. Following each run, the membrane was backwashed with pure methanol and the system was flushed for 30 min with 6 L of pure methanol and drained.

### 7.3.4 Sampling and analysis

Samples from the membrane reactor were taken at various time intervals. The samples were neutralized by the addition of 12N hydrochloric acid to a pH of 7.0. Then, 0.4 g of sample was diluted with 20 g of THF in a 40 mL vial. The sample was then passed through a 0.2 μm polytetrafluoroethylene (PTFE) syringe filter and analyzed by gel-permeation chromatography (GPC) to evaluate the influence of a number of variables affecting the transesterification according to the methods reported by Dubé et al.[20] The GPC system (Waters Corp.) consisted of a pump, a flow and temperature controller, a differential refractive index detector, and two 300 × 7.5 mm Phenogel columns of 3 μm and 100 Å pore size (Phenomenex, Torrance, CA) connected in series. The system was operated by Waters Millennium 32 software. HPLC-grade THF was used as the mobile phase at a flow rate of 0.05 mL/min at 25°C. The sample injection loop was 200 μL and the injected sample volume was 20 μL. The running time required for product characterization was approximately 60 min. Calibration curves were generated for the following standards (Sigma-Aldrich): triolein (TG), diolein (DG), monoolein (MG), methyl oleate (FAME), glycerol and methanol. The areas under the peaks in the chromatograms for the product samples were used, together with the calibration curves, to determine the mass of the constituents (TG, DG, MG, FAME, glycerol and methanol) present in the samples.

## 7.4 Kinetic Model for the Transesterification Process in a Membrane Reactor

The transesterification of TG follows a three-step reaction as shown in Figure 7.2. These steps all occur at different rates of reaction having their own rate constants ($k_n$). In

the first step, TG is converted to DG and a methyl ester, which in turn is converted to MG and a methyl ester in the second step. In the third and final step, MG is converted to glycerol and a methyl ester. In each step, one molecule of methyl ester is formed for every molecule of glyceride reacted. In this study, the shunt reaction involving the direct reaction of TG and methanol proposed by Freedman et al. to yield methyl ester and glycerol was not considered, because the proposed shunt reaction mechanism was not deemed necessary [12,14].

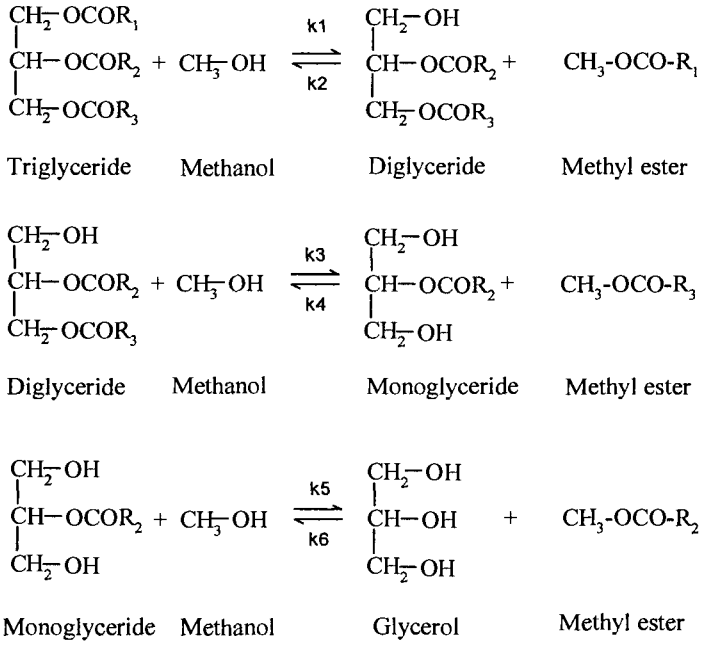


Figure 7.2: Reaction scheme of the transesterification

For the above three-step reversible reaction, the forward and reverse reactions follow second-order overall kinetics. [12,14] The reaction rate can be described as the sum of the rates from both un-catalyzed reactions and catalyzed reactions. Vicente et al. proposed a general form for the governing set of differential equations characterizing the stepwise reactions involved in the transesterification where the catalyzed reactions were first-order with respect to the catalyst concentration. [16] In the Equations 1-6, *r* denotes the reaction rate of 6 components with units of mol/(min·L):

$$r_{TG} = -(k_1 C + k_{10})[TG][Methanol] + (k_2 C + k_{20})[DG][FAME] = -\frac{d[TG]}{dt} \quad (1)$$

$$\begin{aligned} r_{DG} &= (k_1 C + k_{10})[TG][Methanol] - (k_2 C + k_{20})[DG][FAME] \\ &- (k_3 C + k_{30})[DG][Methanol] + (k_4 C + k_{40})[MG][FAME] = \frac{d[DG]}{dt} \end{aligned} \quad (2)$$

$$\begin{aligned} r_{MG} &= (k_3 C + k_{30})[DG][Methanol] - (k_4 C + k_{40})[MG][FAME] \\ &- (k_5 C + k_{50})[MG][Methanol] + (k_6 C + k_{60})[G][FAME] = \frac{d[MG]}{dt} \end{aligned} \quad (3)$$

$$\begin{aligned} r_{FAME} &= (k_1 C + k_{10})[TG][Methanol] - (k_2 C + k_{20})[DG][FAME] \\ &+ (k_3 C + k_{30})[DG][Methanol] - (k_4 C + k_{40})[MG][FAME] \\ &+ (k_5 C + k_{50})[MG][Methanol] - (k_6 C + k_{60})[G][FAME] = \frac{d[FAME]}{dt} \end{aligned} \quad (4)$$

$$r_G = (k_5 C + k_{50})[MG][Methanol] - (k_6 C + k_{60})[G][FAME] = \frac{d[G]}{dt} \quad (5)$$

$$\begin{aligned} r_{Methanol} &= -(k_1 C + k_{10})[TG][Methanol] + (k_2 C + k_{20})[DG][FAME] \\ &- (k_3 C + k_{30})[DG][Methanol] + (k_4 C + k_{40})[MG][FAME] \\ &- (k_5 C + k_{50})[MG][Methnaol] + (k_6 C + k_{60})[G][FAME] \\ &= -\frac{d[Methanol]}{dt} = -r_{FAME} \end{aligned} \quad (6)$$

In the Equations 1-6 above, $k_1$, $k_3$, and $k_5$ are the forward rate constants for the catalyzed reactions, $k_2$, $k_4$, and $k_6$ are the reverse rate constants for the catalyzed reactions, $k_{10}$, $k_{30}$, and $k_{50}$ are the forward rate constants for the un-catalyzed reactions, and $k_{20}$, $k_{40}$, and $k_{60}$ are the reverse rate constants for the un-catalyzed reactions. $C$ is the catalyst concentration.

The catalyst concentration in the reaction mixture remains constant since the catalyst-methanol solution with the same catalyst concentration was fed steadily and the

side reaction that consumed the catalyst could be neglected. Thus, we can use the effective rate constants as shown in Equation 7 to simplify Equations 1-6.

$$k_1^{'} = k_1 C + k_{10}$$
$$k_2^{'} = k_2 C + k_{20}$$
$$k_3^{'} = k_3 C + k_{30} \qquad (7)$$
$$k_4^{'} = k_4 C + k_{40}$$
$$k_5^{'} = k_5 C + k_{50}$$
$$k_6^{'} = k_6 C + k_{60}$$

A schematic representation of the transesterification process in a membrane reactor is illustrated in Figure 7.3. The TG and methanol were fed constantly to the membrane reactor at a known rate, while the mobile phase (methanol-rich phase) in the reactor could leave the reactor through the membrane as it was displaced by the incoming reactants. The circulation rate of the pump in the system allowed for the complete circulation of the reactor contents in 15 s, which permitted excellent mixing in the membrane reactor loop. According to the reaction mechanism shown in Figure 7.2, there are six components (namely TG, DG, MG, FAME, glycerol, methanol) found in the reactor retentate side. Permeate crosses the membrane and is continuously removed from the reactor. TG molecules agglomerate as droplets, and will not pass through the membrane pores unless the reaction mixture becomes a single phase.[9] The circulating mass flow rate in the reactor is about 20 kg/min, and volume of the reactor was 6 L.

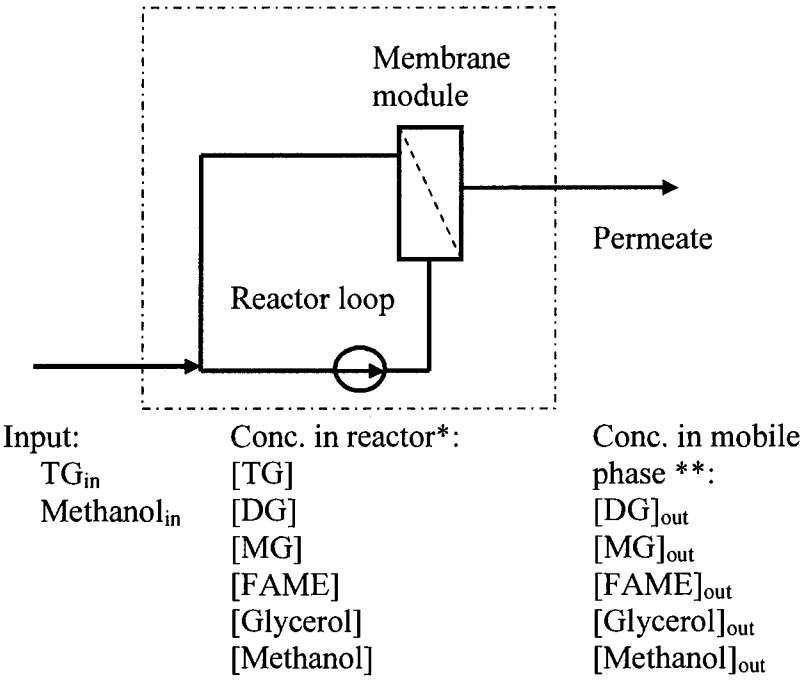


Figure 7.3: Schematic of membrane reactor used for biodiesel production kinetic model

* Based on the total volume of the emulsion in the reactor (6 L)

** Conc. in mobile phase = Conc. of the permeate

For the kinetic study, we assumed that the components on the retentate side of the membrane were perfectly mixed, so that the properties (e.g., concentration, temperature) of the reaction mixture were uniform in the circulating loop of the reactor, and the mass flow rate of the permeate ($M_{Total\text{-}out}$) was also equal to the mass flow rate of the feedstock ($M_{Total\text{-}in}$). Thus,

$$V_{out} = \frac{\mathrm{M_{Total\text{-}in}}}{\rho_{\mathrm{out}}} = \frac{F_{Methanol-in} MW_{Methanol} + F_{TG-in} MW_{TG}}{\rho_{\mathrm{out}}} \qquad (8)$$

For a certain component, $y$, the rate of accumulation in the reactor equals the input rate minus the disappearance by reaction (or plus production by reaction) minus the output rate, i.e.,

$$\frac{dy}{dt} = F_{y-in} + r_y V_0 - F_{y-out} \qquad (9)$$

Thus, for TG, because it is totally retained in the reactor, its accumulation rate will be:

$$\frac{dTG}{dt} = F_{TG-in} + r_{TG}V_0 \tag{10}$$

When Equation 10 is combined with Equations 1 - 7, the TG concentration in the reactor as a function of time can be expressed as:

$$\frac{d[TG]}{dt} = \frac{F_{TG-in}}{V_0} - k_1'[TG][Methanol] + k_2'[DG][FAME] \tag{11}$$

For DG in the membrane reactor:

$$\frac{dDG}{dt} = F_{DG-in} + r_{DG}V_0 - F_{DG-out} \tag{12}$$

$$F_{DG-out} = [DG]_{out}V_{out} \tag{13}$$

$$\frac{d[DG]}{dt} = \frac{(F_{DG-in} - [DG]_{out}V_{out})}{V_0} + k_1'[TG][Methanol] - k_2'[DG][FAME] - k_3'[DG][Methanol] + k_4'[MG][FAME] \tag{14}$$

For MG in the membrane reactor:

$$\frac{dMG}{dt} = r_{MG}V_0 - F_{MG-out} \tag{15}$$

$$F_{MG-out} = [MG]_{out}V_{out} \tag{16}$$

$$\frac{d[MG]}{dt} = \frac{(-[MG]_{out}V_{out})}{V_0} + k_3'[DG][Methanol] - k_4'[MG][FAME] - k_5'[MG][Methanol] + k_6'[G][FAME] \tag{17}$$

For glycerol in the membrane reactor:

$$\frac{dG}{dt} = r_GV_0 - F_{G-out} \tag{18}$$

$$F_{G-out} = [G]_{out}V_{out} \tag{19}$$

$$\frac{d[G]}{dt} = \frac{(-[G]_{out}V_{out})}{V_0} + k_5'[MG][Methanol] - k_6'[G][FAME] \tag{20}$$

For FAME in the membrane reactor:

$$\frac{dFAME}{dt} = r_{FAME}V_0 - F_{FAME-out} \tag{21}$$

$$F_{FAME-out} = [FAME]_{out} V_{out} \tag{22}$$

$$\frac{d[FAME]}{dt} = \frac{(-[FAME]_{out} V_{out})}{V_0} + k_1'[TG][Methanol] - k_2'[DG][FAME] + k_3'[DG][Methanol] - k_4'[MG][FAME] + k_5'[MG][Methanol] - k_6'[G][FAME] \tag{23}$$

For methanol in the membrane reactor:

$$\frac{dMethanol}{dt} = F_{Methanol-in} + r_{Methanol} V_0 - F_{Methanol-out} \tag{24}$$

$$F_{Methanol-out} = [Methanol]_{out} V_{out} \tag{25}$$

$$\frac{d[Methanol]}{dt} = \frac{(F_{Methanol-in} - [Methanol]_{out} V_{out})}{V_0} - k_1'[TG][Methanol] + k_2'[DG][FAME] - k_3'[DG][Methanol] + k_4'[MG][FAME] - k_5'[MG][Methanol] + k_6'[G][FAME] \tag{26}$$

The model also assumes that the DG, MG, FAME, glycerol, and methanol form a single mobile phase while TG forms a separate phase in the retentate stream. The compounds in the mobile phase pass through the membrane pores as a single phase (permeate) which implies that the concentration of DG, MG, FAME, glycerol, and methanol in the permeate stream noted by the subscript "*out*" are equal to their corresponding mobile phase concentrations in the reactor. The volume of the mobile phase ($V_{mobile}$) is

$$V_{mobile} = V_0 - \frac{[TG] V_0 MW_{TG}}{\rho_{TG}} \tag{27}$$

The component concentrations in the permeate can be simply expressed as:

$$[DG]_{out} = \frac{V_0 [DG]}{V_{mobile}} = \frac{[DG]}{\left(1 - \frac{[TG]\ MW_{TG}}{\rho_{TG}}\right)} \tag{28}$$

$$[MG]_{out} = \frac{V_0 [MG]}{V_{mobile}} = \frac{[MG]}{1 - \frac{[TG] MW_{TG}}{\rho_{TG}}} \tag{29}$$

$$[FAME]_{out} = \frac{V_0[FAME]}{V_{mobile}} = \frac{[FAME]}{1 - \frac{[TG]MW_{TG}}{\rho_{TG}}} \tag{30}$$

$$[G]_{out} = \frac{V_0[G]}{V_{mobile}} = \frac{[G]}{1 - \frac{[TG]MW_{TG}}{\rho_{TG}}} \tag{31}$$

$$[Methanol]_{out} = \frac{V_0[Methanol]}{V_{mobile}} = \frac{[Methanol]}{1 - \frac{[TG]MW_{TG}}{\rho_{TG}}} \tag{32}$$

If we incorporate Equations 28-32 into Equations 11, 14, 17, 20, 23, and 26, a set of differential equations of component concentrations in the reactor as a function of time can be derived as shown in Equations 33-38. The 6 component concentrations in the reactor at a given time can be determined from the experimental data. The unknown parameters are the 6 effective rate constants.

$$\frac{d[TG]}{dt} = \frac{F_{TG-in}}{V_0} - k_1'[TG][Methanol] + k_2'[DG][FAME] \tag{33}$$

$$\frac{d[DG\}}{dt} = -\left(\frac{[DG]V_{out}}{V_0 - \frac{[TG]V_0 MW_{TG}}{\rho_{TG}}}\right) + k_1'[TG][Methanol] - k_2'[DG][FAME] \tag{34}$$
$$- k_3'[DG][Methanol] + k_4'[MG][FAME]$$

$$\frac{d[MG]}{dt} = -\left(\frac{[MG]V_{out}}{V_0 - \frac{[TG]V_0 MW_{TG}}{\rho_{TG}}}\right) + k_3'[DG][Methanol] - k_4'[MG][FAME] \tag{35}$$
$$- k_5'[MG][Methanol] + k_6'[G][FAME]$$

$$\frac{d[G]}{dt} = -\left( \frac{[G]V_{out}}{V_0 - \frac{[TG]V_0 MW_{TG}}{\rho_{TG}}} \right) + k_5'[MG][Methanol] - k_6'[G][FAME] \tag{36}$$

$$\frac{d[FAME]}{dt} = -\left( \frac{[FAME]V_{out}}{V_0 - \frac{[TG]V_0 MW_{TG}}{\rho_{TG}}} \right) + k_1'[TG][Methanol] - k_2'[DG][FAME] \tag{37}$$
$$+ k_3'[DG][Methanol] - k_4'[MG][FAME] + k_5'[MG][Methanol] - k_6'[G][FAME]$$

$$\frac{d[Methanol]}{dt} = \frac{F_{Methanol-in}}{V_0} - \frac{[Methanol]V_{out}}{V_0 - \frac{[TG]V_0 MW_{TG}}{\rho_{TG}}} - k_1'[TG][Methanol]$$
$$+ k_2'[DG][FAME] - k_3'[DG][Methanol] + k_4'[MG][FAME] \tag{38}$$
$$- k_5'[MG][Methanol] + k_6'[G][FAME]$$

To calculate the effective rate constants, we need to integrate the Equations 33-38. A computer code for finite difference methods was employed in MATLAB V6.5 (Maths Works Inc.) to solve the governing set of differential equations for the entire experimental reaction time. The size of the time step ($\Delta t$) used in the simulation affected the results; however, a time step less than 1 s gave similar results compared to time steps at 1 s.[15] In this work, a time step of 0.01 min (0.6 s) was used in the simulation; the initial rate constant ranges were selected based on values from the literature. [14] The relative average difference (S%) can be used as the objective criterion of the correctness of the model for base-catalyzed transesterification. [18] We normalized the residuals by dividing that with the experimental values as follow; [15]

$$S\% = \{\sum_{i}^{m}\sum_{0}^{t}\left| y_i(t)_{\exp} - y_i(t)_{cal} \right| / y_i(t)_{\exp}\} \times 100 / N[\%] \tag{39}$$

where m is the number of reactants, $y_i(t)$ is the concentration of component $i$ at time $t$, subscript "exp" denotes the experimental value, subscript "cal" denotes the calculated value, and N is number of total measurements in the interval from time 0 to time $t$. Hence,

S% indicates the average relative difference between all experimental and calculated concentrations of the components.

## 7.5. Results and Discussion

### 7.5.1 Calculation of the effective rate constants

Six reactions were carried out at varying catalyst concentrations and residence times. The temperature was kept at 65°C and the molar ratio of methanol:oil was 23.9:1. Based on the experimental results, the effective rate constants ($k'$) were calculated by the procedure described above in section 3. Table 7.1 lists all the effective rate constants and the corresponding S%. The equations were also modeled using an Excel spreadsheet; the proposed kinetic model for the membrane reactor process was validated by making a mass balance with time for the reactor. The mass balance on the reactor was verified by using the calculated rate constants found in Table 7.1 to determine the mass of permeate leaving the reactor. The differences between the mass fed into the reactor with the mass leaving the reactor were always lower than 2%. This validates the model and the assumption that the volume of the continuous phase (methanol-rich phase) in the reactor can be determined by subtracting the oil phase from the total volume of the reactor.

Table 7.1: Calculated rate constants at 0.5% catalyst in the membrane reactor

| Catalyst conc.(%) | Residence time(min) | S% | **Effective rate constants** (L/(mole.min) | | | | | |
|---|---|---|---|---|---|---|---|---|
| | | | $k_1'$ | $k_2'$ | $k_3'$ | $k_4'$ | $k_5'$ | $k_6'$ |
| 0.5 | 60 | 14.83 | 0.1193 | 0.7414 | 1.4003 | 3.6814 | 0.3914 | 0.0292 |
| 0.5 | 45 | 12.47 | 0.1475 | 0.9227 | 1.7748 | 4.6744 | 0.4815 | 0.0349 |
| 0.5 | 30 | 11.73 | 0.1398 | 0.8742 | 1.6814 | 4.4284 | 0.4562 | 0.0331 |
| 0.5 | 15 | 14.48 | 0.1096 | 0.6857 | 1.3190 | 3.4739 | 0.3586 | 0.0260 |
| 0.1 | 60 | 17.71 | 0.0158 | 0.6620 | 0.4968 | 2.0977 | 0.2344 | 0.0006 |
| 0.05 | 60 | 13.97 | 0.0026 | 0.6450 | 0.1492 | 1.7979 | 0.1365 | 0.00034 |

For the catalyst concentration 0.5% and a 1 h RT reaction, the experimental results and the simulation results for the concentration of the reaction mixture during the first 60 min reaction time are shown in Figure 7.4. The transesterification mechanism consists of

an initial mass transfer controlled region followed by a kinetically controlled region, [14] and the lag time at the initial stage would occur because of poor diffusion between methanol and oil. Figure 7.4 shows the experimental points and simulation curves for the concentration of the reaction mixture during the transesterification in membrane reactor with catalyst concentration 0.5% and 1 h RT. It was found that the concentration of FAME increased rapidly followed by a steady state, and TG conversion did not show a sigmoidal (S-shape) pattern which consists of a slow rate at the beginning followed by a sudden surge and finally a slow rate again,[12,21] even though the TG was continuous fed into the reaction zone. In Table 7.1, the values for the effective rate constants, $k_1^{'}$ to $k_6^{'}$ with 0.5% catalyst concentration did not change significantly at different residence times. Apparently, the residence times did not have a significant impact on the kinetics of transesterification in the membrane reactor. The experimental points and simulation curves for the concentration of the reaction mixture with RT = 45, 30 and 15 min show the same trend (see Figure 7.4).

For the lower catalyst concentrations of 0.1% and 0.05%, Figures 7.5 and 7.6 show both the experimental and the simulated results for the concentration of the reaction mixture during the first 20 min of the experiment. The concentration of FAME and other components changed slowly with the time. The concentration of components at 0.1% reached to a steady state after a longer time than 0.5% catalyst concentration; the concentration of components at 0.05% still didn't approach to steady state when the run was carried out at 20 min. As shown in Table 7.1, the calculated values of the effective rate constants are also much smaller than 0.5% catalyst concentration, which implied that reaction rates for catalyst concentrations of 0.1% and 0.05% are slower. Fortunately, the slow reaction rate does not have a negative effect on the FAME purity in the permeate stream, high quality biodiesel can be achieved through membrane reactor technology at ultra low catalyst concentrations [22].

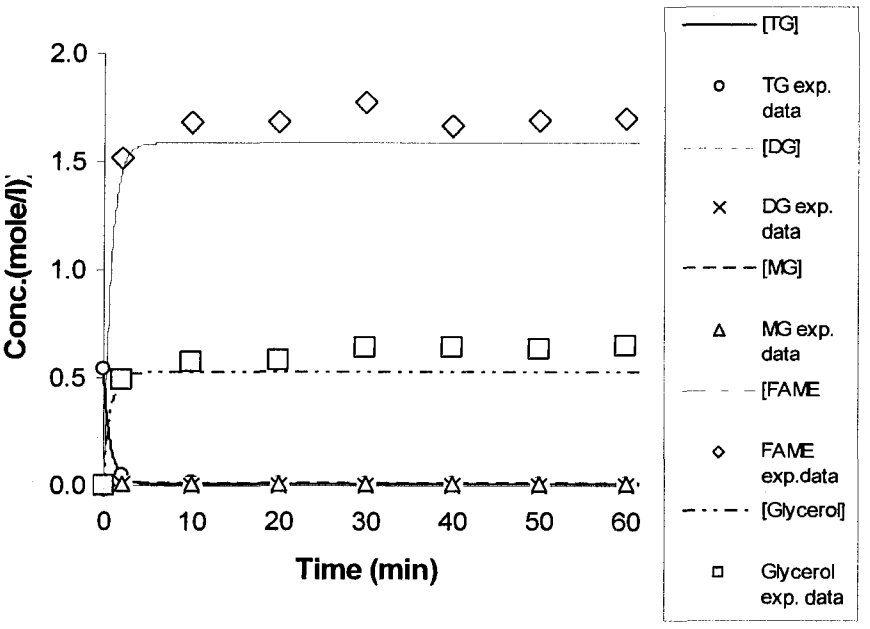


Figure 7.4: Experimental points and simulation curves for the concentration of the reaction mixture during the transesterification in membrane reactor with catalyst concentration 0.5% and 1 hour RT.

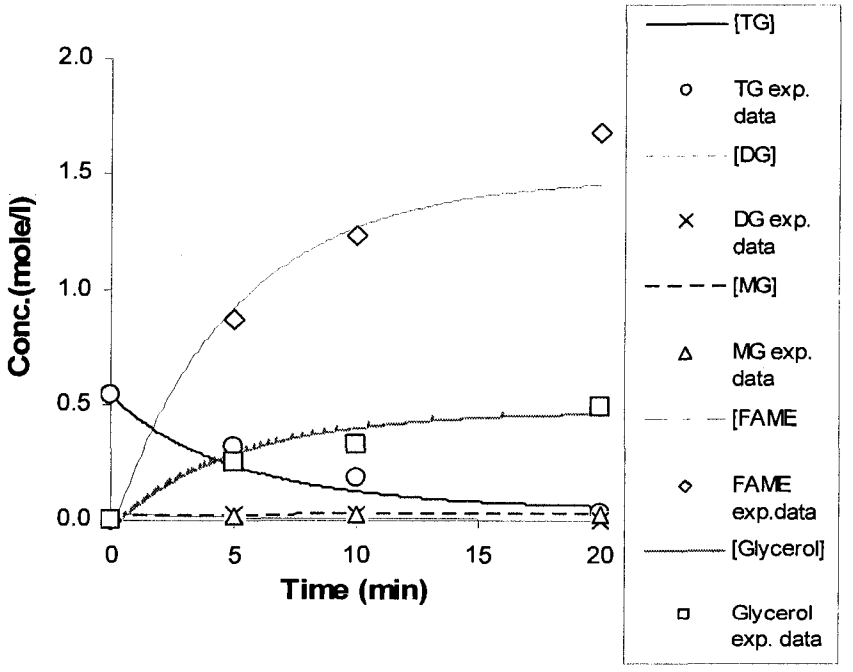


Figure 7.5: Experimental points and simulation curves for the concentration of the reaction mixture during the transesterification in membrane reactor with catalyst concentration 0.1 % and 1 hour RT.

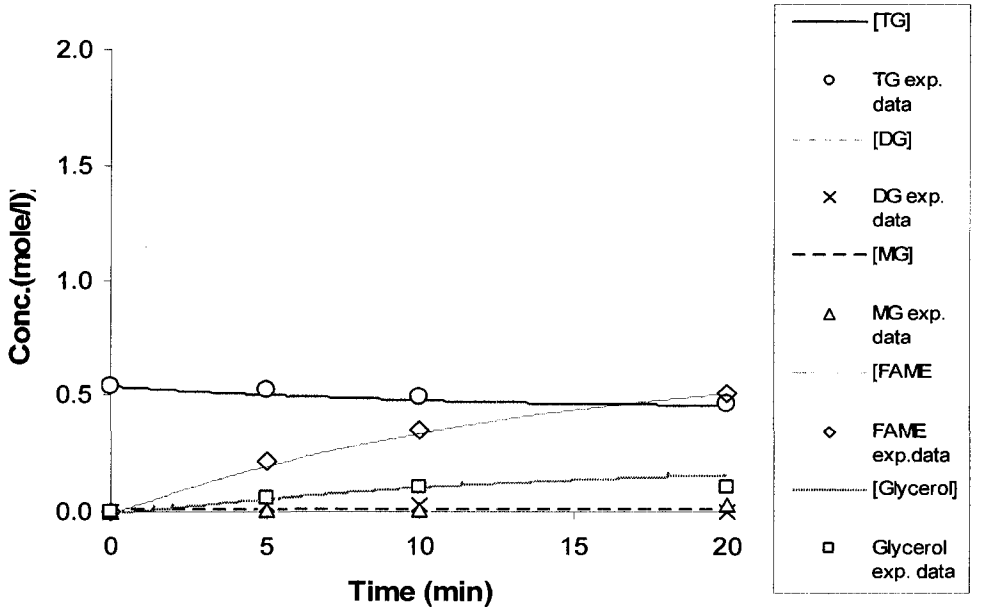


Figure 7.6: Experimental points and simulation curves for the concentration of the reaction mixture during the transesterification in membrane reactor with catalyst concentration 0.05% and 1 hour RT.

### 7.5.2 Effect of catalyst concentrations

Figure 7.7 shows the effect of catalyst on the TG conversion. At the 0.05% catalyst concentration, the TG conversion progressed slowly; an overall TG conversion was only 32.7% after 20 min. The mass transfer limitation resulted from the formation of an emulsion in the reaction mixture, but the membrane reactor takes advantage of this biphasic condition and produces biodiesel without TG. In Figure 7.7, the overall TG conversion for 0.1% catalyst run reached 95.5% after 20 min, and the TG concentration can reach to more than 98% only after 5 min for a 0.5% catalyst concentration.

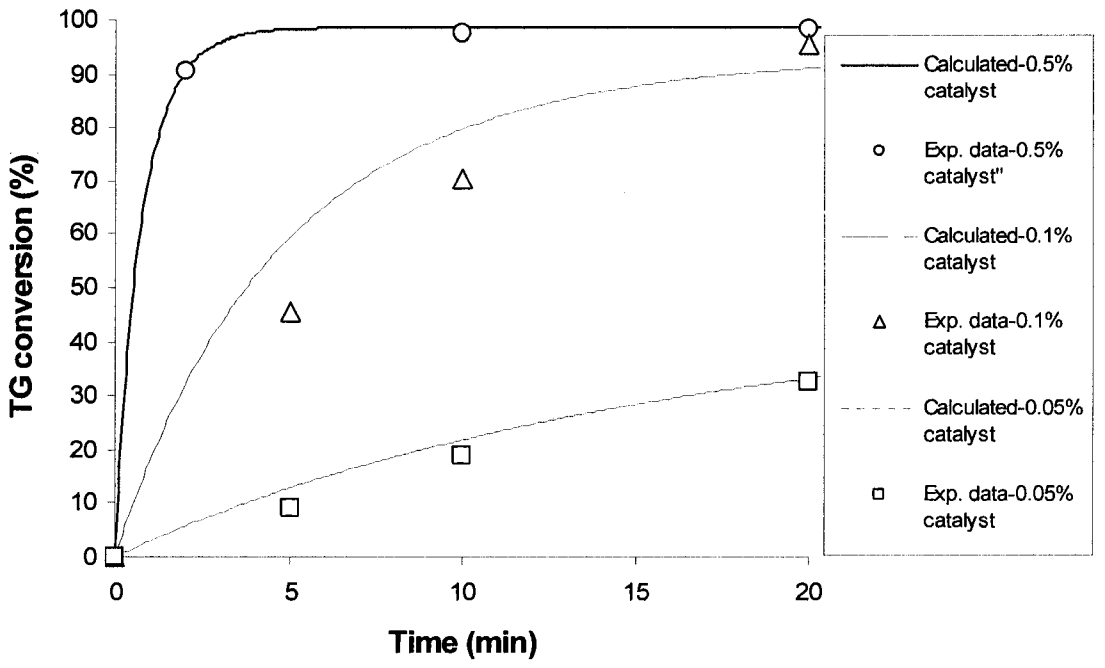


Figure 7.7: TG conversion as function of time

According to the kinetic model, the effective rate constants increased linearly with the catalyst concentration, Figure 7.8 illustrates this linear relationship between effective constants and catalyst concentration, the slopes represented the rate constants of the catalyzed reaction at 65°C. These rate constants irrespective of catalyst concentrations are listed in Table 7.2. As we know, the methanolysis process involves three steps, i.e., from TG to DG, DG to MG, and MG to glycerol; the ratio of $k_{forward}$:$k_{reverse}$ for each step in membrane reactor can be calculated, which is 1.48, 0.629, and 7.46, respectively. The ratio of the last step is greater than that of the second. It indicates that the reaction step MG to glycerol is faster than the step DG to MG, which is also in agreement with the work of Vicente,[16] and the work of Komers et al.[23]. In the membrane reactor, the lowest step of DG to MG is the control step for the canola oil methanolysis; MG reacts with methanol at the most fast rate, and is the least stable component in the membrane reactor, which agrees satisfactorily with MG concentration levels in this work and previous reported values [1,9,10].

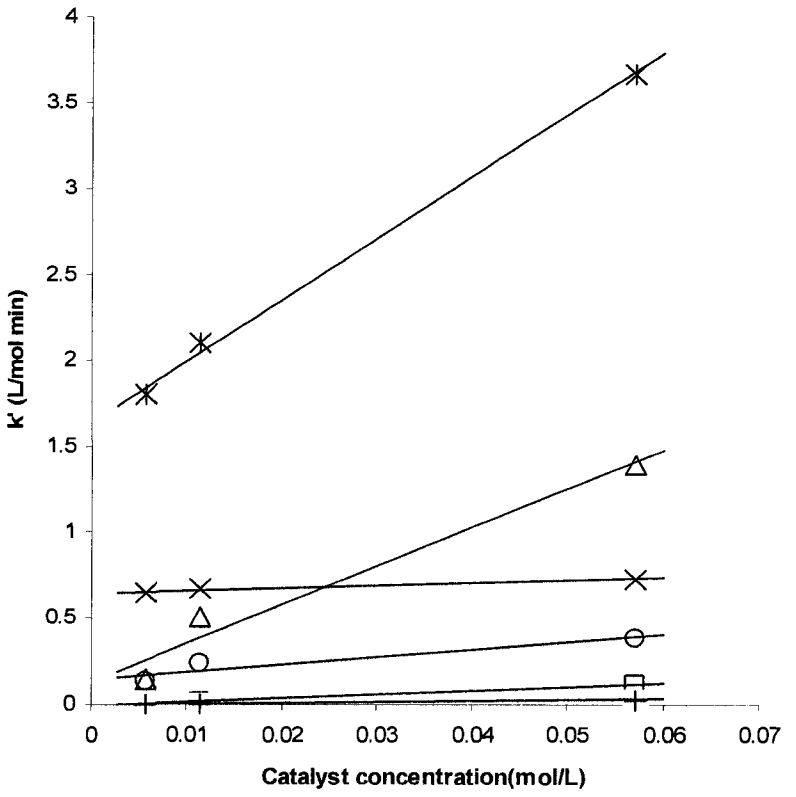


Figure 7.8: Effective rate constantans as a function of catalyst concentration.

$(\square - k_1'; \times - k_2'; \Delta - k_3'; * - k_4'; \mathrm{O} - k_5'; + - k_6')$

Table 7.2: Catalyzed reaction rate constant at 65 $^0$C in the membrane reactor

| Catalyzed reaction rate constants (L/(mole·min) | Present work (Canola oil) | Vicente's work[16] (Sunflower oil) | Vicente's work[24] (Brassica carinata oil) |
|---|---|---|---|
| $k_1$ | 2.1991 | 0.6116 | 0.0510 |
| $k_2$ | 1.4862 | 3.1346 | 0.3823 |
| $k_3$ | 22.466 | 2.0642 | 0.7785 |
| $k_4$ | 35.6950 | 1.6055 | 1.0958 |
| $k_5$ | 4.1078 | 2.0642 | 0.0510 |
| $k_6$ | 0.5503 | -- | -- |

Comparing to the forward rate constants to the work of Vicente,[16, 24] the forward rate constants in continuous membrane reactor were over 450% higher. This was attributed to the greater methanol:oil mole ratio used in this work (24:1 vs. 6:1 used in Vicente's work), excellent mixing in the membrane reactor loop and the continuous removal of product from the reaction medium. The work shows the advantages of product removal in enhancing the reaction rate in transesterifying canola oil in a membrane reactor.

## 7.6 Conclusions

A kinetic model was proposed to simulate the methanolysis of canola oil in the membrane reactor, which gives a good fit to the experimental data for all the conditions tested. It was found that the section of mass transfer control is not significant in the membrane reactor at the methanol to oil molar ratio of 24:1. When the catalyst concentration is at 0.5%, and the TG conversion can reach above 98% only after 5 min. The results obtained show that a decrease in the catalyst concentration lowers the reaction rate, the calculated effective reaction constants increase linearly with the catalyst concentration. Furthermore, the second step of the methanolysis was deemed as the lowest process which controls the overall reaction rates, and MG is the least stable component in the membrane reactor which was found to agree satisfactorily with previously reported values. It was concluded that the residence time did not play an important role in the kinetics of canola oil in the membrane reactor, the rate constants are at same level, but the continuous product removal from the reaction medium enhances the reaction rate in transesterifying canola oil in the membrane reactor.

## 7.7 Acknowledgements

The authors would like to thank the Natural Sciences and Engineering Research Council of Canada (NSERC) and the Ford Foundation for financial support.

## 7.8 References

(1) Cao, P.; Dubé, M. A.; Tremblay, A. Y. High Purity Fatty Acid Methyl Ester Production from Canola, Soybean, Palm and Yellow Grease Lipids by mean of a Membrane Reactor. *Biomass & Bioenergy* (in press), **2008.**

(2) Kusdiana, D.; Saka, S. Kinetics of Transesterification in Rapeseed Oil to Biodiesel Fuel as Treated in Supercritical Methanol. *Fuel,* **2001**, *80*, 693–698.

(3) Boocock, D. G. B.; Konar, S. K.; Mao, V.; Lee, C.; Buligan, S., Fast Formation of High-purity Methyl Esters from Vegetable Oils. *J. Am. Oil Chem. Soc.*, **1998,** *75*, 1167-1172.

(4) Van Gerpen, J; Shanks, B; Pruszko, R; Clements, D; Knothe, G. Biodiesel Production Technology, National Renewable Energy Laboratory, NREL/SR-510-36244, **2004**.

(5) Stavarache, C.; Vinatoru, M.; Nishimura, R.; Maeda, Y. Transesterification of Vegetable Oil in the Presence of Low Ultrasonic Irradiation. *Ultrasonics Sonochemistry,* **2004,** *12*, 367-372.

(6) Barnard, T. M.; Leadbeater, N. E.; Boucher, M. B., Stencel, L. M.; Wilhite, B. A. Continuous-Flow Preparation of Biodiesel Using Microwave Heating. *Energy & Fuels.* **2007,** *21*, 1777-1781.

(7) Tremblay, A. Y.; Dubé, M. A. International patent application, PCT/CA2006/000286, Feb., **2006**.

(8) Dubé, M. A.; Tremblay, A. Y.; Liu, J. Biodiesel Production Using a Membrane Reactor. *Biores. Tech.,* **2007**, *93*, 639-647.

(9) Cao, P.; Tremblay, A. Y.; Dubé, M. A.; Morse, K. Effect of Membrane Pore Size on the Performance of a Membrane Reactor for Biodiesel Production. *Ind. Eng. Chem. Res.,* **2007,** *46*, 52-58.

(10) Cao, P.; Dubé, M. A.; Tremblay, A. Y. Methanol Recycling in the Production of Biodiesel in a Membrane Reactor. *Fuel.* **2008,** *87*, 825-33.

(11) Freedman, B.; Pryde, E. H.; Mounts, T. L. Variables Affecting the Yields of Fatty Esters from Transesterified Vegetable Oils. *J. Am. Oil Chem. Soc.,* 1**984**, *61,* 1638-1643.

(12) Freedman, B.; Butterfield, R. O.; Pryde, E. H. Transesterification Kinetics of Soybean Oil. *J. Am. Oil Chem. Soc.,* **1986,** *63*, 1375-1380.

(13) Mittelbach, M.; Trathnigg, B. Kinetics of Alkaline Catalyzed Methanolysis of Sunflower Oil. *Fat Sci. Technol.*, **1990,** *92*, 145–148.

(14) Noureddini, H.; Zhu, D. Kinetics of Transesterification of Soybean Oil. *J. Am. Oil Chem. Soc.*, **1997,** *74*, 1457-1463.

(15) Leevijit, T.; Wisutmethangoon, W.; Prateepchaikul, G.; Tongurai, C.; Allen, M., A Second Order Kinetics of Palm Oil Transesterification. *The Joint International Conference on "Sustainable Energy and Environment (SEE)"*, Thailand, Dec,, **2004.**

(16) Vicente, G.; Martı´nez, M.; Aracil, J.; Esteban, A. Kinetics of Sunflower Oil Methanolysis, *Ind. Eng. Chem. Res.*, **2005,** *44*, 5447-5454.

(17) Doell, R.; Konar, S. K.; Boocock, D. G. B. Kinetic Parameter of a Homogeneous Transmethylation of Soybean Oil. *J. Am. Oil Chem. Soc.*, **2008,** *85*, 271-276.

(18) Karmee, S. K.; Chadna, D; Ravi, R; Chadha, A. Kinetics of base-catalyzed transesterification of triglycerides from Pongamia oil. *J. Am. Oil Chem. Soc.*, **2006,** *83*, 873–877.

(19) Lang, X.; Dalai, A. K.; Bakhshi, N. N.; Reaney, M. J.; Hertz, P. B. Preparation and Characterization of Bio-diesels from Various Bio-oil. *Biores. Tech.*, **2001,** *80*, 53-62.

(20) Dubé, M. A.; Zheng, S.; McLean, D. D.; Kates, M. A Comparison of Attenuated Total Reflectance-FTIR Spectroscopy and GPC for Monitoring Biodiesel Production. *J. Am. Oil Chem. Soc.*, **2004**, *81*, 599-603.

(21) Darnoko, D; Cheryan, M. Kinetics of palm oil transesterification in a batch reactor. *J. Am. Oil Chem. Soc.*, **2000,** *77*, 1263–1267.

(22) Cao, P.; Tremblay, A. Y.; Dubé, M. A. Biodiesel production using ultra low catalyst concentrations. *Energy & Fuels, in press*, 2008.

(23) Komers, K.; Skopal, F.; Stloukal, R.; Machek, J. Kinetics and Mechanism of the KOH –Catalyzed Methanolysis of Rapeseed Oil for Biodiesel Production. *Eur. J. Lipid Sci. Technol.*, **2002,** *104*, 728–737.

(24) Vicente, G.; Martı´nez, M.; Aracil, J. Kinetics of *Brassica carinata* Oil Methanolysis, *Energy & Fuels,* **2006,** *20*, 1722-1726.

# Chapter 8 General Discussion, Conclusions and Recommendations

The necessity for alternative energy sources across the globe is increasing as non-renewable resources are being depleted. For this reason, biodiesel has been the recent focus of much research. Biodiesel produced by the transesterification of vegetable oils is gaining considerable importance as a renewable fuel.

Transesterification, also referred to as alcoholysis, is a process that combines vegetable oils and/or other lipids with alcohol (usually ethanol or methanol) in the presence of a catalyst (e.g., sodium or potassium hydroxide, sulphuric acid) in order to yield mono-alkyl esters (biodiesel) and glycerol. Chemically, transesterification consists in taking a triglyceride (TG) molecule or a complex fatty acid, neutralizing the free fatty acids, removing the glycerol and creating a fatty acid alkyl ester (FAAE).

Unfortunately the reaction is complicated by its reversibility and the immiscibility of oil and alcohol. The quality of the fuel obtained as a result of batch processing is variable and impurities are often found in the biodiesel product; especially because the unreacted lipids and unsaponifiable materials are retained in the product due to their solubility in FAAE. Although many downstream separation methods have been studied for purifying the biodiesel product, they are often energy intensive and require the addition of extracting solvents to the process. In addition, most of these downstream processes involve the production of wastewaters and these often contain toxic elements (e.g., residual methanol and catalyst) which are evidently not in line with the environmentally driven ideals behind the use and production of biodiesel. In addition to this, most commercially available biodiesel is produced in batch processes which have inherent large scale limitations. All those challenges call for innovative technologies to be developed.

## 8.1 General Discussion and Conclusions

The main objectives of this thesis were to develop a new approach combining membrane separation with the transesterification process, and investigate the effects of different factors on the production process, biodiesel purity and the operation of a membrane reactor. Ideally, the membrane will be able to separate any unreacted material from the product, so that the reactants are retained inside the reactor for a longer

residence time and the products are removed from the reactor in the permeate. The membrane reactor used herein is based on the general principle that oil particles form droplets in hydrophilic environments. When the reactants are mixed, oil droplets form that are hopefully larger than the membrane pores. Subsequently, when the mixture passes by the membrane, only the hydrophilic molecules, namely FAAE, alcohol and glycerol, will be able to permeate through. This selective removal of the products pushes the reaction towards completion.

In Chapter 3 we studied the effects of pore size of the membrane used in the semi-continuous reactor and the initial methanol/canola oil loading. Four carbon membranes having different pore sizes were tested: 0.05, 0.2, 0.5 and 1.4 micron, with four different initial methanol volume fraction ($\phi_1$) 0.29, 0.38, 0.47, and 0.64. It was found that all four membranes retained canola oil in the reactor. Figure 8.1 illustrates that the same amount of injected oil produces almost the same amount of FAME. In other words, the membrane pore size did not affect the final conversion as long as the oil droplet size is larger than the membrane pore size.

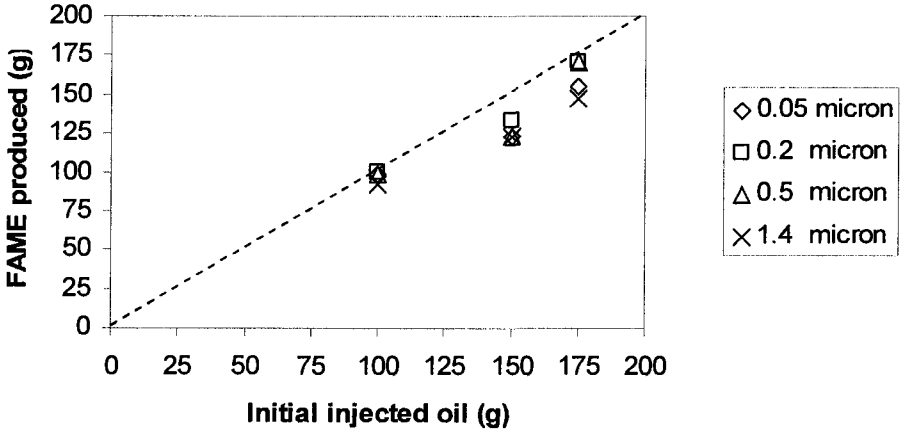


Figure 8.1: Comparison of the amount of FAME produced by transesterification vs. the initial amount of oil in the reactor.

Permeate was observed at the 0.38, 0.47, and 0.64 initial methanol volume fractions whereas it was not observed at $\phi_1 = 0.29$. A semi-empirical model was selected as a predictive equation to determine phase inversion in the reactor (Ho et. al., 1990). This limit was calculated as 0.31 using the following phase distribution equation, which is consistent with experimental results:

$$\frac{\phi_1}{\phi_2} = 1.22 \times \left( \frac{\mu_1}{\mu_2} \right)^{0.29} \qquad (1)$$

For the first time, the value of the octanol-water partition coefficient, $K_{ow}$, was used to illustrate the solubility of the reactants and products in the biodiesel production process. Table 8.1 list the log $K_{ow}$, which represents the tendency of a chemical species to partition itself between an organic and an aqueous phase (or a substance's hydrophilicity and hydrophobicity). This implies that species having closer values of $K_{ow}$ will have a stronger affinity towards each other, and thus be more miscible. It was shown that log $K_{ow}$ values correlated well with the experimental phenomena in the biodiesel production process.

Table 8.1: log $K_{ow}$ values of reaction mixture components in biodiesel production.

| **Chemical Name** | **log $K_{ow}$** |
|---|---|
| Glycerol | -1.76 |
| Water | -1.38 |
| Methanol | -0.77 |
| Ethanol | -0.31 |
| MG (mono-olein) | 6.04 |
| FFA (oleic acid) | 7.64 |
| FAME (methyl oleate) | 8.02 |
| FAEE (ethyl oleate) | 8.51 |
| DG (di-olein) | 14.64 |
| TG ( tri-olein) | 23.29 |

In the next phase of the work, as described in Chapter 4, we proceeded with research on the methanol-rich phase recycling to decrease the overall methanol:oil molar ratio. Three recycle ratios were tested: 100, 75 and 50%, at the same residence time and operating conditions. The permeate consistently separated to yield a FAME-rich non-polar phase containing a minimum of 85 wt.% FAME (the remainder being methanol) as well as a methanol/glycerol polar phase. At the highest recycle ratio, the FAME concentration ranged from 85.7 to 92.4 wt.% in the FAME-rich non-polar phase. In addition, the overall molar ratio of methanol:oil in the reaction system was significantly decreased while maintaining a FAME production rate of 0.04 kg/min. The three lines in Figure 8.2 show the theoretical overall molar ratio trends with time; for the 100% recycle cases, overall molar ratio could approach to 10:1 only after 2 h recycling.

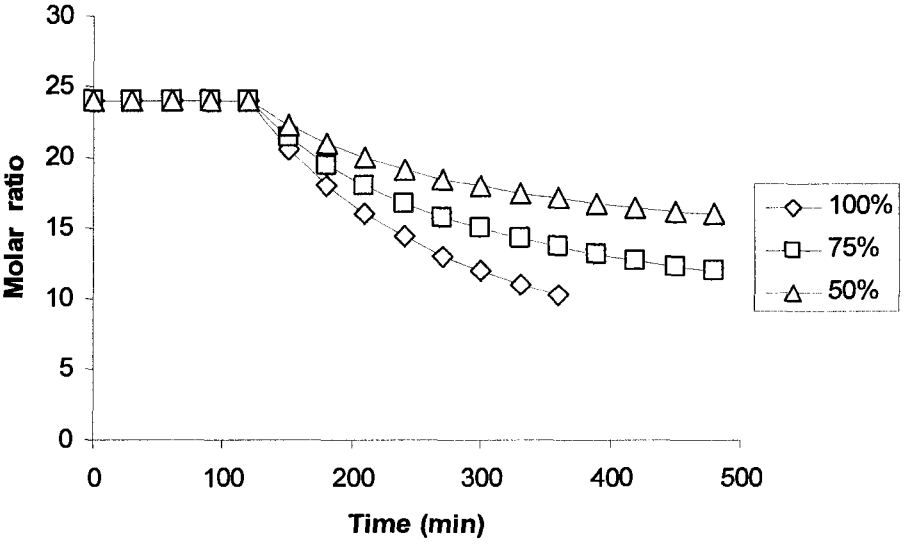


Figure 8.2. Accumulated overall methanol:oil molar ratio trends.

The recycled glycerol was shown to exert significant influence on the fluid density in the reaction loop and to increase the trans-membrane pressure (TMP). It was shown that the reactor could operate at a TMP well beyond that equivalent to a 6:1 methanol:oil molar ratio in a batch reaction. One could, however, operate at recycle and

operating conditions equivalent to a 6:1 overall methanol:oil ratio but the glycerol must be purged to prevent glycerol accumulation within the membrane reactor. In addition, no significant glycerol inhibition during the production of FAME was detected in the membrane reactor. FAME concentrations in the permeate were found to be independent of the recycling ratios, and were maintained between 55 and 60 wt.% after 40 min of reaction time for all recycle ratios tested.

In Chapter 5, the results of using different catalyst concentrations in the membrane reactor were reported. It was demonstrated that a membrane reactor can drive the reversible transesterification towards the product FAME, even at very low catalyst concentrations. A NaOH concentration above 0.05 wt% produced a permeate with very similar FAME concentrations as shown in Figure 8.3.

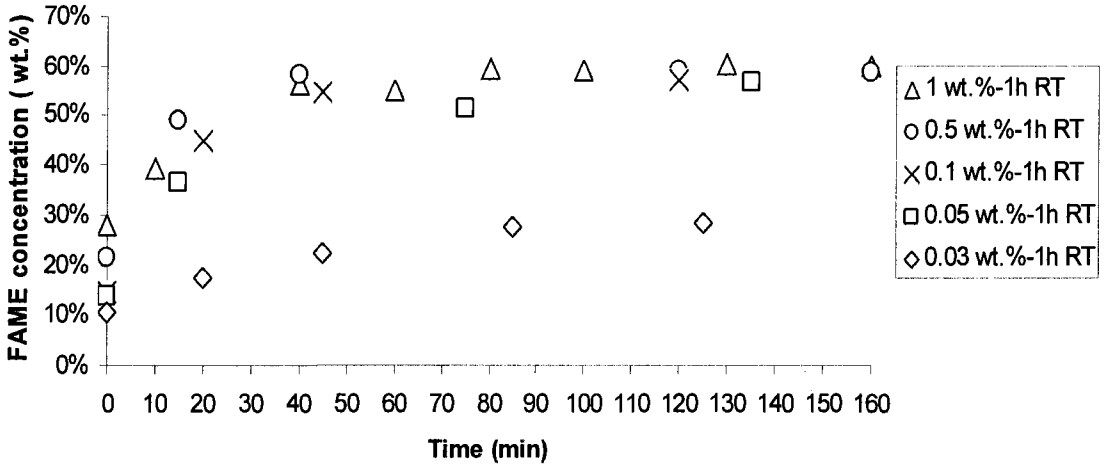


Figure 8.3: The FAME concentration in the permeate as a function of time.

No TG or MG was detected in the permeate stream. Unreacted TG was unable to pass through the membrane and enter the permeate stream to contaminate the biodiesel product. The unique advantage of the membrane reactor of not having to push the reaction to completion before obtaining product, has been fully demonstrated in this work. Furthermore, the concentrations of catalyst used in the reaction have been reduced 10- to 33-fold compared to those used industrially. From the perspective of a long-term, steady biodiesel production, the lowest catalyst concentration for obtaining feasible operation

conditions was 0.05 wt% at a RT of one hour and 0.03 wt% at a RT of two hours. The results illustrate the advantages in using a membrane reactor to produce biodiesel, where products are continuously removed from the reactor in a different phase than the lipid reactant.

Biodiesel production at lower catalyst concentrations will decrease the economic cost of production due to the lower consumption of catalyst, reduction of the downstream processing needed to obtain biodiesel at ASTM specifications and greatly improve the quality of the biodiesel by eliminating unreacted oils and non-saponifiable, oleophilic, substances from entering the biodiesel as is currently occurring in batch processes. Because less water wash steps will be needed to remove residual catalyst in the FAME phase, a higher quality glycerol by-product is obtained, which renders the biodiesel process more in line with the environmentally driven ideals behind the use and production of biodiesel. In addition to this, the visual quality of the co-product glycerol and the biodiesel are improved, indicating less degradation of substances found in the original canola oil feedstock. The RT in the membrane reactor was found not to have any effect on the permeate stream profile, and the FAME-rich phase had a very similar composition for catalyst concentrations above 0.03 wt%. This resulted in phase separation of the permeate stream, a consistent purification process at varying catalyst concentrations and the continuous production of TG free high purity biodiesel.

In the subsequent study reported in Chapter 6, different lipid feedstocks including low quality feedstocks (e.g., yellow grease) with high FFA contents were successfully transesterified in a continuous membrane reactor for biodiesel production under base-catalyzed conditions. Despite the fairly broad range of feedstocks, the membrane reactor delivered a fairly consistent performance at one set of operating conditions and enabled the production of high quality FAME. GC analysis based on the ASTM D6584 standard confirmed the production of high purity FAME from different lipid feedstocks using a continuous membrane reactor. The FAME from each feedstock, including that from waste lipids, completely met and exceeded the ASTM D6751 standard. The glycerine content of FAME produced using a membrane reactor is significantly lower than that produced via a conventional batch reaction as shown in Table 8.3. The FAME produced using methanol/glycerine recycling contained slightly higher glycerine content than that

without recycling. This implies that recycling had no apparently negative impact on biodiesel purity in terms of its free and total glycerine contents.

Table 8.3: GC results according to ASTM D6584

| **Lipid Feedstock** | Biodiesel from membrane reactor (wt.%) | | Biodiesel from batch reaction (wt.%) | |
|---|---|---|---|---|
| | Total glycerine | Free glycerine | Total glycerine | Free glycerine |
| Soybean | 0.0685 | 0.00763 | -- | -- |
| Canola | 0.0712 | 0.00654 | 0.131 | 0.0124 |
| Palm | 0.124 | 0.0117 | -- | -- |
| Yellow grease | 0.0989 | 0.00735 | 0.685* | 0.0234* |
| Brown grease | 0.104 | 0.0138 | 0.797* | 0.0171 |
| Canola oil with methanol recycle | 0.0929 | 0.00749 | -- | -- |

* does not meet the ASTM standard

The effect of the fatty acid composition of feedstock lipids on biodiesel quality was also studied by using the average value of log $K_{ow}$ of the different lipids. Figure 8.4 illustrates the relationship between the total glycerine content in the FAME-rich permeate phase and the average log($K_{ow}$) value for FAME mixtures from different lipid feedstocks. The soybean FAME mixture has the smallest $K_{ow}$ value, which implies that DG would have the least affinity to its corresponding FAME mixture. It was concluded that the biodiesel quality was significantly affected by the fatty acid composition of the lipid feedstocks. The percentage of FAME with less affinity to DG was directly related to the fatty acid composition of the original feedstock. This permitted the production of biodiesel with a total glycerine content lower than the 0.24 wt.% ASTM standard without a post-reaction water wash for soybean and canola oil-based biodiesel. These findings have significant implications for the use of feedstock blending to reduce the need for water washing in biodiesel production.

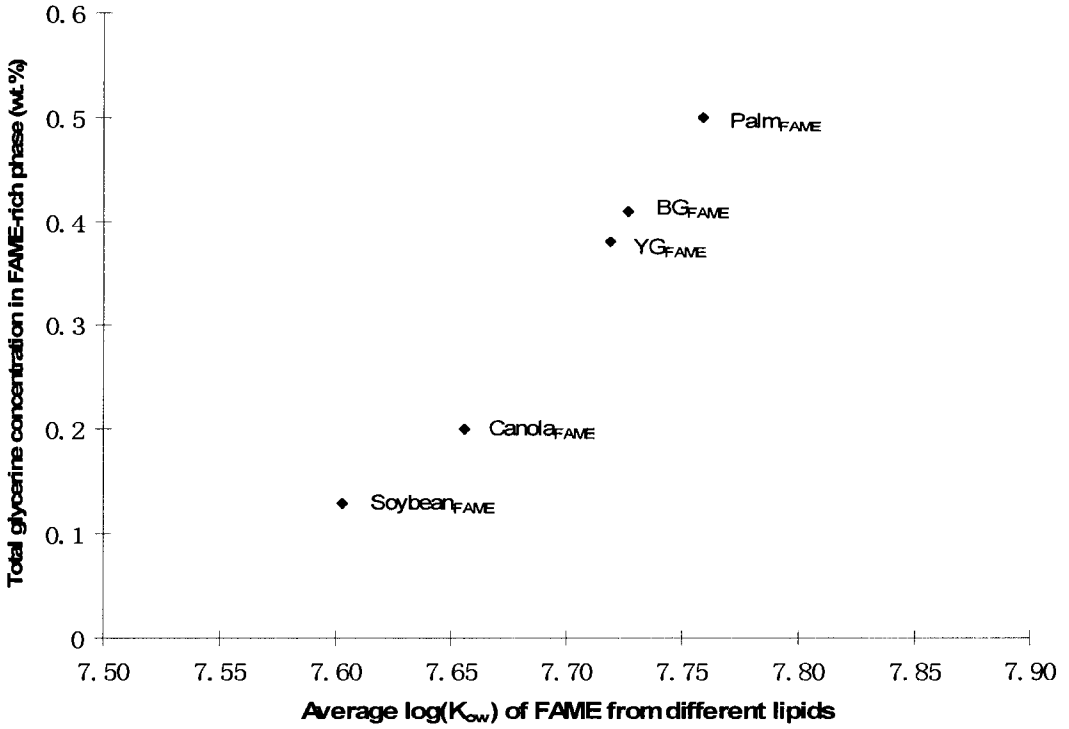


Figure 8.4: Total glycerine concentration in FAME-rich phase vs. average log($K_{ow}$) of FAME from different lipids.

Finally, the kinetics of canola oil transesterification in a membrane reactor were investigated in Chapter 7. The transesterification reaction kinetics are based on a reaction mechanism involving an initial mass transfer-controlled section followed by a kinetically controlled regime. However, the mass transfer-controlled part is not significant when the catalyst concentration is at 0.5%, the TG conversion can reach above 98% only after 5 minutes; Figure 8.5 illustrates this result. The residence time did not play an important role in the canola oil transesterification kinetics in the membrane reactor, the rate constants are clearly at about the same level for all cases. The results obtained show that a decrease in the catalyst concentration lowers the reaction rate, the calculated effective reaction rate constants increased linearly with the catalyst concentration. Continuous product removal from the reaction medium enhances the reaction rate in transesterifying canola oil in a membrane reactor.

The reaction rate constants were calculated based on the proposed kinetic model. The forward rate constants in this continuous membrane reactor were over 450% higher

than the previous work in a batch process as shown in Table 8.4 (Vicente et. al., 2005). This was attributed to the excellent mixing in the membrane reactor loop and the continuous removal of product from the reaction medium. The work shows the advantages of product removal in enhancing the reaction rate in transesterifying canola oil in a membrane reactor.

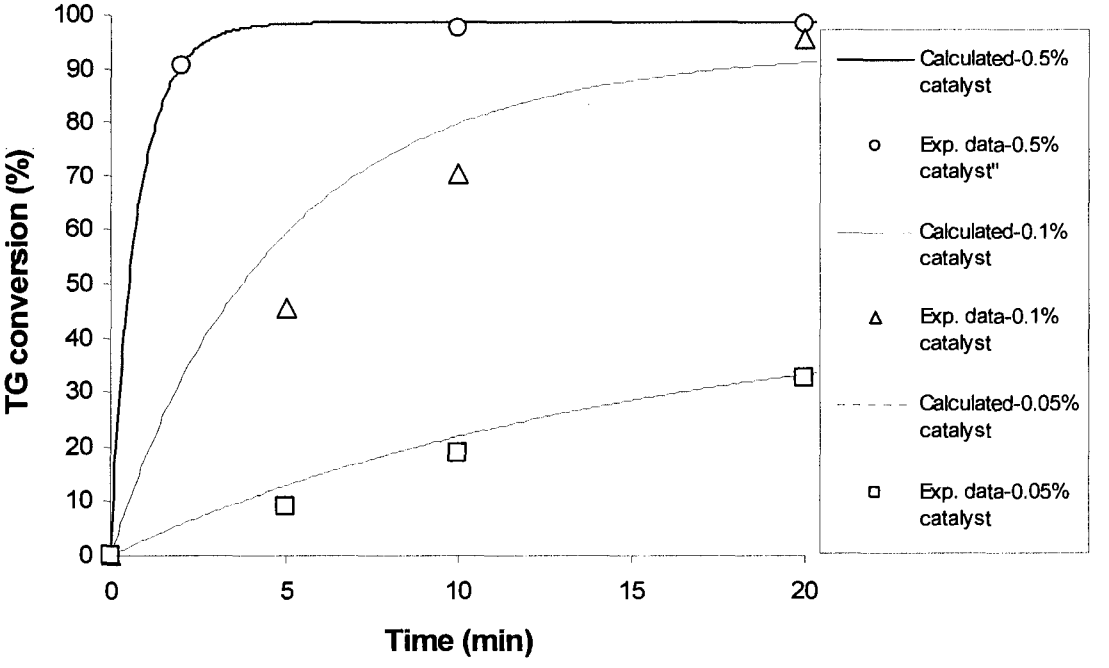


Figure 8.5: TG conversion as function of time

Table 8.4: Catalyzed reaction rate constant at 65°C in the membrane reactor

| Catalyzed reaction rate constants (L/(mole·min) | Present work | Vicente's work |
|---|---|---|
| $k_1$ | 2.1991 | 0.6116 |
| $k_2$ | 1.4862 | 3.1346 |
| $k_3$ | 22.466 | 2.0642 |
| $k_4$ | 35.6950 | 1.6055 |
| $k_5$ | 4.1078 | 2.0642 |
| $k_6$ | 0.5503 | -- |

In this thesis, bench and pilot scale membrane reactors were designed and assembled to carry out the transesterification of vegetable oils and other lipids with methanol. The membrane reactors integrate many procedures and reach several process integration objectives such as: combining reaction and separation in a single unit, continuous mixing of raw materials, maintaining high mass transfer between the immiscible phases and maintaining two phases during the reaction. The membrane reactor was particularly useful in removing unreacted lipids and impurities from the FAME product yielding high purity biodiesel which meets standards such as EN14214 and ASTM D6751. The straightforward separation of the FAME in the permeate stream also enabled the recycling of the polar phase back to the membrane reactor, thus lowering the overall methanol to lipid molar ratio to levels approaching 6:1. Much lower catalyst concentrations can be used in the membrane reactor which brings about the benefit of higher glycerol quality, better product separation and lower costs. In addition, the ability of the membrane reactor to produce biodiesel from a variety of lipid and alcohol feedstocks, some containing high amounts of FFA, has been demonstrated.

## 8.2 Recommendations

Based on the results of this study, the following recommendations are proposed:

In order to increase the yield of biodiesel, further experiments should be carried out in order to assess the limitations of this membrane reactor setup and optimize operational conditions. To decrease the cost of the membrane reactor, a less expensive membrane module, especially membrane materials other than carbon and ceramic, could be tested in this novel reactor system; membranes that are resistant to harsh reaction conditions would be of particular interest. In addition, attempts to evaluate and/or predict the lifetime of the membrane should be undertaken. The continuous biodiesel production with scaled-up multi-membrane modules in the reactor can be applied.

Biodiesel production using alcohols other than methanol should be further investigated. Maintaining a heterogeneous state within the reactor is important for membrane reactor operation. Basically, the membrane separation had no effect on the homogeneous reaction mixture. Preliminary experiments using ethanol have revealed that oil in ethanolysis process could not always form its own dispersion phase at regular

methanolysis condition. If we want to use ethanol instead of methanol, what conditions could guarantee the ethanol/oil system will be maintained in a heterogeneous state, and avoid the permeation of unreacted oil through the membrane? Would a lower reaction temperature help? Could the addition of water or methanol in ethanol assist in the decompatilization and help the oil-FAEE-glycerol-ethanol system create a heterogeneous state? Before the well-designed the experiments, a comprehensive simulation to estimate the transesterification conditions in the membrane reactor using ethanol or propanol could be carried out by HYSYS or other process simulation software.

The transesterification reaction can be catalyzed by both homogeneous and heterogeneous catalysts. Other than the base homogeneous catalyst used in this study, other catalysts such as enzyme or solid acid should be investigated. Those heterogeneous catalysts can be easily incorporated into the volume enhancement section of the membrane reactor. The separation of product from the reaction mixture using a membrane could facilitate the reuse and regeneration of heterogeneous catalysts.

The main difference of a membrane reactor is the use of inorganic membrane, which is now still at a relative high price. With increasing oil prices and the development of new membrane technology may provide lower cost membrane materials. An overall economic assessment based on the updated prices and the latest membrane technology is highly recommended to compare the biodiesel production in a membrane reactor with other conventional processes.

## 8.3 References

Ho, R. M.; Wu C. H.; Su A.C. Morphology of Plastic/Rubber Blends. *Polym. Eng. Sci.*, 30, 511, **1990**.

Vicente, G.; Martı´nez, M.; Aracil, J.; Esteban, A. Kinetics of Sunflower Oil Methanolysis, *Ind. Eng. Chem. Res.*, 44, 5447-5454, **2005**.

# Appendix

## Appendix A Equipment Operation Guidelines and Sample Analysis Procedures

### Appendix A.1 Biodiesel membrane reactor operation manuals

**Start up**

1. Check the reactor loop; make sure all the discharge valves are closed; check the electrical ground.
2. Fully open the manual feed valve and circuit control valve.
3. Turn the pressurized air valve for the filling pump to 30 psi, open the manual fill valve gently to initially fill the reactor with feedstock mixture at a certain molar ratio of alcohol and oil until liquid appears to flow through the highest manual valve (to discharge air while filling), then shut that valve.
4. Turn the pressurized air valve to close the safety valve; the attached pressure gauge was set to 20 psi.
5. Turn on the circulation pump.
6. Turn on the thermocouple to display the temperature.
7. Turn on the power of the Coriolis meter, check and compare the temperature of the thermocouple with that of the Coriolis meter, record the density changes until the end of the experiment.
8. Check the coolant level in the heater bath; turn on the heater power, circulate the coolant to heat the reactor.
9. Turn on the cooling water faucet to decrease the evaporation of alcohol in the permeate stream.
10. Monitor the temperature in the circulating loop. When it approaches $50^0$C, discharge the vapour by quickly opening the top manual valve.
11. Turn on the feed pump after checking and confirming that all the valves are in their correct position. Adjust the flow rate to the intended rate to feed the feedstock.
12. Adjust the heater bath; control the reactor at the intended temperature such as 65 or $70^0$C.

13. Balance the feed pump and the backpressure valve, adjust the permeate flow rate, pressures and pressure difference across membrane.

**Shut down**

1. When the experiment is complete, turn off the feed pump.
2. Turn off the heater bath.
3. When the temperature cools down to $40^0$C, turn off the power to the Coriolis meter. Turn off the circulating pump.
5. Quickly open the top manual valve to release the pressure to zero, and then close again.
6. When the temperature decreases to $45^0$C, turn off the cooling water.
7. Drain all the remains in the reactor from both sides of the membrane using the drain valve.
8. Fill the reactor with pure alcohol and turn on the circulating pump to rinse the reactor.

*Notes: be careful about thermal shock. Due to the ceramics in this system and if operator suddenly inject cold alcohol into the system, it could break the membranes as the thermal expansion of the housing is different from that of the membrane. So operator must allow a sufficient amount of time for the system to cool down to say $45^0$C before putting new fluid in it.*

**Leaving checklist for operator on the novel reactor:**

1. All power supplies should be unplugged, including the main electricity supply to the reactor.
2. Alcohols should always be put in the fume hood; any alcohol-containing liquid should be drained from the reactor and put in the special waste container. Only clean alcohol can be sealed in the reactor at room temperature with zero pressure (atmospheric pressure).
3. The cooling water faucet should be turned off.
4. Both of the two pressurized air valves in the right position: normally the pressure of diaphragm pump for feeding oil should be set to zero, i.e., turn off that valve; the

pressure of the safety valve should be set to 20 psi if there is a flammable liquid in the reactor, otherwise, it can be set to zero, i.e., turn off the valve.

5. All the samples are to be labelled and sealed.
6. Check outside the fume hood and flammable cabinet to ensure that there are no toxic or flammable chemicals laying around. Otherwise, put them into safe storage areas.
7. Check any potential leakage of the whole reactor system, and fix any leakage.
8. Turn off all power. Clean table and floor, turn off light in lab.

## Appendix A.2 HPLC/GPC operation guide for biodiesel sample analysis

### Sample preparation:

Sample work-up and analysis are as follows:

- About 20 mL of permeate (or retentate) is placed in a 40 mL vial (when the sample cools, it may become cloudy and de-phase into a FAAE-rich layer and glycerol-rich layer).
- For the base catalyzed case: A 12N HCl solution is immediately used to neutralize the sample to pH=7 indicated by pH paper. This should stop the transesterification reaction immediately. Normally one drop of 12N HCl is all that is necessary for a 20 mL sample when 0.5% base catalyst is used.
- For the acid catalyzed case: A 6N NaOH solution is immediately used to neutralize the sample to pH=7 as indicated by pH paper. This should stop the transesterification reaction immediately.
- The neutralized solution is filtered through a 0.2 micrometer PTFE syringe filter into a clean vial, this step also can be done later just before instrumental analysis.
- Normally the permeate sample is either cloudy or displays two distinct phases. If this is the case, the sample is heated to 50°C using a hot water bath to homogenize it prior to quantizing; if the sample remains heterogeneous after heating, the upper and lower phases are analyzed separately.

### GPC manual:

1. Turn the computer on
2. Session Manager → Stand by (Millenum V2.10)
3. Turn on
   - water 996
   - 717
   - 600
4. User name = System

5. Pass word = Manager
6. Log in → biodiesel
7. Metho view button → all the existing method can be seen
8. Quick start
9. Biodiesel 1 → use existing method
10. Instrument method (before setting the instrument)
11. Pump 600 → (I should change the flow rate, pressure)
12. Pressure high limit = 1500
13. Pressure low limit = 0.5
14. Flow rate = 0.0
15. % C = 100
16. % A = 0.0
17. High temperature = 20.0

    I should also change the pressure and flow rate in the modified
18. At this time, manually start increasing the flow rate from 0.0 up to 0.5 (gradually)
19. The pressure will increase (by itself) up to 732 psi
20. Instrument method = biodieselTHFinsmethod
21. Setup instrument → "yes"
22. The "Sample loading table" can be seen
23. Pull out the air or bubbles from W600
24. W717 → purge page
25. Start purge
26. Purge 996 by pushing the blue button ($2^{nd}$ function) and then no. 9 (purge)
27. After purging, the machine is ready to analyse the samples
28. W996 → sensitivity of detector, it can be changed by pushing "sens" button; 22.3 / 64 / 128 / 256 / 512
29. Usually we choose "64" by pushing the "sens" button
30. On w717, we should be on the main page
31. In W600, set up → silk should be "on" by pressing the key no. 1
32. The "Direct" button will change the page to the main menu

33. I can decrease the flow rate and increase it again to reach the desired pressure (732 psi)
34. Quick Set → (then we have the sample table)
35. Inject sample
36. Method set report → biodiesel 1
37. Injection volume → 10/15/20 (depends)
38. Run time → 60 minutes
39. Sample weight = 1.000
40. Leave other columns just check they are ok
41. Mode → Sample sat mode
    (if you have just one sample, you can choose "single set mode")
42. "run try" button
43. Save as "name"
44. A window will show up → selected samples
    The machine will start to do the analysis
45. Project Biodiesel
46. Click on "up date" → the last sampling information will be shown in the first rows of the table
47. By double clicking on each of the samples, the peaks related to that sample can be seen
48. You can copy the results on a floppy
49. Copy / Select the desired files
50. tools / process and report
51. Use specified processing method
52. Pro-export
53. Uncheck "print report"
54. Use acquisition / pro
55. Export
56. Use specified process report method
57. Peigang
58. (Alt + tab) → program manager

59. File manager → my file (Peigang) will be shown
60. Select them
61. F7 (move)
62. Then type ( A:\ .... )
63. To finish working with GPC, just close all the windows in the computer and check the W600, 996 and 717 one more time.
64. How to calculate or estimate the peak areas?
65. Biodiesel Project
66. Double click on your sample
67. Integrate
68. View
69. Result table / for negative peaks:
70. Enlarge the peaks to change the two ends of the lines on the points you need
71. Manually change the lines (move line AB to CD)

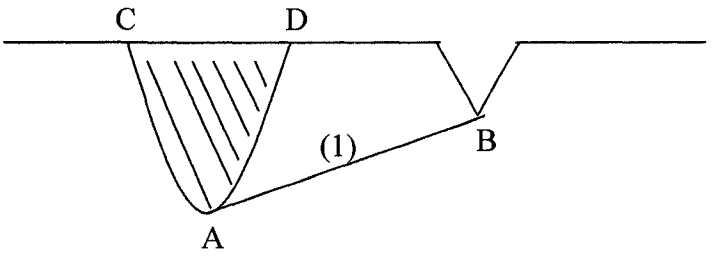


72. The given area in the table is the negative peak area.

**GPC analysis conditions**

| **Items** | **Name** |
|---|---|
| Column | Phenogel 3μm 100Å 300×7.5mm |
| Eluent flow rate | 0.5 mL/min |
| Sample injection volume | 20 μL |
| Eluent | THF |
| Temperature | 25 °C |
| Pump | Waters 600-MS |
| Detector | Waters 410 differential refract meter |
| Analysis time | 60 min |

**GPC retention times of standards**

| Standard | Retention time (min) |
|---|---|
| Triolein (TG) | 24.57 |
| Diolein (DG) | 25.45 |
| Monoolein (MG) | 27.12 |
| Methyl oleate (FAME) | 28.68 |
| Glycerol | 30.95 |
| Methanol | 35.20 |
| Ethanol | 33.75 |
| Ethyl oleate (FAEE) | 28.33 |

**Calibrations of standard solutions,**

**Injection mass (mg) =$a$× Peak Area +$b$**

| Component | Molecular Weight | a | b |
|---|---|---|---|
| Triolein (TG) | 885.46 | $4.530\times10^{-8}$ | 0.0003927 |
| Diolein (DG) | 621.01 | $4.550\times10^{-8}$ | 0.00009567 |
| Monoolein (MG) | 356.55 | $4.612\times10^{-8}$ | -0.00009703 |
| Oleic acid (FFA) | 282.47 | $5.075\times10^{-8}$ | 0 |
| Methyl oleate (FAME) | 296.5 | $6.299\times10^{-8}$ | 0.0001564 |
| Glycerol | 92.09 | $5.566\times10^{-8}$ | 0.0003673 |
| Methanol | 32.04 | $3.560\text{x}10^{-8}$ | 0.0005007 |

## Appendix A.3 GC operation guide (ASTM D6584 - Cold on column injector)

### Sample Preparation

*(All steps written below are done under nitrogen in the glove compartment)*

1. Weigh 100 mg of sample into a 10 mL septa vial.
2. Add 100 µL of each Butanetriol (internal standard 1), Tricaprin (internal standard 2), and MSTFA into the sample vial. Both internal standards are located in the refrigerator in room D403 - *Make sure you put the standard solutions back in the refrigerator after you're done.*
3. Shake the vial and let it set for 20 minutes at room temperature.
4. Add 8 mL of high grade n-heptane into the vial and shake for a few seconds.
5. Remove approximately 1 mL of the sample mixture into GC auto sampler vials.
6. Label the 10 mL vial and the auto sampler vial accordingly.

### Getting Ready

1. Check that gas filters are still functional. All carrier and detector filters should be changed when indicator shows filter is spent. Oxygen contamination in carrier gas can produce excessive column bleed and hydrocarbons cause ghost peaks or increase detector noise.
2. Open the valves on the helium, air, and hydrogen tanks. Verify that they are set to the appropriate pressures; if not, adjust the set-screw accordingly.
   - Helium, carrier gas, set point is ~80 psi
   - Compressed air, set point is ~60 psi
   - Hydrogen, set point is ~40 psi
3. Always leave at least 400 psi residual gas in a depleted cylinder. As the cylinder pressure drops, the concentration of the impurities such as moisture and hydrocarbons increase which will lead to column damage. In addition, if the cylinder pressure drops below the supply pressure required by the GC, retention times and detector sensitivities can slowly change and affect the validity of data gathered.

**6584 Data Handling Method**

1. 8410 Autosampler

Syringe size: 10 µL

Injection mode: User defined

Solvent penetration depth: 90%

Sample penetration depth: 90%

Default clean vial: I

Default clean volume: 5 µL

Default clean strokes: 1

Default clean draw up speed: 5 µL/sec

Clean mode pre-inj solvent flushes: 2

Clean mode post-inj solvent flushes: 2

Clean mode pre-inj sample flushes: 2

Clean Mode solvent source: I & III

Use internal standard: no

Internal standard vial: II

Internal standard volume: 1 µL

Internal standard drawup speed: 5 µL/sec

Internal standard pause time: 0 sec

Internal standard air gap: no

Solvent plug vial: III

Solvent plug volume: 0 µL

Solvent plug draw up speed: 5 µL/sec

Solvent plug pause time: 0 sec

Solvent plug air gap: no

Viscosity delay: 6 sec

Plunger fill speed: 2 µL/sec

Plunger inject speed: 5 µL/sec

Pre-injection delay: 0 sec

Post-injection delay: 6 sec

Fill volume: 5 µL

Fill strokes: 0

Sample air gap: yes

Air plug after sample: 1 µL

Use prepahead: no

Delay time: 0 min

2. Injector

- Front injector type 1079

  Oven power: on

  Coolant: on

  Enable coolant at: 300 °C

  Coolant timeout: 20 min

| Temp (C) | Rate (C/min) | Hold (min) | Total (min) |
|---|---|---|---|
| 50 | 0 | 0.10 | 0.10 |
| 370 | 150 | 32.50 | 34.73 |

| Time (min) | Split state | Split ratio |
|---|---|---|
| Initial | off | off |

- Middle injector type 1177 (not in use)

  Oven power: on

  Temperature: 100 °C

- Rear injector type 1041 (not in use)

Oven power: on

Temperature: 100 °C

3. Flow/Pressure
    - Front injector EFC type 1

        Constant column flow: 3 mL/min

        Pressure pulse: none
    - Middle EFC type 1 (not in use)
    - Rear EFC type 3 (not in use)

4. Column oven

    Coolant: off

    Enable coolant at: 50 °C

    Coolant timeout: 20 min

    Stabilization time: 0 min

| Temp (C) | Rate (C/min) | Hold (min) | Total (min) |
|---|---|---|---|
| 50 | 0 | 1 | 1 |
| 180 | 15 | 0 | 9.67 |
| 230 | 7 | 0 | 16.81 |
| 370 | 10 | 4.19 | 35 |

5. Detector
    - Front FID Detector

        Oven power: on

        Temperature: 380 °C

        Electronics: On

        Time constant: fast

| Time (min) | Range | Autozero |
|---|---|---|
| Initial | 12 | yes |

Front type 11 Detector EFC

Make up flow: 28 mL/min

$H_2$ flow: 30 mL/min

Air flow: 300 mL/min

6. Output

   Time: initial

   Port A signal source: front

   Attenuation: 1

7. Data acquisition

   Detector bunch rate: 4 points

   Noise monitor length: 64

   FID/TCD detector full scale for front, middle, and rear: 1 V

**GC Instructions**

1. Turn on GC (external switch).
2. As the GC begin its initializing step, click the *ComputerLike* button located on the top left hand corner on Varian workstation toolbar to achieve a communication between the software and the GC instrument.
3. "System Control - Configuration" window appears. Working from the Workstation Star software to change method and parameters is preferable than from CP-3800 GC keyboard.
4. Select File → Activate Method. The "Activate a System Control Method File" window opens and select Biodiesel-ASTM6584 folder → Biodiesel6584, press Open. The method name that is activated will now shown in the System Control window's toolbar.
5. Always check the column, injector and detector status; and confirm that the GC is in the Ready state for sample injection. The amber "Ready" light should be

illuminated and green circles should be shown for all the parameters set in the system control window. The red "Not Ready" light will be illuminated and red circles will appear if one or more of the set conditions are not reached.

6. You can inject a single sample or multiple samples from System Control.
    a) Select Inject → Inject Single Sample or by clicking on the *Inject Single Sample* button in the toolbar.
    b) Select File → New SampleList or by clicking on the *New or Open Automation File* button on the tool bar.
7. Both functions on step 6 will open up a sample dialog box.
    - Sample name
    - Sample type → set as Analysis
    - Number of Injection needed
    - Injection notes
    - AutoLink → leave as None
    - Vial position number
    - Injection Volume → set as 0.5 μL
    - Injectors Used → set as position 1
    - Click the scroll bar to scroll past the list of values for the Amount Standard, Unid Peak Factor, Multiplier, and Divisor. Leave them set to their default values.
8. After filling all the parameters mentioned in step 7, below the row of the last sample Select Sample Type → Activate Method and click on *None* button under AutoLink column. The "Activate Method" window opens and select Biodiesel-ASTM6584 folder → Stdby, press Open.
9. Click the *Inject* button to start the run.

**Remarks**

- All samples' chromatogram are saved in the "Data" folder automatically and it's preferred that the chromatograms are copied into a disk to be analyzed.
- GC can be left in Stdby mode for 2 weeks in between sample analysis. If it is predicted that it will not be used for long time i.e., a month or longer then it can be turn off to preserve the gas carrier. The shut down procedure is turning off GC,

closing the air and hydrogen tank valves, and finally the carrier gas, both the regulator valve and the top tank valve.

**Operating conditions for GC (from ASTM D 6584-00)**

| | | |
|---|---|---|
| **Injector** | | |
| Cool on column injection | | |
| Sample size | 1 μ L | |
| **Column Temperature Program** | | |
| Initial temperature | 50 $^0$C | hold 1 min |
| Rate 1 | 15 C/min to 180 $^0$C | |
| Rate 2 | 7 C/min to 230 $^0$C | |
| Rate 3 | 30 C/min to 380 $^0$C | hold 10 min |
| **Detector** | | |
| Type | Flame ionization | |
| Temperature | 380 $^0$C | |
| **Carrier Gas** | | |
| Type | Hydrogen or Helium | measured at 50 $^0$C |
| Flow rate | 3 mL/min | |

**The retention times of standards for GC**

| Standard | Retention time (min) | Relative Retention Times (RRT) |
|---|---|---|
| Triolein (TG) | 30.424 | 1.44 |
| Diolein (DG) | 24.890 | 1.18 |
| Internal STD 2 | 21.082 | 1 |
| Monoolein (MG) | 16.219 | 0.76 |
| Internal STD 1 | 6.198 | 1 |
| Glycerol | 5.695 | 0.91 |

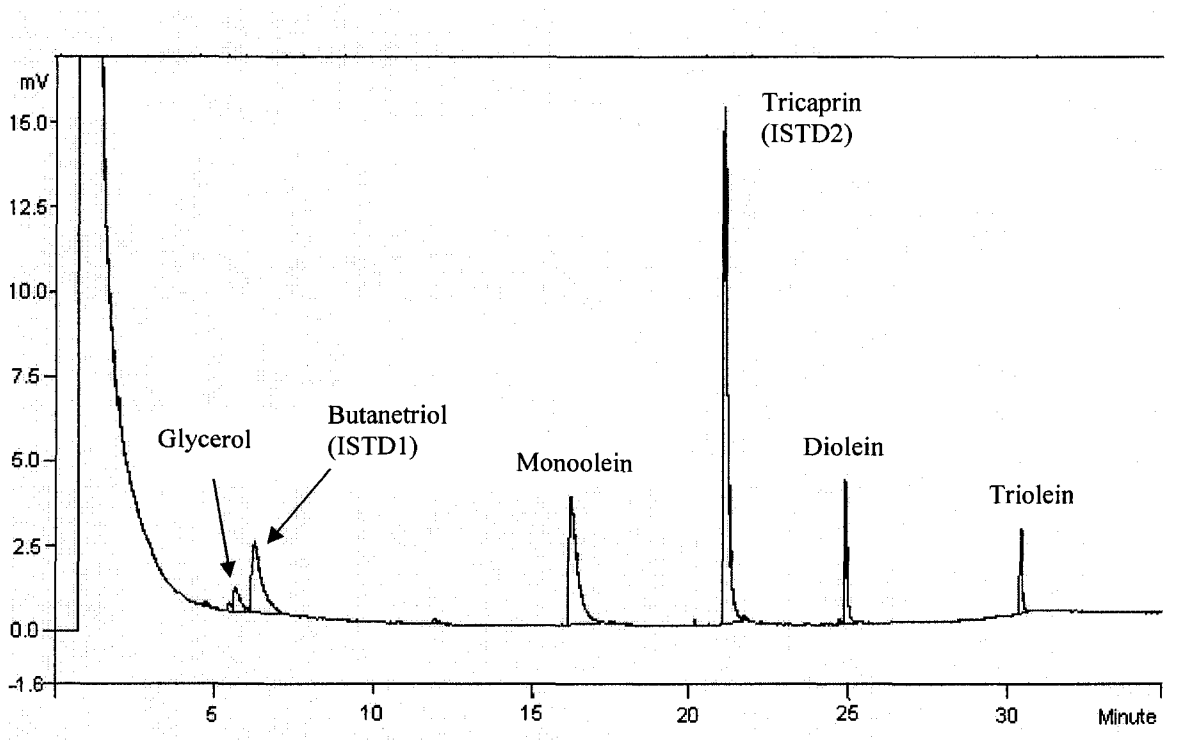


Figure A.4: GC Chromatograph of mixture of standards.

## Appendix B Raw Data for Chapter 3-7

### Experiments performed for chapter 3.

Experimental mode: Semi-continuous mode.

| Carbon Membrane pore size | 100g oil Injected initially | 150g oil Injected initially | 175g oil Injected initially |
|---|---|---|---|
| Old 0.05μm | I-#1* | I-#2 | I-#3 |
| New0.05μm | I-#4 | I-#5 | I-#6* |
| New 0.2μm | I-#7 | I-#8 | I-#9 |
| New 0.5μm | I-#10 | I-#11 | I-#12 |
| New 1.4μm | I-#13 | I-#14 | I-#15 |

*Notes: Catalyst (con.): base 0.5%; total alcohol mass: methanol 800mL; Reactor temperature: 65 $^0$C, reactor pressure: 20 psi; Lipid: virgin canola oil. Flowrate is unregular due to the backpressure valves' inconsistency, The total volume of the reactor was 320 mL.*

**0.05 µm**

| ***100 g oil*** | | | |
|---|---|---|---|
| Volume of MeOH that has passed through the reactor (mL) | **Mass % FAME** | **Mole % FAME** | **Integrated area** |
| 0 | 17.73839527 | 2.405138802 | |
| 125 | 23.01712139 | 3.222528952 | 2547.219791 |
| 250 | 27.68267218 | 4.919029327 | 3168.737098 |
| 375 | 19.89501963 | 2.67653561 | 2973.605738 |
| 500 | 15.26314325 | 1.929436023 | 2197.38518 |
| | | | 10886.94781 |
| ***150 g oil*** | | | |
| 0 | 22.59286497 | 3.245712059 | |
| 100 | 24.62459018 | 3.549221652 | 2360.872757 |
| 400 | 26.09448685 | 4.28702363 | 7607.861555 |
| 500 | 21.96556804 | 3.143437237 | 2403.002744 |
| | | | 12371.73706 |
| ***175 g oil*** | | | |
| 0 | 22.90612788 | 3.262541208 | |
| 166.6666667 | 34.07213365 | 5.44999798 | 4748.188461 |
| 333.3333333 | 28.64768574 | 4.063936881 | 5226.651615 |
| 500 | 25.64768574 | 3.793936881 | 4524.614289 |
| | | | 14499.45437 |

## 0.2 µm

| ***100 g oil*** | | | |
|---|---|---|---|
| Volume of MeOH that has passed through the reactor (mL) | **Mass % FAME** | **Mole % FAME** | **Integrated area** |
| 0 | 26.69954916 | 3.965075613 | |
| 125 | 20.73600893 | 2.791688067 | 2964.722 |
| 250 | 19.88595887 | 2.650156977 | 2538.873 |
| 500 | 19.09466723 | 2.318792982 | 4872.578 |
| | | | 10376.17 |
| ***150 g oil*** | | | |
| 0 | 25.0143654 | 3.77639639 | |
| 83.33333 | 31.9842561 | 4.914567643 | 2374.943 |
| 125 | 30.0498753 | 4.538532996 | 1292.378 |
| 166.6667 | 40.1567896 | 6.727843365 | 1462.639 |
| 229.1667 | 35.2469125 | 5.220451506 | 2356.366 |
| 291.6667 | 34.8651326 | 4.930706571 | 2191.001 |
| 375 | 34.2564389 | 4.82158311 | 2880.065 |
| 437.5 | 30.5046123 | 4.128627555 | 2023.783 |
| 500 | 22.3841262 | 3.20505366 | 1652.773 |
| | | | 16233.95 |
| ***175 g oil*** | | | |
| 0 | 19.53229267 | 2.718746964 | |
| 33.33333 | 34.25846364 | 5.632223436 | 896.5126 |
| 66.66667 | 45.98061927 | 8.880470623 | 1337.318 |
| 100 | 44.6948243 | 8.407385323 | 1511.257 |
| 133.3333 | 48.59479107 | 9.769279354 | 1554.827 |
| 166.6667 | 50.27913842 | 10.18279047 | 1647.899 |
| 233.3333 | 50.99578559 | 10.61947087 | 3375.831 |
| 300 | 45.69498241 | 8.680468189 | 3223.026 |
| 350 | 35.37579504 | 5.809294674 | 2026.769 |
| 400 | 36.4973806 | 6.037911891 | 1796.829 |
| 500 | 29.08454212 | 4.793814215 | 3279.096 |
| | | | 20649.37 |

**0.5 µm**

| ***100 g oil*** | | | |
|---|---|---|---|
| Volume of MeOH that has passed through the reactor (mL) | **Mass % FAME** | **Mole % FAME** | **Integrated area** |
| 0 | 24.81399853 | 3.512504159 | |
| 41.66666667 | 25.90743689 | 3.718011684 | 1056.697 |
| 83.33333333 | 25.24124221 | 3.588359061 | 1065.597 |
| 125 | 24.08715001 | 3.381740186 | 1027.675 |
| 166.6666667 | 23.78107317 | 3.326543724 | 997.2546 |
| 208.3333333 | 24.31493742 | 3.418971321 | 1002 |
| 250 | 28.40608047 | 4.249229072 | 1098.355 |
| 312.5 | 21.77729608 | 2.96989222 | 1568.231 |
| 375 | 18.22694776 | 2.389827953 | 1250.133 |
| 500 | 16.14081557 | 2.082643524 | 2147.985 |
| | | | 11213.93 |
| ***150 g oil*** | | | |
| 0 | 41.12196029 | 7.359957457 | |
| 142.8571429 | 32.88184081 | 5.197566171 | 5285.986 |
| 285.7142857 | 24.16547412 | 3.443970703 | 4074.808 |
| 400 | 23.55323833 | 3.37061881 | 2726.784 |
| 500 | 19.27432844 | 0.840610292 | 2141.378 |
| | | | 14228.96 |
| ***175 g oil*** | | | |
| 0 | 29.62810001 | 4.664999795 | |
| 41.66666667 | 47.47392794 | 9.38941883 | 1606.292 |
| 83.33333333 | 48.68696592 | 9.855981521 | 2003.352 |
| 166.6666667 | 42.87827745 | 7.8337875 | 3815.218 |
| 250 | 39.17536816 | 6.752081711 | 3418.902 |
| 375 | 30.54858329 | 4.819973744 | 4357.747 |
| 500 | 29.21711364 | 4.372589147 | 3735.356 |
| | | | 18936.87 |

**1.4 µm**

| ***100 g oil*** | | | |
|---|---|---|---|
| Volume of MeOH that has passed through the reactor (mL) | **Mass % FAME** | **Mole % FAME** | **Integrated area** |
| 0 | 30.25972881 | 5.42868987 | |
| 208.3333333 | 24.70031527 | 3.490076954 | 5725.005 |
| 375 | 20.45161954 | 2.741864176 | 3762.661 |
| 500 | 11.5828215 | 1.405234934 | 2002.153 |
| | | | 11489.82 |
| ***150 g oil*** | | | |
| 0 | 43.73582988 | 7.878078083 | |
| 83.33333333 | 32.91167862 | 5.579936098 | 3193.646 |
| 500 | 19.52056799 | 1.843277379 | 10923.38 |
| | | | 14117.03 |
| ***175 g oil*** | | | |
| 0 | 61.97016385 | 15.86654368 | |
| 166.6666667 | 30.38077793 | 5.625304547 | 7695.912 |
| 500 | 24.15226321 | 2.205287997 | 9088.84 |
| | | | 16784.75 |

**Experiments performed for chapter 4.**

Experimental mode: continuous mode with recycling.

**50% Recycling**

| Time (min.) | phases | Component | comp. wt.% |
|---|---|---|---|
| 0 | upper POLAR | FAME | 16.07 |
| | | GLYCEROL | 11.01 |
| | | METHANOL | 72.91 |
| | Lower FAME | FAME | 85.71 |
| | | GLYCEROL | 0.00 |
| | | METHANOL | 14.29 |
| 20 | upper POLAR | FAME | 15.52 |
| | | GLYCEROL | 11.96 |
| | | METHANOL | 72.52 |
| | Lower FAME | FAME | 86.17 |
| | | GLYCEROL | 0.00 |
| | | METHANOL | 13.83 |
| 40 | upper POLAR | FAME | 11.10 |
| | | GLYCEROL | 13.18 |
| | | METHANOL | 75.72 |
| | Lower FAME | FAME | 86.39 |
| | | GLYCEROL | 0.00 |
| | | METHANOL | 13.61 |
| 60 | upper POLAR | FAME | 10.77 |
| | | GLYCEROL | 13.67 |
| | | METHANOL | 75.56 |
| | Lower FAME | FAME | 87.06 |
| | | GLYCEROL | 0.00 |
| | | METHANOL | 12.94 |
| 80 | upper POLAR | FAME | 14.25 |
| | | GLYCEROL | 12.82 |
| | | METHANOL | 72.92 |
| | Lower FAME | FAME | 87.05 |
| | | GLYCEROL | 0.00 |
| | | METHANOL | 12.95 |
| 120 | upper POLAR | FAME | 18.80 |
| | | GLYCEROL | 11.44 |
| | | METHANOL | 69.76 |
| | Lower FAME | FAME | 86.67 |
| | | GLYCEROL | 0.00 |
| | | METHANOL | 13.33 |
| 140 | upper POLAR | FAME | 19.06 |
| | | GLYCEROL | 11.55 |
| | | METHANOL | 69.39 |

| | | | |
|---|---|---|---|
| | Lower FAME | FAME | 85.96 |
| | | GLYCEROL | 0.00 |
| | | METHANOL | 14.04 |
| 160 | upper POLAR | FAME | 17.75 |
| | | GLYCEROL | 12.92 |
| | | METHANOL | 69.33 |
| | Lower FAME | FAME | 86.50 |
| | | GLYCEROL | 0.00 |
| | | METHANOL | 13.50 |
| 180 | upper POLAR | FAME | 16.58 |
| | | GLYCEROL | 13.79 |
| | | METHANOL | 69.64 |
| | Lower FAME | FAME | 86.73 |
| | | GLYCEROL | 0.00 |
| | | METHANOL | 13.27 |
| 200 | upper POLAR | FAME | 14.68 |
| | | GLYCEROL | 13.62 |
| | | METHANOL | 71.70 |
| | Lower FAME | FAME | 86.69 |
| | | GLYCEROL | 0.00 |
| | | METHANOL | 13.31 |
| 240 | upper FAME | FAME | 87.31 |
| | | GLYCEROL | 0.00 |
| | | METHANOL | 12.69 |
| | Lower polar | FAME | 8.87 |
| | | GLYCEROL | 19.02 |
| | | METHANOL | 72.11 |
| 260 | upper FAME | FAME | 86.83 |
| | | GLYCEROL | 0.00 |
| | | METHANOL | 13.17 |
| | Lower polar | FAME | 10.43 |
| | | GLYCEROL | 19.77 |
| | | METHANOL | 69.80 |
| 300 | upper FAME | FAME | 88.03 |
| | | GLYCEROL | 0.00 |
| | | METHANOL | 11.97 |
| | Lower polar | FAME | 10.36 |
| | | GLYCEROL | 18.86 |
| | | METHANOL | 70.78 |
| 360 | upper FAME | FAME | 88.35 |
| | | GLYCEROL | 0.00 |
| | | METHANOL | 11.65 |
| | Lower polar | FAME | 8.20 |
| | | GLYCEROL | 20.28 |
| | | METHANOL | 71.52 |
| 380 | upper FAME | FAME | 88.61 |
| | | GLYCEROL | 0.00 |
| | | METHANOL | 11.39 |
| | Lower polar | FAME | 7.07 |

| | | | |
|---|---|---|---|
| | | GLYCEROL | 22.10 |
| | | METHANOL | 70.84 |
| 420 | upper FAME | FAME | 88.70 |
| | | GLYCEROL | 0.00 |
| | | METHANOL | 11.30 |
| | Lower polar | FAME | 7.43 |
| | | GLYCEROL | 22.21 |
| | | METHANOL | 70.36 |
| 480 | upper FAME | FAME | 88.73 |
| | | GLYCEROL | 0.00 |
| | | METHANOL | 11.27 |
| | Lower polar | FAME | 6.11 |
| | | GLYCEROL | 24.30 |
| | | METHANOL | 69.60 |

**50% recycling (overall permeate)**

| **Time (min.)** | Aver. MOH wt.% | Aver. Gly. wt.% | Aver. FAME wt. % |
|---|---|---|---|
| 0 | 68.41 | 4.23 | 27.37 |
| 20 | 58.45 | 4.80 | 36.75 |
| 40 | 40.40 | 5.12 | 54.48 |
| 60 | 37.25 | 5.27 | 57.48 |
| 80 | 38.65 | 4.67 | 56.68 |
| 120 | 41.13 | 5.50 | 53.37 |
| 140 | 41.66 | 6.68 | 51.66 |
| 160 | 43.68 | 7.53 | 48.80 |
| 180 | 39.40 | 7.51 | 53.09 |
| 200 | 37.00 | 5.80 | 57.19 |
| 240 | 35.60 | 5.38 | 59.02 |
| 260 | 35.43 | 4.52 | 60.05 |
| 300 | 34.59 | 7.25 | 58.16 |
| 360 | 35.92 | 8.22 | 55.86 |
| 380 | 35.91 | 9.35 | 54.74 |
| 420 | 37.35 | 9.80 | 52.85 |
| 480 | 35.60 | 10.33 | 54.07 |

**Main parameters of the membrane reactor for 50% recycling**

| Time | Mass flowrate(g/min) | Density(g/mL) | TMP(kPa) |
|---|---|---|---|
| 8:40 | | | |
| 9:10 | 18764 | 0.8149 | 48.263 |
| 9:40 | 19098 | 0.8143 | 48.263 |
| 10:20 | 19840 | 0.8152 | 48.263 |
| 10:40 | 19675 | 0.8144 | 48.263 |
| 11:10 | 19463 | 0.8206 | 48.263 |
| 11:50 | 19439 | 0.8221 | 48.263 |
| 12:10 | 19384 | 0.8211 | 55.158 |
| 12:40 | 19254 | 0.8287 | 62.052 |
| 1:10 | 19135 | 0.8271 | 68.947 |
| 1:50 | 18903 | 0.8286 | 68.947 |
| 2:10 | 18708 | 0.8304 | 68.947 |
| 2:40 | 18534 | 0.8329 | 82.736 |
| 3:00 | 18357 | 0.8319 | 82.736 |
| 3:40 | 18025 | 0.8330 | 89.631 |
| 4:20 | 17202 | 0.8360 | 89.631 |
| 4:35 | 16764 | 0.8365 | 89.631 |
| 4:40 | 16764 | 0.8365 | 89.631 |

**75 % Recycling**

| Time (min.) | phases | Component | comp. wt.% |
|---|---|---|---|
| 0 | upper POLAR | FAME | 16.07 |
| | | GLYCEROL | 11.01 |
| | | METHANOL | 72.91 |
| | Lower FAME | FAME | 85.71 |
| | | GLYCEROL | 0.00 |
| | | METHANOL | 14.29 |
| 20 | upper POLAR | FAME | 15.52 |
| | | GLYCEROL | 11.96 |
| | | METHANOL | 72.52 |
| | Lower FAME | FAME | 86.17 |
| | | GLYCEROL | 0.00 |
| | | METHANOL | 13.83 |
| 40 | upper POLAR | FAME | 11.10 |
| | | GLYCEROL | 13.18 |
| | | METHANOL | 75.72 |
| | Lower FAME | FAME | 86.39 |
| | | GLYCEROL | 0.00 |
| | | METHANOL | 13.61 |
| 60 | upper POLAR | FAME | 10.77 |
| | | GLYCEROL | 13.67 |
| | | METHANOL | 75.56 |
| | Lower FAME | FAME | 86.46 |
| | | GLYCEROL | 0.00 |
| | | METHANOL | 13.54 |
| 80 | upper POLAR | FAME | 15.25 |
| | | GLYCEROL | 11.82 |
| | | METHANOL | 72.92 |
| | Lower FAME | FAME | 87.05 |
| | | GLYCEROL | 0.00 |
| | | METHANOL | 12.95 |
| 120 | upper POLAR | FAME | 17.82 |
| | | GLYCEROL | 12.08 |
| | | METHANOL | 70.11 |
| | Lower FAME | FAME | 86.09 |
| | | GLYCEROL | 0.00 |
| | | METHANOL | 13.91 |
| 140 | upper POLAR | FAME | 17.82 |
| | | GLYCEROL | 12.08 |
| | | METHANOL | 70.11 |
| | Lower FAME | FAME | 86.90 |
| | | GLYCEROL | 0.00 |
| | | METHANOL | 12.84 |
| 180 | upper POLAR | FAME | 13.06 |

| | | | |
|---|---|---|---|
| | | GLYCEROL | 15.88 |
| | | METHANOL | 70.83 |
| | Lower FAME | FAME | 87.75 |
| | | GLYCEROL | 0.00 |
| | | METHANOL | 11.93 |
| 185 | upper FAME | FAME | 87.55 |
| | | GLYCEROL | 0.00 |
| | | METHANOL | 12.45 |
| | Lower polar | FAME | 14.76 |
| | | GLYCEROL | 15.94 |
| | | METHANOL | 69.30 |
| 200 | upper FAME | FAME | 88.81 |
| | | GLYCEROL | 0.00 |
| | | METHANOL | 11.19 |
| | Lower polar | FAME | 12.97 |
| | | GLYCEROL | 18.65 |
| | | METHANOL | 68.38 |
| 240 | upper FAME | FAME | 90.10 |
| | | GLYCEROL | 0.00 |
| | | METHANOL | 9.90 |
| | Lower polar | FAME | 6.68 |
| | | GLYCEROL | 25.16 |
| | | METHANOL | 68.16 |
| 280 | upper FAME | FAME | 90.86 |
| | | GLYCEROL | 0.00 |
| | | METHANOL | 9.14 |
| | Lower polar | FAME | 5.53 |
| | | GLYCEROL | 28.03 |
| | | METHANOL | 66.44 |
| 340 | upper FAME | FAME | 90.68 |
| | | GLYCEROL | 0.00 |
| | | METHANOL | 9.32 |
| | Lower polar | FAME | 5.20 |
| | | GLYCEROL | 28.73 |
| | | METHANOL | 66.07 |
| 380 | upper FAME | FAME | 91.07 |
| | | GLYCEROL | 0.00 |
| | | METHANOL | 8.93 |
| | Lower polar | FAME | 4.82 |
| | | GLYCEROL | 32.24 |
| | | METHANOL | 62.94 |
| 480 | upper FAME | FAME | 91.83 |
| | | GLYCEROL | 0.00 |
| | | METHANOL | 8.17 |
| | Lower polar | FAME | 3.59 |
| | | GLYCEROL | 35.68 |
| | | METHANOL | 60.73 |

**75% recycling (overall permeate)**

| Time (min.) | Aver. MOH wt.% | Aver. Gly. wt.% | Aver. FAME wt. % |
|---|---|---|---|
| 0 | 68.41 | 4.23 | 27.37 |
| 20 | 59.45 | 5.80 | 34.75 |
| 40 | 37.25 | 5.27 | 57.48 |
| 60 | 36.40 | 6.12 | 57.48 |
| 80 | 38.65 | 4.67 | 56.68 |
| 100 | 38.81 | 4.52 | 56.68 |
| 120 | 35.60 | 4.73 | 59.68 |
| 140 | 36.21 | 5.87 | 57.93 |
| 180 | 35.69 | 3.63 | 60.68 |
| 185 | 35.19 | 6.38 | 58.43 |
| 200 | 35.33 | 7.87 | 56.79 |
| 240 | 34.87 | 10.78 | 54.35 |
| 280 | 33.69 | 12.01 | 54.29 |
| 340 | 29.78 | 9.85 | 60.37 |
| 380 | 28.99 | 11.97 | 59.04 |
| 480 | 29.92 | 14.76 | 55.32 |

**Main parameters of the membrane reactor for 75% recycling**

| Time (min.) | Mass flowrate(g/min) | Density(g/mL) | TMP(kPa) |
|---|---|---|---|
| 8:40 | | | |
| 9:20 | 19011 | 0.8147 | 48.263 |
| 9:50 | 19261 | 0.8161 | 48.263 |
| 10:20 | 19604 | 0.8152 | 48.263 |
| 10:40 | 19675 | 0.8154 | 48.263 |
| 11:07 | 19463 | 0.8206 | 48.263 |
| 11:35 | 18642 | 0.8273 | 55.158 |
| 12:05 | 17902 | 0.8346 | 68.947 |
| 12:20 | 17856 | 0.8365 | 75.842 |
| 12:50 | 16945 | 0.8418 | 82.736 |
| 1:20 | 16660 | 0.8421 | 103.421 |
| 1:50 | 16559 | 0.8413 | 110.315 |
| 2:10 | 16515 | 0.8424 | 117.210 |
| 2:25 | 16434 | 0.8429 | 124.105 |
| 3:00 | 16446 | 0.8474 | 137.894 |
| 3:30 | 16581 | 0.8496 | 144.789 |
| 4:00 | 16386 | 0.8493 | 151.683 |
| 4:30 | 16315 | 0.8513 | 155.131 |
| 4:40 | 16315 | 0.8513 | 155.131 |

**100% Recycling**

| Time (min.) | phases | Component | comp. wt.% |
|---|---|---|---|
| 0 | upper POLAR | FAME | 16.07 |
| | | GLYCEROL | 11.01 |
| | | METHANOL | 72.91 |
| | Lower FAME | FAME | 85.71 |
| | | GLYCEROL | 0.00 |
| | | METHANOL | 14.29 |
| 20 | upper POLAR | FAME | 15.52 |
| | | GLYCEROL | 11.96 |
| | | METHANOL | 72.52 |
| | Lower FAME | FAME | 86.17 |
| | | GLYCEROL | 0.00 |
| | | METHANOL | 13.83 |
| 40 | upper POLAR | FAME | 11.10 |
| | | GLYCEROL | 13.18 |
| | | METHANOL | 75.72 |
| | Lower FAME | FAME | 86.39 |
| | | GLYCEROL | 0.00 |
| | | METHANOL | 13.61 |
| 60 | upper POLAR | FAME | 10.77 |
| | | GLYCEROL | 13.67 |
| | | METHANOL | 75.56 |
| | Lower FAME | FAME | 87.06 |
| | | GLYCEROL | 0.00 |
| | | METHANOL | 12.94 |
| 80 | upper POLAR | FAME | 14.50 |
| | | GLYCEROL | 12.85 |
| | | METHANOL | 72.65 |
| | Lower FAME | FAME | 86.77 |
| | | GLYCEROL | 0.00 |
| | | METHANOL | 13.23 |
| 100 | upper POLAR | FAME | 14.80 |
| | | GLYCEROL | 12.44 |
| | | METHANOL | 72.76 |
| | Lower FAME | FAME | 85.67 |
| | | GLYCEROL | 0.00 |
| | | METHANOL | 14.33 |
| 130 | upper POLAR | FAME | 18.30 |
| | | GLYCEROL | 11.57 |
| | | METHANOL | 70.13 |
| | Lower FAME | FAME | 85.56 |
| | | GLYCEROL | 0.00 |
| | | METHANOL | 14.44 |
| 160 | upper POLAR | FAME | 12.53 |

| | | | |
|---|---|---|---|
| | | GLYCEROL | 15.62 |
| | | METHANOL | 71.84 |
| | Lower FAME | FAME | 87.60 |
| | | GLYCEROL | 0.00 |
| | | METHANOL | 12.40 |
| 180 | upper FAME | FAME | 88.04 |
| | | GLYCEROL | 0.00 |
| | | METHANOL | 11.96 |
| | Lower polar | FAME | 12.75 |
| | | GLYCEROL | 18.15 |
| | | METHANOL | 69.09 |
| 200 | upper FAME | FAME | 88.87 |
| | | GLYCEROL | 0.00 |
| | | METHANOL | 11.13 |
| | Lower polar | FAME | 7.59 |
| | | GLYCEROL | 23.30 |
| | | METHANOL | 69.11 |
| 230 | upper FAME | FAME | 89.56 |
| | | GLYCEROL | 0.00 |
| | | METHANOL | 10.44 |
| | Lower polar | FAME | 5.66 |
| | | GLYCEROL | 26.11 |
| | | METHANOL | 68.23 |
| 260 | upper FAME | FAME | 90.67 |
| | | GLYCEROL | 0.00 |
| | | METHANOL | 9.33 |
| | Lower polar | FAME | 4.76 |
| | | GLYCEROL | 29.54 |
| | | METHANOL | 65.70 |
| 340 | upper FAME | FAME | 92.03 |
| | | GLYCEROL | 0.00 |
| | | METHANOL | 7.97 |
| | Lower polar | FAME | 2.98 |
| | | GLYCEROL | 37.61 |
| | | METHANOL | 59.41 |
| 360 | upper FAME | FAME | 92.49 |
| | | GLYCEROL | 0.00 |
| | | METHANOL | 7.51 |
| | Lower polar | FAME | 3.47 |
| | | GLYCEROL | 40.44 |
| | | METHANOL | 56.09 |

**100% recycling (overall permeate)**

| Time (min.) | Aver. MOH wt.% | Aver. Gly. wt.% | Aver. FAME wt. % |
|---|---|---|---|
| 0 | 68.41 | 4.23 | 27.37 |
| 20 | 58.45 | 4.80 | 36.75 |
| 40 | 40.40 | 5.12 | 54.48 |
| 60 | 37.25 | 5.27 | 57.48 |
| 80 | 38.65 | 4.67 | 56.68 |
| 100 | 41.13 | 5.50 | 53.37 |
| 120 | 42.29 | 5.79 | 51.93 |
| 140 | 36.10 | 6.50 | 57.40 |
| 160 | 33.18 | 5.57 | 61.25 |
| 180 | 32.65 | 5.70 | 61.66 |
| 200 | 34.02 | 9.20 | 56.78 |
| 230 | 35.63 | 11.38 | 52.99 |
| 260 | 35.10 | 13.50 | 51.40 |
| 300 | 33.70 | 15.24 | 51.07 |
| 340 | 32.08 | 17.63 | 50.29 |
| 360 | 32.08 | 17.63 | 50.29 |

**Main parameters of the membrane reactor for 100% recycling**

| Time (min.) | Mass flowrate(g/min) | Density(g/mL) | TMP(kPa) |
|---|---|---|---|
| 9:20 | | | |
| 9:25 | 18721 | 0.8087 | 48.263 |
| 9:50 | 18785 | 0.8139 | 48.263 |
| 10:20 | 19181 | 0.8140 | 44.816 |
| 10:50 | 19708 | 0.8150 | 44.816 |
| 11:20 | 19722 | 0.8160 | 48.263 |
| 11:50 | 18584 | 0.8297 | 55.158 |
| 12:20 | 18286 | 0.8343 | 62.052 |
| 1:00 | 17053 | 0.8407 | 96.526 |
| 1:50 | 16944 | 0.8443 | 120.657 |
| 2:20 | 17006 | 0.8460 | 124.105 |
| 2:50 | 16966 | 0.8495 | 130.999 |
| 3:10 | 16867 | 0.8539 | 151.683 |
| 3:20 | 16275 | 0.8550 | 165.473 |

**Experiments performed for chapter 5**: Permeate composition. Experimental mode: continuous mode without recycling.

| 1%-1hRT | | | | |
|---|---|---|---|---|
| Time(min) | DG(wt.%) | FAME(wt.%) | Glycerol(wt.%) | Methanol(wt.%) |
| 0 | 0.00% | 27.95% | 2.80% | 69.25% |
| 10 | 0.14% | 39.10% | 3.89% | 56.87% |
| 40 | 0.14% | 56.14% | 4.64% | 39.08% |
| 60 | 0.17% | 55.01% | 4.56% | 40.26% |
| 80 | 0.22% | 59.60% | 4.83% | 35.35% |
| 100 | 0.17% | 59.20% | 4.76% | 35.88% |
| 130 | 0.17% | 60.14% | 4.37% | 35.31% |
| 160 | 0.15% | 59.76% | 4.15% | 35.94% |

| | FAME | | | | | | POLAR | | | | | |
|---|---|---|---|---|---|---|---|---|---|---|---|---|
| Time (min) | TG (wt.%) | DG (wt.%) | MG (wt.%) | FAME (wt.%) | Glycerol (wt.%) | Methanol (wt.%) | TG (wt.%) | DG (wt.%) | MG (wt.%) | FAME (wt.%) | Glycerol (wt.%) | Methanol (wt.%) |
| 0 | 0.00 | 0.00 | 0.00 | 85.71 | 0.00 | 14.29 | 0.00 | 0.00 | 0.00 | 16.07 | 3.38 | 80.55 |
| 10 | 0.00 | 0.44 | 0.00 | 86.17 | 0.00 | 13.39 | 0.00 | 0.00 | 0.00 | 17.13 | 5.69 | 77.18 |
| 40 | 0.00 | 0.23 | 0.00 | 86.39 | 0.00 | 13.38 | 0.00 | 0.00 | 0.00 | 11.10 | 11.56 | 77.34 |
| 60 | 0.00 | 0.30 | 0.00 | 87.06 | 0.00 | 12.64 | 0.00 | 0.00 | 0.00 | 11.96 | 10.58 | 77.46 |
| 80 | 0.00 | 0.35 | 0.00 | 86.77 | 0.00 | 12.88 | 0.00 | 0.00 | 0.00 | 14.50 | 12.85 | 72.65 |
| 100 | 0.00 | 0.27 | 0.00 | 86.67 | 0.00 | 13.06 | 0.00 | 0.00 | 0.00 | 14.80 | 12.44 | 72.76 |
| 130 | 0.00 | 0.27 | 0.00 | 85.56 | 0.00 | 14.17 | 0.00 | 0.00 | 0.00 | 14.76 | 12.18 | 73.06 |
| 160 | 0.00 | 0.24 | 0.00 | 86.93 | 0.00 | 12.83 | 0.00 | 0.00 | 0.00 | 11.92 | 11.44 | 76.64 |

| 0.5%-1hRT | | | | |
|---|---|---|---|---|
| Time(min) | DG(wt.%) | FAME(wt.%) | Glycerol(wt.%) | Methanol(wt.%) |
| 0 | 0.00% | 21.41% | 2.48% | 76.11% |
| 15 | 0.18% | 49.06% | 4.56% | 46.20% |
| 40 | 0.30% | 58.38% | 4.39% | 36.94% |
| 120 | 0.27% | 59.05% | 4.53% | 36.16% |
| 160 | 0.20% | 58.67% | 4.55% | 36.58% |

| FAME PHASE | | | | | | POLAR PHASE | | | | | | |
|---|---|---|---|---|---|---|---|---|---|---|---|---|
| TG (wt.%) | DG (wt.%) | MG (wt.%) | FAME (wt.%) | Glycerol (wt.%) | Methanol (wt.%) | TG (wt.%) | DG (wt.%) | MG (wt.%) | FAME (wt.%) | Glycerol (wt.%) | Methanol (wt.%) | Time (min) |
| 0.00 | 0.00 | 0.00 | 85.71 | 0.00 | 14.29 | 0.00 | 0.00 | 0.00 | 12.82 | 2.81 | 84.36 | 0 |
| 0.00 | 0.39 | 0.00 | 86.17 | 0.00 | 13.44 | 0.00 | 0.00 | 0.00 | 17.44 | 8.45 | 74.11 | 15 |
| 0.00 | 0.49 | 0.00 | 86.39 | 0.00 | 13.12 | 0.00 | 0.00 | 0.00 | 14.96 | 11.18 | 73.85 | 40 |
| 0.00 | 0.43 | 0.00 | 86.93 | 0.00 | 12.64 | 0.00 | 0.00 | 0.00 | 14.79 | 11.71 | 73.50 | 120 |
| 0.00 | 0.32 | 0.00 | 86.77 | 0.00 | 12.91 | 0.00 | 0.00 | 0.00 | 11.77 | 12.14 | 76.09 | 160 |

| 0.1%-1hRT | | | | |
|---|---|---|---|---|
| Time(min) | DG(wt.%) | FAME(wt.%) | Glycerol(wt.%) | Methanol(wt.%) |
| 0 | 0.00% | 14.75% | 3.74% | 81.51% |
| 20 | 0.18% | 45.10% | 4.56% | 50.16% |
| 45 | 0.16% | 54.66% | 4.70% | 40.48% |
| 120 | 0.20% | 56.99% | 4.83% | 37.98% |

| FAME PHASE | | | | | | POLAR PHASE | | | | | | |
|---|---|---|---|---|---|---|---|---|---|---|---|---|
| TG (wt.%) | DG (wt.%) | MG (wt.%) | FAME (wt.%) | Glycerol (wt.%) | Methanol (wt.%) | TG (wt.%) | DG (wt.%) | MG (wt.%) | FAME (wt.%) | Glycerol (wt.%) | Methanol (wt.%) | Time (min) |
| | | | | | | | | | | | | 0 |
| 0.00 | 0.38 | 0.00 | 83.026 | 0.00 | 16.59 | 0.00 | 0.00 | 0.00 | 12.73 | 8.45 | 78.81 | 20 |
| 0.00 | 0.26 | 0.00 | 83.956 | 0.00 | 15.78 | 0.00 | 0.00 | 0.00 | 10.17 | 11.84 | 77.99 | 45 |
| 0.00 | 0.31 | 0.00 | 84.274 | 0.00 | 15.41 | 0.00 | 0.00 | 0.00 | 10.24 | 13.10 | 76.66 | 120 |

| 0.05-1hRT | | | | |
|---|---|---|---|---|
| Time(min) | DG(wt.%) | FAME(wt.%) | Glycerol(wt.%) | Methanol(wt.%) |
| 0 | 0.00% | 13.61% | 4.04% | 82.35% |
| 15 | 0.00% | 36.34% | 5.51% | 58.15% |
| 75 | 0.13% | 51.26% | 5.23% | 43.38% |
| 135 | 0.14% | 56.60% | 5.27% | 37.99% |

| FAME PHASE | | | | | | POLAR PHASE | | | | | | |
|---|---|---|---|---|---|---|---|---|---|---|---|---|
| TG (wt.%) | DG (wt.%) | MG (wt.%) | FAME (wt.%) | Glycerol (wt.%) | Methanol (wt.%) | TG (wt.%) | DG (wt.%) | MG (wt.%) | FAME (wt.%) | Glycerol (wt.%) | Methanol (wt.%) | Time (min) |
| | | | | | | | | | | | | 0 |
| 0.00 | 0.00 | 0.00 | 85.12 | 0.00 | 14.88 | 0.00 | 0.00 | 0.00 | 13.68 | 8.07 | 78.25 | 15 |
| 0.00 | 0.25 | 0.00 | 86.07 | 0.00 | 13.68 | 0.00 | 0.00 | 0.00 | 10.65 | 11.33 | 78.02 | 75 |
| 0.00 | 0.24 | 0.00 | 84.97 | 0.00 | 14.79 | 0.00 | 0.00 | 0.00 | 13.77 | 13.22 | 73.01 | 135 |

| 0.03%-1hRT | | | | |
|---|---|---|---|---|
| Time(min) | DG(wt.%) | FAME(wt.%) | Glycerol(wt.%) | Methanol(wt.%) |
| 0 | 0 | 10.61% | 1.23% | 88.16% |
| 20 | 0 | 17.35% | 3.85% | 78.80% |
| 45 | 0 | 22.44% | 3.97% | 73.59% |
| 85 | 0 | 27.42% | 5.68% | 66.90% |
| 125 | 0 | 28.36% | 6.24% | 65.40% |

| FAME PHASE | | | | | | POLAR PHASE | | | | | | |
|---|---|---|---|---|---|---|---|---|---|---|---|---|
| TG (wt.%) | DG (wt.%) | MG (wt.%) | FAME (wt.%) | Glycerol (wt.%) | Methanol (wt.%) | TG (wt.%) | DG (wt.%) | MG (wt.%) | FAME (wt.%) | Glycerol (wt.%) | Methanol (wt.%) | Time (min) |
| | | | | | | | | | | | | 0 |
| | | | | | | | | | | | | 20 |
| 0.00 | 0.00 | 0.00 | 83.95 | 0.00 | 16.05 | 0.00 | 0.00 | 0.00 | 9.80 | 4.79 | 85.42 | 45 |
| 0.00 | 0.00 | 0.00 | 84.3 | 0.00 | 15.70 | 0.00 | 0.00 | 0.00 | 12.50 | 7.17 | 80.33 | 85 |
| 0.00 | 0.00 | 0.00 | 83.95 | 0.00 | 16.05 | 0.00 | 0.00 | 0.00 | 9.58 | 8.35 | 82.07 | 125 |

| 0.05%-2hRT | | | | |
|---|---|---|---|---|
| Time(min) | DG(wt.%) | FAME(wt.%) | Glycerol(wt.%) | Methanol(wt.%) |
| 0 | 0.00% | 13.61% | 4.04% | 82.35% |
| 20 | 0.13% | 40.36% | 5.60% | 53.91% |
| 35 | 0.12% | 46.44% | 5.74% | 47.70% |
| 60 | 0.15% | 49.90% | 5.13% | 44.81% |
| 120 | 0.17% | 56.66% | 5.41% | 37.75% |

| FAME PHASE | | | | | | POLAR PHASE | | | | | | |
|---|---|---|---|---|---|---|---|---|---|---|---|---|
| TG (wt.%) | DG (wt.%) | MG (wt.%) | FAME (wt.%) | Glycerol (wt.%) | Methanol (wt.%) | TG (wt.%) | DG (wt.%) | MG (wt.%) | FAME wt.%) | Glycerol (wt.%) | Methanol (wt.%) | Time (min) |
| | | | | | | | | | | | | 0 |
| 0.00 | 0.34 | 0.00 | 85.12 | 0.00 | 14.54 | 0.00 | 0.00 | 0.00 | 13.14 | 9.01 | 77.85 | 20 |
| 0.00 | 0.25 | 0.00 | 86.07 | 0.00 | 13.68 | 0.00 | 0.00 | 0.00 | 12.81 | 10.60 | 76.58 | 35 |
| 0.00 | 0.29 | 0.00 | 84.97 | 0.00 | 14.73 | 0.00 | 0.00 | 0.00 | 11.40 | 10.77 | 77.83 | 60 |
| 0.00 | 0.28 | 0.00 | 84.97 | 0.00 | 14.74 | 0.00 | 0.00 | 0.00 | 14.00 | 13.57 | 72.43 | 120 |

| 0.03%-2hRT | | | | |
|---|---|---|---|---|
| Time(min) | DG(wt.%) | FAME(wt.%) | Glycerol(wt.%) | Methanol(wt.%) |
| 0 | 0 | 9.61% | 1.06% | 89.33% |
| 30 | 0 | 18.46% | 3.51% | 78.02% |
| 60 | 0 | 26.53% | 4.07% | 69.40% |
| 90 | 0 | 28.27% | 4.19% | 67.54% |
| 120 | 0 | 29.49% | 3.41% | 67.10% |

| FAME PHASE | | | | | | POLAR PHASE | | | | | | |
|---|---|---|---|---|---|---|---|---|---|---|---|---|
| TG (wt.%) | DG (wt.%) | MG (wt.%) | FAME (wt.%) | Glycerol (wt.%) | Methanol (wt.%) | TG(wt.%) | DG (wt.%) | MG (wt.%) | FAME (wt.%) | Glycerol (wt.%) | Methanol (wt.%) | Time (min) |
| | | | | | | | | | | | | 0 |
| | | | | | | | | | | | | 30 |
| 0.00 | 0.00 | 0.00 | 82.449 | 0.00 | 17.55 | 0.00 | 0.00 | 0.00 | 12.28 | 5.10 | 82.62 | 60 |
| 0.00 | 0.00 | 0.00 | 83.954 | 0.00 | 16.05 | 0.00 | 0.00 | 0.00 | 10.61 | 5.52 | 83.88 | 90 |
| 0.00 | 0.00 | 0.00 | 84.296 | 0.00 | 15.70 | 0.00 | 0.00 | 0.00 | 12.04 | 6.93 | 81.02 | 120 |

| 0.01%-2hRT | | | | |
|---|---|---|---|---|
| Time(min) | DG(wt.%) | FAME(wt.%) | Glycerol(wt.%) | Methanol(wt.%) |
| 0 | 0 | 4.44% | 0.53% | 95.03% |
| 10 | 0 | 6.10% | 1.37% | 92.53% |
| 20 | 0 | 7.87% | 1.98% | 90.15% |
| 50 | 0 | 10.84% | 2.64% | 86.52% |
| 80 | 0 | 11.41% | 2.89% | 85.70% |
| 100 | 0 | 12.61% | 2.94% | 84.45% |

| 0%-2hRT | | | | |
|---|---|---|---|---|
| Time(min) | DG(wt.%) | FAME(wt.%) | Glycerol(wt.%) | Methanol(wt.%) |
| 0 | 0 | 3.44% | 0.37% | 96.19% |
| 15 | 0 | 5.60% | 1.37% | 93.03% |
| 30 | 0 | 6.76% | 1.98% | 91.26% |
| 45 | 0 | 7.88% | 2.64% | 89.48% |
| 60 | 0 | 8.41% | 2.89% | 88.70% |

**Average $K_{ow}$ calculation for chapter 6:**

Experimental mode: continuous mode without recycling.

| **Lipids** | | | **Fatty acid composition (wt.%)** | | | | | **AVE.** |
|---|---|---|---|---|---|---|---|---|
| | **Fatty acid** | **Myristic: 14:0** | **Palmitic:** (16:0) | **Stearic:** (18:0) | **Oleic:** (18:1) | **Linoleic:** (18:2) | **Linolenic:** (18:3) | $k_{ow}$ |
| | **Stru-cture** | R = - $(CH_2)_{12}$ – $CH_3$ | R = - $(CH_2)_{14}$ – $CH_3$ | R = - $(CH_2)_{16}$ – $CH_3$ | R = - $(CH_2)_7$ CH=CH- $(CH_2)_7CH_3$ | R = - $(CH_2)_7$ CH=CH- $CH_2$-CH=CH $(CH_2)_4CH_3$ | R= - $(CH_2)_7$ CH=CH-$CH_2$- CH=CH-$CH_2$- CH=CH-$CH_2$-$CH_3$ | |
| Log $k_{ow}$ | | 6.27 | 7.25 | 8.23 | 7.73 | 7.51 | 7.3 | |
| $k_{ow}$ | | 1862087 | 17782794 | 169824365 | 5.4E+07 | 32359366 | 19952623 | |
| Canola | | 1.25 | 3.75 | 1.75 | 59.45 | 23.55 | 10.25 | |
| | | 2.33E+06 | 6.67E+07 | 2.97E+08 | 3.19E+09 | 7.62E+08 | 2.05E+08 | 7.656 |
| Soybean | | 4.45 | 7.8 | 4.2 | 24.25 | 53.05 | 6.25 | |
| | | 8.29E+06 | 1.39E+08 | 7.13E+08 | 1.30E+09 | 1.72E+09 | 1.25E+08 | 7.602 |
| Palm | | 1.4 | 43.9 | 17 | 30.1 | -- | -- | |
| | | 2.61E+06 | 7.81E+08 | 2.89E+09 | 1.62E+09 | 0.00E+00 | 0.00E+00 | 7.759 |
| YG | | 0.84 | 15.88 | 8.43 | 48.43 | 20.11 | 1.89 | |
| | | 1.56E+06 | 2.82E+08 | 1.43E+09 | 2.60E+09 | 6.51E+08 | 3.77E+07 | 7.719 |
| BG | | 1 | 23 | 10 | 50 | 15 | -- | |
| | | 1.86E+06 | 4.09E+08 | 1.70E+09 | 2.69E+09 | 4.85E+08 | 0.00E+00 | 7.727 |

**Experiments performed for chapter 7: Samples composition in the membrane reactor.**

Experimental mode: continuous mode without recycling.

RT = 60 minutes, with 0.5 wt.% catalyst concentration

| Time(min) | TG (mol/L) | DG (mol/L) | MG] (mol/L) | FAME (mol/L) | Glycerol (mol/L) | Methanol (mol/L) |
|---|---|---|---|---|---|---|
| 0 | 0.53883 | 0.00000 | 0.00000 | 0.00000 | 0.00000 | 12.91061 |
| 2 | 0.05148 | 0.00571 | 0.00719 | 1.51256 | 0.49411 | 10.78697 |
| 10 | 0.01557 | 0.00409 | 0.00700 | 1.68147 | 0.57203 | 10.02745 |
| 20 | 0.01122 | 0.00366 | 0.00697 | 1.68248 | 0.58137 | 10.12032 |
| 30 | 0.00600 | 0.00345 | 0.00657 | 1.77204 | 0.63988 | 9.83262 |
| 40 | 0.00930 | 0.00314 | 0.00712 | 1.66761 | 0.64021 | 10.15000 |
| 50 | 0.00839 | 0.00310 | 0.00864 | 1.69049 | 0.63150 | 9.97265 |
| 60 | 0.00849 | 0.00408 | 0.00701 | 1.69585 | 0.65045 | 9.86504 |
| 90 | 0.00846 | 0.00297 | 0.00718 | 1.67865 | 0.66619 | 9.99897 |
| 120 | 0.00846 | 0.00533 | 0.00955 | 1.72440 | 0.65576 | 9.53445 |

RT = 45 minutes, with 0.5 wt.% catalyst concentration

| Time(min) | TG (mol/L) | DG (mol/L) | MG] (mol/L) | FAME (mol/L) | Glycerol (mol/L) | Methanol (mol/L) |
|---|---|---|---|---|---|---|
| 0 | 0.53883 | 0.00000 | 0.00000 | 0.00000 | 0.00000 | 12.91061 |
| 10 | 0.01770 | 0.00388 | 0.00652 | 1.73978 | 0.59824 | 9.36356 |
| 20 | 0.01504 | 0.00322 | 0.00591 | 1.73081 | 0.62464 | 9.46350 |
| 30 | 0.01073 | 0.00326 | 0.00649 | 1.71217 | 0.66237 | 9.63935 |
| 40 | 0.00876 | 0.00322 | 0.00504 | 1.67861 | 0.68185 | 9.96489 |
| 50 | 0.00801 | 0.00320 | 0.00598 | 1.64661 | 0.68923 | 10.25066 |
| 60 | 0.00712 | 0.00317 | 0.00778 | 1.63162 | 0.68799 | 10.39796 |
| 90 | 0.00920 | 0.00317 | 0.01481 | 1.55605 | 0.68379 | 10.97319 |
| 120 | 0.01000 | 0.00372 | 0.00875 | 1.49408 | 0.61406 | 11.78170 |

RT = 30 minutes, with 0.5 wt.% catalyst concentration

| Time(min) | TG (mol/L) | DG (mol/L) | MG] (mol/L) | FAME (mol/L) | Glycerol (mol/L) | Methanol (mol/L) |
|---|---|---|---|---|---|---|
| 0 | 0.53883 | 0.00000 | 0.00000 | 0.00000 | 0.00000 | 12.91061 |
| 10 | 0.01932 | 0.00351 | 0.01277 | 1.52238 | 0.57263 | 11.34070 |
| 20 | 0.01612 | 0.00309 | 0.01344 | 1.54601 | 0.53253 | 11.32637 |
| 30 | 0.01349 | 0.00302 | 0.00697 | 1.55193 | 0.58312 | 11.27235 |
| 40 | 0.01044 | 0.00419 | 0.01739 | 1.50357 | 0.64047 | 11.50071 |
| 50 | 0.01076 | 0.00336 | 0.01658 | 1.49062 | 0.66720 | 11.55982 |
| 60 | 0.00990 | 0.00354 | 0.01638 | 1.46367 | 0.67921 | 11.79721 |
| 90 | 0.00988 | 0.00319 | 0.00977 | 1.55222 | 0.67116 | 11.08194 |
| 120 | 0.00965 | 0.00354 | 0.00666 | 1.52288 | 0.65016 | 11.44805 |

RT = 15 minutes, with 0.5 wt.% catalyst concentration

| Time(min) | TG (mol/L) | DG (mol/L) | MG] (mol/L) | FAME (mol/L) | Glycerol (mol/L) | Methanol (mol/L) |
|---|---|---|---|---|---|---|
| 0 | 0.53883 | 0.00000 | 0.00000 | 0.00000 | 0.00000 | 12.91061 |
| 10 | 0.02104 | 0.00428 | 0.01152 | 1.66577 | 0.51448 | 10.13297 |
| 20 | 0.02124 | 0.00488 | 0.00607 | 1.53720 | 0.60729 | 11.09910 |
| 30 | 0.02104 | 0.00601 | 0.01712 | 1.48114 | 0.58779 | 11.53467 |
| 40 | 0.02083 | 0.00705 | 0.00560 | 1.43790 | 0.57083 | 12.09742 |
| 50 | 0.02579 | 0.00930 | 0.00569 | 1.39678 | 0.57912 | 12.27313 |

RT = 60 minutes, with 0.1 wt.% catalyst concentration

| Time(min) | TG (mol/L) | DG (mol/L) | MG] (mol/L) | FAME (mol/L) | Glycerol (mol/L) | Methanol (mol/L) |
|---|---|---|---|---|---|---|
| 0 | 0.53883 | 0.00000 | 0.00000 | 0.00000 | 0.00000 | 12.91061 |
| 5 | 0.31708 | 0.02736 | 0.01702 | 0.86919 | 0.25633 | 9.55362 |
| 10 | 0.18384 | 0.02679 | 0.02620 | 1.23373 | 0.33229 | 9.55687 |
| 20 | 0.03150 | 0.00321 | 0.02946 | 1.68222 | 0.49108 | 9.14808 |

RT = 60 minutes, with 0.05 wt.% catalyst concentration

| Time(min) | TG (mol/L) | DG (mol/L) | MG] (mol/L) | FAME (mol/L) | Glycerol (mol/L) | Methanol (mol/L) |
|---|---|---|---|---|---|---|
| 0 | 0.53883 | 0.00000 | 0.00000 | 0.00000 | 0.00000 | 12.91061 |
| 5 | 0.52388 | 0.02736 | 0.00800 | 0.21472 | 0.06253 | 9.64603 |
| 10 | 0.49675 | 0.02679 | 0.00800 | 0.35522 | 0.10135 | 8.70391 |
| 20 | 0.46219 | 0.00321 | 0.02879 | 0.50770 | 0.10816 | 8.17052 |

## Appendix C Oil Droplet Size, $P_{crit}$, and Permeat Flux

For the purposes of membrane selection, it is important to know the size and distribution of the dispersed oil droplets in the continuous alcohol phase at membrane reactor condition. Mugele and Evan (1951) proposed a general equation for various average droplet diameters.

$$D_{qP}^{q-p} = \int_0^\infty D^q f(D)dD \Big/ \int_0^\infty D^p f(D)dD \qquad (1)$$
$$(q > p; q = 1,2,3; p = 0,1,2)$$

The oil droplet size distribution is defined by the Sauter mean diameter ($d_{32}$), which is obtained with q=3, p=2. The Sauter mean diameter ($d_{32}$) expresses the average ratio between the volume and the surface area of the droplets, and is the most appropriate mean diameter to represent the size distribution in liquid-liquid dispersed systems. To account for the dispersed phase viscosity effect, the following equation was derived which correlated the data very well (Sleicher, 1962):

$$\frac{D_{\max}\rho_c U^2}{\sigma}\sqrt{\frac{\mu_c U}{\sigma}} = 38\left[1+0.7\left(\frac{\mu_d U}{\sigma}\right)^{0.7}\right] \qquad (2)$$

where $\rho$ = density (kg/m$^3$), U = average velocity (m/s), $\sigma$ = interfacial tension (N/m), $\mu$ = coefficient of viscosity (kg/(m.s)), D or d = drop diameter (m or μm), and the subscripts c = continuous phase (i.e. methanol phase) and d = dispersed phase (i.e. oil phase).

A simple relation between the maximum and Sauter mean droplet diameter is $d_{32} = \alpha_4 d_{\max}$, where $\alpha_4$ has been determined to be 2/3 (Berkmann et al., 1988).

From eq. (2), we can predict the oil droplet size in methanol at different conditions using the following semi-empirical equation:

$$d_{32} = \frac{25.33\sigma}{\rho_c U^2}\left[1+0.7\left(\frac{\mu_d U}{\sigma}\right)^{0.7}\right] \Big/ \sqrt{\frac{\mu_c U}{\sigma}} \qquad (3)$$

As discussed in chapter 3, four membranes with different pore sizes were assessed: 0.05, 0.2, 0.5 and 1.4 μm. It was observed that no TG was found in the permeate stream for all runs. At our experimental conditions, the calculated mean diameter range for canola oil droplet in methanol was 63.9 to 1719.7 micron, which is consistent with Collin

and Knudsen's experimental results (Collins and Knudsen, 1970). They showed an immiscible liquid droplet size distribution ranging from 20 to 900 microns. An important result of their study was the demonstration of the existence of a critical droplet diameter range within which droplets are stable. Oil as the dispersed phase in the methanol continuous phase, therefore will assume a droplet size that can neither be bigger than the upper limit due to breakup, nor smaller than the lower limit due to coalescence.

In emulsions, pore blockage can be caused by the entry of oil droplets into a membrane pore if the operating pressure exceeds the critical capillary pressure ($P_{crit}$) (Nazzal and Wiesner, 1996). The critical pressure $P_{crit}$ at which an oil droplet enters a pore can be expressed by:

$$P_{crti} = 2\sigma \frac{\cos\theta}{r_{pore}} \times \left\{ 1 - \left[ \frac{2 + 3\cos\theta - \cos\theta^3}{4(\frac{r_{oil}}{r_{pore}})^3 \cos\theta^3 - (2 - \sin\theta + \sin\theta^3)} \right]^{1/3} \right\} \qquad (4)$$

A TMP above $P_{crit}$ will also cause the oil to permeate though membrane pores and contaminate the biodiesel for membrane reactor. Critical pressures were anticipated through the model of eq. (5) by assuming a contact angle of 25 deg, interfacial tension of 52 dynes/cm. Figure C.1 illustrate the critical pressures for the different membrane pore size and smallest oil droplet 12 micron (Cao et al., 2007) in methanol at 65 $^0$C. For the 300KD MWCO membrane installed in the prototype membrane reactor, we assume the largest membrane pore size is 0.05 micron, it could endure 40000 kPa TMP without oil (TG) being pushed though the membrane pore. Even for the 1.4 micron pore size carbon membrane which was used in lab-scale reactor, its theoretical critical pressure is still above 1000 kPa, which means TMP for biodiesel production can operated as high as 1000 kPa. Practical experimental TMP is always in the range from 12 to 210 kPa, which is far below the critical pressure, which explained why no oil was detected by GPC for all cases.

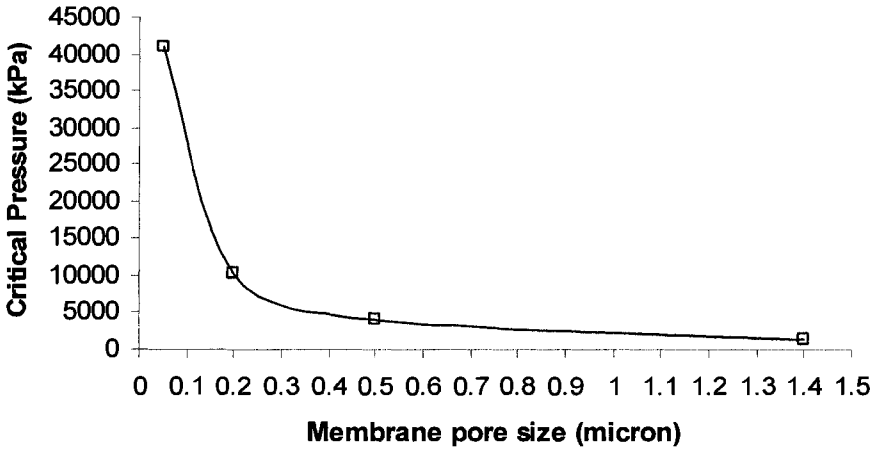


Figure C.1. Critical pressure as a function of pore size

For biodiesel production process in the membrane reactor, TMP reaches to a steady state after a short period of time (Cao et al., 2007). Table C.1 list the TMP values of the four runs with 0.5% catalyst concentration in chapter 7. The lower residence time result higher TMP in the membrane reactor, that was because the permeate flux increases linearly when RT decreases.

Table C.1: Steady state TMP values for different residence time.

| RT(min) | TMP (kPa) |
|---|---|
| 60 | 20.68 |
| 45 | 31.03 |
| 30 | 41.37 |
| 15 | 62.05 |

During the membrane separation process, Darcy's law can be used to explain the relation ship between the permeate flux and TMP (Mallevialle et al., 1996), a modified form of Darcy's law is introduced in equation 6 as following:

$$J_p = \frac{(dV/dt)}{A} = \frac{\Delta P}{\mu R_t} = K\Delta P \qquad (6)$$

Where, $J_p$ is the volumetric flux permeate flux (L/(h.m$^2$)), A is the membrane area (m$^2$) (for this study, the membrane area is 0.3 m$^2$); V is the volume of the permeate (L), t is the time (hour), Rt represents total resistance to flow (1/m), $\mu$ is dynamic viscosity (Pa.h). For the biodiesel production process, if we assume that the Rt and $\mu$ are constant with time, the linear relationship can be derived in equation 6. Figure C.2 illustrated the experimental results of permeate flux and TMP, as we can see a roughly linear line can be drawn.

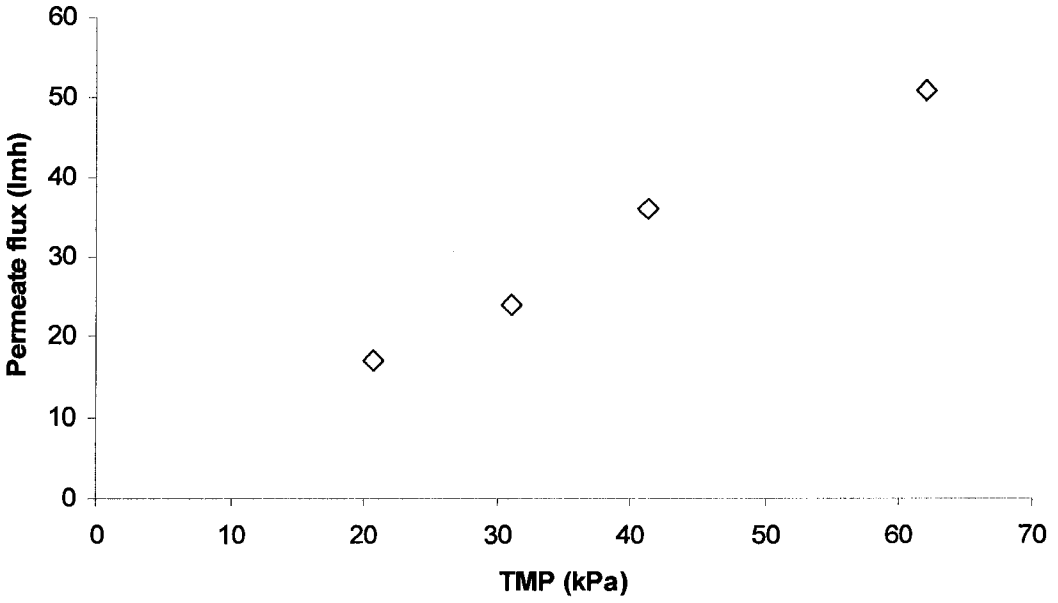


Figure C.2: Permeate flux and TMP using 300KD membrane

**References**

Berkmann P. D.; Calabrese R. V. Dispersion of Viscous Fluids by Turbulent Flow in a Static Mixer. *AIChE J.*, 34, 602, **1988**.

Cao P.; Tremblay A.Y.; Dubé M.A.; Morse K., Effect of Membrane Pore Size on the Performance of a Membrane Reactor for Biodiesel Production, *Ind. Eng. Chem. Res.*, 46, 52-58, **2007**.

Collins S. B.; Knudsen J. G. Drop-size distribution produced by turbulent pipe flow of immiscible liquids. *AIChE J.*, 11, 1074**, 1970**.

Mallevialle J.; Odendaal P.E.; Wiesner M.R., Coagulation and Membrane Separation, In: Water Treatment Membrane Processes, *McGraw-Hill,* New York, **1996**.

Mugele R.C.; Evans H.D., Droplet Size Distribution in Sprays, *Ind. Eng. Chem. Res.*, 43, 1317, **1951**.

Nazzal F.F.; Wiesner M.R., Mirofiltration of Oil-in-water Emulsions, *Water Environment Research,* **1996.**

Sleicher C. A., Maximum Stable Drop Size in Turbulent Flow, *A.I.Ch.E. J.*, 8, 471**, 1962**.